NOAA Technical Report NMFS 139

November 1998

Seasonal, Horizontal, and Vertical Distribution of Phytoplankton Chlorophyll *a* in the Northeast U.S. Continental Shelf Ecosystem

John E. O'Reilly
Christine Zetlin

Library
NOAA, National Marine Fisheries Service
SWFC Honolulu Laboratory F/SWC2
2570 Dole Street
Honolulu, HI 96822-2396

U.S. Department of Commerce

U.S. DEPARTMENT OF COMMERCE

WILLIAM M. DALEY
SECRETARY

National Oceanic and Atmospheric Administration

D. James Baker
Under Secretary for
Oceans and Atmosphere

National Marine Fisheries Service

Rolland A. Schmitten
Assistant Administrator
for Fisheries

NOAA Technical Reports NMFS

Technical Reports of the *Fishery Bulletin*

Scientific Editor
Dr. John B. Pearce
Northeast Fisheries Science Center
National Marine Fisheries Service, NOAA
166 Water Street
Woods Hole, Massachusetts 02543-1097

Editorial Committee
Dr. Andrew E. Dizon National Marine Fisheries Service
Dr. Linda L. Jones National Marine Fisheries Service
Dr. Richard D. Methot National Marine Fisheries Service
Dr. Theodore W. Pietsch University of Washington
Dr. Joseph E. Powers National Marine Fisheries Service
Dr. Tim D. Smith National Marine Fisheries Service

Managing Editor
Shelley E. Arenas
Scientific Publications Office
National Marine Fisheries Service, NOAA
7600 Sand Point Way N.E.
Seattle, Washington 98115-0070

The *NOAA Technical Report NMFS* (ISSN 0892-8908) series is published by the Scientific Publications Office, National Marine Fisheries Service, NOAA, 7600 Sand Point Way N.E., Seattle, WA 98115-0070.

The Secretary of Commerce has determined that the publication of this series is necessary in the transaction of the public business required by law of this Department. Use of funds for printing of this series has been approved by the Director of the Office of Management and Budget.

The *NOAA Technical Report NMFS* series of the *Fishery Bulletin* carries peer-reviewed, lengthy original research reports, taxonomic keys, species synopses, flora and fauna studies, and data intensive reports on investigations in fishery science, engineering, and economics. The series was established in 1983 to replace two subcategories of the Technical Report series: "Special Scientific Report—Fisheries" and "Circular." Copies of the *NOAA Technical Report NMFS* are available free in limited numbers to government agencies, both federal and state. They are also available in exchange for other scientific and technical publications in the marine sciences.

NMFS Honolulu Library
00000000004864

NOAA Technical Report NMFS 139
A Technical Report of the *Fishery Bulletin*

Seasonal, Horizontal, and Vertical Distribution of Phytoplankton Chlorophyll *a* in the Northeast U.S. Continental Shelf Ecosystem

John E. O'Reilly
Christine Zetlin

November 1998

U.S. Department of Commerce
Seattle, Washington

Library
NOAA, National Marine Fisheries Service
SWFC Honolulu Laboratory F/SWC2
2570 Dole Street
Honolulu, HI 96822-2396

NOAA
Tech
Rept
NMFS
139
c.2

Suggested reference
O'Reilly, John E., and Christine Zetlin. Seasonal, horizontal, and vertical distribution of phytoplankton chlorophyll *a* in the northeast U.S. continental shelf ecosystem. U.S. Dep. Commer., NOAA Tech. Rep. NMFS 139, 119 p.

Purchasing additional copies
Additional copies of this report are available for purchase in paper copy or microfiche from the National Technical Information Service, 5285 Port Royal Road, Springfield, VA 22161; 1-800-553-NTIS; http://www.ntis.gov.

Copyright law
Although the contents of the Technical Reports have not been copyrighted and may be reprinted entirely, reference to source is appreciated.

Proprietary products
The National Marine Fisheries Service (NMFS) does not approve, recommend, or endorse any proprietary product or proprietary material mentioned in this publication. No reference shall be made to NMFS, or to this publication furnished by NMFS, in any advertising or sales promotion which would indicate or imply that NMFS approves, recommends, or endorses any proprietary product or proprietary material mentioned herein, or which has as its purpose an intent to cause directly or indirectly the advertised product to be used or purchased because of this NMFS publication.

Contents

Introduction 2
- Description of Study Area 4
  - Gulf of Maine 4
  - Georges Bank 6
  - Middle Atlantic Bight 7

Methods 8
- Data Sources 8
- Sampling 10
- Measurement of Chlorophyll *a* 10
- Computations 11
- Contouring 11
- Standard Sampling Stations (Tiles) 12
- Statistical Subareas 12

Results and Discussion 16
- Range of Chlorophyll Concentrations 16
- Size Composition of Phytoplankton 16
- Horizontal Distribution of Chlorophyll 17
- Horizontal Distribution of Netplankton/Nanoplankton 21
- Percent Phaeopigment 23
- Recurring Patterns in Phytoplankton Biomass 25
- Cross-Shelf Chl_w Gradient 26
- Recurring Patterns in Phytoplankton Size Composition 28
- Annual Cycle of Chl_w 28
- Vertical Distribution of Chlorophyll 32
  - Middle Atlantic Bight 37
  - Georges Bank 40
  - Gulf of Maine 42
- Winter-Spring Bloom 44
- The Fate of WS-bloom 44
- Stratified Season: Subsurface Chlorophyll Maxima 46
- Seasonal Changes in Subsurface Maxima 47
- Spatial Distribution of Subsurface/Surface Ratio 47
- Fall Bloom 54

Summary 55

Acknowledgments 57

Citations 57

APPENDIX A

Figure A1. Locations of stations sampled during the 78 surveys considered in this report. 64

Figure A2. Temporal distribution of chlorophyll sampling in subareas of the Middle Atlantic Bight, Georges Bank, and Gulf of Maine, 1977-1988. 68

APPENDIX B

Figures B1-38. Chlorophyll distribution from 38 MARMAP surveys. 71-108

APPENDIX C

Table C1. Chronological listing of surveys, dates of sampling, number of vertical profiles, number of samples, number of samples taken 3 m below surface while underway, and summary by field program. 109

Table C2. Coordinates of standard MARMAP stations used in the Dirichlet tesselation to define tiles. 111

Table C3. Mean water column concentration of chlorophyll *a* and associated statistics by tile and by two-month periods. 115

Seasonal, Horizontal, and Vertical Distribution of Phytoplankton Chlorophyll *a* in the Northeast U.S. Continental Shelf Ecosystem

JOHN E. O'REILLY

Northeast Fisheries Science Center
National Marine Fisheries Service, NOAA
28 Tarzwell Drive
Narragansett, Rhode Island 02882-1199

CHRISTINE ZETLIN

Northeast Fisheries Science Center
National Marine Fisheries Service, NOAA
Bldg. 74 McGruder Road
Highlands, New Jersey 07732

ABSTRACT

The broad scale features in the horizontal, vertical, and seasonal distribution of phytoplankton chlorophyll *a* on the northeast U.S. continental shelf are described based on 57,088 measurements made during 78 oceanographic surveys from 1977 through 1988. Highest mean water column chlorophyll concentration (Chl_w) is usually observed in nearshore areas adjacent to the mouths of the estuaries in the Middle Atlantic Bight (MAB), over the shallow water on Georges Bank, and a small area sampled along the southeast edge of Nantucket Shoals. Lowest Chl_w (<0.125 $\mu g\ l^{-1}$) is usually restricted to the most seaward stations sampled along the shelf-break and the central deep waters in the Gulf of Maine. There is at least a twofold seasonal variation in phytoplankton biomass in all areas, with highest phytoplankton concentrations (m^3) and highest integrated standing stocks (m^2) occurring during the winter-spring (WS) bloom, and the lowest during summer, when vertical density stratification is maximal. In most regions, a secondary phytoplankton biomass pulse is evident during convective destratification in fall, usually in October. Fall bloom in some areas of Georges Bank approaches the magnitude of the WS-bloom, but Georges Bank and Middle Atlantic Bight fall blooms are clearly subordinate to WS-blooms.

Measurements of chlorophyll in two size-fractions of the phytoplankton, netplankton (>20 μm) and nanoplankton (<20 μm), revealed that the smaller nanoplankton are responsible for most of the phytoplankton biomass on the northeast U.S. shelf. Netplankton tend to be more abundant in nearshore areas of the MAB and shallow water on Georges Bank, where chlorophyll *a* is usually high; nanoplankton dominate deeper water at the shelf-break and deep water in the Gulf of Maine, where Chl_w is usually low. As a general rule, the percent of phytoplankton in the netplankton size-fraction increases with increasing depth below surface and decreases proceeding offshore.

There are distinct seasonal and regional patterns in the vertical distribution of chlorophyll *a* and percent netplankton, as revealed in composite vertical profiles of chlorophyll *a* constructed for 11 layers of the water column. Subsurface chlorophyll *a* maxima are ubiquitous during summer in stratified water. Chlorophyll *a* in the subsurface maximum layer is generally 2–8 times the concentration in the overlying and underlying water and approaches 50 to 75% of the levels observed in surface water during WS-bloom. The distribution of the ratio of the subsurface maximum chlorophyll *a* to surface chlorophyll *a* (SSR) during summer parallels the shelfwide pattern for stability, indexed as the difference in density (sigma-*t*) between 40 m and surface ($stability_{40}$). The weakest stability and lowest SSR's are found in shallow tidally-mixed water on Georges Bank; the greatest stability and

highest SSR's (8–12:1) are along the mid and outer MAB shelf, over the winter residual water known as the "cold band." On Georges Bank, the distribution of SSR and the stability$_{40}$ are roughly congruent with the pattern for maximum surface tidal current velocity, with values above 50 cms^{-1} defining SSR's less than 2:1 and the well-mixed area.

Physical factors (bathymetry, vertical mixing by strong tidal currents, and seasonal and regional differences in the intensity and duration of vertical stratification) appear to explain much of the variability in phytoplankton chlorophyll *a* throughout this ecosystem.

Introduction

Continental shelves are a disproportionately important part of the marine realm, occupying only 10% of the world's oceans but supporting a rich fishery where 99% of the global fish harvest is taken (Walsh, 1981). This rich fishery is nourished by high rates of phytoplankton productivity and high concentrations of phytoplankton (Raymont, 1949; Esaias et al., 1986; Nixon, 1992; Hooker et al., 1993) characteristic of shallow coastal environments having ample supply of nutrients and light for photosynthesis.

This report focuses on seasonal and spatial variations in phytoplankton biomass over the northeast U.S. continental shelf. One of the most productive shelf ecosystems in the world, it encompasses the Middle Atlantic Bight, Georges Bank, and the Gulf of Maine (Fig. 1). Annual phytoplankton production in the tidally-mixed shallow waters on Georges Bank and in the shallow nearshore waters of the Middle Atlantic Bight is three times the mean for world continental shelves (O'Reilly et al., 1987). However there are large seasonal and regional differences in primary productivity. These are mainly related to variations in phytoplankton biomass, as well as the rate of light absorption by phytoplankton, and seasonal changes in incident light and efficiency of light utilization (Campbell and O'Reilly, 1988).

There is great interest in the abundance and distribution of phytoplankton because they play a pivotal role in the trophodynamics of aquatic ecosystems (Lasker, 1978; Smith and Eppley, 1982). Most marine fish larvae feed on young stages of copepods (Hunter, 1981), and copepods feed on phytoplankton. Reports of the significance of phytoplankton to the nutrition and survival of higher trophic levels are numerous. As early as 1941, Hjort proposed a relationship between the timing of the spring phytoplankton bloom, the spawning of Norwegian spring-spawning herring, and the success of the year-class recruitment (May, 1974).

A strong association exists between landings of finfish and shellfish, annual phytoplankton primary production, and the input of nitrogen to estuarine and marine ecosystems, with the fisheries yield approaching 1% of the phytoplankton carbon production in the most productive systems (Nixon, 1988, 1992). In some areas the ratio of phytoplankton production to fish production is used to estimate size of fish stock, which in turn can be related to fish catch, to determine the percentage of the community taken through fishing (Steven, 1975). Iverson (1990) developed convincing arguments that carnivorous fish production in coastal and open ocean environments (including the Gulf of Maine) is controlled by the amount of new nitrogen entering the euphotic layer and consequent new phytoplankton production, and not by systemic differences in trophic transfer efficiency or number of steps in the food chain. On Georges Bank, a high level of fish production is, in part, traceable to the high level of primary production (Cohen and Grosslein, 1987). The phytoplankton requirements of scallop populations in the eastern half of Georges Bank could potentially be met from the flux of nitrate across the tidal front and consequent phytoplankton production (Horne et al., 1989).

There is also keen interest in the role played by phytoplankton, presumably responding to nutrients from agriculture and sewage wastes, in the eutrophication of many coastal environments worldwide (Walsh, 1981; Larsson et al., 1985; Rosenberg, 1985; Stoddard et al., 1986; Smith et al., 1987; Mahoney et al., 1990; Smayda, 1990, 1991; Hinga et al., 1991). Additionally, concerns over the buildup of atmospheric carbon dioxide and global climate change have led to renewed interest in phytoplankton as principal intermediaries in the flux of carbon from the atmosphere to the marine biosphere and sediments (Keeling et al., 1976; Broeker et al., 1979; Walsh et al., 1981; Malone et al., 1983b). For example, in the central North Pacific Ocean since 1968, there has been a doubling in phytoplankton biomass (vertically integrated chlorophyll) which is believed to be caused by climate change: increased winter winds and decreased sea surface temperature (Venrick et al., 1987).

Measurements of phytoplankton chlorophyll throughout the euphotic and upper mixed layers are essential for the calibration (Gordon et al., 1980; Smith, 1981; Gordon, 1987) and interpretation (Collins, 1989) of pigment distributions derived from satellite spectral

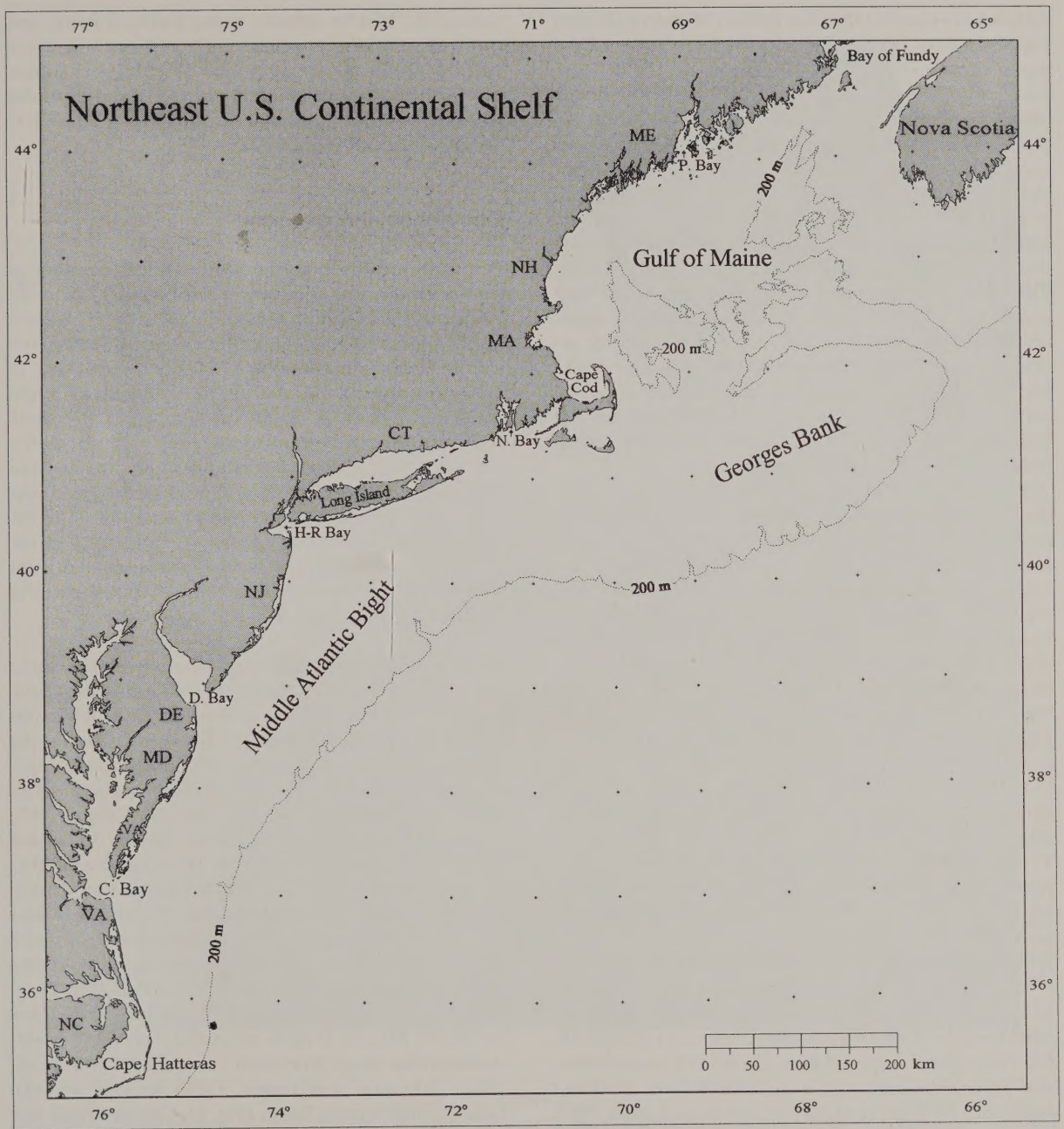

Figure 1

The northeast U.S. continental shelf and its major oceanographic regions: Gulf of Maine, Georges Bank, and Middle Atlantic Bight; major estuaries: Penobscot Bay (P. Bay), Narragansett Bay (N. Bay), Hudson-Raritan Bay (H-R. Bay), Delaware Bay (D. Bay), Chesapeake Bay (C. Bay); and coastal points of reference: Nova Scotia, Maine (ME), New Hampshire (NH), Massachusetts (MA), Cape Cod, Connecticut (CT), Long Island, New Jersey (NJ), Delaware (DE), Maryland (MD), Virginia (VA), North Carolina (NC), Cape Hatteras.

radiometers such as the Coastal Zone Color Scanner (CZCS) and the Sea-viewing Wide Field-of-view Sensor (SeaWiFS) (Hooker and Esaias, 1993). Since the launch of the CZCS in 1978, synoptic descriptions of fine scale

features (1–4 km) in the distribution of phytoplankton pigments have been generated for large areas of the ocean (Yoder et al., 1988; Hooker et al., 1993). However, radiometers such as the CZCS indirectly detect plant pigments in just the upper one-fifth of the euphotic layer (Campbell and O'Reilly, 1988). Their accuracy, using a general algorithm relating ocean color to chlorophyll, is only 0.3–0.5 log chlorophyll (Gordon et al., 1980; Balch et al., 1992) but may improve to ±40% using ship data from the study region to optimize the chlorophyll algorithm (Smith and Baker, 1982). Thus it is becoming widely recognized that direct measurements of chlorophyll and remote measurements are complementary; both are required to generate accurate assessments of phytoplankton standing stocks and phytoplankton production at a number of spatial scales for large areas of the ocean (Sathyendranath and Platt 1989; Kuring et al., 1990; Platt et al., 1991; Sathyendranath et al., 1991; Antoine et al., 1996).

Therefore, it is important to understand the abundance and distribution of phytoplankton, to delineate regional and seasonal and long-term patterns in their abundance, and to determine the oceanographic and ecological factors responsible for such distributions (e.g. Walsh et al., 1978; Marra et al., 1982; Malone et al.,1983a; Campbell and Esais, 1985; Eslinger and Iverson, 1986). Some of the major features in the horizontal and seasonal distribution of chlorophyll *a* have been described for portions of the northeast U.S. continental shelf based on relatively short studies: New York Bight (e.g. Ryther and Yentsch, 1958; Mandelli et al., 1970; Malone, 1976; Yentsch, 1977; Falkowski et al., 1983; Malone et al. 1983b; Falkowski et al., 1988); Georges Bank (e.g. Riley, 1941; Colton et al., 1968; Yentsch et al., 1994; Thomas et al.[1]); and Gulf of Maine (e.g. Bigelow, 1926; Bigelow et al., 1940; Cohen, 1976; Yentsch and Garfield, 1981). Only the New York Bight has been comprehensively described at a high level (monthly) of temporal resolution (Malone, 1976; Malone et al., 1983b).

The purpose of this report is to illustrate and characterize typical (mean) coarse-scale features in the horizontal, seasonal, and vertical distribution of phytoplankton chlorophyll *a* over the northeast U.S. continental shelf. Our characterizations are derived from an extensive series of shipboard surveys conducted from 1977 through 1988. Previous studies did not routinely survey the entire ecosystem. Our report establishes ecological baselines, defines the annual cycle of phytoplankton abundance, and identifies similarities and differences among the Middle Atlantic Bight, Georges Bank, and the Gulf of Maine. Baselines such as these may prove useful in understanding regional differences in fishery productivity (e.g. Sherman et al., 1984) and in assessments of long term ecological change (e.g. Venrick et al., 1987; Radach et al., 1990).

Description of Study Area

Our study area includes the northeast U.S. continental shelf and adjacent continental slope (Fig. 1). It spans 10 degrees latitude and longitude, from Cape Hatteras in the southwest to Nova Scotia in the northeast, and encompasses approximately 275,000 km^2. The Gulf of Maine, Georges Bank, and the Middle Atlantic Bight constitute the three major subdivisions of the shelf, based on diverse bottom topography (Fig. 2); differences in fresh water sources and inputs, water mass characteristics, circulation, and tidal mixing; and zoogeographic provinces (Sherman et al., 1988). The following brief description of the oceanography of the study area provides background and perspective for subsequent discussion of seasonal and spatial patterns in phytoplankton biomass.

Gulf of Maine—The Gulf of Maine, a semi-enclosed continental shelf sea, is bounded landward by the northeast U.S. and Nova Scotia coasts and includes waters west of longitude –66° between Georges Bank and the entrance to the Bay of Fundy (Fig. 1). Bottom depth throughout much of the Gulf of Maine is greater than 100 m, and averages 150 m (Uchupi and Austin, 1987). Three large basins (Georges Basin, 377 m; Wilkinson Basin, 295 m; and Jordan Basin, 311 m) and a number of smaller basins (Uchupi, 1965; Uchupi and Austin, 1987) are deeper than 200 m (Fig. 2). Shallow water <60 m is mostly confined to a relatively narrow band along the coast and on Stellwagen Bank, which is west of the Jordan Basin and north of Cape Cod (Fig. 2).

Seawater exchange between the Gulf of Maine and the North Atlantic is fairly restricted, occurring mostly through the deep Northeast Channel (Ramp et al., 1985; Mountain and Jessen, 1987) located between Georges and Browns Banks (Fig. 2). Georges Bank limits the flow of water such that only the upper 20 m of Gulf of Maine water can pass over it, while flow in the Great South Channel is limited to the upper 70 m (Butman and Beardsley, 1987). Waters deeper than 70 m communicate with the gulf only through the Northeast Channel, the principal entry point for slope water into the region. Freshwater enters the Gulf of Maine from rivers in Maine, the Bay of Fundy (St. Johns River), and the Scotian Shelf where the freshwater originates from the Gulf of St. Lawrence. Maine rivers, principally

[1] Thomas, J. P., H. Mustafa, A. A. Tvirbutas, C. A. McPherson, and J. B. Suomala. 1982. Seasonal patterns of surface temperature and phytoplankton pigments in the Georges Bank region. Int. Coun. Explor. Sea, Biol. Oceanogr. Comm. Doc. Council Meeting 1982/ L:14 (poster).

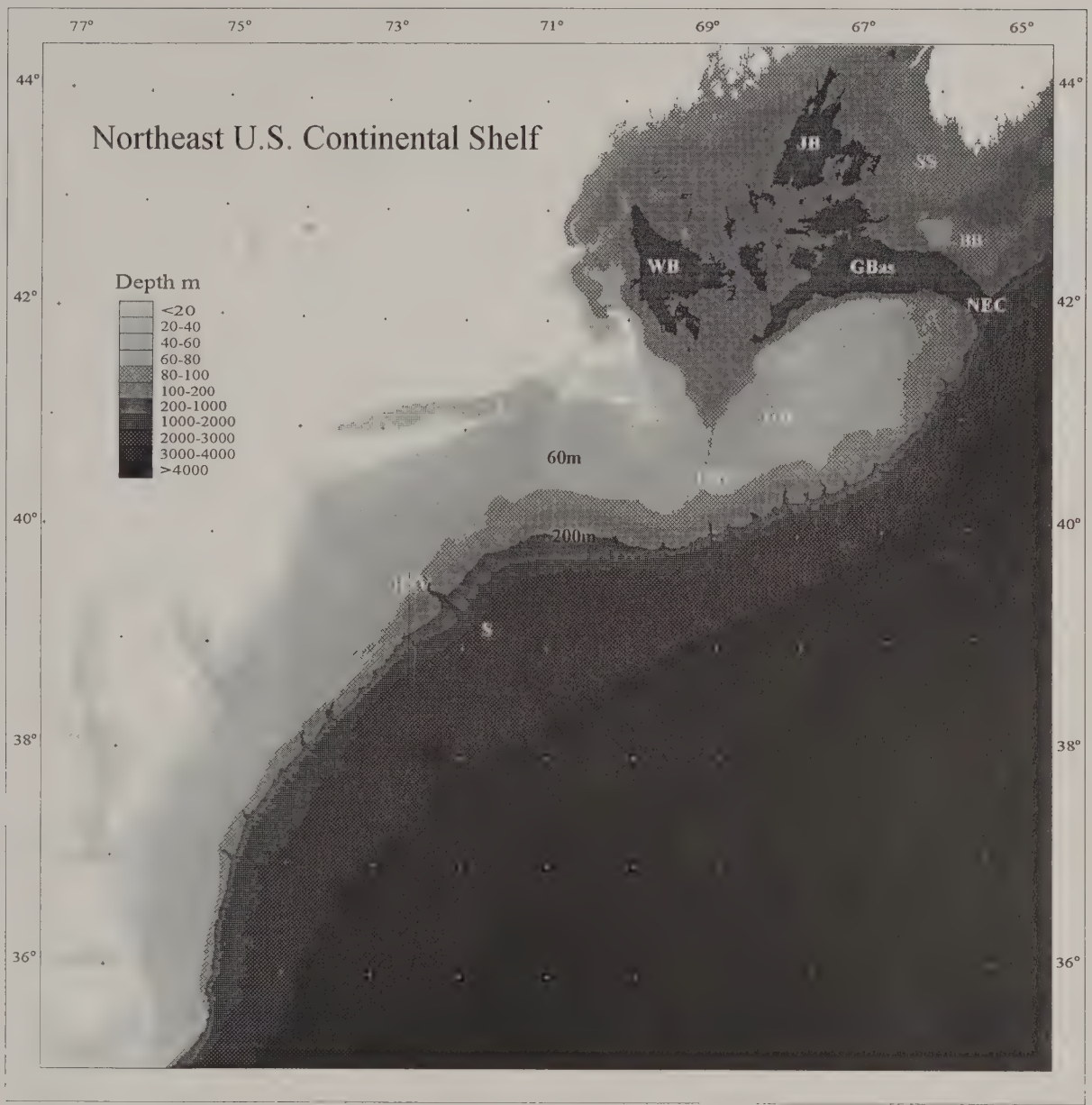

Figure 2

Major bathymetric features of the northeast U.S. continental shelf: Browns Bank (BB), Scotian Shelf (SS), Northeast Channel (NEC), Georges Basin (GBas), Wilkinson Basin (WB), Jordan Basin (JB), Georges Bank (GB), Great South Channel (GSC), Nantucket Shoals (NS), Hudson Shelf Valley (HSV), Continental Slope (S).

the Androskogen, Penobscott, Merrimak, and Kennebeck, flow into the gulf and, during spring, form a plume of relatively brackish stratified waters in the western gulf (Franks and Anderson, 1992a, 1992b). Most of the land drainage (~90%) occurs north of Cape Elizabeth (TRIGOM, 1974) and, in response to snow melt, maximum river runoff occurs in the south earlier than in the north. In the northern Gulf of Maine, a cold buoyant coastal current (Townsend et al., 1987) may extend from the Bay of Fundy to Penobscott Bay where it may split into a nearshore and offshore limb (Bisagni et al., 1996b). Local rivers have a significant contribu-

tion to the upper 40 m of the water column (Brown and Irish, 1993). Along with the outflow of the Bay of Fundy and the east-to-west flow of slope water, they maintain the gulf's counterclockwise circulation, which seems strongest in spring (Sherman et. al., 1988). The most significant input of fresh water to the gulf comes from the Scotian Shelf. Based on the total volume of water in the Gulf of Maine, most of the fresh-water input derives from cold, low-salinity Scotian Shelf water (Hopkins and Garfield, 1979) that enters through the Northeast Channel and through passages formed between Cape Sable and Browns Bank (Brown and Irish, 1993).

Upwelling is common along the coastal areas in the western Gulf of Maine, off Nova Scotia, and on the Scotian Shelf (Garrett and Loucks, 1976). In comparison with deep waters of the central basin, northwestern coastal waters are turbid with reduced transparency due to river runoff (TRIGOM, 1974). During warmer months, stratification occurs where bottom depth exceeds 20 m. At shallower depths, tidal mixing and coastal currents prevent stratification (TRIGOM, 1974). Waters along the Scotian Shelf, at the mouth of the Bay of Fundy, and nearshore, north of Penobscott Bay, are only weakly stratified during summer as a consequence of strong tidal currents (Moody et al., 1984).

Based on hydrographic features, Gulf of Maine waters are divided vertically into three layers: Maine surface water (MSW), water less than 50 m; Maine intermediate water (MIW), water between 50–100 m; and Maine bottom water (MBW), water greater than 100 m (Hopkins and Garfield, 1979). During summer, the temperature minimum is found in MIW that is isolated from the warmer layers above and below. During spring the relatively fresh MSW is warmed through solar heating. Maine bottom water is warmer because it is derived from warmer and saltier continental slope water that enters the Northeast Channel. During this time the isolation of this water is similar to the isolation of Georges Bank-Middle Atlantic Bight cold band water described below. During winter months the water column is mixed to about 100 m and only two layers are present.

Georges Bank—Georges Bank is generally delineated by the 200 m isobath except in the west and northwest (Fig. 2). Along the northern flank, sharp bathymetric gradients between Georges Basin and Georges Bank define the bank. Here water shoals quickly from 200 m to 60 m within a relatively short distance (< 30 km). The eastern and southern extent, where shoaling from the 200 m isobath is more gradual, is defined by the Northeast Channel and the shelf-break, respectively (Fig. 2). Georges Bank is defined in the west by the western edge of the Great South Channel, which separates Georges Bank from Nantucket Shoals, and in the northwest by the 100 m isobath (Fig. 2). The shallowest waters—Georges, Cultivator, and some unnamed shoals—are found on the northwestern part of the bank within the 60 m isobath, where shifting medium-to-coarse sand ridges cover most of the bottom and contribute to the turbulence (Uchupi and Austin, 1987) and turbidity of overlying waters (Butman, 1987; Twichell et. al., 1987). Diurnal and semidiurnal tides interacting with the shallow bottom topography of the bank generate exceptionally strong currents (Butman and Beardsley, 1987) that maintain a vertically well-mixed water column within the 60 m isobath throughout the year (Yentsch and Garfield, 1981; Bisagni and Sano, 1993). The maximum tidal current speed near surface on the bank increases gradually from 10–20 cm s^{-1} at the 200 m isobath along the southern flank, to 60–70 cm s^{-1} over the shallow area (Fig. 3). Maximum tidal current speeds decrease sharply from the northern edge of the bank into Georges Basin.

During spring and summer, a clockwise recirculation pattern sets up around the shallow water on the bank (Limeburner and Beardsley, 1996). This recirculation prolongs mean residence time (~60 days) of shallow water (Colton and Anderson, 1983) and limits exchange with surrounding waters. During winter, recirculation is minimal, prevailing northwest winds drive surface water offshore (Bumpus, 1976), and generally more exchange occurs between the shallow Georges Bank water and Gulf of Maine and Scotian Shelf water (Flagg, 1987). In the deeper areas of the bank, the water column is vertically mixed during winter but thermally stratified during summer, and subject to variations from advection of slope water onto the bank (Bisagni and Sano, 1993). During summer, a tidally-induced front, found around the 60 m isobath and often extending across the Great South Channel toward Nantucket Shoals, separates the vertically-mixed shallow water from deeper stratified water on the bank (Butman and Beardsley, 1987).

The mean flow of water beyond the 60 m isobath is to the southwest, and is strongest in late summer and weakest in winter (Butman and Beardsley, 1987). Physical properties of deeper Georges Bank waters are influenced by the advection of slope water onto the bank (Bisagni and Sano, 1993) and by entrainment of bank water by warm core rings passing along the southern flank (Bisagni, 1983; Evans et al., 1985). During spring, cold, low salinity water from the Scotian Shelf may move onto the southern flank of Georges Bank (Bisagni et al., 1996a). From spring through fall turnover, cold, winter-residual water, known as the "cold band" or "cold pool," occurs beneath the seasonal thermocline, within the 60–100 m isobaths from the Northeast Peak of Georges Bank south to near Cape Hatteras (Butman and Beardsley, 1987; Flagg, 1987). The axis of the cold band is along the 80 m isobath on Georges Bank (Flagg, 1987), the 65 m isobath off Long Island, and the 55–60 m isobath in the Middle Atlantic Bight offshore of

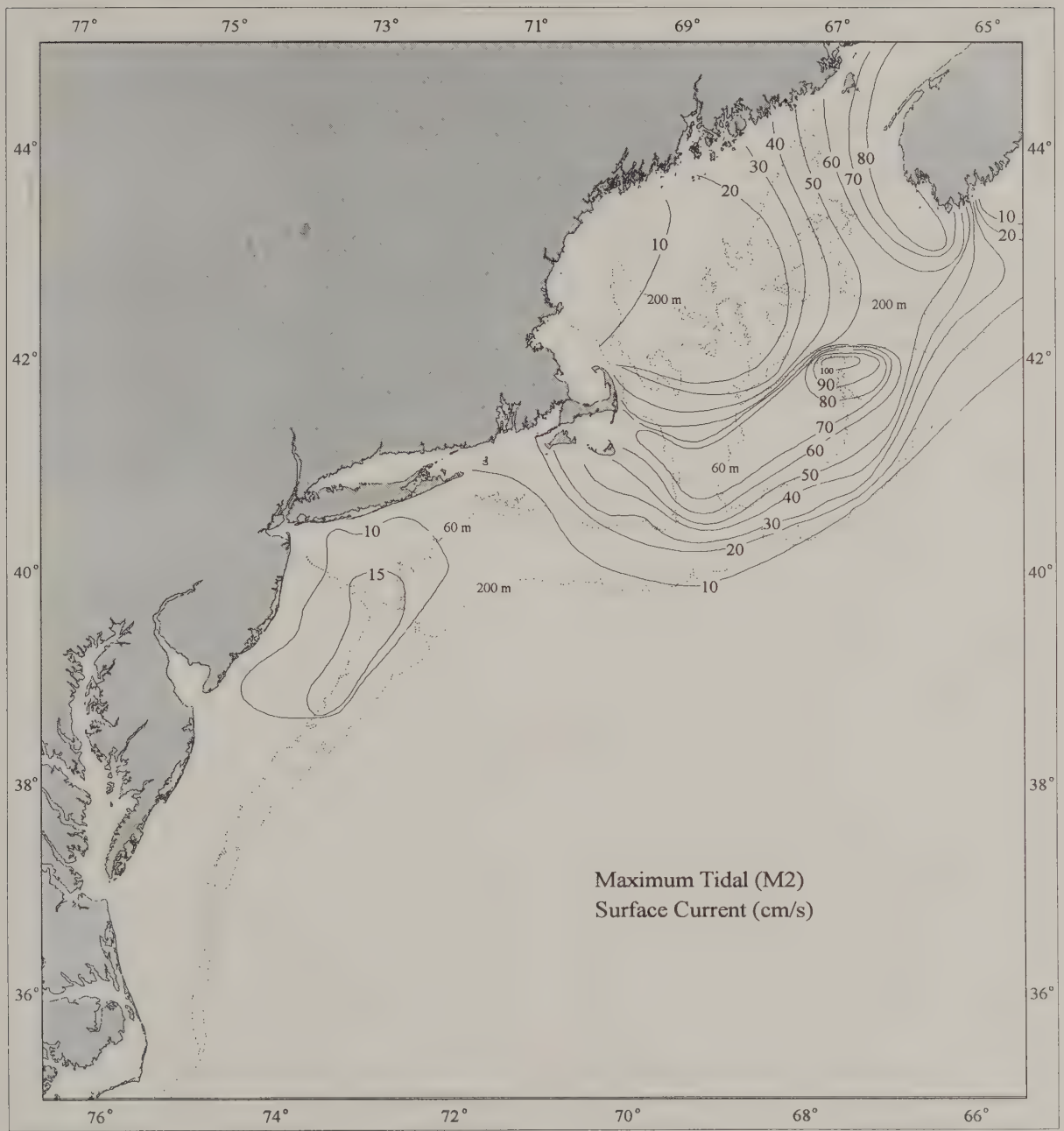

Figure 3
Maximum tidal current velocity (M2 current, cm/s) of surface water. Redrawn from Moody et al. (1984).

Chesapeake Bay (Ketchum and Corwin, 1964; Colton et al., 1968; Houghton et al., 1982; Flagg, 1987).

Middle Atlantic Bight—The Middle Atlantic Bight includes the shelf area between Cape Hatteras and the Great South Channel. The shelf in the Middle Atlantic Bight slopes gently offshore and is shallow compared with the Gulf of Maine and Georges Bank; much of the bight from Long Island south is less than 60 m deep (Fig. 2).

A retrograde shelf-slope front, delineated by the 34.5 salinity isohaline (Wright, 1976; Mooers et al., 1979), is located along the shelf-break in the Middle Atlantic Bight and on Georges Bank. It is generally centered near the 200 m isobath, however since it is angled and not vertical the location of the surface and bottom of the front is not the same. The bottom of the front is anchored closely to the 80–100 m isobath year round, but the front in surface water undergoes seasonal onshore-offshore excursions, reaching its maximum seaward extension during June–August when it is approximately 100 km seaward of the shelf-break, over the ~2000 m isobath.

Waters in the Middle Atlantic Bight are well mixed during winter and strongly stratified during summer with the exception of shallow coastal areas which experience episodes of vertical mixing from storms, upwelling, and downwelling (Ingham and Eberwine, 1984). Nearshore waters are more turbid than offshore because of their shallowness, resuspension of sediment, and from estuarine outflow they receive. Fresh water enters the Middle Atlantic Bight at the mouth of the Hudson-Raritan, Delaware, and Chesapeake bays. These local sources are responsible for approximately 70% of the large interannual variation in salinity in the bight (Manning, 1991). Runoff peaks in spring, when about half the annual runoff occurs (Bigelow and Sears, 1935). While the inflow of freshwater is predictable, removal of shelf water is not. Shelf water predictably travels from Georges Bank in a southwesterly direction with some loss at Cape Hatteras; however, loss of shelf water can also occur erratically around the shelf-break. Though the shelf-slope front is coherent from Georges Bank to the Cape Hatteras; warm core rings drifting southwest between the northern edge of the Gulf Stream current and the continental shelf-break, and intrusions of Gulf Stream water along the southern portion of the Middle Atlantic Bight, may entrain and displace significant amounts of shelf water (Churchill and Cornillon, 1991).

The cold band is present throughout the summer in the Middle Atlantic Bight and disappears during fall overturn. The inshore edge of the cold band is at shallower depths in the Middle Atlantic Bight (30–40 m) than on Georges Bank (70–80 m). Presumably this is a consequence of the relatively greater surface and bottom tidal current mixing (at comparable depths) along the southern flank of Georges Bank, relative to the outer Middle Atlantic Bight (Moody et al., 1984). In the New York Bight the cold band is typically 6°C during the early summer and warms to about 10–12°C just before convective overturn in fall. The coldest part of the cold band is usually between the 40 and 80 m isobaths (Ketchum and Corwin, 1964), whereas on the southern flank of Georges Bank, it is centered along the 80 m isobath and spans between the 65 and 95 m depths. In the Middle Atlantic Bight the greatest thermal contrast appears during June, when the cold band is 6–7°C and surface water temperature is 22°C (Benway et al., 1993). At that time the inshore edge of the cold band is 80 km offshore, at about the 40 m isobath. During fall overturn, when the water column becomes nearly vertically isothermal, the winter residual water disappears first in the shallow nearshore area (early September) and last in the outer shelf area in early December (Benway et al., 1993). The annual maximum bottom water temperature (16°C nearshore, 13°C offshore to the shelf-slope front) occurs during the fall overturn (Benway et al., 1993). In nearshore waters off the Raritan Estuary the annual minimum surface water salinity occurs during March–April, with a secondary minimum in August (Benway et al., 1993). Along the outer Middle Atlantic Bight the minimum appears during July–August (31.5–32‰), when temperature is at its annual maximum across the shelf (22–24°C; Benway et al., 1993), reinforcing density stratification.

Methods

Data Sources

Data presented in this monograph were collected during several multidisciplinary field programs conducted by the National Oceanographic and Atmospheric Administration, Northeast Fisheries Science Center, between 1977 and 1987 (Append. Table C1). Major field programs included the Marine Resources Monitoring, Assessment, and Prediction Program (MARMAP) described by Sherman (1980); the Northeast Monitoring Program (NEMP) described by Pearce (1981); and the Warm Core Ring (WCR) Program (Evans et al., 1985). The objectives and sampling areas of these programs differed but phytoplankton chlorophyll sampling and measurement protocols were consistent.

During MARMAP surveys, vertical profiles of temperature, salinity, chlorophyll, and primary productivity were routinely measured from hydrocasts and by using expendable bathythermographs (XBT's) (temperature). Mountain and Holzwarth (1989) and Mountain and Manning (1994) summarized hydrographic data from MARMAP surveys. Major plant nutrients were also measured on some surveys (Draxler et al., 1985; Sibunka and Silverman, 1989). Double oblique net tows were made to 200 m to determine the abundance and species composition of zooplankton and ichthyoplankton (Morse et al., 1987; Sherman, 1988; Sibunka and Silverman, 1989). MARMAP surveys occupied up to 193 standard sites (Fig. 4). Usually surveys progressed from south to north and lasted four weeks. Stations

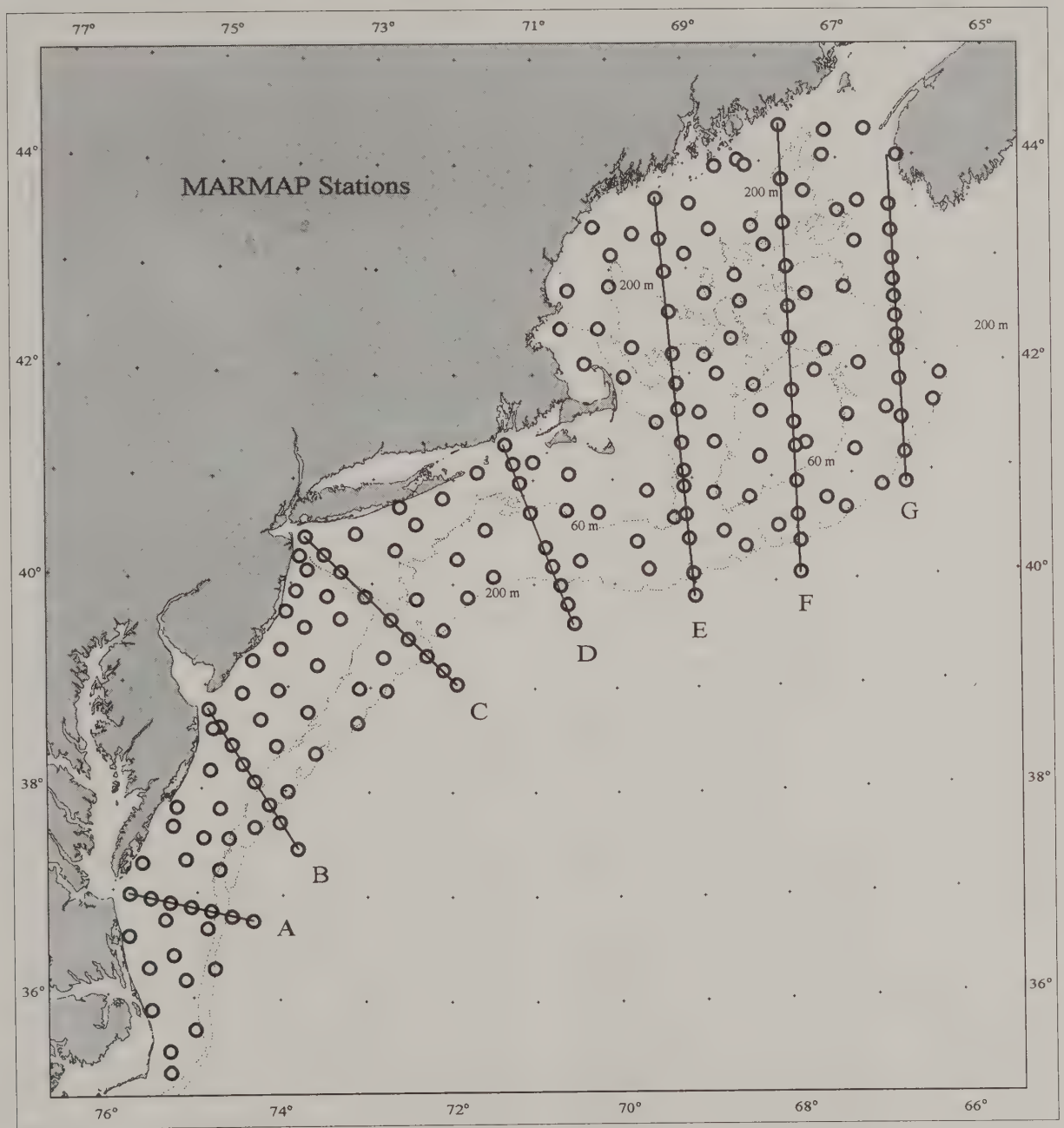

Figure 4

Locations of Standard 193 MARMAP sampling sites, onshore-offshore transects (A, B, C, D, E, F, G), and the 60 m and 200 m isobaths (only the 200 m isobath is shown north of Cape Cod).

along transects A, B, C, D; those portions of transects E, F, and G on Georges Bank; and transects E, F, and G in the Gulf of Maine, were usually sampled sequentially to obtain synoptic data (Fig. 4).

NEMP surveys involved collection of water samples from hydrocasts, demersal fish using trawls, and benthic invertebrate community and sediment contaminants using grab samplers. Surveys took two weeks to com-

plete. The stations were sparsely distributed throughout the study area since the objective of the program was to sample key sites that represented the range of conditions in the ecosystem. The distribution of stations during a typical NEMP survey is illustrated in Append. Fig. A1 (survey AL8009). There was some overlap between NEMP and MARMAP sites.

Warm core ring surveys were conducted in deeper water near and beyond the shelf and focused on the entrainment of filaments of shelf water and associated biota (Colton and Anderson, 1983). Both underway and hydrocast sampling were conducted (Append. Table C1). Surveys labeled "Other" (Append. Table C1) had various objectives, areas of interest, and sampling intensities (e.g. Append. Fig. A1: AD7701, EV8002).

Of the 78 oceanographic surveys considered in this analysis, only a few covered the entire study area (Append. Fig. A1). The combined data set consists of 61,533 discrete measurements of phytoplankton chlorophyll (Append. Table C1). The majority of chlorophyll measurements were made during MARMAP surveys (Append. Table C1, bottom). Most of the measurements were taken from 6,686 hydrocast profiles of the upper 100 m of the water column. Some of the surveys obtained samples inside the mouths of estuaries and seaward of the continental slope; those samples are not considered here (Append. Fig. A1). The focus of this report is on the 57,088 samples from the upper ~100 m of the water column on the continental shelf and adjacent slope.

Sampling

Generally, water samples were collected using 5-l opaque PVC Niskin bottles suspended within the water column from a hydrowire at standard depths, i.e. 1, 5, 10, 15, 20, 25, 30, 35, 50, and 75 m below sea surface. Prior to being sequentially tripped, Niskin bottles were equilibrated (flushed) with water at the desired depth for at least five minutes. At stations where bottom depth was less than 75 m, an additional sample was collected within ~2–3 m of bottom. Beginning in October 1979, a bottom-trip bottle (rigged to close when a tripping device contacted the seabed) collected near-bottom water within 1 m of the seabed. After spring 1980, the sampling protocol included samples from 100 m and from within 1 m of bottom, when bottom depths were approximately 100 m or less. Additional nonstandard depths were sampled to coincide with depths sampled for measurements of simulated in situ primary production (O'Reilly and Thomas, 1983; O'Reilly et al., 1987).

On all surveys, samples were collected from the hydrocast except DL8510, DL8601, DL8603, DL8607, Dl8610, Dl8701, and DL8704 (Append. Fig. A1) during which water for chlorophyll analyses was obtained only from the vessel's saltwater intake (~3 m) while the ship was underway. During warm core ring surveys, samples were collected from hydrocasts and the vessel's saltwater intake (Append. Table C1).

Measurement of Chlorophyll *a*

The concentration of chlorophyll *a*, the dominant photosynthetic pigment in phytoplankton, is widely used by biological oceanographers as a proxy for phytoplankton carbon biomass. However, the relationship between chlorophyll *a* and phytoplankton biomass is not constant, but varies widely in space and time with the species composition and physiological state of the phytoplankton (Banse, 1977; Cullen, 1982). Because it is operationally difficult to distinguish routinely organic carbon in autotrophic phytoplankton from that in microheterotrophs and detritus, measurements of chlorophyll *a* remain the best chemical index of the biomass of natural assemblages of autotrophic phytoplankton (Cullen, 1982). In this report, the expressions "phytoplankton biomass," or "biomass," are used frequently as shorthand notation for "the concentration of chlorophyll *a* in a liter of seawater," but the distinction should be remembered.

Immediately following retrieval of Niskin bottles, subsamples were drawn through silicon tubing into opaque 1-l polyethylene bottles. During subsampling, zooplankton >300 µm were removed by an in-line, 1-in diameter, 300 µm mesh nylon filter. Water samples were size-fractionated immediately after collection by serial filtration, using 25-mm diameter Nitex Nylon filters (20 µm mesh) in the upper stage and 25-mm diameter Whatman GF/F glass fiber filters (~0.7 µm mesh) in the lower stage of a filtration manifold, which allowed up to 10 samples to be processed simultaneously. Vacuum pressure on the lower filter stage was regulated by a manostat and did not exceed 55 mm Hg. Usually from 200 to 900 ml of seawater were filtered, the amount chosen to avoid filter clogging and yet achieve a fluorescence measurement significantly above blanks and within the accurate range of a Turner Designs fluorometer.

Phytoplankton retained on the upper 20 µm mesh are defined operationally as netplankton, while phytoplankton passing the 20 µm and retained on ~0.7 µm GF/F filters are defined as nanoplankton. This size-fractionation scheme follows that established by Malone (1976).

Phytoplankton chlorophyll *a* concentration was determined following the methods of Yentsch and Menzel (1963) and Holm-Hansen et al. (1965) where the in vitro fluorescence of pigments extracted into 90% ac-

etone is measured. Through August 1985, pigments were extracted by grinding filters and retained particulate matter in a glass grinding vessel (Arthur H. Thomas) with a teflon-tip rod driven by an electric hand drill at ~500 rpm for <1 minute. Prior to grinding, samples were covered with 3–4 ml 90% acetone and chilled in a refrigerator. A Whatman GFF glass fiber filter was added to the Nitex nylon filter to facilitate grinding. Following grinding, additional 90% acetone was added to the vessel to obtain 10 ml. Samples were mixed and allowed to extract in dark for 5 minutes, then this was repeated. Extracts, while in the grinding vessels, were centrifuged at 4000 r/min for 2 minutes, and a 5–6 ml aliquot was decanted into a fluorometer cuvette (13 × 100 mm).

Due to loss of equipment in a fire, after September 1985 the extraction procedure was modified. Following Parsons et al. (1984), pigments were extracted by submerging filters and phytoplankton in 90% acetone and refrigerating for 12–24 hours. Following extraction, samples were mixed and particulates allowed to settle through centrifugation or gravity. The supernatant liquid was decanted into a fluorometer cuvette.

Following extraction, sample fluorescence was measured using a Turner Designs fluorometer equipped with a 10–045 blue lamp, a red-sensitive photomultiplier tube, and Corning filters 10–050, 10–051, and 10–052 for excitation, emission, and reference light paths, respectively. Fluorescence of the extract was measured before and after the addition of two drops of 5% HCl to the cuvette to determine corrected chlorophyll *a* concentration as well as phaeophytin *a* concentration (Holm-Hansen and Riemann, 1978).

Fluorometers were calibrated immediately before and after each survey using a 90% acetone solution of pure chlorophyll *a* (Sigma Chemical Company). The fluorescence of individual (not serial) dilutions (1, 0.1, 0.04, 0.02, 0.01, 0.002, and 0.001) of this calibration solution (approx. 1 mg/l) were measured to check linearity of the fluorometer over the working range of the instrument. Additionally, the fluorescence of aliquots of the calibration solution (kept in dark in a freezer) was recorded approximately each night at sea to detect any drift or change in the calibration during the survey.

The concentration of chlorophyll *a* in the calibration solution was determined using the method outlined by Holm-Hansen and Riemann (1978). The absorption of the pure chlorophyll *a* stock solution at 480, 630, 645, 663, 665, and 750 nm, before and after acidification (2 drops of 5% HCl per 10 ml aliquot), was determined using a dual-beam Perkin-Elmer #550 spectrophotometer and a 5 cm cuvette. A specific absorption coefficient of 89.31 l/g cm for chlorophyll *a* (UNESCO, 1966) was applied. The accuracy of the calibration was routinely checked against the chlorophyll *a* calibration standard obtained from U.S. EPA, Quality Assurance Branch, Cincinnati, Ohio. The coefficient of variation (standard error × 100/average) among 10 replicate size-fractionated seawater subsamples is usually 6–7% at 1 µg chlorophyll/l. Evans et al. (1987) describes additional details of our method.

Computations

Chlorophyll *a* concentrations measured in the netplankton and nanoplankton size-fractions are added to generate an estimate of total chlorophyll *a* concentration at each sampling depth. Standing stocks of water column chlorophyll *a* (µg m^{-2}) in the upper 75 m (or bottom depth if < 75 m) is computed by arithmetically integrating values over depth using the trapezoidal rule. In the integration, the measured value at 1 m below surface is used as the estimate for 0 m. In water deeper than 75 m, when sampling did not exactly coincide with 75 m, the chlorophyll *a* concentration at 75 m was estimated by linear interpolation, using measurements from the two adjacent sampling depths. Water column concentration of chlorophyll *a* (µg l^{-1}), abbreviated as Chl_w, is computed by dividing the water column integral (µg chlorophyll *a* m^{-2}) by the depth of integration (m). The percent netplankton in the water column is calculated as 100 times water column netplankton chlorophyll *a*, divided by water column total chlorophyll *a*. Similarly, percent phaeopigment in the water column is calculated as 100 times phaeophytin *a*, divided by (phaeophytin *a* + chlorophyll *a*). Venrick (1978) provides an indication of the statistical precision of estimated Chl_w based on the systematic sampling used during our study.

Contouring

Contoured distributions of chlorophyll *a* were generated using Surface III (Sampson, 1988). Latitude and longitude coordinates of each station were transformed into map coordinates using Lambert's conic conformal map projection (Uchupi, 1965; Snyder, 1987). The grid resolution used for contoured horizontal distribution maps is 10.2 km/grid. That used for cross sections is 2 km and 2 m per grid. Grid values were estimated from a distance-weighted average ($1/d^2$) of the nearest eight data values. Prior to generating contoured cross sections, original data were linearly interpolated, first vertically (1 m), then horizontally (1 km) between transect stations. This provided the "control points" (Sampson, 1988) necessary to avoid artifacts in the contouring of vertically clustered transect data.

The sampling density and coverage of the continental shelf during MARMAP surveys permitted contouring. The distance between stations along the seven MARMAP cross-shelf transects is approximately 25 km (Fig. 4). Stations on these transects were usually sampled sequentially over a 24–48 hr period. This spatial resolution and synopticity permitted the construction of cross section portrayals. Inter-station distances during NEMP surveys were judged too large to generate representative contours. Contoured distributions of chlorophyll from WCR surveys are also not portrayed here since the focus of WCR surveys was the outer shelf-slope region under the influence of several specific warm core rings.

Contoured distributional maps of mean water column chlorophyll concentration (chl_w) and contoured cross-shelf sections of chlorophyll *a* are presented for 38 MARMAP surveys in Append. B. Contoured maps of data, composited and averaged by tile, used the standard station location coordinate to represent data (see below).

Standard Sampling Stations (Tiles)

To unify data from several field programs, each with different spatial sampling patterns, all data were assigned to standard locations. This enabled the construction of composite horizontal, vertical, and temporal portrayals. The coordinates of the 193 MARMAP stations (Fig. 4, Append. Table C2) were used to define the standard locations since these sites were repeatedly sampled during MARMAP surveys, where most of the chlorophyll observations were measured (Append. Table C1). Dirichlet cells (Ripley, 1981) or tiles (Green and Sibson, 1978) were constructed around each standard location (Fig. 5). The northeast U.S. continental shelf was thus subdivided into 193 areas or tiles such that all samples within a tile were closer to the standard coordinate used to generate the polygon tile than to any other standard coordinate. Additional artificial sites were employed to constrain the offshore extent of tiles along the outer continental shelf-break (Fig. 5). The median distance between standard MARMAP coordinates defining the 193 tiles is 42 km (Fig. 6). Using this partitioning scheme, 84% of the 6,344 stations occupied in the study area were within 10 km of the standard site, and 96% were within 20 km (Fig. 7).

The resulting temporal sampling intensity for each tile, grouped by subarea and region, is depicted in Append. Fig. A2. Sampling intensity was highest in 1978 through 1980. Tiles surrounding stations at the offshore terminus of MARMAP transects (18, 36, 63, 84, 116, 152) were sampled infrequently as were tiles along the eastern edge of Georges Bank (180, 191, 192). Similarly, northern and eastern areas of the Gulf of Maine (tiles 168, 169, 171, 172, 173, 181, 189, 190) were sampled infrequently because many of the surveys abbreviated by inclement weather began off Cape Hatteras and proceeded northward.

Statistical Subareas

Data were grouped into subareas to construct generalized monthly representations of chlorophyll over broad but relatively homogeneous areas of the shelf. Clustering techniques (Fastclus, SAS Inst., 1990) were employed as an exploratory tool to aid the definition of subareas. Two expressions of the chlorophyll data were used in separate clustering analyses: two-month mean water column chlorophyll and percent netplankton, averaged by tile; and chlorophyll concentration averaged by tile (193), depth strata (11), and month (12). The first expression emphasizes areas having similar annual cycles in the magnitude and size composition of Chl_w, while the second expression groups tiles with similar annual cycles in the magnitude and shape of the vertical profile of chlorophyll *a*. We also examined monthly composite profiles constructed for each of the 193 tiles. These provided a number of features useful in identifying tiles which were similar and therefore could be grouped into subareas: the magnitude of chlorophyll, the occurrence and timing of a distinct winter-spring bloom and fall bloom, the shapes of the vertical profiles of chlorophyll concentration and percent netplankton throughout the annual cycle, and the presence/absence of a distinct subsurface chlorophyll maximum layer during the summer (indicative of physical and biological vertical stratification). Thus, these composite profiles, recurring patterns in contoured distributions of Chl_w from surveys, and results from clustering explorations were considered in the development of subareas shown in Fig. 8. An analysis of variance of mean water column chlorophyll *a* concentration indicates the efficacy of our partitioning scheme, with highly significant differences among subareas as well as signifi-

Table 1
Two-way analysis of variance in Chl_w among subareas and months.

Source	Degrees of freedom	Mean square	Frequency	Probability
Subareas	25	184.9	123.5	<0.0001
Months	11	54.7	36.5	<0.0001
Interaction	275	10.6	7.1	<0.0001
Residual	6,252	1.5		

Figure 5

Tiles (polygons) surrounding each of the 193 MARMAP station coordinates. Tile numbers are centered on MARMAP station coordinates except for tiles 184, 140, and 148, which were adjusted to enhance legibility.

cant variability among months and interaction effects between subareas and months (Table 1).

Our partitioning of Georges Bank approximates the physical regimes defined by Butman and Beardsley (1987) and Flagg (1987), which are based primarily on tidal current velocity, water properties, locations of hydrographic fronts, bottom topography, and bottom type. The partitioning between Georges Bank and Gulf of

Maine, along the northern flank, corresponds with the 100 m isobath and follows the Chl_w patterns as well as the relatively restricted cross-bank transport during summer (Perry et al., 1993).

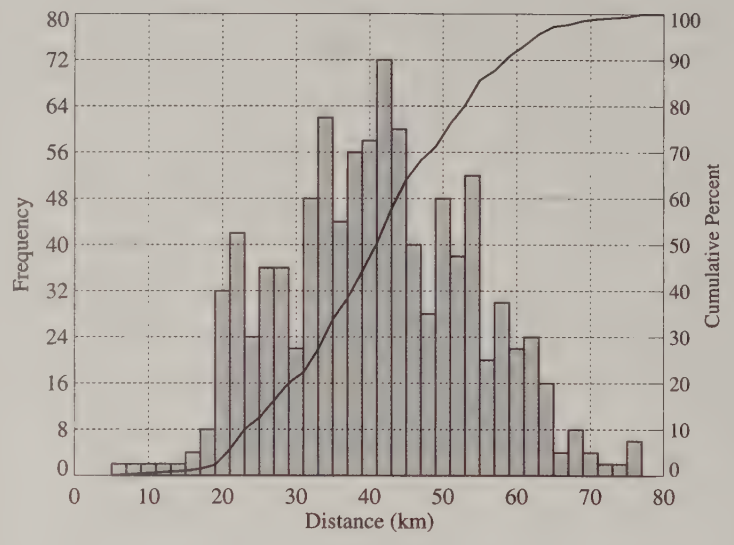

Figure 6
The frequency and cumulative percent distribution of average distance between each MARMAP standard station and its neighboring stations.

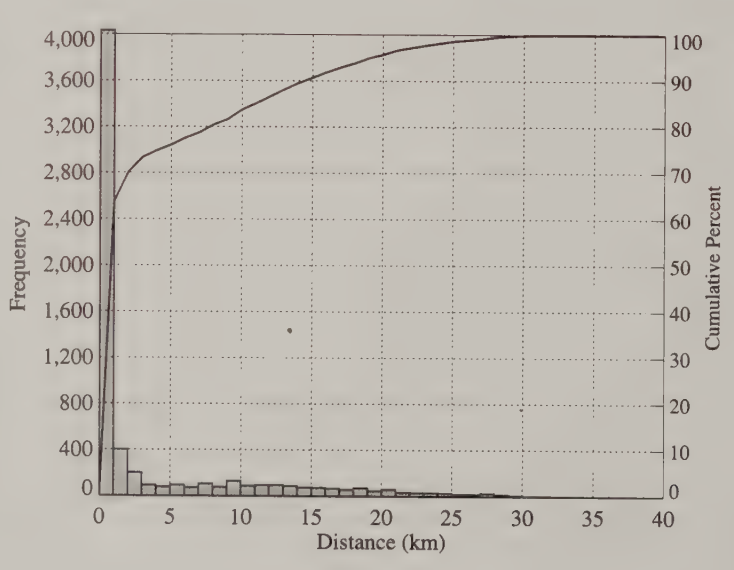

Figure 7
The frequency and cumulative percent distribution of distance between sampling coordinates and MARMAP standard station coordinates for all 193 tiles.

In the Gulf of Maine, as will be discussed later, recurring Chl_w distribution patterns are not as obvious as in the Middle Atlantic Bight and Georges Bank, partly because sampling in the gulf was sparser than in other areas. Nevertheless, the west-east distinction between the Scotian Shelf, Georges Basin, Wilkinson Basin, and the coastal water in the western Gulf of Maine is similar to the partitioning based on cluster analysis of standardized anomalies of sea surface temperature and salinity data collected along a transect-swath between Massachusetts Bay and the southern tip of Nova Scotia (Benway et al., 1993).

Subareas in the Middle Atlantic Bight are bathymetrically defined into nearshore (<30 m), midshelf (30–60 m), outer shelf (60–100 m), and shelf-break (>100 m). The nearshore region is influenced by brackish, nutrient-enriched plumes from the Hudson-Raritan, Delaware, and Chesapeake bays. These plumes tend to hug the coasts south of the estuarine mouths (Bowman and Wunderlich, 1976; Fedosh and Munday, 1982). During summer, the nearshore is also subject to episodes of wind-forced destratification, upwelling, and downwelling (Ingham and Eberwine, 1984). The nearshore region is separated into several subareas: one adjacent to each of the three estuaries and others that include remaining nearshore tiles which are not as obviously influenced by estuarine plumes. Analyses of chlorophyll data (chl_w) variances in the New York Bight by Malone et al. (1983b) indicated statistically insignificant variation among stations within bathymetric regions relative to the high variability among regions and monthly variability within a region. Our depth-based subareas differ somewhat from those used by Malone et al., (1983b) (<= 40 m, 41–80 m, 81–1000 m). We partition the shelf into four subareas, nearshore (<=30 m),

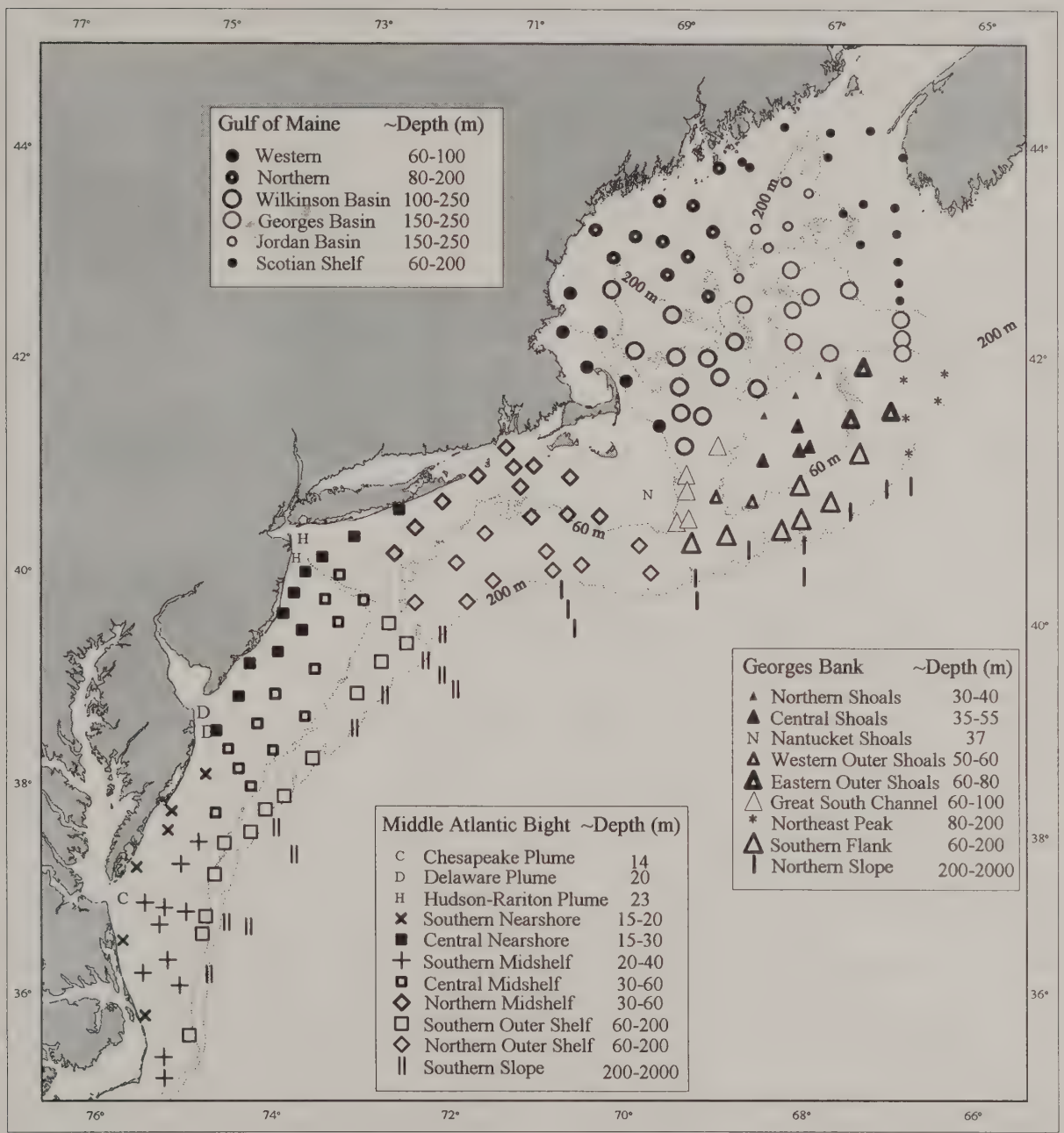

Figure 8

Subareas in the Gulf of Maine, Georges Bank, and Middle Atlantic Bight. Symbols indicate locations of standard MARMAP stations used to define tiles.

midshelf (>30<= 60 m), outer shelf (60–200 m), and slope adjacent to Middle Atlantic Bight and Georges Bank (>200<2,000 m) to accommodate the distribution of standard sampling stations during MARMAP surveys.

The shelf-break subarea includes waters seaward of the 100 m isobath, on Georges Bank and in the Middle Atlantic Bight. This is a region of transition between continental shelf and continental slope waters (Colton

et al., 1985). Along the shelf-break, a coherent shelf water-slope front is present throughout the year (Butman and Beardsley, 1987). Its mean position varies seasonally, moving seaward during summer and landward during winter (Wright, 1976; Flagg, 1987; Benway et al., 1993). During summer, in the lower water column, a cold band (winter residual water) extends offshore to ~95 m along the southern flank of Georges Bank (Flagg, 1987) and to ~100 m in the Middle Atlantic Bight (Bowman and Wunderlich, 1977). This cold band serves to further delineate the outer shelf from the shelf-break region. Near surface, the shelf-slope front, defined by the 34.5 ps isohal, is found landward of the 100 m isobath only a small fraction of the time (Flagg, 1987; Benway et al., 1993). Therefore, the shelf-break region includes shelf water the majority of the time but is likely to be overrun by surface slope water from October through March.

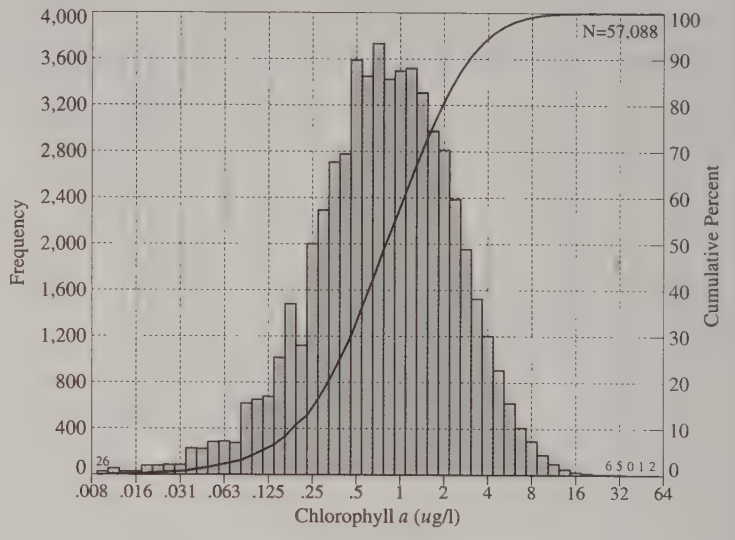

Figure 9
Frequency and cumulative percent distributions of chlorophyll concentration measured during 78 surveys of the northeast U.S. continental shelf (57,088 discrete samples).

It should be kept in mind that no single partitioning scheme will be the best fit throughout all seasons, given the diversity and complexity in the distribution of water masses, circulation, degree of mixing by tides and winds, and stratification by seasonal heating and brackish plumes from estuaries. Nevertheless, the partitioning scheme employed here does embody the major coarse-scale differences among regions of the shelf.

Results and Discussion

Range of Chlorophyll Concentrations

The frequency distribution of phytoplankton chlorophyll *a* in 57,088 water samples collected throughout the study area from 1977–1988 is depicted in Fig. 9. Data were $\log_2$-transformed prior to generating the frequency histogram to normalize the wide distribution (<.01 and 57.8 $\mu g\ l^{-1}$) encompassed by all samples, from varying regions, depths, and seasons. The resulting distribution is still platykurtic and skewed toward lower values. A broad mode, centered at ~ 1 $\mu g\ l^{-1}$, is evident. The median value is 0.87 µg/l and the geometric mean ($mean_g$) is 0.84 µg/l. Chlorophyll *a* exceeding 4, 8, and 16 µg/l are observed 6.7%, 1.1%, and 0.1% of the time, respectively, while concentrations below 0.13, 0.06, and 0.03 µg/l occur at frequencies of 5.3%, 2.1%, and 0.6%, respectively.

Size Composition of Phytoplankton

When considering all samples without regard to sampling depth, season, or geographic region, nanoplankton (<20 µm) dominate the phytoplankton. The frequency distribution is strongly skewed toward low percent netplankton, with a median value of ~29% netplankton (Fig. 10). Chlorophyll *a* in the netplankton (>20 µm) exceeds 50% of the total chlorophyll in only 30% of the 57,019 paired measurements; the remainder of the time (70%), nanoplankton dominate (Fig. 10). Strong dominance (>90%) by netplankton is rare (only ~2% of the samples), but strong dominance by nanoplankton is common (25% of the samples). When the samples are grouped by depth strata, a vertical progression emerges in the median percent netplankton value. Percent netplankton increases with increasing depth, to ~50 m below surface. In subsequent sections we illustrate that phytoplankton size composition varies not only with depth, but also seasonally and regionally.

Horizontal Distribution of Chlorophyll

A wide range in mean water column chlorophyll concentration (Chl_w) is obvious in each of the two-month composite distributions (Fig. 11) and in most of the distributions based on individual surveys (Append. B). The contoured two-month distributions are generated from Chl_w averaged by tile. The range, mean, and coefficient of variation of Chl_w for each of the 193 tiles, tabulated by two-month periods, is provided in Table C3. The precision (coefficient of variation or CV) of the Chl_w estimates is depicted in Fig. 12. The sampling frequency per tile was judged insufficient for constructing representative contours of the monthly distribution of Chl_w. The two-month composites will obscure, in the mean, shorter-period chlorophyll events or pulses such as those obvious from survey to survey (Append. B). For the climatological intent of this monograph, the two-month portrayals adequately represent the major broadscale and seasonal features of interest, except perhaps in portions of the Gulf of Maine which were sampled infrequently during January–February and March–April (Fig. 13).

High levels of Chl_w, between 4 and 16 µg/l, occur in the shallow nearshore waters (~<30 m) of the Middle Atlantic Bight during the January–February period. These concentrations are about double those observed in November–December, and indicate that the WS-bloom commences relatively early in nearshore water. The 2 µg/l isochlor parallels the 60 m isobath from Nantucket Shoals to Cape Hatteras, but not on Georges Bank (Fig. 11). Water column chlorophyll concentration exceeding 2 µg/l is restricted to a small area in the shallow water on Georges Bank, and Chl_w during January–February is generally lower than the proceeding November–December period. This suggests that the WS-bloom has not yet begun on Georges Bank. An early WS-bloom also occurs in isolated nearshore areas of the western Gulf of Maine, between Cape Cod and Penobscot Bay. Here, mean chlorophyll concentrations are modest, between 1 and 4 µg/l, but nevertheless represent a doubling over mean values in November–December. Along the outer shelf, Chl_w is approximately 0.5–1 µg/l on Georges Bank and increases to ~1–2 µg/l in the southern end of the Middle Atlantic Bight. The lowest values (0.25–0.5 µg/l) during January–February occur in the northern Gulf of Maine and at some of the most seaward stations sampled along the shelf-break. The distributional pattern and magnitude of Chl_w along

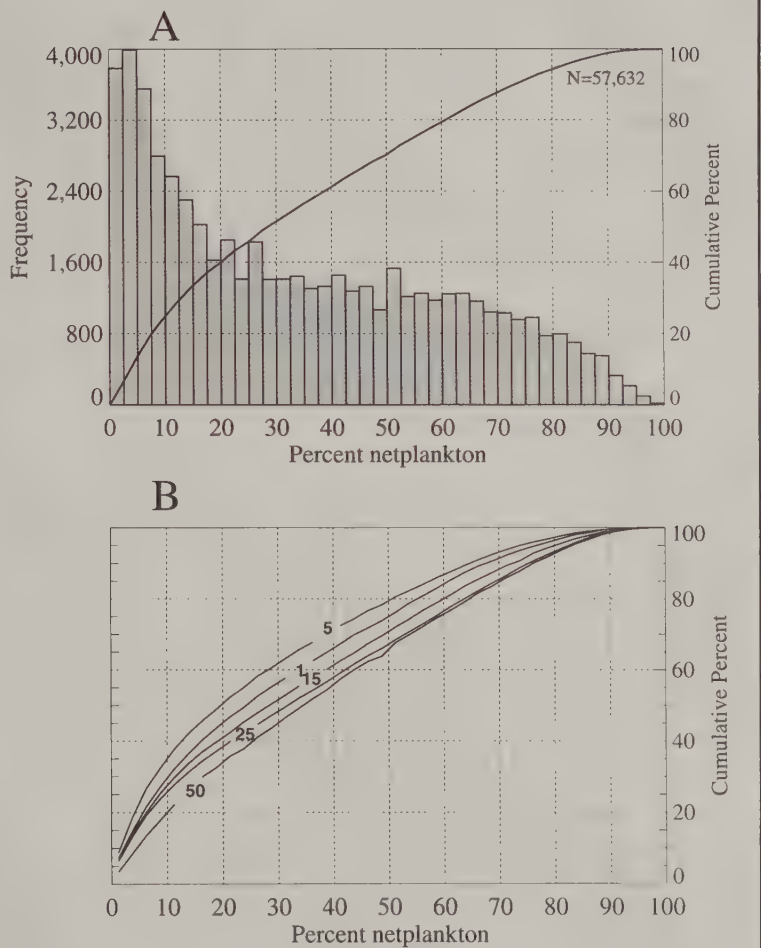

Figure 10

(A) Frequency and cumulative percent distributions of the percent of chloroplyll *a* in netplankton size-fraction (>20 µm) in 56,632 discrete water samples. (Samples having total chlorophyll concentrations less than 0.04 µg/l are not included since the estimates of percent netplankton would be imprecise.) (B) Cumulative percent distributions of percent of chlorophyll *a* in netplankton for five depth strata: 1 (0<3 m); 5 (3<8 m); 15 (13<18 m); 25 (23<28 m); 50 (38<63 m).

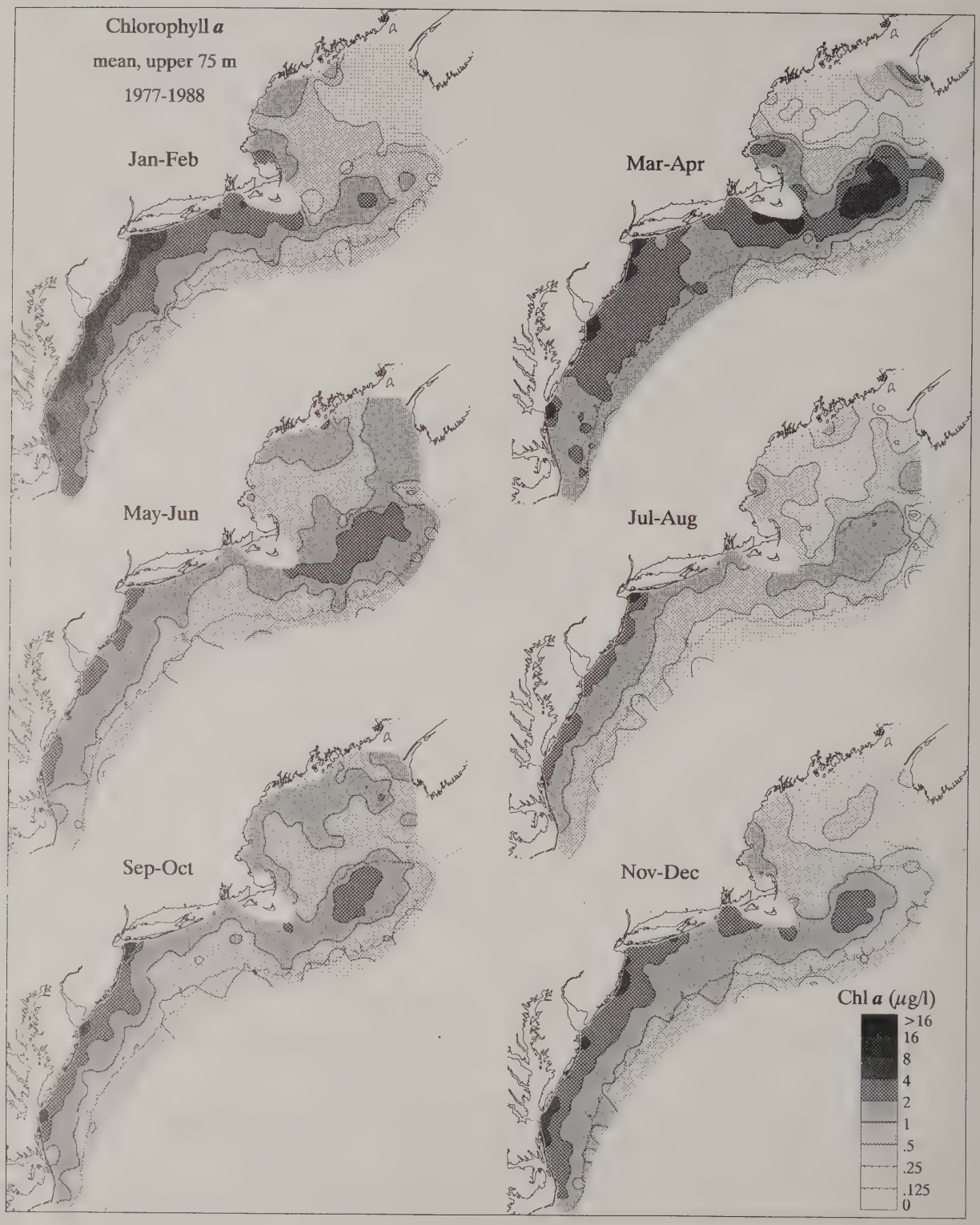

Figure 11

Contoured distribution of chlorophyll *a* in the upper 75 m of the water column during Jan-Feb, March–Apr, May–June, July–Aug, Sept-Oct, and Nov-Dec. Depth-weighted means (Chl_w) were composited by tile and 2-mo periods before contouring.

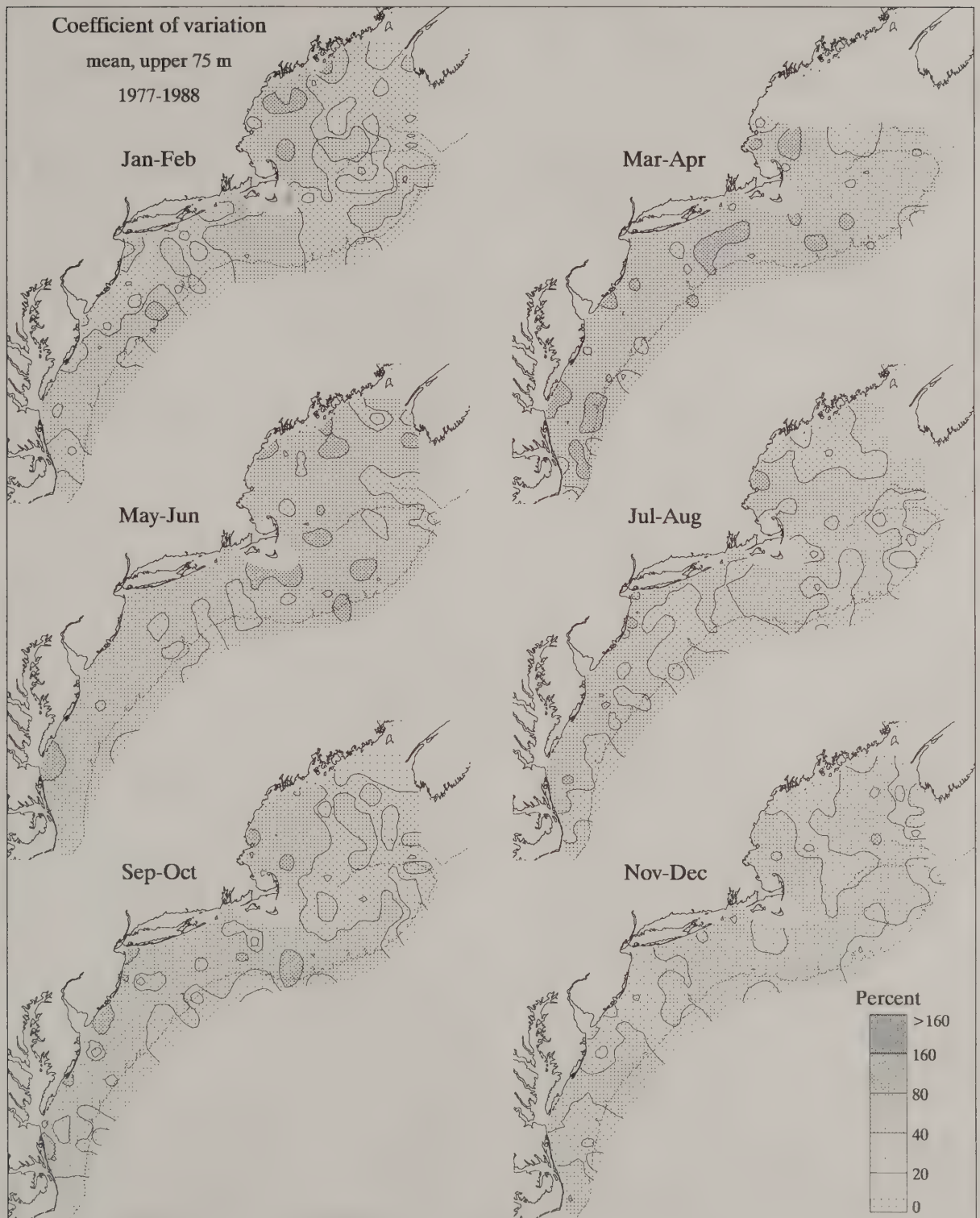

Figure 12

Contoured distribution of percent coefficient of variation (C.V.) of average concentration of chlorophyll *a* in the upper 75 m of the water column during Jan-Feb, March–Apr, May–June, July–Aug, Sept-Oct, and Nov-Dec. Depth-weighted means (Chl_w) were composited by tile and 2-mo periods before contouring.

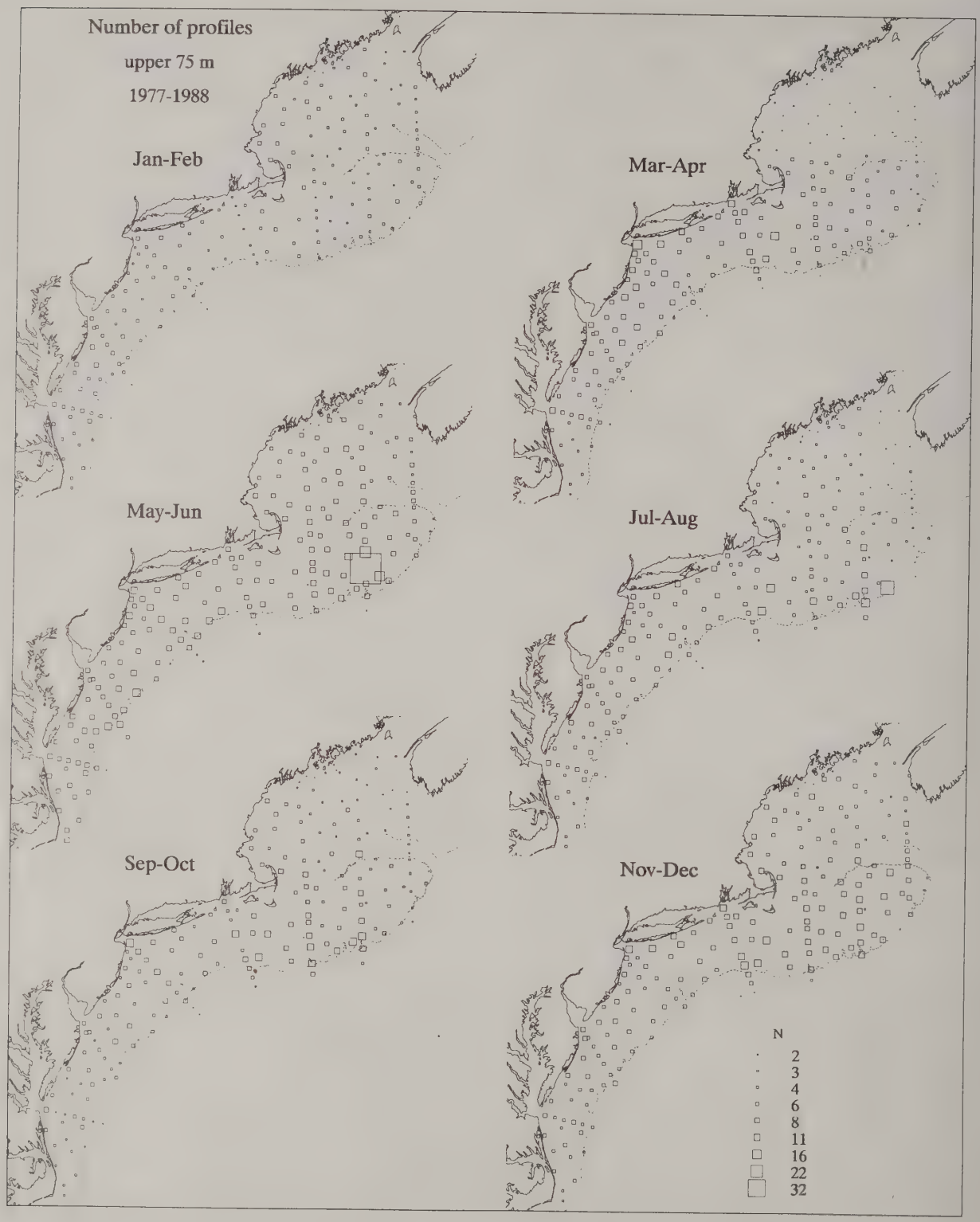

Figure 13

Number of vertical profiles (stations) used in calculation of Chl_w and related calculations, during Jan-Feb, March–Apr, May–June, July–Aug, Sept-Oct, and Nov-Dec.

the shelf-break and in offshore areas of the Gulf of Maine in January–February are essentially unchanged from November–December.

In March–April, Chl_w over the shallows on Georges Bank and flanking Nantucket Shoals reaches WS-bloom levels (2–8 μg/l). In the Middle Atlantic Bight, between Long Island and north of Chesapeake Bay, the WS-bloom extends from the coast to the shelf-break (Fig. 11). High Chl_w is also observed adjacent to the mouths of estuaries in the Middle Atlantic Bight, but Chl_w in the nearshore bight has generally decreased from the January–February period. Some exceptionally low values (0.13–0.25 μg/l) are present in the central region of the Gulf of Maine. (Note, however, that the composite distribution in March–April for the northern half of the Gulf of Maine is based on very few observations (Fig. 13) and may not represent true mean conditions).

In May–June, the highest Chl_w values (~2–4 μg/l) occur near the Middle Atlantic Bight estuaries and over shallow areas on Georges Bank. In both areas values are lower than in the preceding period. The lowest Chl_w (0.25–0.5 μg l^{-1}) is found along the shelf-break in the Middle Atlantic Bight.

Overall, the July–August period represents the annual minimum in mean water column concentrations of chlorophyll *a*. On Georges Bank, Chl_w has decreased progressively since the annual peak in March–April. In the Middle Atlantic Bight, the 2 μg l^{-1} isochlor has receded from the 60 m to the ~40 m isobath since the May–June period. Water column chlorophyll concentration is again highest in the nearshore Middle Atlantic Bight and the shallow water on Georges Bank.

The pattern of Chl_w distribution in the Middle Atlantic Bight during September–October is similar to the distribution during July–August, except that in the nearshore area (~<30 m) levels during September–October are higher (Fig. 11). Similar increases are evident in the shallow water on Georges Bank, Western Gulf of Maine, and off the coast of Nova Scotia. These relative increases constitute the fall bloom, an event of lesser magnitude than the WS-bloom.

During November–December, phytoplankton distribution on Georges Bank is similar to the pattern in September–October. In the nearshore Middle Atlantic Bight, Chl_w ranges between 2 and 5 μg l^{-1}, a slight increase over the September–October period. Mean values exceeding 2 μg l^{-1} occur nearshore, between Narragansett Bay and the southern flank of Nantucket Shoals (Fig. 11). In the Middle Atlantic Bight, the 2 μg l^{-1} and 1 μg l^{-1} isochlors extend farther offshore in November–December than during the preceding period, indicating a seaward extension of the fall bloom. Throughout much of the northern Gulf of Maine, chlorophyll concentrations are below 0.5 μg l^{-1}, much less than values on Georges Bank and the nearshore Middle Atlantic Bight.

Horizontal Distribution of Netplankton/Nanoplankton

There is considerable horizontal and temporal variation in the size composition of the phytoplankton community, indexed as percent netplankton (Fig. 14). Throughout most of the year, percent netplankton generally decreases from the nearshore to offshore Middle Atlantic Bight. Similarly, an annular, bathymetric pattern in phytoplankton size composition is evident on Georges Bank, where percent netplankton usually decreases from the shallow to deeper water.

In the nearshore areas of the Middle Atlantic Bight, the shallow water on Georges Bank, and in western Gulf of Maine, 40–80% of the chlorophyll is bound in the netplankton size-fraction during January–February. Elevated percent netplankton occurs in areas with elevated Chl_w (cf. Figs. 11 and 14) and reflects the initiation of a WS-bloom, presumably comprised of large diatoms and chains or colonies of smaller diatoms retained on a 20 m mesh. The areas with lowest Chl_w also have the lowest percent netplankton (cf. Figs. 11 and 14). The spatial contrasts in the size composition of the phytoplankton at this time are extreme: netplankton predominate in nearshore areas of the Middle Atlantic Bight and shallow water on Georges Bank, while nanoplankton predominate in deeper water on Georges Bank, along the shelf-break, and surrounding the Jordan Basin in the Gulf of Maine.

The advance of the WS-bloom across the Middle Atlantic Bight and deeper areas on Georges Bank during March–April is evident in the distribution of percent netplankton (Fig. 14). The initiation of the WS-bloom in the western Gulf of Maine and easterly sweep across the gulf, noted by Curra (1987), is also evident. March–April is the peak period of netplankton dominance on the northeast U.S. continental shelf. Netplankton exceeds 60% of the total biomass throughout a large portion of the Middle Atlantic Bight and Georges Bank. Although chlorophyll concentrations are still elevated in the nearshore region of the Middle Atlantic Bight, there is an overall decrease in percent netplankton from the January–February period. This may indicate a successional change toward post-WS-bloom phytoplankton assemblages.

The composite distributions for May–June and July–August periods indicate that nanoplankton generally dominate the phytoplankton (Fig. 14). However, in the Middle Atlantic Bight, south of Long Island, a broad band exists where netplankton and nanoplankton are approximately equal. A similar phytoplankton size composition is evident in the shallow water on Georges Bank. Percent netplankton is relatively high in patches in the western Gulf of Maine, off Casco Bay and Penobscott Bay. July–August is the only period when mean

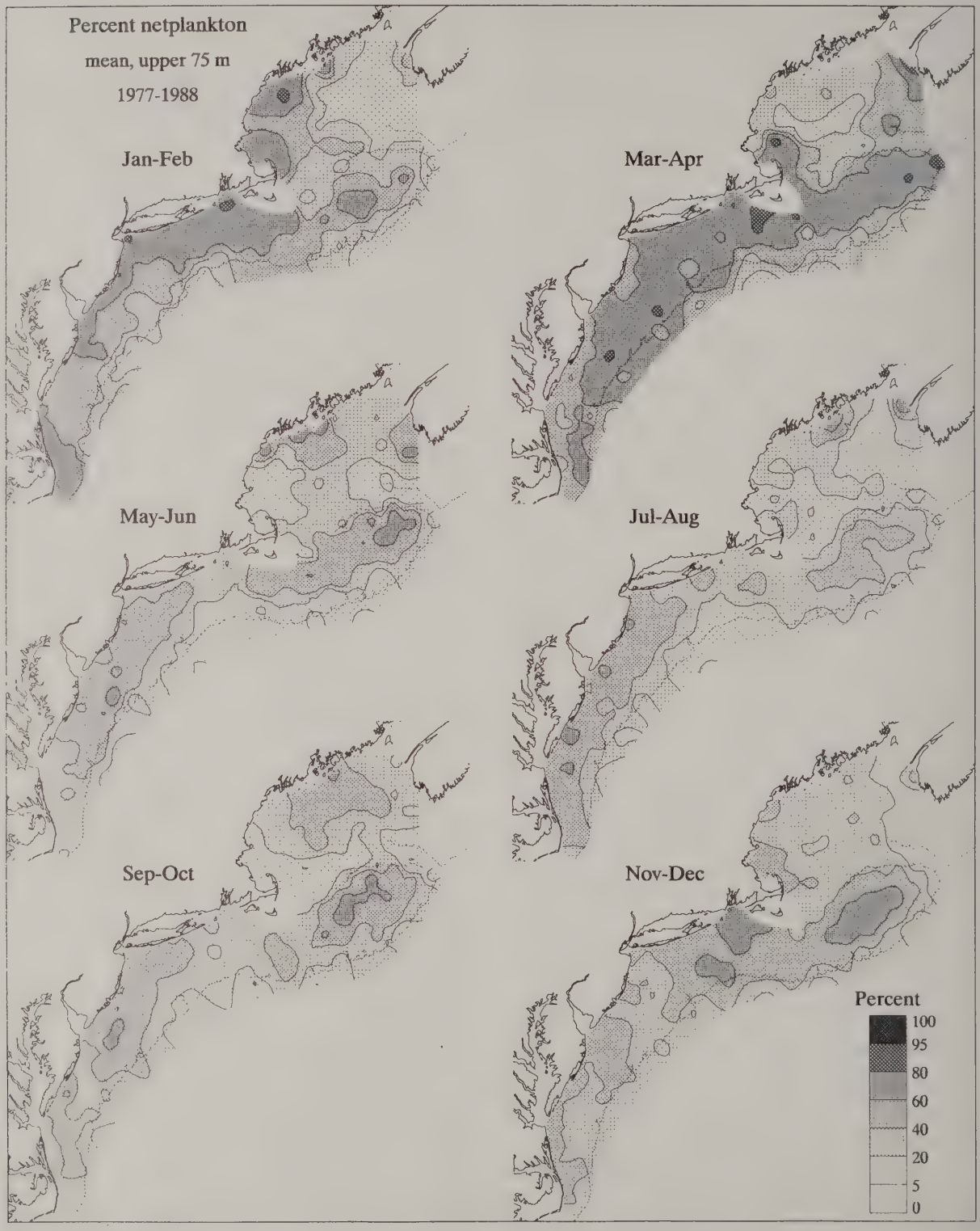

Figure 14

Distribution of percent netplankton chlorophyll *a* in the upper 75 m of the water column during Jan-Feb, March–Apr, May–June, July–Aug, Sept-Oct, and Nov-Dec. Depth-weighted means (Chl_w) were composited by tile and 2-mo periods before contouring.

percent netplankton values do not exceed 60% in the shallow areas of Georges Bank. During September–October and continuing through November–December, percent netplankton increases on Georges Bank, reaching 60–80%. In contrast, except for patches off Narragansett Bay, only modest changes in percent netplankton are seen in the Middle Atlantic Bight from July–August to November–December.

There is a direct relationship between mean Chl_w and mean percent netplankton throughout the annual cycle (Fig. 15) and increases in Chl_w, particularly above 1 $\mu g\ l^{-1}$, are more related to netplankton increases than to nanoplankton increases. During many of the two-month periods, elevated levels of Chl_w are observed in areas adjacent to the three Middle Atlantic Bight estuaries. Malone et al. (1980) suggested that during winter-spring periods of netplankton abundance in coastal water, the coastal water acts as a source and the estuary as a sink for netplankton. In the stratified season, the nanoplankton and flagellate blooms in the estuarine surface water represent a source of new phytoplankton and the coastal water a sink.

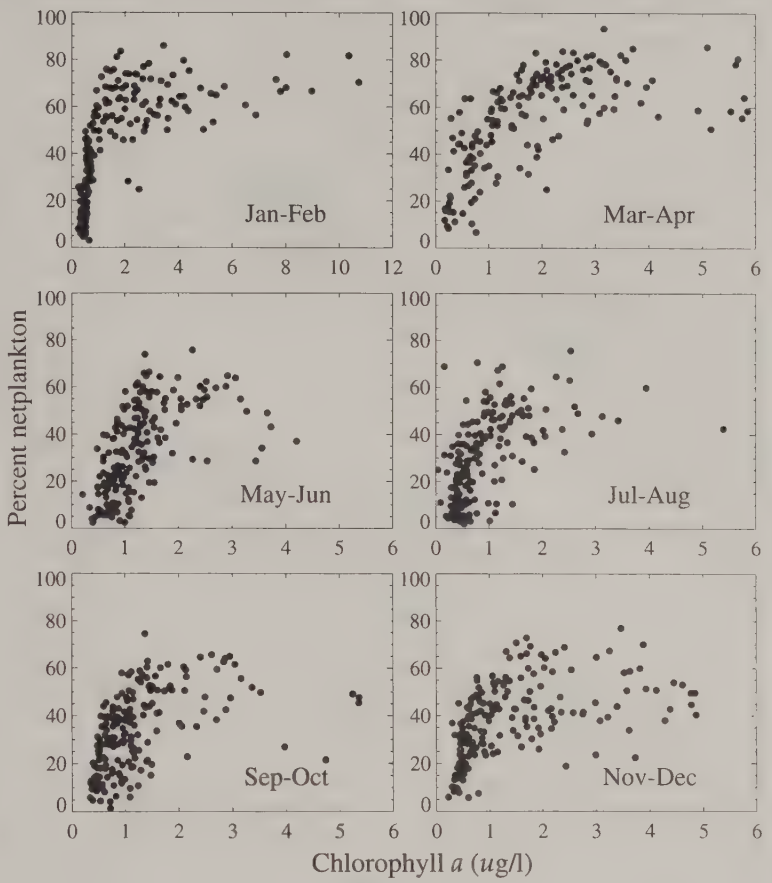

Figure 15
Relationship between mean percent of water column chlorophyll in netplankton and mean water column chlorophyll *a* concentration for Jan-Feb, March–Apr, May–June, July–Aug, Sept-Oct, and Nov-Dec. Data points represent means for each tile.

Percent Phaeopigment

The percent phaeopigment index provides additional diagnostic information on the plankton community. Very low values indicate rapid phytoplankton growth combined with minimal grazing by zooplankton. High values are not as unambiguously interpreted. They would indicate either a senescent phytoplankton community or extensive grazing by copepods (Downs and Lorenzen, 1985; Falkowski et al., 1988), or methodological error due to chlorophyll *b* and *c* (Trees et al., 1985).

Despite this ambiguity, regular, distinct patterns of increasing percent phaeopigment from shallow to deep water are evident in the two-month composite distributions (Fig. 16). Percent phaeophytin is relatively low in Middle Atlantic Bight shelf water and shallow water over Georges Bank and relatively high in the offshore Gulf of Maine and along the shelf-break. In many of the subareas, seasonal variation in median percent phaeopigment is modest or not apparent. Over the annual cycle the range of median values is ~20% and in some areas only 10%. The largest seasonal variation appears in subareas where WS-bloom is intense or prolonged.

During January–February, the lowest percent phaeopigment occurs in regions with highest Chl_w and highest percent netplankton (cf. Figs. 11, 14, and 16). Values below 20% are evident nearshore, in large patches adjacent to the Hudson-Raritan and Delaware estuaries, Narragansett Bay, and the western Gulf of Maine (Fig. 16). Over most of Georges Bank and the eastern half of the Gulf of Maine, values exceed 30%, whereas

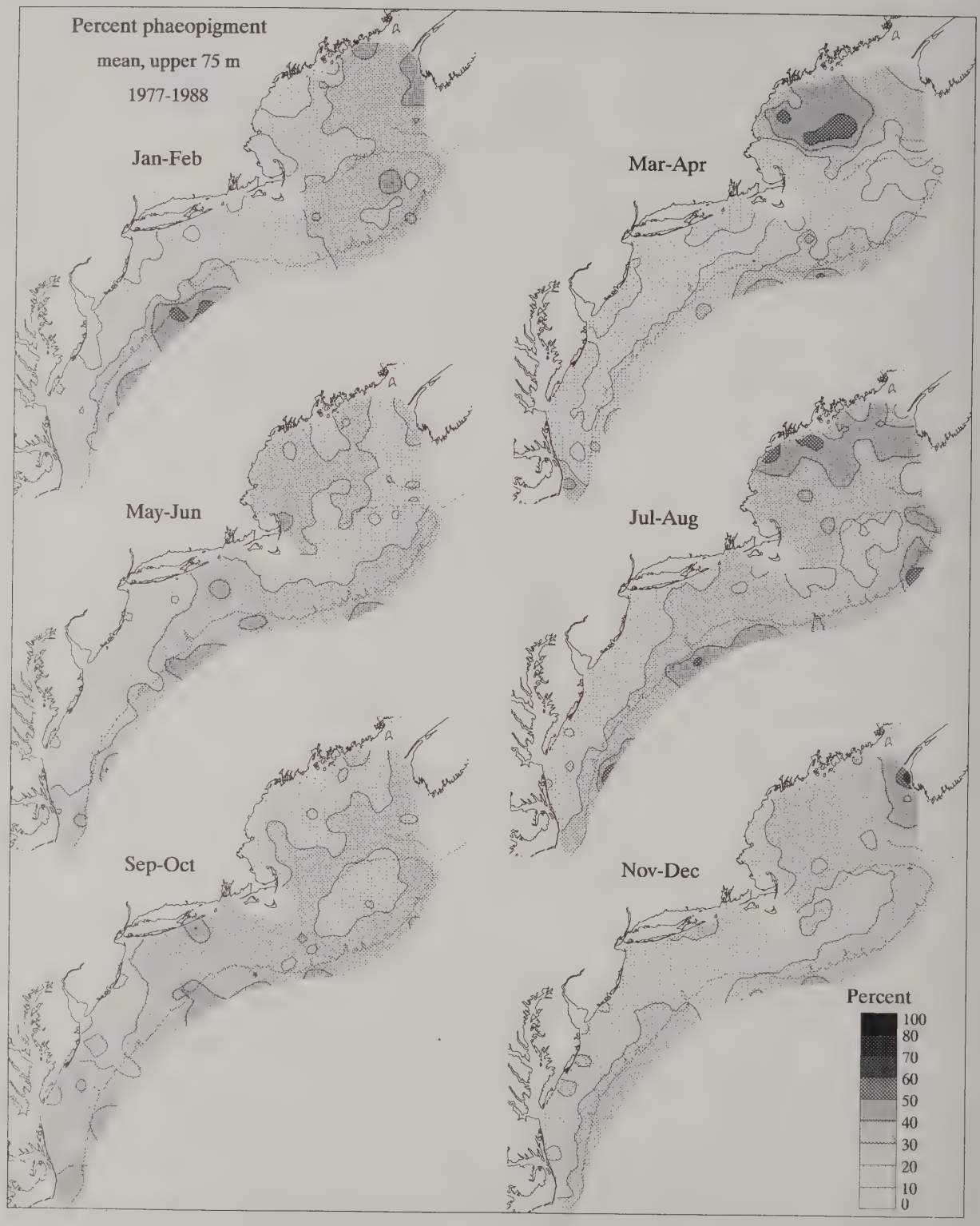

Figure 16

Distribution of average percent phaeopigment in the upper 75 m of the water column during Jan-Feb, March–Apr, May–June, July–Aug, Sept-Oct, and Nov-Dec. Depth-weighted means (Chl_w) were composited by tile and 2-mo periods before contouring.

throughout most of the Middle Atlantic Bight shelf water, values are less. The percent phaeopigment index reinforces the generalization, based on increases in Chl_w and increases in percent netplankton, that the WS-bloom commences in January–February in the nearshore areas of the Middle Atlantic Bight and the western Gulf of Maine, and extends throughout the Middle Atlantic Bight and over Georges Bank during March–April.

Overall, the percent phaeopigment index is highest during the July–August and September–October periods. In November–December, percent phaeophytin is high (>30%) throughout most of the Gulf of Maine, when compared with the band of relatively lower values extending throughout most of the Middle Atlantic Bight and onto the shallow water on Georges Bank.

Throughout the annual cycle, percent phaeopigment generally decreases as the percent netplankton and Chl_w increase (Fig. 17). Since the increases in Chl_w above 1 g l^{-1} are primarily due to the netplankton (Fig. 15), low percent phaeopigment values probably reflect relatively rapid (netplankton) growth. Alternatively, actively dividing chain and colonial forms of phytoplankton and larger dinoflagellates are likely to be retained in the netplankton pigment fraction, whereas chlorophyll degradation products such as phaeophytin *a* would tend to be decimated and more likely recovered in the particulate fraction passing the 20 m mesh (nanoplankton). These percent phaeopigment patterns reported may also reflect temporal and spatial variation in phytoplankton species composition and pigment composition (the relative amounts chlorophylls *a*, *b*, and *c*), because the fluorometric method used here to derive chlorophyll *a* and phaeophytin *a* is known to be influenced adversely by moderate concentrations of chlorophyll *b* and chlorophyll *c* (Trees et al., 1985; Welschmeyer, 1994).

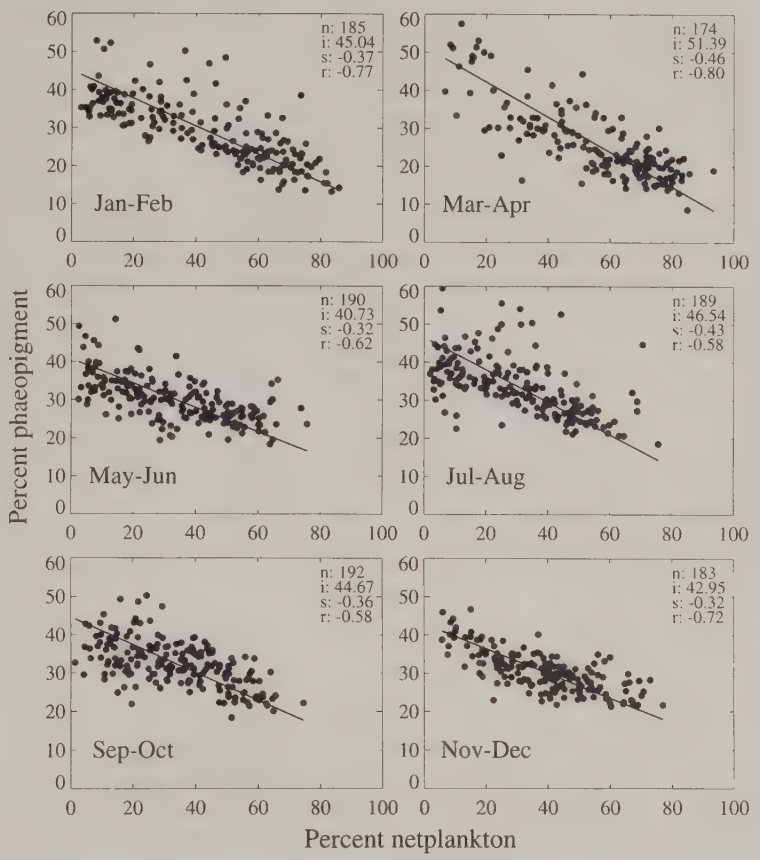

Figure 17

Relationship between mean percent phaeopigment and mean percent netplankton in the upper 75 m of the water column during Jan-Feb, March–Apr, May–June, July–Aug, Sept-Oct, and Nov-Dec. Data points represent means for each tile. Line represents functional regression (n=number of observations, r=correlation coefficient, s=functional slope, i=functional intercept).

Recurring Patterns in Phytoplankton Biomass

There are recurring patterns in the distribution of phytoplankton chlorophyll on the northeast U.S. shelf that are evident throughout most of the year (Append. Fig. B1–B38). In general, chlorophyll concentrations decrease with increasing bottom depth and distance from shore. On Georges Bank, relatively high concentrations of Chl_w are consistently found within the shallow, tidally well-mixed waters approximately delineated by the 60 m isobath. Chloropleths which decrease from shallow to deep (e.g. Append. Figs. B11, B15, B20, B22, B33, B34, and B35) are roughly concentric (annular)

around the epicenter which is generally found toward the middle of the southern half of the shallows (Fig. 5: Tiles 123, 147, 148, 156). Similarly, in the MAB, chloropleths frequently parallel isobaths. Water column chlorophyll concentration is usually highest in shallow water and decreases offshore with increasing bottom depth until minima are reached along the shelf-break. Exceptionally high (>8 μg l^{-1}) Chl_w, when present in the Middle Atlantic Bight (Table 2), usually occurs near the mouths of the Hudson-Raritan, Delaware, and Chesapeake bays, areas receiving high concentrations of river-borne nutrients (e.g. Malone, 1976; Malone, 1984). Occasionally, high Chl_w concentrations are found in Middle Atlantic Bight coastal waters not in close proximity to estuaries, and may reflect upwelling episodes. High Chl_w are also found in a small area along the southeast edge of Nantucket Shoals (Table 2). In the Gulf of Maine, Chl_w is usually greatest near the coast in pockets near Cape Cod Bay, Massachusetts Bay, Casco Bay, and Penobscott Bay. Highest concentrations are generally found between Penobscot and Casco bays. Lowest values are generally found in the deeper water over the offshore basins.

Table 2
Ranking of tiles with Chl_w exceeding 8 μg l^{-1} two or more times.

Tile	Subarea	Frequency
55	MAB[1] Hudson-Raritan plume	28.0
187	MAB Hudson-Raritan plume	17.0
12	MAB Chesapeake plume	11.0
185	MAB central nearshore	9.0
29	MAB Delaware plume	9.0
184	MAB Delaware plume	7.0
28	MAB southern nearshore	7.0
23	MAB southern nearshore	5.0
93	GB[2] Nantucket shoals	4.0
13	MAB southern midshelf	3.0
56	MAB central nearshore	3.0
53	MAB central nearshore	3.0
41	MAB central nearshore	2.0
42	MAB central nearshore	2.0
68	MAB central nearshore	2.0
21	MAB southern nearshore	2.0
11	MAB southern nearshore	2.0
76	MAB northern midshelf	2.0
123	GB central shoals	2.0
148	GB central shoals	2.0
126	GOM[3] Wilkinson Basin	2.0

[1] MAB=Middle Atlantic Bight.
[2] GB=Georges Bank.
[3] GOM=Gulf of Maine.

Cross-Shelf Chl_w Gradients

A significant portion of the spatial variation in phytoplankton biomass is related to bottom depth. When considering the entire dataset, there is nearly an eight-fold decrease in Chl_w from the shallowest to the deepest water column sampled (Fig. 18). The correlation coefficient between $\log_2$(Chl_w, μg l^{-1}) and $\log_2$ (bottom depth, meters) is –0.53 and the linear regression (least-squares-y) is highly significant at <0.00001 *P*. The regression line in Fig. 18 does not represent well those areas deeper than ~250 m, because sampling was usually limited to the upper 100 m and chlorophyll concentrations below 100 m are less than those above. Therefore, values in the deep water overestimate Chl_w and are above the regression line. The independence between Chl_w and bottom depths greater than ~250 m suggests that the depth of the permanent thermocline over slope water (and the relevant vertical mixing depth for plankton in these areas) may express the relationship more appropriately.

When we examine the data by region and season we find significant exceptions to the above-generalized cross-shelf Chl_w gradient. In fact, there is a distinct seasonality in the magnitude of the cross-shelf chlorophyll gradient and notable differences among shelf regions (Fig. 19). The steepest cross-shelf Chl_w gradients on Georges Bank occur during February and March. Water column chlorophyll concentration in the shallowest water sampled is approximately 25–38 times Chl_w in the deepest water. This is a significant departure from the mean cross-shelf gradient of 8:1 shown in Fig. 18, and reflects the initiation of the WS-bloom in shallow central Georges Bank. Similarly, the steepest gradients in the Middle Atlantic Bight reflect the appearance of the WS-bloom nearshore in January–February. As the WS-bloom spreads offshore in the Middle Atlantic Bight during March–April and into deeper water on Georges Bank during April, cross-shelf Chl_w gradients drop precipitously, approaching the annual minimum. In a number of surveys that captured WS-bloom conditions, cross-shelf gradients in chlorophyll are not obvious (Append. Figs. B16, B17, B22, B23, and B26).

On Georges Bank, Chl_w gradients are low from June through August when the central tidally-mixed area reaches its annual Chl_w minimum (Fig. 11; Append. Figs. B6 and B19). During summer the presence of a pronounced subsurface chlorophyll maximum layer in the seasonal thermocline in deeper, stratified waters also tends to diminish the magnitude of the cross-bank Chl_w gradient (see section "Subsurface Chlorophyll Maximum" below).

In the Gulf of Maine, Chl_w gradients are muted relative to the Middle Atlantic Bight and Georges Bank. Many of the estimated gradients (linear regression

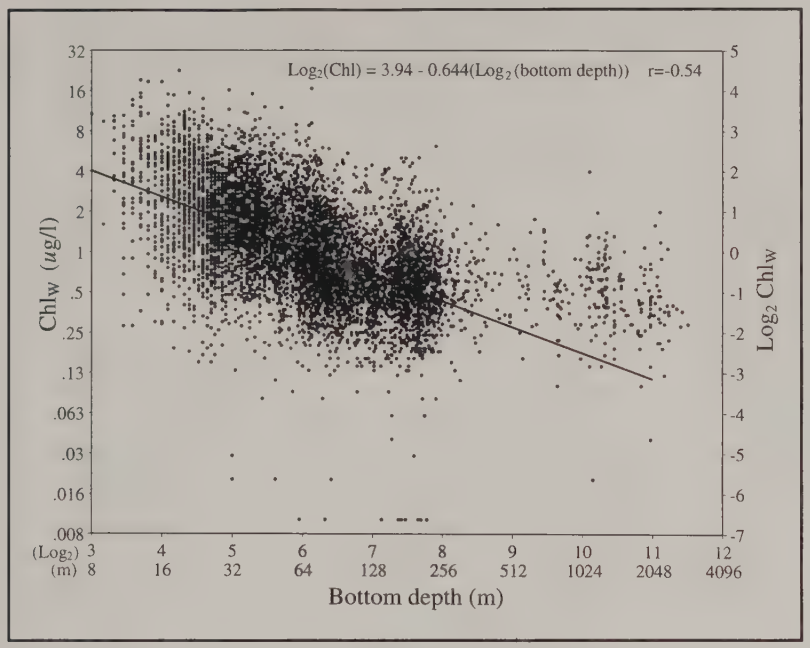

Figure 18

(Above) Relationship between Chl_w and bottom depth (all data). Line represents least-squares linear regression (r=correlation coefficient).

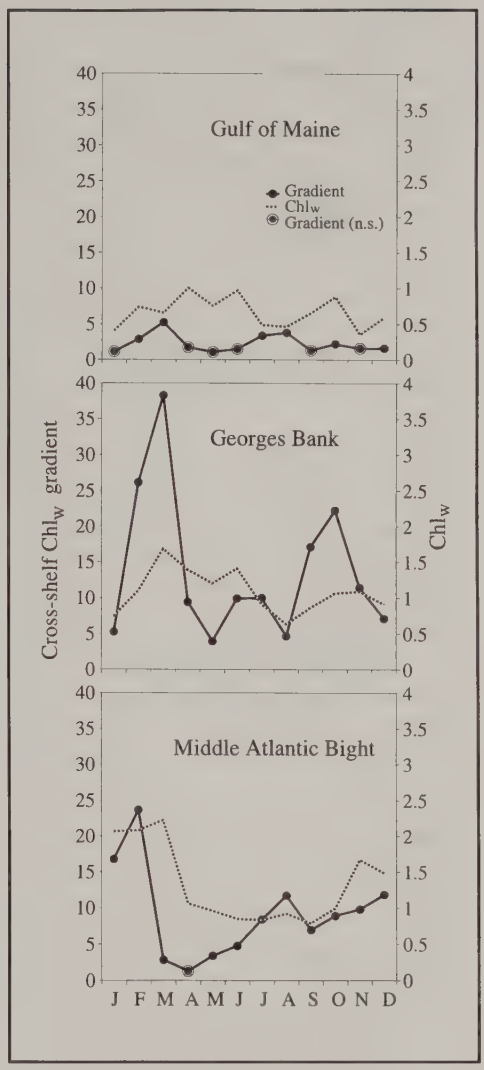

Figure 19

(Right) Cross-shelf (bathymetric) gradient in Chl_w and mean Chl_w versus month for Gulf of Maine, Georges Bank, and Middle Atlantic Bight regions. Cross-shelf gradients were computed as the product of the slopes from least-squares-y regressions of $\log_2$ (water column chlorophyll *a*) on $\log_2$ (bottom depth) times the depth range for each region (Gulf of Maine: 32–256 m, Georges Bank: 22.6–256 m, Middle Atlantic Bight: 8–256 m). Bottom depths greater than 256 m were ignored in the regression. The linear regression model explained a significant portion of the chlorophyll variation (probability of a larger F-value<0.001) and computed regression slopes were significantly different from zero ($p<0.001$) for all gradient values except those circled (not significant, n.s.).

slopes) are not significantly different from zero. Still, the annual maximum gradient occurs during March, the time of the WS-bloom in the western gulf.

The cross-shelf, depth-related decrease in the mean water column chlorophyll *a* reported here has also been observed during oceanographic surveys of other shelf ecosystems, such as the Southern California Bight (Eppley et al., 1978), the Southeast Atlantic Bight (Haines and Dunstan, 1975), and in coastal waters off Washington and Oregon (Anderson, 1964). The general cross-shelf gradient in phytoplankton pigment concentrations in near surface water on the northeast U.S. continental shelf is also evident in monthly composites of satellite images remotely sensed using the CZCS (Feldman et al., 1989). Off the coast of Georgia, in the Southeast Atlantic Bight, Bishop et al. (1980) found high concentrations of chlorophyll in nearshore surface water (1.9–8.0 µg/l), and lower concentrations at midshelf, 20–30 km offshore (<1.0 µg/l). Along the shelf-break, 100 km offshore, they observed even lower values (0.1–0.2 µg) in surface water throughout the year, except during upwelling episodes when concentrations reached ~2–6 µg/l. Occasionally our surveys detected small patches of high Chl_w along the shelf-break (Append. B), where low concentrations are usually observed. Phytoplankton in these areas may be responding to localized nutrient enrichment due to upwelling along the shelf-break, although this process is not as obvious or recurrent in our data as in other studies of the area (Marra et al., 1990) or along the

shelf-break south of Cape Hatteras (Yoder et al., 1983, 1985).

A somewhat different pattern from water column average chlorophyll emerges when the chlorophyll data are integrated to 75 m (Chl_i) and expressed as standing stocks per m^2 (Fig. 20). Integrated chlorophyll will naturally underestimate standing stocks in water deeper than 75 m, and more so during the unstratified season than the stratified season, when concentrations are modest below 75 m. As is the case for Chl_w, bathymetric gradients in Chl_i are present on Georges Bank during each of the two-month periods, the most pronounced during the March–April WS-bloom. However, the cross-shelf gradient in Chl_i in the Middle Atlantic Bight differs from the cross-shelf decreases in Chl_w (cf. Fig. 11, 20). During the March–April WS-bloom, Chl_i is higher at mid- and outer shelf and shelf-break areas than nearshore, except for small patches near the estuaries. These observations agree with those reported for the New York Bight (Malone et al., 1983b). Off Chesapeake Bay, Chl_i increases from the coast to the shelf-break (March–April, May–June) or is relatively uniform across the shelf (remaining periods). In this area, there is no strong onshore-offshore bathymetric gradient as found to the north (Fig. 20); the 60 m isobath converges offshore with the 200 m isobath, resulting in a narrow, uniformly shallow shelf.

Recurring Patterns in Phytoplankton Size Composition

Recurring onshore-offshore patterns in the size composition of the phytoplankton on the northeast U.S. shelf are also evident in the two-month composite maps of size-fractionated Chl_w (Fig. 14) and in the distributions from individual surveys (Append. B). However, the size-structure pattern varies more by season and region than does biomass. Generally netplankton dominate phytoplankton in areas where Chl_w is consistently high, such as the nearshore Middle Atlantic Bight and the shallow water on Georges Bank, while nanoplankton dominate in areas that have low Chl_w, such as deeper water along the slope and in deep offshore water in the Gulf of Maine. These general gradients in size composition reflect the shift from a predominantly diatom flora nearshore to a phytoflagellate flora offshore (Marshall, 1976, 1984; Malone et al., 1983b). Curra (1987) reported that total phytoplankton cell abundance (primarily diatoms) during early spring and summer in the shallow waters on Georges Bank is at least ten times that observed in the surrounding deeper water (primarily dinoflagellates). The prolonged presence of diatoms following the WS-bloom seems to be a characteristic feature of shallow, vertically well-mixed waters on Georges Bank. In contrast, diatoms are particularly sparse in the central Gulf of Maine during summer (Curra, 1987).

Onshore-offshore gradients in the size composition of the phytoplankton have been observed on other continental shelves. Bishop et al. (1980) reported a seaward decrease in percent netplankton (>10 μm) in the South Atlantic Bight off the coast of Georgia.

Annual Cycle of Chl_w

Water column chlorophyll concentration generally follow an annual cycle typical of temperate shelf ecosystems. In most shelf areas, Chl_w is low from late spring through late summer, the period of strongest vertical density stratification of the water column, and relatively high during the unstratified season, with highest values observed during spring and fall blooms (Fig. 21). Fall bloom is generally subordinate in magnitude to spring bloom. Minor blooms or "bursts" occur outside of spring and fall bloom time periods but their duration is short and their occurrence unpredictable from year to year as they result from conditions temporarily favorable for phytoplankton growth or accumulation.

This general cycle is most recognizable in the central and northern midshelf areas of the Middle Atlantic Bight (Fig. 21). However, it is also obvious that there is considerable variation among shelf areas in the timing and duration of winter-spring and fall blooms, and in the overall magnitude of Chl_w. WS-bloom begins earlier (January–February) and persists longer in southern and/or shallow waters than in northern and/or deeper waters. By March, WS-bloom is in progress over most of the shelf between Long Island and north of Chesapeake Bay. By April, WS-bloom is past throughout most of the shelf except deeper northern waters which have Chl_w peaks in April (Gulf of Maine Wilkinson Basin, Georges Bank southern flank, and Georges Bank Great South Channel) and April–May (Georges Bank northern slope).

With the exception of areas in the Middle Atlantic Bight influenced by river plumes, Chl_w over the entire shelf are at or near annual minima during July and August (Figs. 11 and 22). Only during this period are most stratified shelf areas at the same stage of the annual cycle, when cross-shelf gradients in Chl_w are weakest (Fig. 19). Water column chlorophyll concentration is low from May through September throughout the Middle Atlantic Bight, and in subareas—Georges Bank southern flank, Georges Bank northern slope, and Gulf of Maine western, Wilkinson Basin, and Georges Basin. Like spring bloom, fall bloom progresses from shallow to deeper water, beginning early in southern shallow water in October and starting in deeper water in October–November.

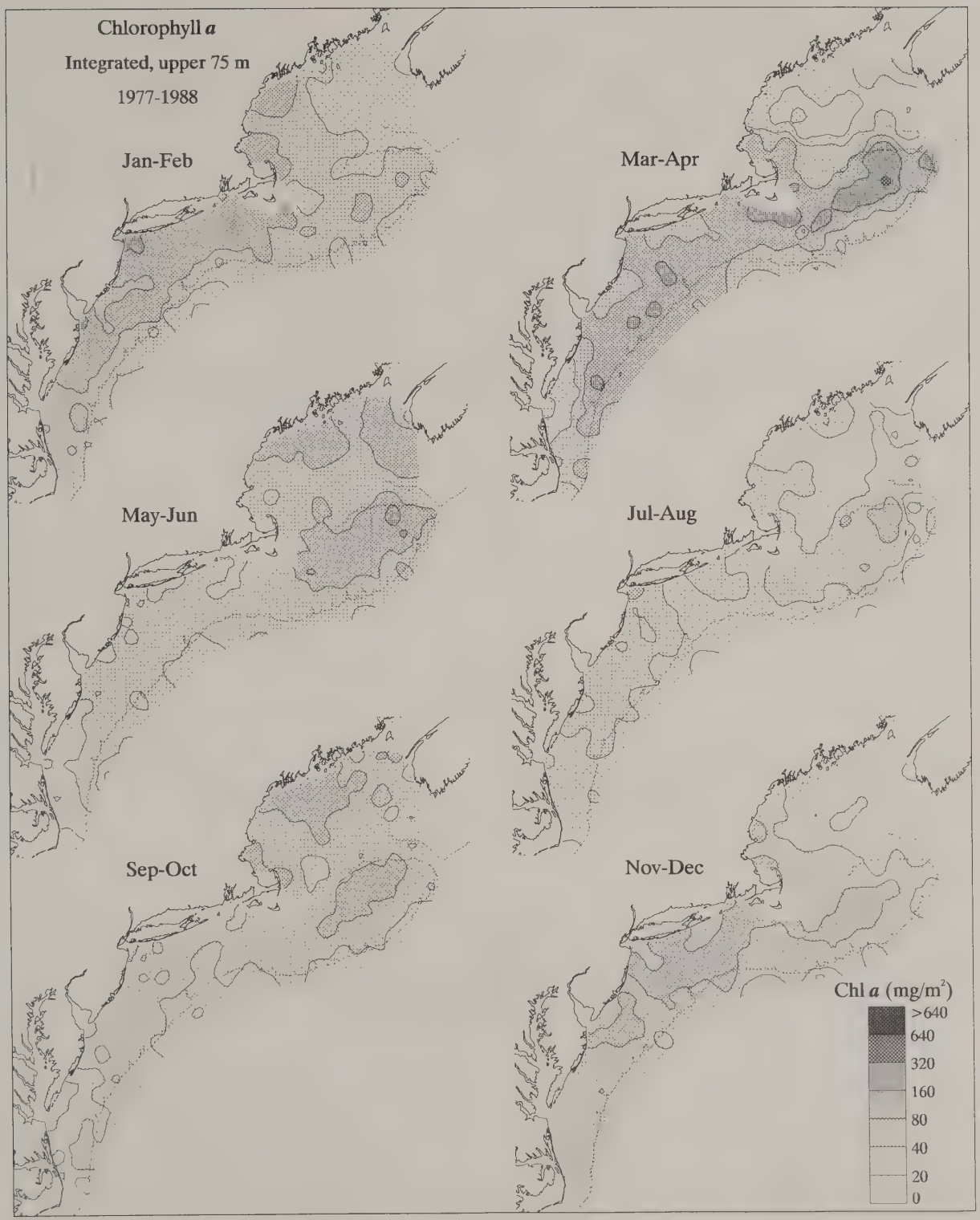

Figure 20

Contoured distribution of integrated chlorophyll *a* in the upper 75 m of the water column during Jan-Feb, March–Apr, May–June, July–Aug, Sept-Oct, and Nov-Dec. Integrated chlorophyll *a* data were composited by tile and 2-mo periods before contouring.

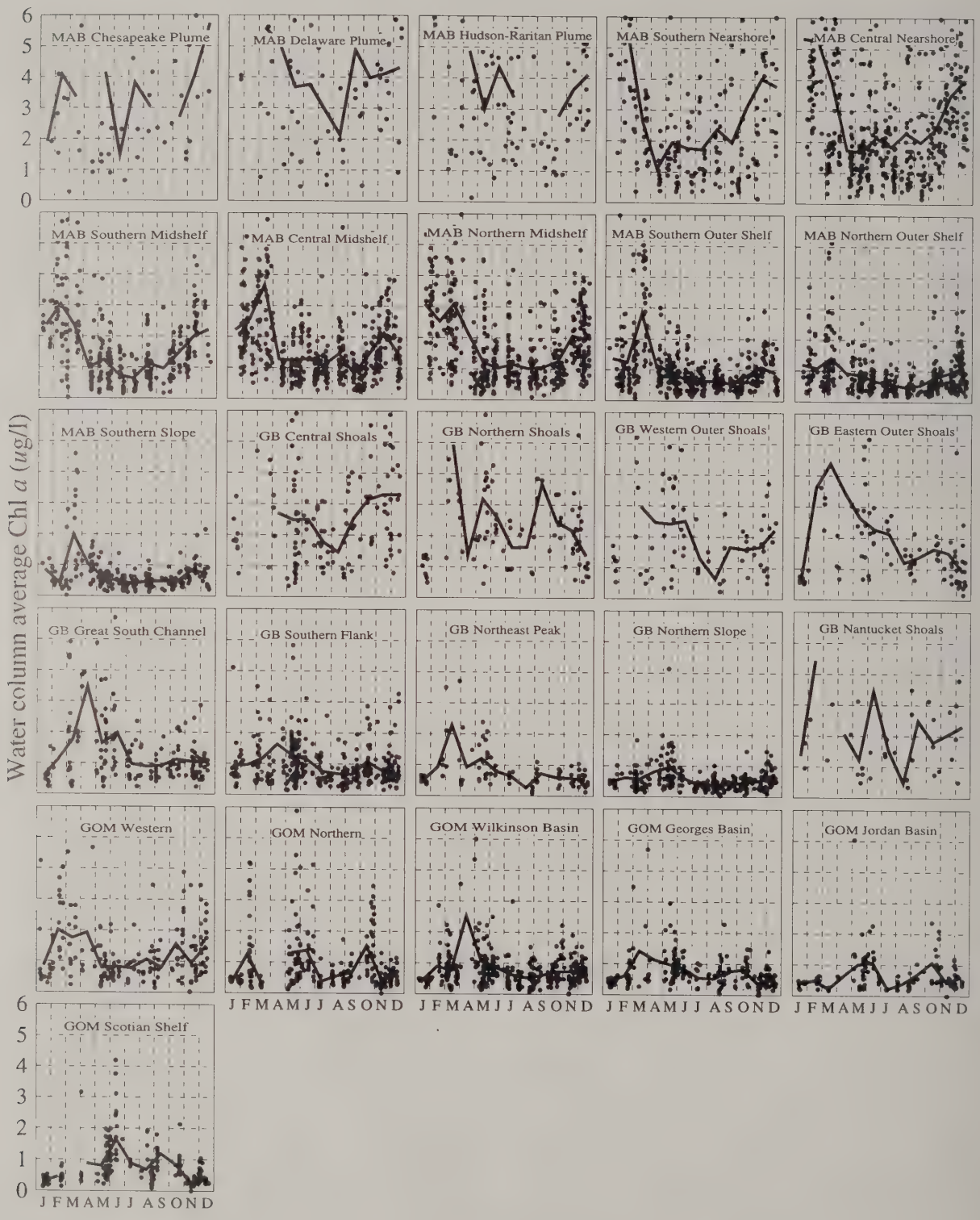

Figure 21

Mean water column concentration of chlorophyll *a* versus month for 26 subareas of the northeast U.S. continental shelf. Individual observations are represented as dots. The solid line connects monthly means.

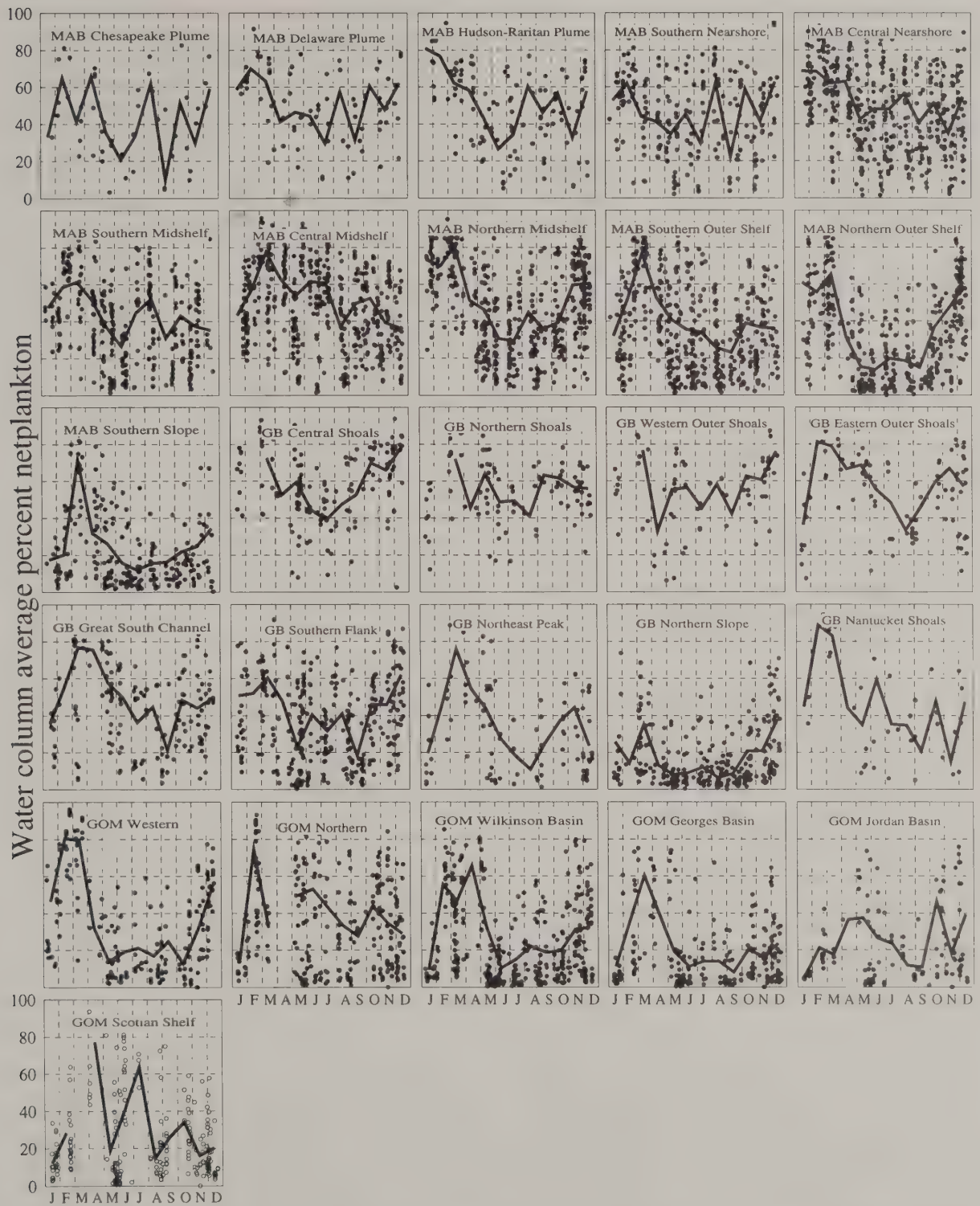

Figure 22

Mean water column percent netplankton versus month for 26 subareas of the northeast U.S. continental shelf. Individual observations are represented as dots. The solid line connects monthly means.

A regular seasonal progression of netplankton/nanoplankton is evident, with percent netplankton maxima usually coinciding with Chl_w maxima during spring and fall blooms (Fig. 22). However, even though percent netplankton is at its annual maximum, the phytoplankton community is not necessarily strongly dominated everywhere by netplankton as might be expected based on the spring bloom paradigm. In deeper areas of the Middle Atlantic Bight, on Georges Bank, and in the Gulf of Maine, the annual cycle of percent netplankton generally follows that of chlorophyll (cf. Figs. 21 and 22). In shallow waters less than 60 m during stratification, neither netplankton nor nanoplankton strongly dominate (percent netplankton ~40–60%). In the outer shelf and slope, nanoplankton generally are strongly dominant through September (percent netplankton~10–30%) and become less dominant in October when Chl_w begins to increase.

The summer pattern in the southern part of the Gulf of Maine (western Gulf of Maine, Wilkinson Basin, and Georges Basin) is similar to that of the Middle Atlantic Bight. Following the WS-bloom, Chl_w is low (~.75–1.0) and in the western Gulf of Maine increases in October. The percent netplankton in the southern Gulf of Maine follows the pattern of outer shelf (Middle Atlantic Bight) waters. It ranges from ~10–20% and increases during October (Georges Basin) and November (western Gulf of Maine and Wilkinson Basin).

Vertical Distribution of Chlorophyll

Some extremely interesting and regular features in the vertical distribution of phytoplankton are obscured in portrayals of average water column concentrations previously described. The vertical distribution of chlorophyll *a* across the continental shelf is illustrated as cross-sections for individual MARMAP surveys in Apend. B. To characterize typical regional and seasonal patterns in vertical distribution of phytoplankton biomass and size composition, monthly mean profiles were constructed for subareas of the Middle Atlantic Bight, Georges Bank, and the Gulf of Maine (Figs. 23–25). Depending on bottom depth, up to 11 layers of the water column are represented in a mean chlorophyll *a* profile. Layers (depth strata) are approximately centered on standard sampling depths: 1, 5, 10, 15, 20, 25, 30, 35, 50, 75, and 100 m. These composite profiles complement two-month shelfwide distributional contours described earlier (Figs. 11 and 14) by providing greater temporal and vertical resolution but less horizontal resolution of trends, since many tiles are grouped into each subarea. To enhance legibility and enable seasonal and regional comparisons, estimates of data dispersion about the mean values forming each profile are not graphed.

There are large seasonal changes in the vertical distribution of phytoplankton which are mostly related to seasonal changes in density stratification (Figs. 23–25). Four general profile shapes are evident: uniform, declining, bell, and inverted. Vertically uniform chlorophyll *a* profiles are most obvious from November through February, the period of minimal density stratification (e.g. January–April, outer Middle Atlantic Bight), and year-round in the tidally well-mixed shallow water on Georges Bank (e.g. Georges Bank northern and central shoals). Declining vertical profiles occur during the winter-spring and fall blooms, where highest biomass appears in the upper 20–30 m of the column (e.g. September–November, nearshore Middle Atlantic Bight). Inverted profiles occur infrequently. They are most obvious following the WS-bloom, when elevated concentrations of chlorophyll *a* appear near the bottom of the water column in the midshelf region of the Middle Atlantic Bight, but they are not found on Georges Bank and in the Gulf of Maine. Bell-shaped profiles characterize periods of vertical density stratification. Chlorophyll *a* is relatively low near surface, progressively increases forming a subsurface chlorophyll maximum layer generally in the pycnocline (20–35 m below surface), and then progressively decreases over the remaining deeper portion of the profile. Subsurface chlorophyll *a* maxima are ubiquitous during summer in stratified water. Chlorophyll *a* in the subsurface maximum layer is generally 2–8 times the concentration in the overlying and underlying water and approaches 50–75% of the levels observed throughout the upper mixed layer during WS-bloom.

The composite profiles of chlorophyll *a* also reveal large vertical gradients in the size composition of phytoplankton during the stratified season. Usually, percent netplankton increases with increasing depth below surface. In some areas, such as the midshelf and outer shelf Middle Atlantic Bight (Fig. 23), percent netplankton increases from ~10–20% at surface to 40–70% at 50 m below surface, suggesting substantial vertical differences in the species composition of phytoplankton. Similar but less sharp gradients are observed during summer in the deeper stratified water on Georges Bank and in the Gulf of Maine.

In general, during late fall and winter the water column is well-mixed and chlorophyll *a* is evenly distributed throughout the water column in shallower areas and to ~35–50 or 100 m in some of the deepest areas sampled (Figs. 23–25). The transition between summer stratification and well-mixed conditions begins as the upper mixed layer deepens, the water column chlorophyll *a* maximum is found near surface, and the distributional pattern changes to declining. Subsequent deepening of this upper mixed layer leads to the uniform chlorophyll *a* distribution observed during winter. This

pattern is clear in the Gulf of Maine, deeper waters of Georges Bank, and in the Middle Atlantic Bight from midshelf to the slope. In general, the bell shape disappears during September (Jordan Basin, Georges Basin, and the northern Gulf of Maine) or October (remaining areas where summer stratification is observed). By November, chlorophyll *a* is vertically uniform in the upper 35–50 m and remains so until February–March when the transition to stratified conditions begins. In the Gulf of Maine (except the western gulf) and the

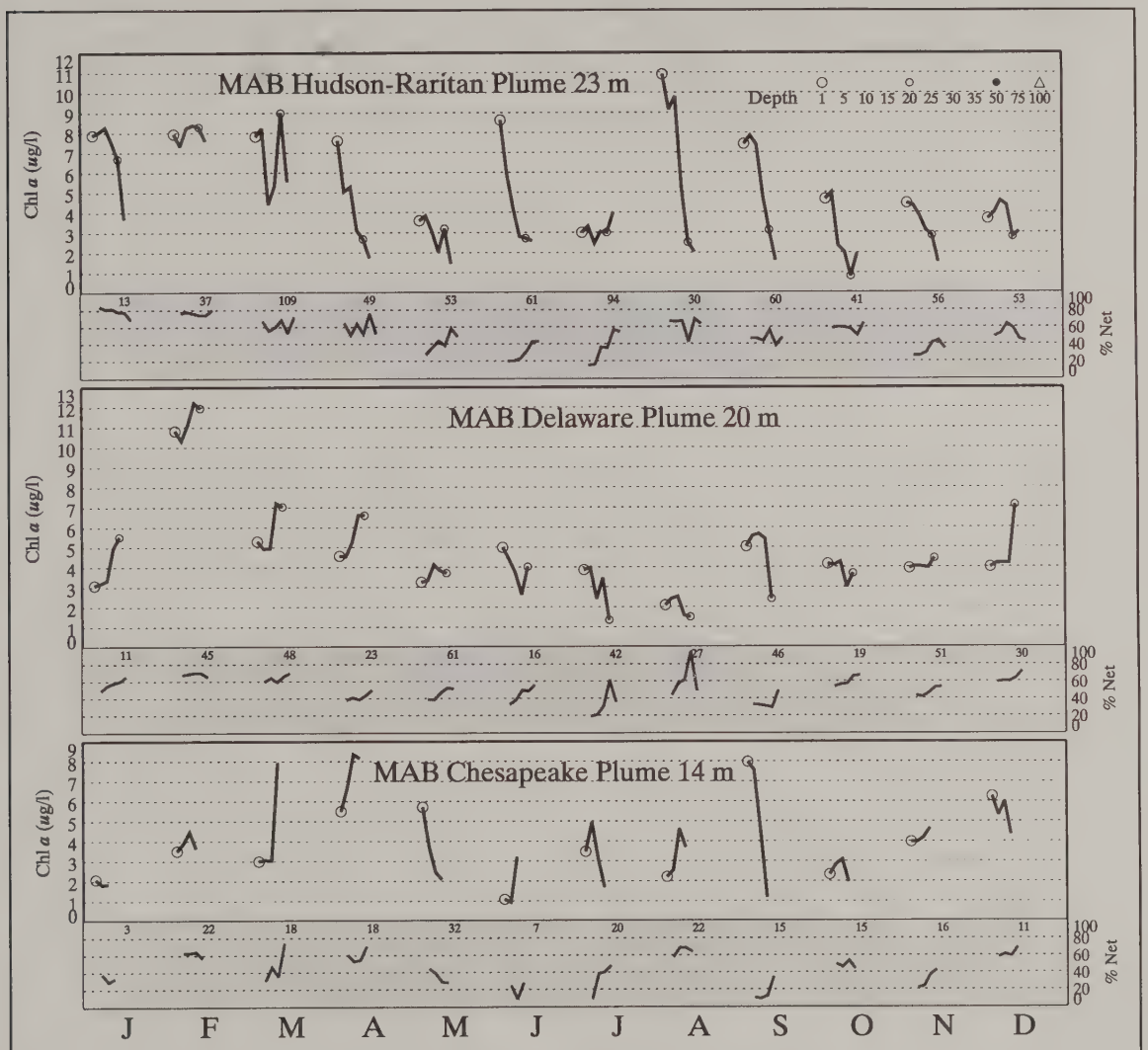

Figure 23

Monthly composite profiles of chlorophyll *a* and percent netplankton for subareas in the Middle Atlantic Bight. (See Fig. 8 for location of subareas.) The profiles were generated by averaging all observations within each of 11 depth strata by month. Depth strata bracketed standard sampling depths; 1 m (0<3); 5 m (3<8); 10 m (8<13); 15 m (13<18); 20 m (18<23); 25 m (23<28); 30 m (28<33); 35 m (33<38); 50 m (38<63); 75 m (63<88); 100 m (88<113). Four strata are marked: 1 m (large open circle), 20 m (small open circle), 50 m (small solid circle), and 100 m (large open triangle). The number of water samples in the monthly composite is shown below each chlorophyll *a* profile.

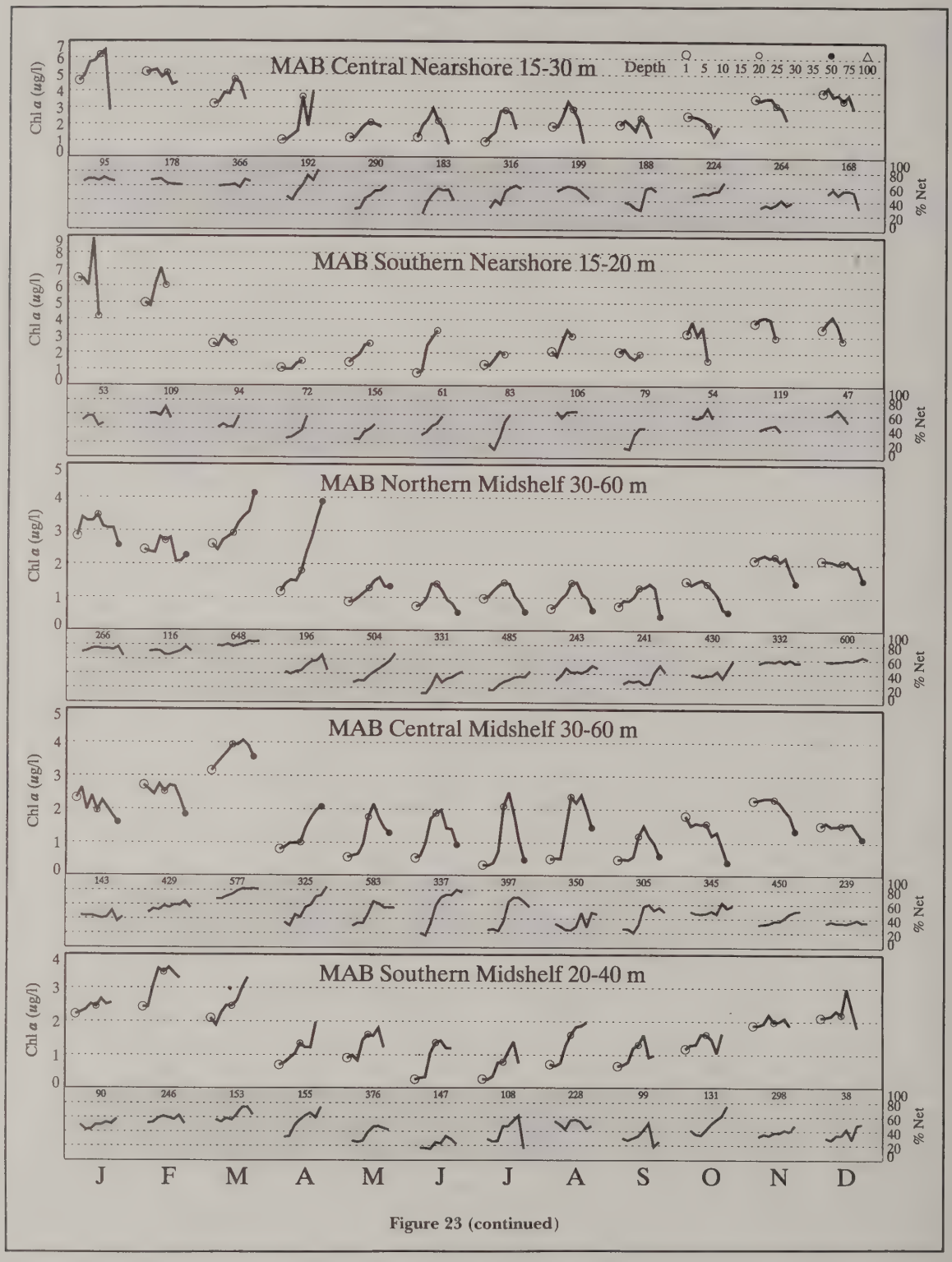

Figure 23 (continued)

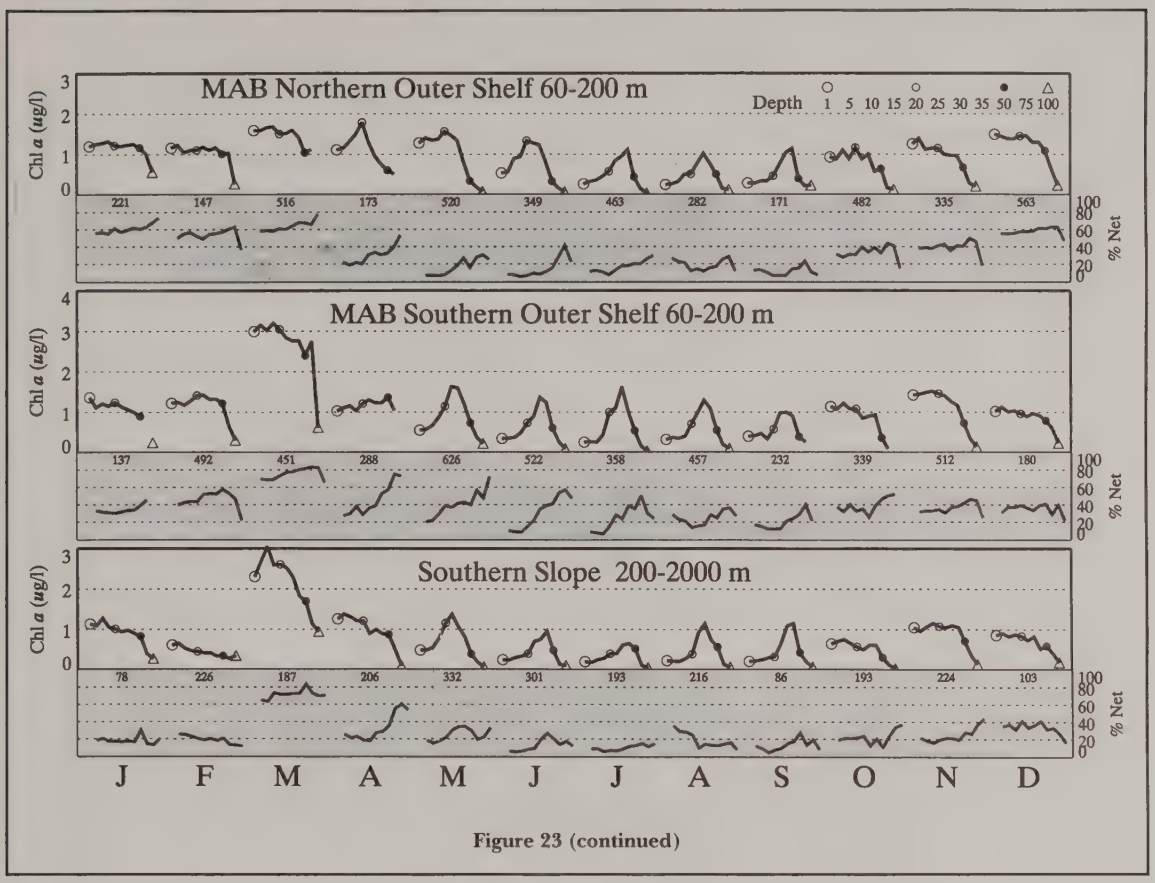

Figure 23 (continued)

southern slope of the Middle Atlantic Bight, the depth of uniform chlorophyll distribution deepens to 100 m in January and/or February.

Unlike the fall transition, when water column distribution patterns are similar among all areas that are stratified, the distributional pattern in the water column during spring transition varies among areas. By February or March in nearshore and midshelf Middle Atlantic Bight, chlorophyll *a* is distributed in the water column in an inverted pattern and remains so until the appearance of the bell-shaped distribution. In slope waters, outer shelf Middle Atlantic Bight, and the Gulf of Maine, the spring profile is declining. Generally the transition starts in March in southern waters and in April in northern gulf and Georges Bank waters. Regardless of area, it generally takes two months for the bell-shaped distribution and subsurface maximum to appear, occurring in May in the south and June in the north. Once formed, the bell shape is most distinct in the Middle Atlantic Bight (central nearshore, northern and central midshelf, outer shelf and slope); Georges Bank southern flank and northern slope; and Gulf of Maine, all regions except Scotian Shelf. In other areas, subsurface maxima are present but the bell shape is missing (Middle Atlantic Bight southern nearshore; Scotian Shelf) or weakly defined (Middle Atlantic Bight southern midshelf; Georges Bank Great South Channel, eastern outer shoals, and southern flank).

In shallow areas influenced by estuarine plumes and in the shoal areas of Georges Bank (Figs. 23- 25), the vertical distribution of chlorophyll *a* does not fit the seasonal cycle described above. Vertical profiles for subareas adjacent to the Hudson-Raritan, Delaware, and Chesapeake estuaries are "noisier" than comparable nearshore areas remote from the estuaries. This is expected, given the high temporal variability, sharp horizontal gradients associated with estuarine plumes, the small size of these subareas, and our infrequent sampling. In the Hudson-Raritan Plume, for instance, the chlorophyll profile shape is declining within the water column throughout the year except during February, March, July, and December, when a subsurface maximum is present (Fig. 23).

The following sections characterize monthly variation in the vertical distribution of chlorophyll *a* by region and subarea, beginning with the Middle Atlantic

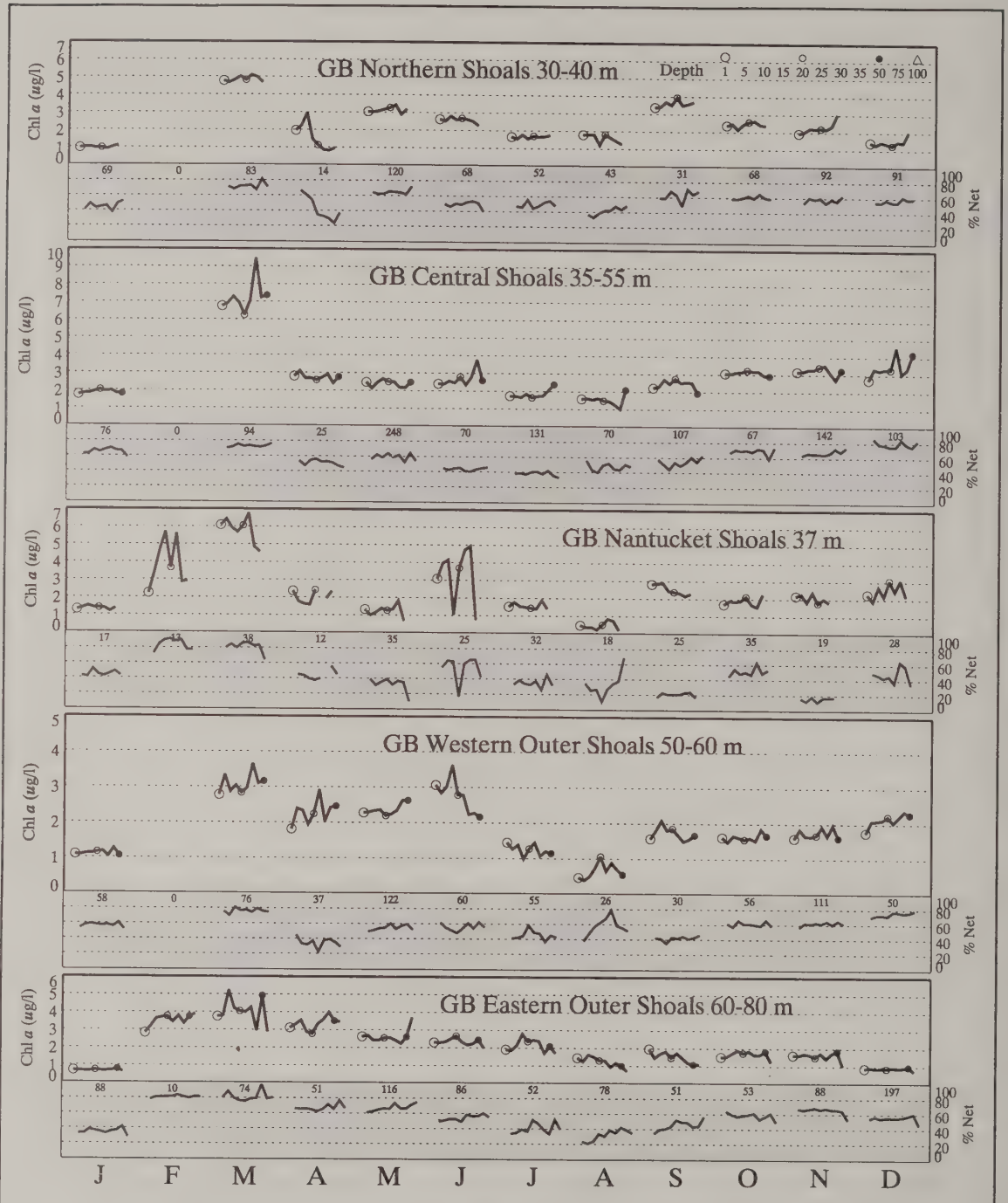
GB Northern Shoals 30-40 m
Depth 1 5 10 15 20 25 30 35 50 75 100
GB Central Shoals 35-55 m
GB Nantucket Shoals 37 m
GB Western Outer Shoals 50-60 m
GB Eastern Outer Shoals 60-80 m
Chl a (ug/l)
% Net
J F M A M J J A S O N D

Figure 24

Monthly composite profiles of chlorophyll *a* and percent netplankton for subareas on Georges Bank. See Fig. 8 for location of subareas and Fig. 23 caption for additional details.

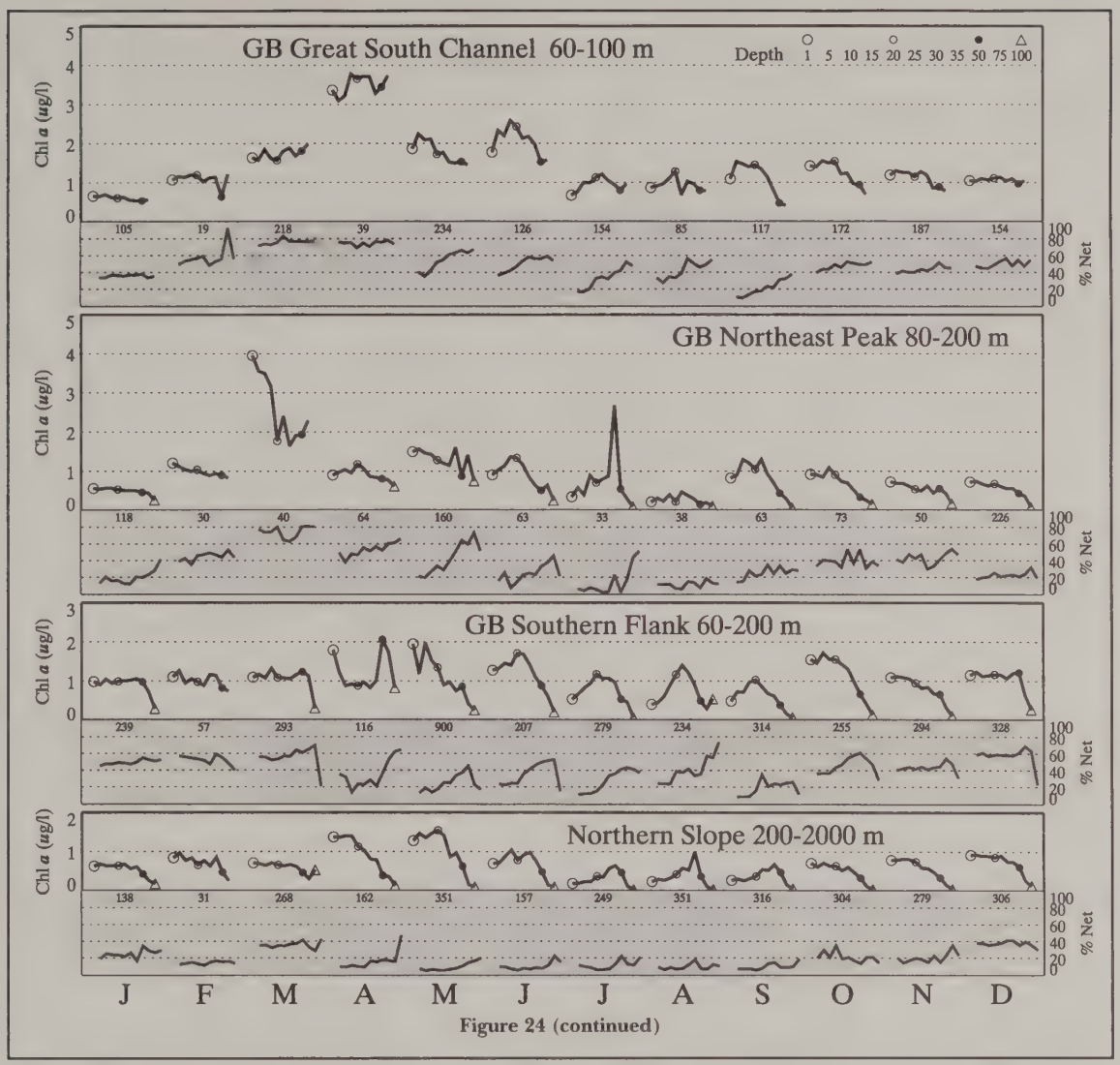

Figure 24 (continued)

Bight. Once basic patterns in the annual cycle are familiar, only noteworthy similarities and differences between previously described subareas are presented to avoid repetitious descriptions.

Middle Atlantic Bight—A number of temporal and spatial distributional features evident in the water column average concentrations discussed earlier are also evident in the composite vertical profiles for the Middle Atlantic Bight (Fig. 23). The general trend of decreasing phytoplankton biomass from nearshore to slope water is readily discerned. With some exceptions, this onshore-offshore gradient is present at each depth stratum year-round; however, the gradient is steeper in surface water than at mid-depths in the column. The general trend of decreasing netplankton dominance from nearshore to the slope is also illustrated in the composite profiles and is particularly evident during summer (Fig. 23).

Hudson-Raritan Plume—In the Hudson-Raritan Plume subarea, highest chlorophyll *a* is usually observed in the surface; chlorophyll *a* generally decreases toward the bottom of the water column. The WS-bloom appears during January–February as an increase in both chlorophyll *a* and percent netplankton from November–December. Winter-spring bloom is strongly dominated by netplankton, presumably diatoms. The annual maximum biomass in surface water appears in August when brackish water from the estuary generates the annual minimum surface salinity (Benway et al., 1993).

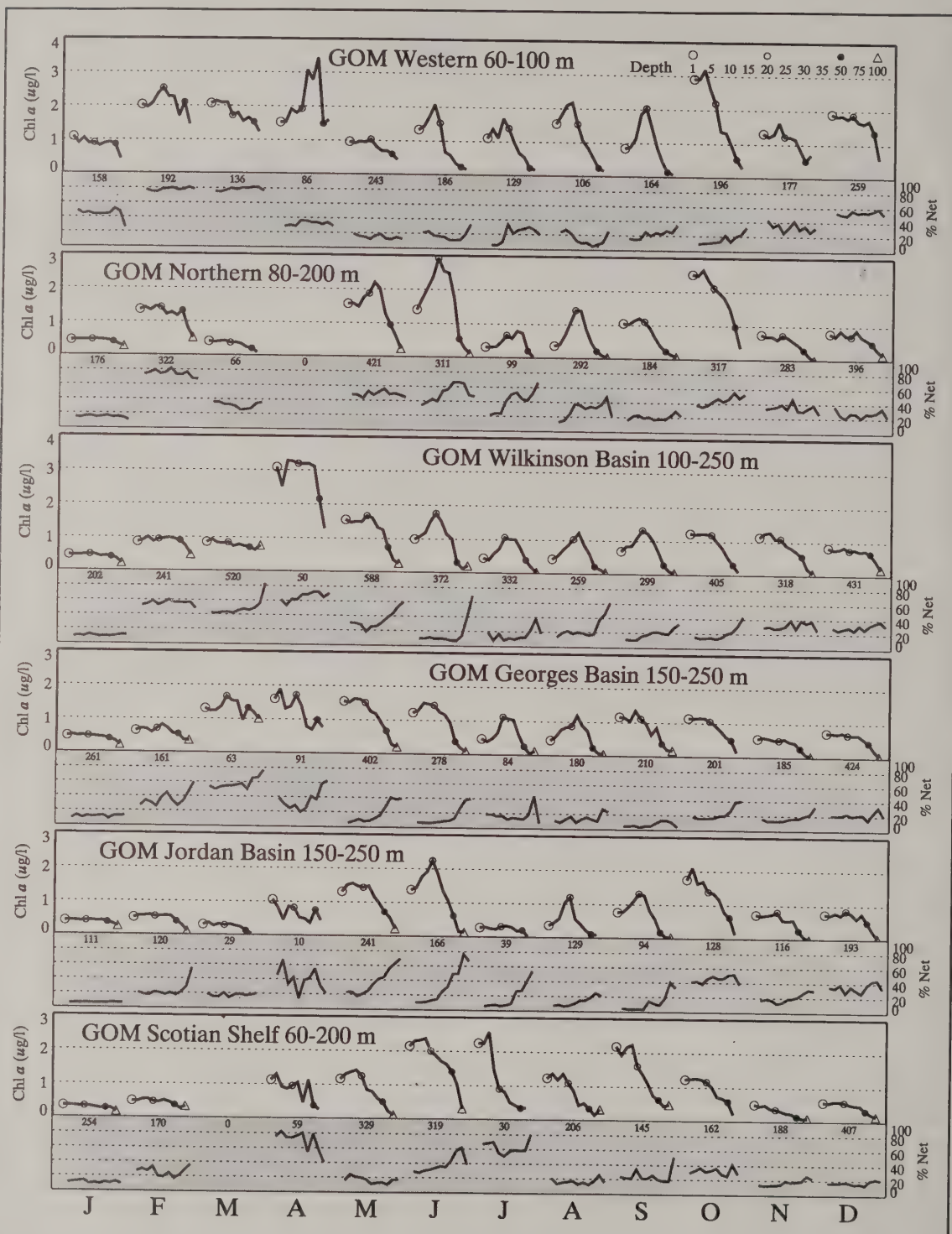

Figure 25

Monthly composite profiles of chlorophyll *a* and percent netplankton subareas of the Gulf of Maine. See Fig. 8 for location of subareas and Fig. 23 caption for additional details.

Over the annual cycle, netplankton prevail over nanoplankton, except during May–June when nanoplankton dominate in the upper layer. During the remaining months, vertical gradients in size composition are weak.

Delaware Plume—Despite the small sample size used to form composite profiles, an annual chlorophyll *a* cycle is evident (Fig. 23). A vigorous WS-bloom, strongly dominated by netplankton with chlorophyll *a* exceeding 10 µg/l, is observed in February (in January there is insufficient sampling). Following WS-bloom, chlorophyll *a* declines, reaching minima during the stratified season as netplankton are replaced by nanoplankton. Vertical size composition gradients are weak except perhaps during May–August when percent netplankton increases with depth.

Chesapeake Plume—Sampling frequency is inadequate to characterize well the general vertical and seasonal trends in the Chesapeake Plume subarea, except to note that chlorophyll *a* is generally elevated and in the same range as observed for the Hudson-Raritan and Delaware Plume subareas. In August, a species-succession favoring netplankton occurs here, as well as in the Delaware and Hudson-Raritan subareas.

Nearshore—In the central and southern nearshore, mean chlorophyll *a* is elevated above 1 µg l^{-1} throughout the year in nearly all depth strata (Fig. 23). The annual cycle is well defined, with minima during the stratified season and maxima during the unstratified season. Chlorophyll *a* and netplankton increase progressively from September to the WS-bloom maxima. Thus, WS-bloom is defined more by the timing of the annual peak than by abrupt changes in either biomass or phytoplankton size composition. Winter-spring bloom in the southern nearshore occurs during January–February but in the central nearshore it persists from January through March, and netplankton are more abundant.

During October, a fall bloom is indicated by chlorophyll *a* and netplankton increases over September values. The fall bloom in the southern nearshore is marked by more abrupt increases in chlorophyll *a* and percent netplankton than that in the central nearshore. Furthermore, the fall bloom does not constitute the secondary annual maximum since biomass following the bloom, in November–December, is higher.

Subsurface chlorophyll *a* maxima (SSM) emerge 15–20 m below surface during June–August. Chlorophyll *a* in these maxima is more than half the concentration observed during WS-bloom. Subsurface maxima tend to be near bottom in the relatively shallow southern nearshore water column; in the central nearshore, profiles take on a bell shape with lower chlorophyll *a* above and below the SSM. Bell shape profiles weaken in September and are replaced by more vertically uniform chlorophyll *a* and percent netplankton profiles during October. Presumably this is the result of destratification of nearshore water which can begin, with significant interannual variation, throughout September and is usually complete by mid October (Ingham et al., 1982).

From October through March, the period when vertical density stratification is weak and intermittent in the nearshore Middle Atlantic Bight, there are shifts in the size composition of the phytoplankton and in the magnitude of chlorophyll *a*, but the percent netplankton profiles are essentially vertically uniform (Fig. 23). In contrast, during the stratified season, there are vertical gradients in phytoplankton size composition. For instance, during July percent netplankton increases from ~10% near surface to ~60% at the bottom of the southern nearshore profile (Fig. 23). The percent netplankton profile for August presents an exception to this pattern; netplankton prevail throughout the water column. Perhaps this netplankton shift from the preceding month reflects the appearance of large motile dinoflagellates? Alternatively, nonmotile netplankton may be responsible. Benway et al. (1993) report relatively large temperature variations nearshore during August, which they attributed to wind-forced mixing of the shallow water column and upwelling/downwelling events. Presumably these interruptions of stratification enrich the surface waters with subpycnocline nutrients as well as reinject netplankton species, already abundant near the bottom of the column, into the upper layer.

In the nearshore Middle Atlantic Bight, netplankton are an important component of the plankton from October through April, and during August (Fig. 23). In fact, this sustained contribution by netplankton throughout much of the year is a characteristic feature of the nearshore bight.

Midshelf—As in the nearshore, a clear annual chlorophyll *a* cycle is evident in the three midshelf subareas (Fig. 23). Netplankton increase during a prolonged WS-bloom beginning in January, achieving maximum dominance in March. The precipitous netplankton decline in April, particularly in the upper column, signifies the end of the WS-bloom.

A secondary biomass peak, half that achieved during WS-bloom, appears during the October fall bloom. There are important differences between WS-bloom and fall bloom. During the WS-bloom, biomass is elevated throughout the water column and netplankton clearly dominate, but during fall bloom biomass increases are restricted to the upper 20 m and netplankton and nanoplankton are approximately equal.

There is indication that WS-bloom diatoms are settling out of the water column in March and April; the shape of the composite chlorophyll *a* profile (inverse) is very different from the vertically uniform profiles in January and February and from those constructed for the rest of the year. April biomass progressively in-

creases fourfold from surface to near bottom in the northern midshelf, and twofold in the central midshelf and southern midshelf. Additionally, large vertical gradients in phytoplankton size composition and presumably species composition are established in April following WS-bloom; nanoplankton replace netplankton in the upper column and netplankton continue their prevalence in the lower column.

The annual minimum surface chlorophyll *a* is during June–August when pronounced SSM appear in the seasonal thermocline 20–25 m below surface. Biomass in the central midshelf SSM approaches values observed during WS-bloom. Steep vertical gradients in phytoplankton size composition appear from April through September, the steepest in the central midshelf. Similar to the nearshore, there is an August netplankton pulse in the southern midshelf and an increase in percent netplankton without concomitant increase in biomass in the northern midshelf.

Outer Shelf—The basic features of the annual cycle in the outer shelf regions are similar to those for midshelf and nearshore areas, but there are notable differences in the shapes of the composite vertical profiles, the magnitude and timing of maxima, and in the size composition of the phytoplankton. In the midshelf region, WS-bloom is prolonged from January through March; in the outer shelf WS-bloom appears distinctly during March.

In the southern outer shelf, netplankton achieve their maximum dominance during March, as biomass triples over values during February. Netplankton in the northern outer shelf are dominant as early as January, but increases in biomass also do not occur until March. The WS-bloom in the southern outer shelf is twice as intense as the northern outer shelf. A marked shift from netplankton to nanoplankton dominance from March to April signals the conclusion of WS-bloom. Netplankton are still relatively abundant toward bottom following WS-bloom, but phytoplankton do not appear to accumulate in the lower water column in April, as in the midshelf bight.

Phytoplankton size composition is vertically uniform, or percent netplankton increases slightly with increasing depth from October through March. Exceptionally large vertical gradients in phytoplankton size composition are established in the southern outer shelf during April–July. For example percent netplankton grades from ~10% in surface waters to ~60% near bottom in June. Presumably, this reflects major vertical gradients in the species-composition of the phytoplankton. Vertical gradients in phytoplankton size composition are less sharp in the northern outer shelf.

During the October fall bloom, biomass increases in the upper 30–35 m of the column but not below. Nanoplankton dominate the fall bloom, in sharp contrast to the strong netplankton dominance during WS-bloom. The fall bloom, though modest compared with the WS-bloom, nevertheless represents a four- to fivefold increase in biomass over levels in the upper surface layer during stratified conditions. Moreover, as in the nearshore Middle Atlantic Bight, biomass throughout the column in November–December exceeds that of the fall bloom.

Southern Slope—The annual biomass cycle in the southern slope is similar to that observed in adjacent outer shelf areas of the Middle Atlantic Bight, but biomass is generally lower in slope water. A distinct and intense WS-bloom occurs in March. The WS-bloom represents a fivefold increase in chlorophyll *a* over values during February and a shift from 20% to 70% netplankton. The WS-bloom collapse in April is marked by a decrease in chlorophyll *a* and a shift to strong dominance by nanoplankton in the upper column. Note that netplankton are still relatively abundant toward the bottom of the April profile, possibly indicating a residual WS-bloom community which is subsequently replaced by nanoplankton in May.

Over the annual cycle, netplankton are not as abundant in the southern slope as in the adjacent southern outer shelf. Netplankton dominate only during March and near the bottom of the water column during April. The remainder of the time, including the October fall bloom, nanoplankton predominate.

Beginning in May and continuing through September, SSM develop in the seasonal thermocline 25–35 m below surface. Vertical gradients in percent netplankton are much less pronounced at this time than in the adjacent southern outer shelf. Percent netplankton is quite low in the SSM layer, suggesting that floristic composition of the thermocline community in the southern slope differs greatly from that of the outer and midshelf Middle Atlantic Bight.

Following the modest October fall bloom in the upper 40 m, biomass becomes more vertically uniform, with increasing destratification from November through January. By February the most vertically homogeneous conditions are established in the slope water.

Georges Bank

Northern and Central Shoals—Phytoplankton biomass in the northern and central shoals is comparable to the high levels observed in central nearshore and southern nearshore areas of the Middle Atlantic Bight but less than nearshore areas of the bight influenced by estuarine plumes (cf. Figs. 23 and 24; also see Table 3).

The annual chlorophyll *a* maximum (~5–7 µg/l) is observed in March. There are no observations in February. However, biomass is exceptionally high throughout the water column during March, as percent netplankton exceeds 70% and biomass declines markedly

Table 3

Water column chlorophyll *a* concentration (μg l^{-1}) by subarea and month. Underlined entries indicate WS-bloom period; bold font indicates the probable peak in WS-bloom.

Region	Subarea	JAN	FEB	MAR	APR	MAY	JUN	JUL	AUG	SEP	OCT	NOV	DEC	Mean	Rank
Middle Atlantic Bight	Hudson-Raritan plume	7.63	**8.14**	6.23	4.87	2.99	4.36	3.38	6.09	6.83	2.77	3.63	4.11	5.09	1
	Delaware plume	3.99	**11.25**	5.59	5.06	3.67	3.76	2.95	2.13	4.89	3.98	4.11	4.31	4.64	2
	Chesapeake plume	1.91	**4.06**	3.35	8.36	4.15	1.47	3.82	3.03	6.78	2.69	4.06	5.73	4.12	3
	Central nearshore	5.32	**5.25**	3.88	1.72	1.67	2.13	1.84	2.28	1.98	2.42	3.49	4.00	3.00	6
	Southern nearshore	6.69	**5.37**	2.62	1.11	1.93	1.77	1.72	2.38	1.95	3.08	4.01	3.76	3.03	5
	Northern midshelf	3.08	2.53	**3.08**	2.11	1.19	1.03	1.14	1.02	1.06	1.23	2.06	1.96	1.79	11
	Central midshelf	2.21	2.55	**3.67**	1.28	1.24	1.30	1.09	1.45	0.81	1.44	2.13	1.45	1.72	12
	Southern midshelf	2.36	**3.04**	2.32	1.00	1.24	0.74	0.64	1.12	0.96	1.45	1.99	2.21	1.59	13
	Northern outer shelf	1.19	1.07	**1.40**	0.93	0.85	0.66	0.55	0.48	0.53	0.78	0.93	1.12	0.87	18
	Southern outer shelf	1.36	1.25	**2.81**	1.16	0.92	0.68	0.63	0.65	0.56	0.79	1.09	0.90	1.07	16
	Southern slope	0.85	0.42	**1.98**	1.01	0.61	0.48	0.40	0.47	0.48	0.48	0.85	0.71	0.73	24
Georges Bank	Northern shoals	0.99		**4.93**	1.36	3.18	2.58	1.62	1.64	3.68	2.44	2.18	1.36	2.50	7
	Central shoals	1.90		**7.29**	2.70	2.49	2.50	1.77	1.45	2.52	3.14	3.30	3.30	3.05	4
	Nantucket shoals	1.37	4.43	**6.39**	2.06	1.23	3.43	1.54	0.48	2.48	1.80	2.04	2.31	2.46	8
	Western outer shoals	1.15		**2.98**	2.47	2.41	2.51	1.30	0.65	1.67	1.61	1.67	2.22	1.95	10
	Eastern outer shoals	0.70	3.62	**4.38**	3.43	2.64	2.27	2.13	1.20	1.38	1.64	1.51	0.90	2.15	9
	Great South Channel	0.58	1.13	1.76	**3.47**	1.65	1.98	0.97	0.89	0.91	1.13	1.06	1.04	1.38	14
	Northeast peak	0.50	0.93	**2.28**	0.91	1.21	0.80	0.63	0.26	0.72	0.60	0.57	0.53	0.83	22
	Southern flank	0.94	**0.96**	1.18	1.63	1.27	1.14	0.76	0.68	0.66	1.08	0.79	1.06	1.01	17
	Northern slope	0.50	0.61	0.57	0.81	0.96	0.60	0.37	0.39	0.41	0.45	0.51	0.67	0.57	26
Gulf of Maine	Western	0.86	**2.01**	1.75	1.91	0.79	0.82	0.78	1.07	0.80	1.57	0.95	1.50	1.23	15
	Northern	0.41	**1.24**	0.29		1.31	1.38	0.38	0.55	0.67	1.52	0.45	0.57	0.85	20
	Wilkinson Basin	0.43	0.89	0.75	**2.51**	1.07	0.86	0.63	0.53	0.59	0.72	0.74	0.71	0.87	19
	Georges Basin	0.43	0.60	**1.41**	1.13	0.98	0.84	0.55	0.52	0.75	0.81	0.36	0.55	0.74	23
	Jordan Basin	0.39	0.48	0.21	**0.63**	1.00	1.07	0.21	0.38	0.68	1.07	0.43	0.61	0.60	25
	Scotian Shelf	0.31	0.46		**0.88**	0.80	1.64	0.89	0.68	1.19	0.85	0.27	0.46	0.85	21

from March to April. Taken together, this suggests the WS-bloom probably begins in February, peaks during March, and is over by April. This is supported by Curra (1987) who examined phytoplankton counts and changes in species-composition. The magnitude of WS-bloom is comparable but it does not persist as long as the nearshore Middle Atlantic Bight WS-bloom.

Following WS-bloom, chlorophyll *a* is sustained at high levels (~2 μg l^{-1}) throughout the water column through June. Annual chlorophyll *a* minima are during July–August and in January. The January minimum is lower than January biomass in comparably deep areas of the midshelf Middle Atlantic Bight where WS-bloom is already underway (cf. Figs. 23 and 24).

Fall bloom appears during September, with chlorophyll *a* increases above the summer minimum and netplankton more dominant. But fall bloom in the northern shoals appears greater than in the central shoals. Following fall bloom, chlorophyll *a* increases through December in the central shoals but decreases in the northern shoals.

A strong seasonality in the phytoplankton size composition is present in the central shoals. Netplankton dominate standing stocks from October through March when peak dominance (75% netplankton) occurs, whereas nanoplankton achieve only weak dominance (40% netplankton) from June through August. The abundance of netplankton throughout the year is a characteristic feature of the shallow water on Georges Bank.

The vertical distribution of chlorophyll *a* is essentially uniform throughout the year, as are composite profiles of phytoplankton size composition. There is no well-defined SSM layer characteristically found in areas that undergo vertical density stratification during summer. Temperature and salinity are also vertically uniform throughout the year (Bisagni and Sano, 1993). This vertical uniformity is the consequence of vigorous mixing, primarily by tidal currents which reach magnitudes of 70–80 cm s^{-1} over the shoals (Fig. 3). Perhaps only during December is the estimated critical depth (O'Reilly et al., 1987) below the seafloor in the shallow water on the Bank.

Nantucket Shoals—Even though sampling in this subarea is suboptimal, the annual phytoplankton cycle resembles that of the northern and central shoals. Similarities include the magnitude and timing of WS-bloom and fall bloom, the occurrence of annual minima in

January and August, and the size composition of the phytoplankton throughout the year.

Western and Eastern Outer Shoals—The annual chlorophyll *a* cycle in the western and eastern outer shoals (Fig. 8) has many features in common with the northern and central shoals: Winter-spring bloom peaks in March, there is a modest fall bloom in September, and there are annual chlorophyll *a* minima in January and August. Chlorophyll *a* and percent netplankton are also vertically uniform but biomass profile is more variable, and well-defined SSM do not persist during summer. The major difference is that biomass is generally lower in the western and eastern outer shoals than in the northern and central shoals (also see Table 3).

Following WS-bloom, netplankton persist in the eastern outer shoals in April but are replaced by nanoplankton (the usual successional pattern) in the western outer shoals. There is also a trend of higher chlorophyll *a* during December and January in the western outer shoals.

Great South Channel—This subarea is slightly deeper than the adjacent western outer shoals (Fig. 8). Following the annual biomass minimum in January, netplankton steadily accrue until the March–April WS-bloom. From May through September, netplankton are replaced by nanoplankton in the upper column but continue to prevail in the lower column, and weak SSM are present in the seasonal thermocline. As in the western outer shoals, high chlorophyll *a* persists until June, followed by a secondary annual biomass minimum during July–August.

Fall bloom in September is modest, limited to the upper column, and dominated by nanoplankton. From October to January, netplankton become as abundant as nanoplankton, chlorophyll *a* decreases near surface but increases at the bottom of the column, and chlorophyll *a* and percent netplankton profiles become increasingly more vertically uniform, as expected with increasing wind mixing.

Northeast Peak—Chlorophyll *a* and netplankton steadily increase from January to WS-bloom climax during March. Sharp vertical gradients in size composition appear during May, and perhaps June–July, but not the remainder of the year. Nanoplankton are responsible for a greater share of biomass during summer here than in the shallower areas of Georges Bank.

Southern Flank—Perhaps the most interesting feature in the biomass cycle in the southern flank is the relatively weak netplankton dominance and low biomass achieved during WS-bloom. The bloom is not easily discerned; based on phytoplankton size composition, the peak may be in March, but biomass levels are higher in April (upper 15 m) and even higher in May when nanoplankton species prevail. This pattern contrasts sharply with the intense, distinct WS-bloom in the comparably deep southern outer Middle Atlantic Bight shelf (cf. Figs. 23 and 24).

A weak SSM is present in the thermocline and relatively steep vertical gradients in the size composition of the phytoplankton occur from May throughout September, but not during the remainder of the year when the water column is not well-stratified. The October fall bloom occurs one month later than the bloom in other areas of Georges Bank and is not dominated by nanoplankton. There is a trend of increasing vertical homogeneity in chlorophyll *a* and percent netplankton profiles from October to January, presumably the consequence of increased wind mixing of the column during winter. This is also evident in individual synoptic cross-bank sections (Append. B).

Northern Slope—The overall annual cycle is similar to the cycle in the southern slope, except WS-bloom in the northern slope is much weaker, appears later (in April), and is comprised of nanoplankton (cf. Figs. 23 and 24). Low chlorophyll *a* ($<0.5\ \mu g\ l^{-1}$), typically observed in stratified surface waters, appears during May in the southern slope but not until July in the northern slope.

Nanoplankton dominate the community throughout the water column during all months. During summer, netplankton do not increase toward the bottom of the column in the northern slope as they do in the adjacent southern flank of Georges Bank. This is a major difference between these two areas, and matches the floristic transition from the southern outer Middle Atlantic Bight shelf to the adjacent southern slope.

Gulf of Maine

Western Gulf of Maine—The annual minimum surface chlorophyll *a* occurs during January. Netplankton become strongly dominant as chlorophyll *a* doubles to $2\ \mu g\ l^{-1}$ during February, and persist at this level through March (Fig. 25). The February–March bloom is weak relative to WS-blooms in the Middle Atlantic Bight and the shallow area on Georges Bank. Like most other WS-blooms in the study area, it is strongly dominated (80%) by species in the netplankton, presumably diatoms.

During April, a second, more intense nanoplankton-dominated WS-bloom appears. Tentatively, we suggest that this is a second WS-bloom because its size composition, and presumably species composition, is very different from the February–March bloom. (The composite profile for April is based on few observations so it must be considered with caution.) Biomass is greatest 25–35 m below surface. The size composition of the community is vertically uniform, without indication that netplankton from the preceding bloom are accumulating in the lower column, as is the case in midshelf Middle Atlantic Bight.

Biomass again increases in the upper column during June, but there are no obvious changes in phytoplankton size composition. Subsurface chlorophyll maxima

(~2 μg l^{-1}) emerge 15–20 m below surface from June through September. Biomass in the SSM is similar to the high levels in the thermocline community in central Middle Atlantic Bight. Note that vertical gradients in size composition during summer are weak when contrasted with stratified areas of Georges Bank and the Middle Atlantic Bight. The bell-shaped profiles are not as symmetrical as those for stratified waters in the Middle Atlantic Bight and Georges Bank. In part this is because chlorophyll *a* in the upper mixed layer during summer is greater than that observed in stratified areas of the Middle Atlantic Bight and Georges Bank. Also, biomass is quite low at the bottom of the column during summer: at 50 m below surface, chlorophyll *a* is roughly one-third the values observed at comparable depths along the southern flank of Georges Bank and outer shelf areas of the Middle Atlantic Bight.

The annual surface biomass maximum is during the October fall bloom. The bloom is largely confined to the upper 25 m and represents a fivefold biomass increase above September levels. This peak is strongly dominated by the nanoplankton and surpasses fall blooms in all other subareas except the nearshore Middle Atlantic Bight and the shallow water on Georges Bank (cf. Figs. 23, 24, and 25). Moreover, this annual cycle differs greatly from those constructed for the Middle Atlantic Bight, Georges Bank, and slope areas, in which fall bloom is clearly subordinate to the WS-bloom.

Northern Gulf of Maine—Annual minima surface chlorophyll *a* occur in January and March, just before and after the weak WS-bloom in February (Fig. 25). Netplankton are exceptionally low (<10%) during January. This is a characteristic feature of deep regions within the study area, such as the entire Gulf of Maine (except western gulf), northeast peak on Georges Bank, and northern and southern slope subareas.

Biomass in the upper 30 m during May–June is high relative to levels achieved during the WS-bloom, and consists of equal proportions of netplankton and nanoplankton. Moderate vertical gradients in size composition are established from June through September and netplankton are relatively more abundant during summer here than in the western gulf. As in the western gulf, a fall bloom which exceeds the WS-bloom is evident in surface water during October.

Wilkinson Basin—During February, biomass increases above the annual minimum in January and netplankton begin to prevail, but maximum biomass is not reached until April (Fig. 25). This slowly developing WS-bloom surpasses those in other areas of the Gulf of Maine. The bloom is over by April as indicated in the nanoplankton dominance in the upper layer. An SSM is present in the general vicinity of the seasonal thermocline from June–September. Biomass in the SSM is generally less than in the western gulf.

Georges Basin—The essential features of the annual phytoplankton cycle are similar to those of Wilkinson Basin. The biggest difference involves the progression and makeup of the WS-bloom(s). From February through March, netplankton dominance and biomass increase. But biomass does not peak until April, when the community shifts to nanoplankton. Our tentative interpretation is that the March and April peaks represent two distinct but modest WS-blooms comprised of different species of phytoplankton. Perhaps what is lacking in the annual progression is the usual precipitous decline in biomass that punctuates the conclusion of the WS-bloom and the start of nanoplankton prevalence as seasonal stratification intensifies.

Biomass doubles in surface water in September and nanoplankton achieve maximal dominance. Fall bloom starts one month earlier here than in the Wilkinson Basin, perhaps resulting from lower water column stability (see below) and earlier destratification. Only during April do netplankton achieve weak dominance over nanoplankton; the rest of the year nanoplankton strongly dominate.

Jordan Basin—It appears that a netplankton WS-bloom does not occur in the Jordan Basin until April and it is weak relative to WS-blooms in Wilkinson and Georges Basin. Biomass during April barely exceeds 1 μg l^{-1}. This conclusion must be tentative since sampling frequency in March and April was poor.

A nanoplankton increase in the upper layer appears in May and is sustained through June, as is the case in the Wilkinson and Georges Basins and northern gulf subarea. The steepest vertical gradients in size composition in the Gulf of Maine appear over Jordan Basin during May, June, and July. Fall bloom appears during October; netplankton play a larger role in the bloom than in any other subareas in the gulf where the fall bloom is strongly dominated by nanoplankton.

Scotian Shelf—Surface concentrations decline from October to January, the annual minimum. Except for the vertically uniform chlorophyll *a* profile during January and February, most of the chlorophyll *a* decreases with increasing depth. Subsurface chlorophyll *a* maxima are weak and very near surface from May through September. The relatively high chlorophyll *a* and percent netplankton during April, and the abrupt shift to nanoplankton in May, suggest that the WS-bloom may peak during April. This conclusion is tentative since data are lacking for March.

There is a suggestion of a trend of increasing percent netplankton from May through June, followed by a return to strong dominance by nanoplankton in August. This pattern is not evident in other areas of the Gulf of Maine. The contribution by netplankton to annual standing phytoplankton stocks is generally greater in the Scotian Shelf and other northerly subar-

eas of the Gulf of Maine (Jordan Basin and northern gulf), than in southerly gulf areas.

Winter-Spring Bloom

Sverdrup (1955) introduced the concept of critical depth to explain increases in phytoplankton biomass such as spring bloom. The critical depth is the depth in the water column at which phytoplankton respiration, vertically integrated from surface, equals integrated photosynthesis. The upper mixed layer must be less than critical depth for a net increase in phytoplankton biomass to occur, assuming nutrients are not limiting growth, and grazing and other biomass losses are held constant. Riley (1957) expanded on this and reported a mean radiation of about 0.03 g-cal cm^{-2} min^{-1} or about 40 ly d^{-1} was critical to the onset of flowering. In support, Riley (1957) cited the occurrence of increases in phytoplankton biomass between December and March in Cape Cod Bay (Bigelow, 1926), Long Island Sound (Riley, 1956), coastal waters of Woods Hole (Lillick, 1937), Block Island Sound (Riley, 1952), and Georges Bank (Riley, 1941). More recent observations by Townsend and Spinrad (1986) of the WS-bloom in the Gulf of Maine support Riley's work. Surveys of nearshore shallow water over the past several decades have also revealed that the bloom may commence and even culminate during winter, as early as January or December (Hitchcock and Smayda, 1977). Therefore, "winter-spring bloom" seems a more accurate label than "spring bloom" for this pulse in the annual cycle.

Thus, a strong pulse of phytoplankton growth and increase in biomass occurs during late winter-early spring following increases in incident solar radiation, water temperature and stratification, and reductions in wind velocity and turbulence (Riley, 1957; Yentsch, 1977; Eslinger and Iverson, 1986; Mann, 1993). In shallow water, suitable conditions for the bloom may be met through seasonal increase in incident solar radiation and concomitant increase in mean radiation in the mixed column. In deeper waters, bloom conditions are met through a combination of increased solar radiation and shoaling of the upper mixed layer that occurs with increased stability within the water column. This stability can be accomplished in several ways: by fresh water forming a low salinity surface layer, such as in coastal areas where there is river runoff; by vernal heating of the upper water column and formation of the pycnocline; and by "doming," whereby water from below pushes the mixed layer higher into the water column. Combining with the above is the winter to summer reduction in the average number of wind events that mix the water column (Walsh et. al., 1978; Eslinger and Iverson, 1986).

In a broad temporal sense the above classical picture of WS-bloom is correct. However, recent intensive studies by Falkowski (1991) and others suggest that the WS-bloom paradigm needs reexamination. They found that the WS-bloom does not continuously build, but instead develops as a series of short (3–5 day) pulses of phytoplankton increases. Therefore, our characterizations of WS-bloom based on composited data (multi-year means) at a monthly temporal resolution do not represent well the actual dynamics which proceed at short time scales.

On the northeast U.S. shelf, there are differences among and within regions in the timing, magnitude, duration, and size composition of the WS-bloom. In Table 3 we summarize these differences based on Figs. 23–25 by highlighting (underlining) the WS-bloom period when netplankton biomass increases, and defining peaks (bold entries) for each of the subareas. Winter-spring bloom is prolonged, from January through March, in nearshore, midshelf, and northern outer shelf areas of the Middle Atlantic Bight. The peak occurs earlier in shallow water in the nearshore and midshelf areas, as might be expected based on the critical depth concept. In fact, in the nearshore shallow column, biomass is elevated during November and December, such that additional biomass increases of the WS-bloom seem less dramatic when compared with deeper areas of the shelf. This contrasts with the relatively rapid change in mean photic light levels resulting from spring stratification in the outer shelf and slope regions of the Middle Atlantic Bight (where a distinct pulse is evident in surface waters during spring and fall).

A relatively prolonged WS-bloom also occurs in Great South Channel, Wilkinson Basin, and the Scotian Shelf, with peaks achieved in April. In contrast, more distinct WS-bloom occurs during March in the deep water over the southern slope, April in the northern slope, and March in the northern Gulf of Maine. WS-blooms in subareas of Georges Bank and the Gulf of Maine start later and are generally not as prolonged as those in the Middle Atlantic Bight. Some areas of the shelf appear to have very weak (or ill-defined in our data set) WS-blooms (e.g. southern flank of Georges Bank).

The end of the WS-bloom is most easily discerned by rapid decreases in biomass and a shift to nanoplankton in the upper layer. In some areas (Western Gulf of Maine, Georges Basin, Jordan Basin), the shift to nanoplankton occurs but biomass persists at high levels, leading to the question: Are there two distinct WS-blooms in these areas?

The Fate of WS-bloom

In addition to differences among subareas with respect to the course and magnitude of WS-bloom, there are

also differences among areas following the bloom which have potentially significant consequences to shelf ecosystem trophodynamics. The composite vertical profiles (Figs. 23–25) provide insight into regional differences in the amount and vertical distribution of phytoplankton biomass following WS-bloom, and suggest differences in the fate of the WS-bloom. The inverted profiles provide insight into the near-term fate of the WS-bloom. They are easily identified in March and April profiles for the midshelf Middle Atlantic Bight and perhaps in the central nearshore bight, but are not obvious in mean portrayals for Georges Bank and the Gulf of Maine (Figs. 23–25). The most remarkable inverted profile occurs in the northern midshelf Middle Atlantic Bight in April, and marks the conclusion of the WS-bloom. Here, surface concentrations average ~1 $\mu g\ l^{-1}$ and bottom concentrations average 4 $\mu g\ l^{-1}$ (Fig. 23).

Accumulations of phytoplankton biomass near bottom during March and April 1984 have been reported by Falkowski et al. (1988) and Falkowski (1991), with the largest buildup in the midshelf Middle Atlantic Bight. They observed highest chlorophyll *a* accumulations (10–25 $\mu g\ l^{-1}$) in April in the Middle Atlantic Bight midshelf between the 30–60 m isobath. The mean values we report are less than this, but values exceeding 10 $\mu g\ l^{-1}$ were observed during several surveys (Append. B). These inverted profiles are not an artifact of compositing very diverse vertical distributions, since the preponderance of phytoplankton biomass in near bottom water at this time is seen midshelf in most of the vertical cross-sections along transects A, B, and C (Append. B). These inverted chlorophyll *a* profiles, plus the progressive relative increase in netplankton (presumably diatoms) with depth, indicate the near-term fate of the WS-bloom in these waters: sinking and accumulating in the lower water column and on the seafloor.

Evidence is mounting that much of the WS-bloom is not assimilated in the water column by zooplankton but instead sinks to the lower column (e.g. Lignell et al., 1993) where its subsequent fate (1–4 months) is uncertain. It may be advected off the shelf to the continental slope (Walsh, 1981; Dagg and Turner, 1982), consumed by the benthic community (Townsend and Cammen, 1988), or be remineralized on the shelf (Rowe et al., 1986; Falkowski et al., 1988). Malone et al. (1983b) indicate that between wind events, the netplankton diatom blooms sink and accumulate near bottom but that 90% of the biomass produced during the diatom bloom period is exported to the continental slope. Falkowski et al. (1988) and Falkowski (1991) estimate that 51% of the 1984 spring bloom off the coast of Long Island sank, forming a near-bottom nepheloid layer which was subsequently oxidized. Falkowski et al. (1988) further reported that along-shelf transport of particles in the Middle Atlantic Bight dominates cross-shelf transport during spring and that 50–60% of the along-shelf transport leaves the shelf at Cape Hatteras.

Our composite profiles suggest yet an additional fate for a portion of the WS-bloom phytoplankton. Following WS-bloom, sharp vertical gradients in size composition become established in shelf areas undergoing seasonal density stratification. Nanoplankton prevail in the upper column and netplankton in the lower. For example, in the central midshelf Middle Atlantic Bight, biomass in the lower column steadily declines following the WS-bloom through July, yet netplankton continue to prevail over nanoplankton in the lower column. This leaves open the possibility that residual WS-bloom species may be influencing the floristic composition of phytoplankton below the thermocline during the ensuing summer months, and acting as a seed stock for the fall bloom. Alternatively, the netplankton in the lower column may be comprised of dinoflagellates. Evaluation of this hypothesis will require vertically detailed examinations of the successional patterns of phytoplankton species from spring through summer. To our knowledge, such examinations are lacking.

Despite the manifold trajectories available to WS-blooms on continental shelves, evidence is accumulating that a large portion of the WS-bloom is not grazed by pelagic herbivores but sinks to the bottom of the water column, where it is more likely to enter demersal fishery food webs than pelagic webs. Townsend and Cammen (1988) suggest that benthic production may be enhanced in years with early WS-blooms. In their paradigm, early blooms would persist longer because the relatively cold water present earlier in the annual cycle would retard zooplankton development, growth, and grazing pressure. Conversely, WS-blooms arriving late would be expected to enhance zooplankton production and survival of pelagic fish larvae. They suggest further that variations in the onset and duration of WS-bloom are potentially relevant to understanding variability in recruitment success for some coastal fisheries.

Sampling frequency during our study is insufficient to resolve conclusively interannual variability. However, the concept may be useful in understanding the potential ecological significance of the systematic differences in mean conditions among regions of the continental shelf during and following WS-bloom. For instance, greatest near bottom accumulations of biomass occur during the final stage of prolonged and intense WS-bloom in the midshelf Middle Atlantic Bight. In the portrayals of mean vertical distribution of chlorophyll *a*, inverted profiles characterize the vertical distribution of phytoplankton, where chlorophyll *a* increases from surface to bottom and netplankton are disproportionately more abundant near bottom. The prolonged WS-bloom, characteristic of this area, may explain why these near bottom accumulations are observed here

but not in the Gulf of Maine or on Georges Bank. It seems reasonable to speculate that the benthic community here would benefit more from this pulse than benthos in deep waters of the Gulf of Maine, where netplankton do not appear (on average) to accumulate in the lower column we sampled following WS-bloom. However, since our sampling was limited to the upper 100 m, this conclusion must be tentative for the deep basins in the Gulf of Maine.

Our composite profiles indicate the disappearance in May of the high levels of netplankton chlorophyll observed near bottom during the preceding two months. We suggest that a potentially significant fraction of the spring diatom bloom remains on the shelf in the cold band, influencing the floristic composition of phytoplankton in and below the thermocline during the ensuing summer months. The biomass and percent netplankton profiles in May and June suggest that a fraction of the netplankton WS-bloom persists near bottom. To examine this hypothesis, a detailed knowledge is needed of phytoplankton species successional patterns near bottom following the WS-bloom and into summer.

Stratified Season: Subsurface Chlorophyll Maxima

A pronounced subsurface chlorophyll maximum emerges 20–35 m below surface from May through September in those regions of the continental shelf which undergo and sustain vertical density stratification (Figs. 23–25). Thus, the vertical chlorophyll profile takes a characteristic bell-shape; mean chlorophyll *a* increases from surface to 20–35 m below surface, then decreases progressively toward bottom. The position of the SSM layer during the stratified season is generally coincident with the mean depth of the thermocline and tends to track the thermocline's seasonal and onshore-offshore deepening.

Phytoplankton biomass in the SSM layer may be substantial, between 50–70% of the levels attained during the WS-bloom. Consequently, the amplitude of the seasonal fluctuation in biomass is greatly reduced by these subsurface maxima. For instance, in the southern outer shelf Middle Atlantic Bight, mean surface chlorophyll *a* during July (~0.3 μg l–1) is approximately one-tenth the March value (~3 μg l–1), whereas 30 m below surface, in the SSM layer, chlorophyll *a* (1.8 μg l^{-1}) is more than one-half the WS-bloom chlorophyll *a* maximum (Fig. 23).

Typically, strong vertical gradients in phytoplankton size composition also begin to appear in April–May and persist through the stratified season. These gradients represent a large change from relatively vertically uniform profiles of percent netplankton in March, to profiles which show nanoplankton dominance in the upper layer and increasing netplankton contribution with depth (Figs. 23–25).

Based on extensive hydrographic surveys of shelf water from Cape Sable to Long Island, from 1964–66, Colton (1972) reported that whenever marked vertical density gradients were present: "chlorophyll was concentrated within the thermocline, the maximum depth limit of which seldom exceeded 40 m." Moreover, a series of 2-hour profiles made in June 1966 over a 42-hour period off Cape Cod (41.5°N, 69°W; 100 m) revealed a pronounced SSM layer at an average depth of 30 m (Colton, 1972). In the outer Middle Atlantic Bight during June–July 1979, vertical sections portrayed by Cosper and Stepien (1984) show an SSM layer at 20–40 m. In deeper slope water seaward of the 200 m isobath in the Middle Atlantic Bight (67 profiles), the median depth of SSM during June–September is ~40 m below surface, and 75 m in northern Sargasso Sea water (Cox et al., 1981).

The SSM is generally in the lower half (10–1% of surface light) of the euphotic zone. Though light is suboptimal, the SSM has relatively greater access to higher concentrations of inorganic nitrogen present in and below the thermocline during summer; whereas phytoplankton in the upper euphotic layer depend more upon nutrients made available through heterotrophic recycling. Thus, with ample light and nutrients for growth, the SSM layer contributes significantly to the overall primary productivity of the water column. In the deeper waters on Georges Bank which stratify during summer, the SSM layer is responsible for 37% of the daily integral primary production (O'Reilly et al., 1987). Similarly, 37% of primary productivity takes place below the seasonal pycnocline in the New York Bight shelf (Malone et al., 1983b). Holligan (1978) estimated phytoplankton in the thermocline in the western English Channel were responsible for 30–80% of daily summer production and may contribute as much as the WS-bloom to annual primary production. In stratified waters surrounding the Dogger Bank in the North Sea, the SSM layer was responsible for up to 70% of the integral primary production in May 1990 (Nielsen et al., 1993). In the southern Kattegat, the SSM layer is responsible for 30% of the annual primary production, whereas the spring bloom is responsible for only 19% (Richardson and Christoffersen, 1991).

A number of investigators have reported associations (juxtapositions) between the depth of the SSM layer, the thermocline, and nitroclines (Anderson, 1964; Herbland and Voiturez, 1979; Cox et al., 1981; Cullen and Eppley, 1981; Kiefer and Kremer, 1981; Cullen et al., 1982; Holligan et al., 1984; Townsend et al., 1984; Nielsen et al., 1993). Cullen (1982) reviewed a number of processes potentially responsible for the persistence

of the SSM layer. These include sinking; physiological changes (decreases in the sinking rate from increased phytoplankton buoyancy, in response to increased nutrient concentrations and decreased photosynthetically active radiation (PAR) at the thermocline); behavioral aggregation at the thermocline by motile phytoplankton; greater stability; residence times which are much greater than phytoplankton generation time in the thermocline relative to waters above and below; and depth-differential grazing.

Our purpose here is not to choose among these mechanisms but to underscore the trophodynamic significance of this layer. The SSM is ubiquitous, persists throughout the stratified season, is a productive layer, and therefore represents a concentrated and renewable source of organic matter for herbivores.

Relatively little is known about the species composition of the SSM in the study area. The magnitude, species composition, and temporal variability of the SSM have been shown to be key determinants in the success of the northern anchovy on the west coast of the United States. The dinoflagellate *Gymnodinium splendens* is a nutritionally important food source for first-feeding northern anchovy larvae, and the success of the year class may be partly dependent upon the availability of this organism or other nutritionally comparable dinoflagellates (Lasker, 1975, 1978, 1981).

Seasonal Changes in Subsurface Maxima

To better understand temporal changes in SSM, and its relationship to surface chlorophyll concentrations, the SSR is computed for each vertical profile and portrayed for each subarea (Fig. 26). Subsurface/surface chlorophyll ratios of 1 indicate that the maximum chlorophyll concentration is at the surface; a value of 2 means that chlorophyll *a* concentration at some depth below surface is twice the concentration observed in surface water.

The monthly geometric mean ($mean_g$) SSR is less than 2 from October through March in nearly all 26 subareas (Fig. 26). These low SSR's indicate that vertical variation in phytoplankton biomass is relatively low during the period of minimal vertical density stratification in the upper 40 m (Fig. 27). In the nearshore Middle Atlantic Bight, $mean_g$ SSR drops below 2 in September when destratification may begin during some years (Fig. 26). One month later during destratification in October, mean SSR drops below 2 throughout most of the study area (Fig. 26). SSR's below 2 correspond to density differences between 40 m and surface which are less than 1 sigma-*t* unit (cf. Figs. 26 and 27).

Subsurface/surface ratios increase markedly during the stratified season. Peaks in the monthly $mean_g$ SSR occur from June through September (Fig. 26). These high SSR's result mostly from bell-shaped profiles where the maximum chlorophyll *a* is in the seasonal thermocline at ~20–35 m. In the Middle Atlantic Bight, individual SSR's above 16 are present in all subareas except those near estuaries; on Georges Bank, values exceed 16 only along the southern flank and adjacent northern slope; and in the Gulf of Maine, values above 16 are found only in Wilkinson Basin, and western and northern subareas. Subsurface/surface ratios above 32 are present only in the Middle Atlantic Bight and $mean_g$ adjacent southern slope.

Highest SSR's usually occur in the Middle Atlantic Bight central midshelf. The $mean_g$ SSR during July is ~10. Note that the relatively high $mean_g$ SSR during April in this area is due to near-bottom, not midwater, chlorophyll maxima (Fig. 23). Lowest SSR's occur in the weakly stratified water on Georges Bank (central shoals, northern shoals, western outer shoals, eastern outer shoals), Nantucket Shoals, and Scotian Shelf. Individual SSR's exceeding 2 are present in these areas but the monthly $mean_g$ SSR persists at very low values from May through September.

In the deeper water on Georges Bank which stratify during summer (Fig. 27), SSR's exceeding 2 are common but SSR's above 8 are rare. In the Gulf of Maine, the monthly $mean_g$ SSR does not surpass 2 until June, two months later than in the outer shelf Middle Atlantic Bight, although a number of individual values above 2 occur in May.

Spatial Distribution of Subsurface/Surface Ratio

Some striking spatial patterns are evident in the shelfwide distribution of SSR during summer (Fig. 28). This is the period of greatest density stratification (Fig. 27), when vertical profiles of phytoplankton chlorophyll *a* are generally bell-shaped in stratified water (e.g. Fig. 23).

Relatively low SSR's are present off the mouths of the Raritan, Delaware, and Chesapeake bays, over the shallow region on Georges Bank, and in the eastern Gulf of Maine (Fig. 28). In the Gulf of Maine, summer SSR is aligned in east to west bands. Values between 2–2.8 characterize the western region of the gulf while values below 2 characterize the eastern region. In between, a band of moderately high SSR's stretches northward, from Wilkinson Basin to the area nearshore, between Casco Bay and Penobscot Bay (Fig. 28). In the Wilkinson Basin (Fig. 5: tiles 106, 107) SSR's are 2.8–4. In the nearshore northern Gulf of Maine (Fig. 5: tile 104), SSR's are 5.6–8 and match well the observations by Holligan et al. (1984) of SSM (~3 $\mu g\ l^{-1}$) 10–20 m below surface and SSR of ~ 6 during June 1979 surveys across the 100 m isobath. The chlorophyll *a* and phytoplank-

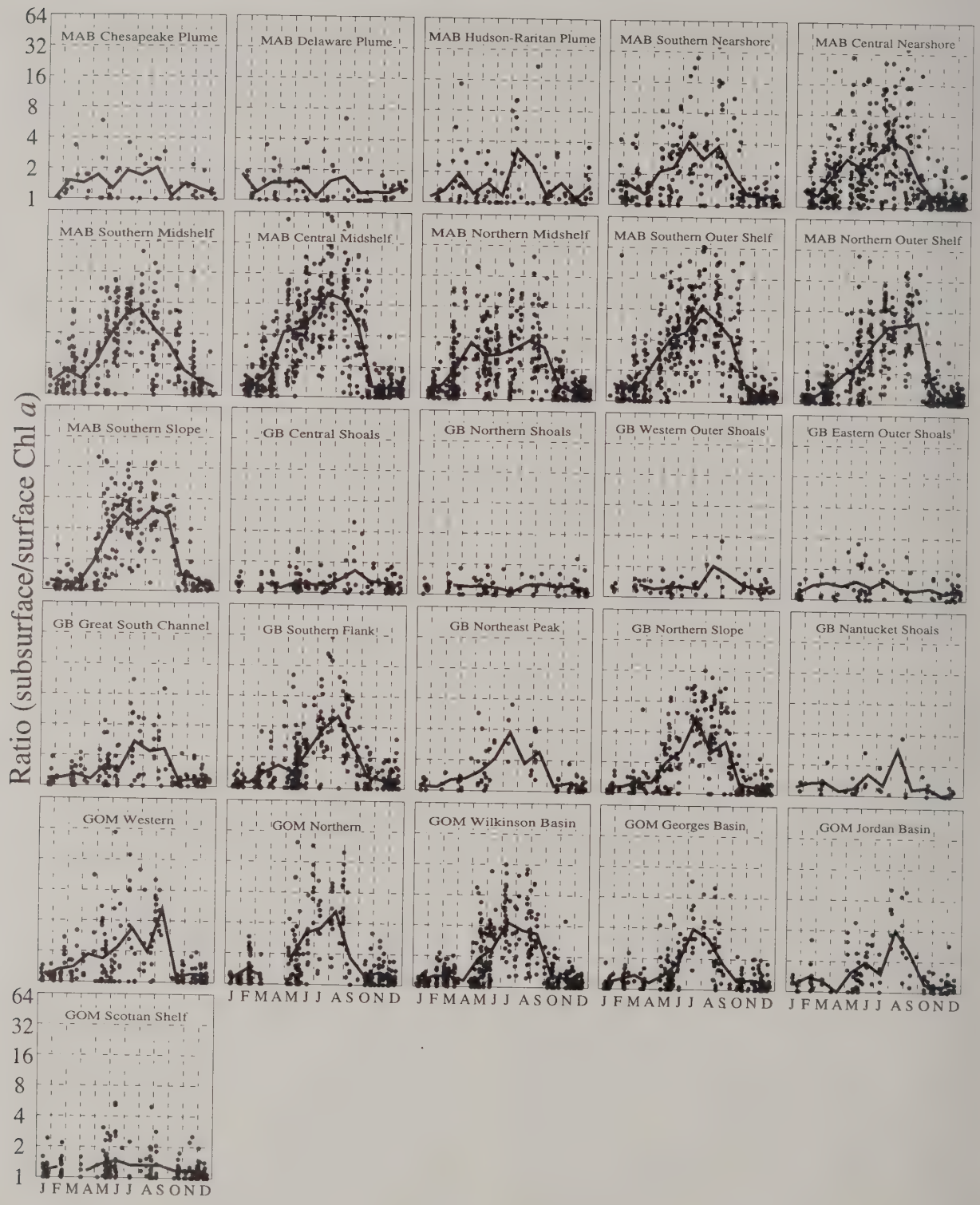

Figure 26

Ratio of the subsurface/surface chlorophyll *a* versus month for 26 subareas of the northeast U.S. continental shelf. Individual observations are represented as open circles. The solid line connects monthly geometric mean ratios.

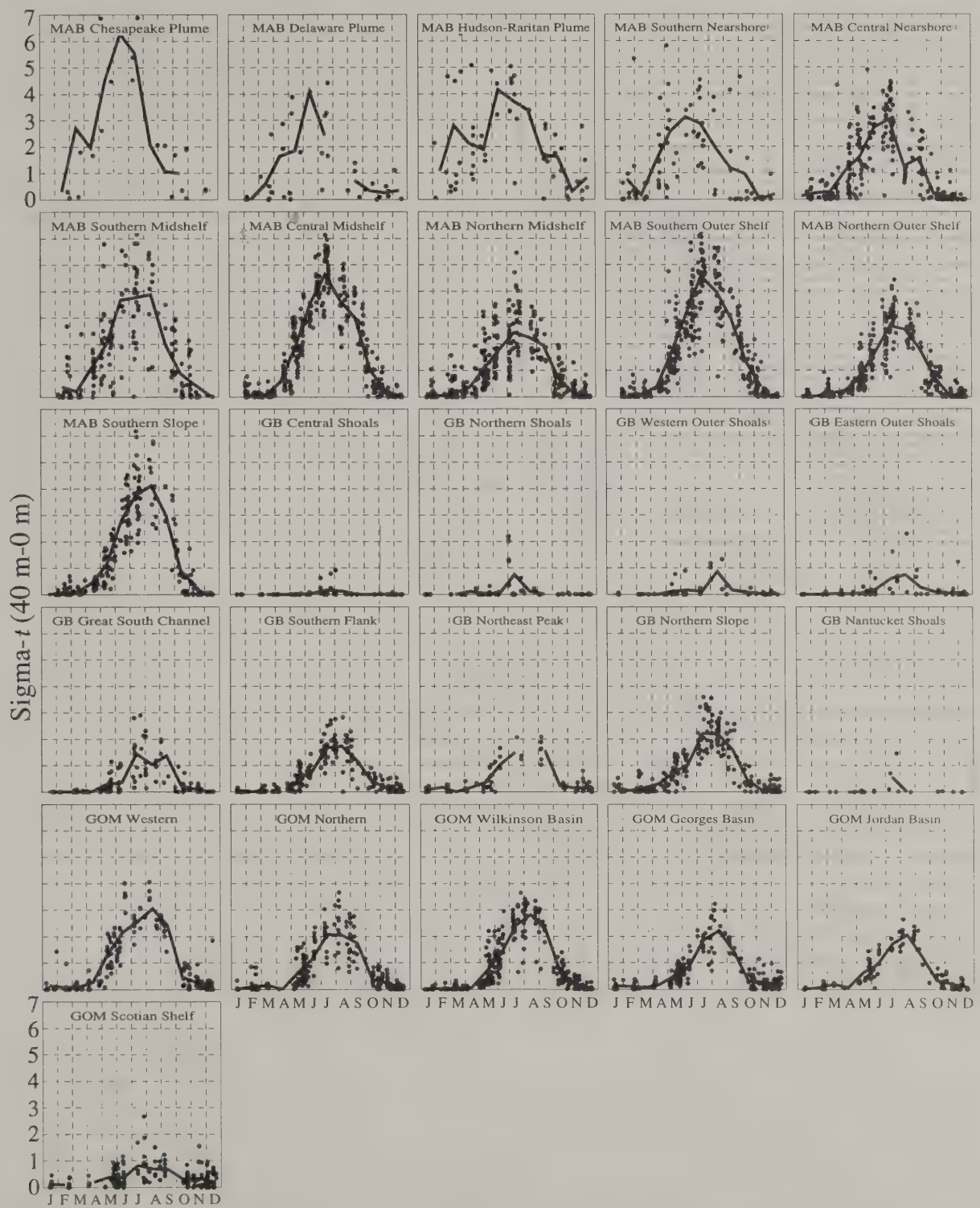

Figure 27

Stability (Sigma-*t* 40 m–0 m) versus month for 26 subareas of the northeast U.S. continental shelf. Individual observations are represented as open circles. The solid line connects monthly means.

ton biomass maxima were present at the base of the seasonal thermocline, at the top of the nitracline, and in the lower euphotic layer at between 1% and 5% of surface light intensity (Holligan et al., 1984).

A general onshore-offshore or bathymetric gradient in mean SSR is evident in the Middle Atlantic Bight and on Georges Bank (Fig. 28). A gradient is also evident proceeding south along the outer continental shelf:

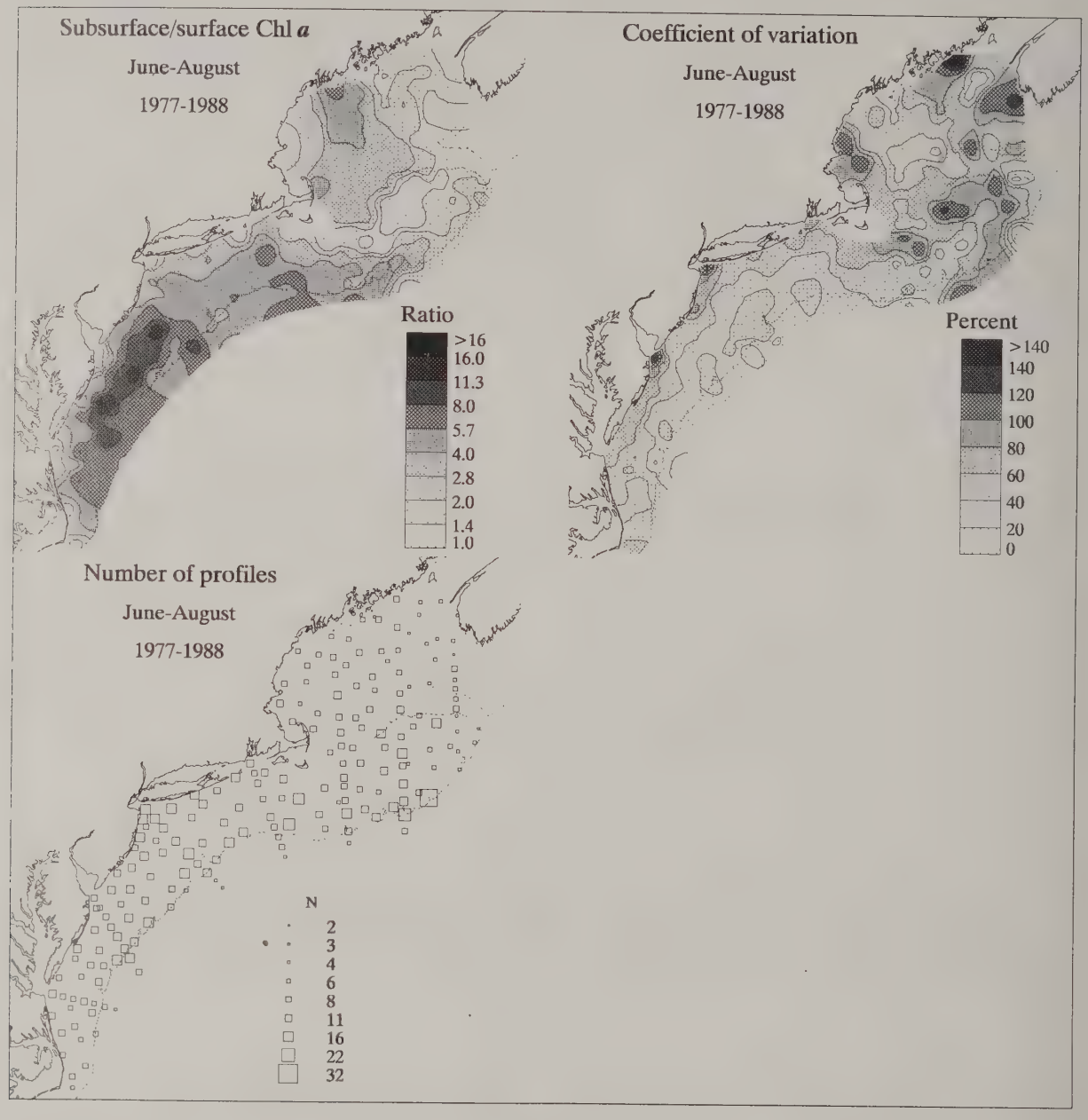

Figure 28

Contoured distribution of the ratio of subsurface/surface chlorophyll concentration, coefficient of variation percentage in the ratio of subsurface/surface chlorophyll concentration, and number of vertical profiles, during the period June–August. Subsurface/surface ratios were $\log_2$-transformed and composited by tile before contouring. The coefficient of variation was based on $\log_2$-transformed ratios.

SSR is 2–2.8 at the southeast flank of Georges Bank; 2.8–4 near Great South Channel; 4–5.6 near the Hudson Shelf Valley; and 5.6–8 offshore of Delaware Bay.

Variability in mean$_g$ SSR is lowest in tiles with highest SSR's and greatest in tiles which, on average, have little vertical structure in chlorophyll concentration (Fig. 29A). This follows the pattern expected: low temporal persistence of vertical structure in areas with weak or intermittent density stratification and high persistence where density stratification is high and continuous during summer. Variance in the composite summer mean$_g$ SSR's includes inter- and intra-annual sources, so high CV's may mean either or both sources are responsible, while low CV's indicate both sources of variation are small. Subsurface/surface ratios also tend to increase with increasing depth below surface (Fig. 29B), following the general onshore-offshore tilt (deepening) of the seasonal thermocline with increasing water column depth. Chlorophyll *a* in the SSM and near surface layers begin to converge (vertical uniformity) at surface chlorophyll *a* concentrations greater than 1 µg/l (Fig. 29C).

There is a distinct band within the Middle Atlantic Bight with elevated SSR's (8–16), roughly between the 30 and 60 m isobaths offshore of Chesapeake Bay, Delaware Bay, and the southern half of New Jersey (Fig. 5: tiles 50, 44, 40, 31, 32, 27, 24, 20, 14, 45, 39, 33, 19). This is a relatively stable feature during the stratified season as the CV's in SSR's are low (Fig. 28). This midshelf band coincides with the location of cold winter residual water known as the "cold pool" (Ketchum and Corwin, 1964) or "cold band" (Houghton et al., 1982). The cold band is approximately bounded between the 30 and 100 m isobaths in the Middle Atlantic Bight (Ketchum and Corwin, 1964; Bowman and Wunderlich, 1977), and extends uninterrupted onto Georges Bank at 65–96 m where it is further offshore than in the bight (Flagg, 1987; Bisagni, 1992).

Overall, the shelfwide pattern in mean summer SSR is similar to the shelfwide pattern in upper water column stability (cf. Figs. 28 and 30), where stability is indexed (stability$_{40}$) as the difference between density (sigma-*t*) at 40 m and surface. The greatest SSR's occur where density stratification is greatest, in the Middle Atlantic Bight midshelf. The Middle Atlantic Bight is among the most stratified coastal regions in the world; density gradients across the summer pycnocline are 0.3–0.4 sigma-*t* units m^{-1} (Falkowski et al., 1983). This is reflected in the distribution of the stability$_{40}$ (Fig. 30). The thermal contrast between the cold band below the seasonal thermocline and the warmest brackish surface water, found in the southern half of the Middle Atlantic Bight (Mountain and Manning, 1994), endows this area with the highest vertical density stratification.

Conversely, lowest summer SSR's are found where stability is lowest (cf. Figs. 28 and 30)—shallow areas on

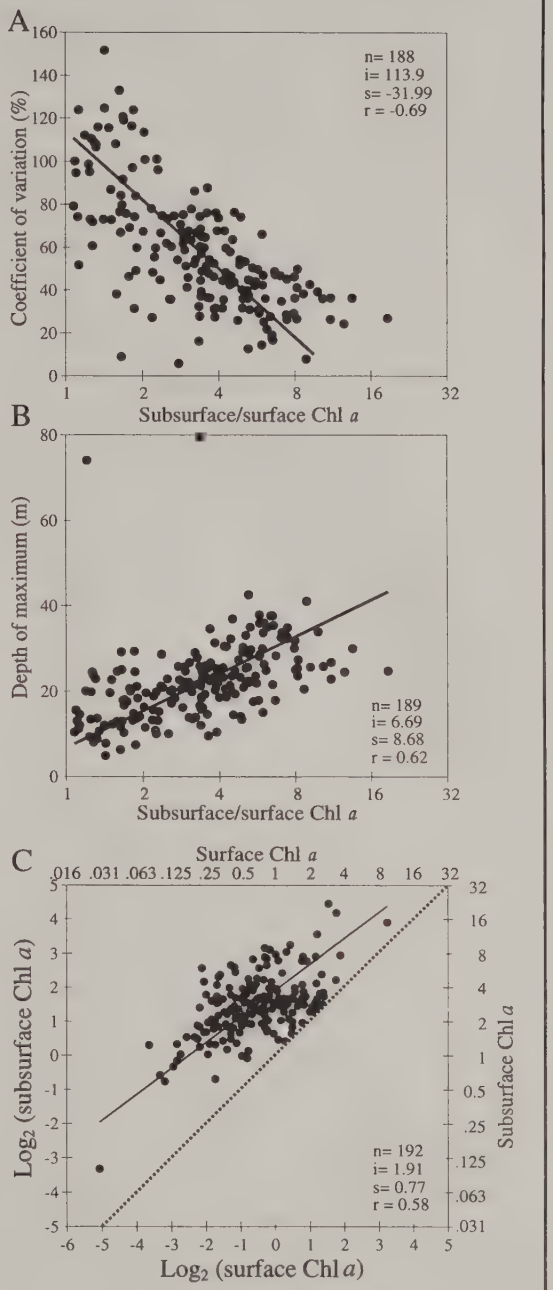

Figure 29

(A) Relationship between coefficient of variability and ratio of subsurface/surface chlorophyll concentration. (B) Depth of maximum chlorophyll versus subsurface/surface chlorophyll concentration. (C) Log_2 (surface chlorophyll *a*) versus log_2 (subsurface chlorophyll *a*). (N=number of observations, r=correlation coefficient, s=functional slope, i=functional intercept.)

Georges Bank, Nantucket Shoals, Browns Bank, and eastern Gulf of Maine. The low stability in these areas is the consequence of vigorous tidal currents (Fig. 3) interacting with shallow topography (Fig. 2) to vertically mix the water column and dissipate density stratification. Despite the spatial coarseness of our observations, there is good agreement between the distribution of $mean_g$ SSR's below 2, $stability_{40}$ below 1, and maximum tidal surface currents exceeding ~50 cm s^{-1} (Fig. 3). These parameters roughly define the mixing front separating well-mixed from surrounding stratified water on Georges Bank. Strong currents and mix-

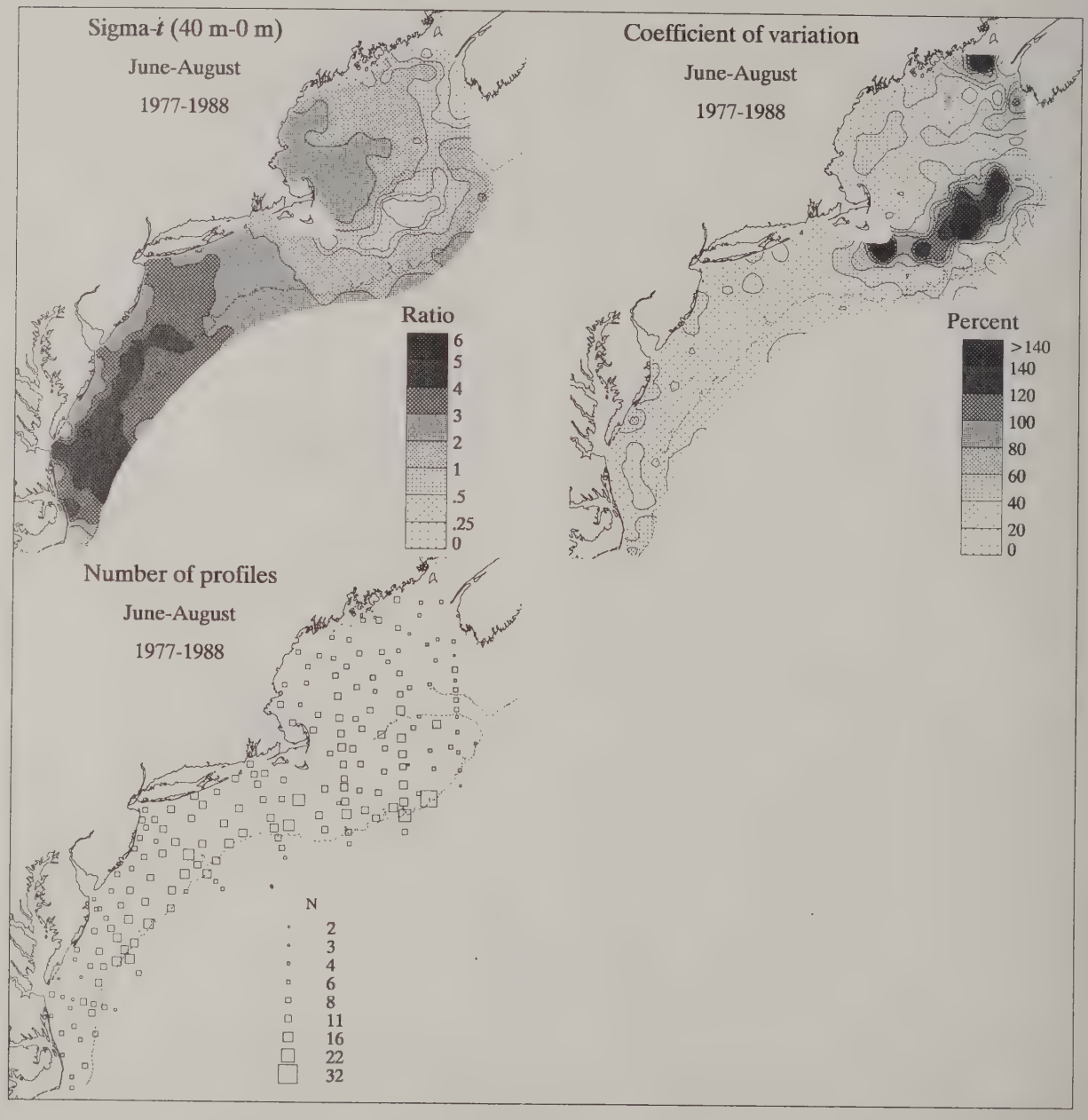

Figure 30

Contoured distribution of mean stability (Sigma-*t* 40 m–0 m), coefficient of variation percentage of stability, and the number of vertical profiles, during the period June–August. Data were composited by tile before contouring.

ing on Georges Bank during summer are dominated by the M2 tidal component. With mixing by summertime wind included, Loder and Greenberg (1986) predict that the position of the mixing front generally parallels the 50 m isobath, except it is shoaler than 50 m along the north and southern edges on Georges Bank and deeper than 50 m along the northeast peak.

On a very coarse scale, the west-east banding of SSR's in the western gulf follows the general west-east banding in stability (cf. Figs. 28 and 30). The pattern for stability probably reflects the greater density differences in the western gulf that result from warm stratified surface water overlying a relatively thick lens of winter residual Maine Intermediate Water (Brown and Irish, 1993). The relatively low SSR's in the extreme western Gulf of Maine are less than would be expected based on stability, and point out the limitations of this simple SSR index. The reason for this departure is that, unlike other well-stratified waters in the study area, chlorophyll *a* is high in the surface layer (Fig. 25). Low SSR's are also found in subareas influenced by plumes from Hudson-Raritan, Delaware, and Chesapeake bays, where stability is quite high (Fig. 31). Highest chlorophyll *a* is not in the thermocline but in the nutrient-enriched surface water entering the coastal zone (Fig. 23).

The SSR is a useful simple index of the degree of vertical stratification of phytoplankton. This index, with the above noted but understandable exceptions, parallels indices of vertical density stratification. The importance of physical stability to the establishment of subsurface chlorophyll maxima during summer has been known for some time (Pingree et al., 1976; Pingree, 1978). Thermoclines and pycnoclines generate sharp biological gradients. These gradients structure the column into approximately three layers. Phytoplankton in the upper mixed layer have optimal light, but nutrient demands must be met largely through recycling processes. Phytoplankton forming SSM in the thermocline layer are exposed to suboptimal light and reduced turbulence, and have relatively greater access to new nutri-

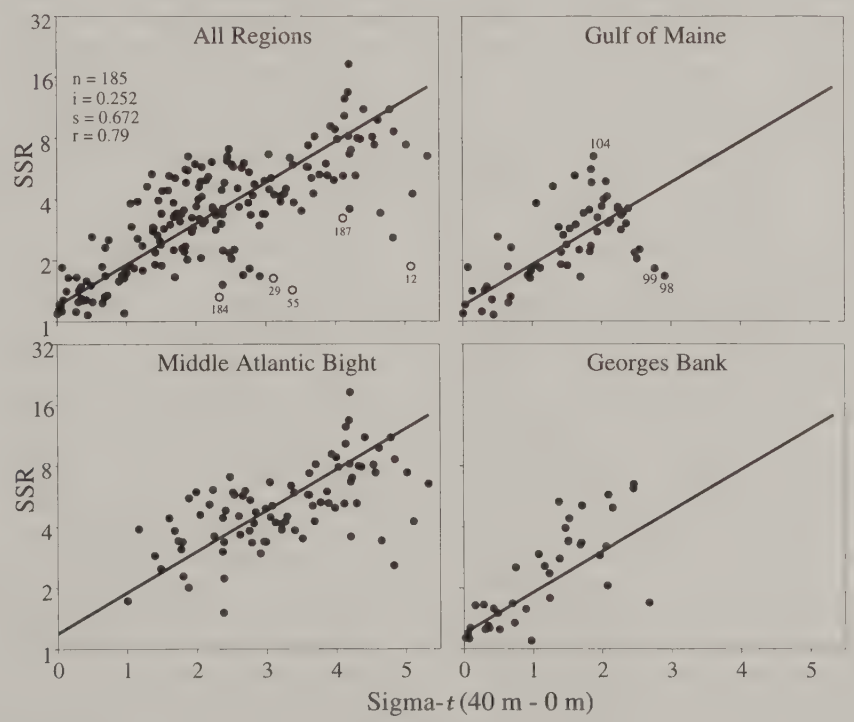

Figure 31

Relationship between the geometric mean ratio of subsurface/surface chlorophyll (SSR) and stability (Sigma-*t* 40 m–0 m) during the period June–August. The line in each panel represents the functional regression slope for all data except tiles adjacent to Middle Atlantic Bight estuaries (labeled 184, 29, 55, 187, 12). (N=number of observations, r=correlation coefficient, s=functional slope, i=functional intercept.)

ents present in the nitrocline. Below the thermocline community, light intensity decreases to levels which permit only very modest growth above respiratory demands. The SSR may provide an index of the relative importance of new versus recycled nutrients during stratified conditions. It seems reasonable to infer that the supply of new nitrogen to the upper mixed layer would be minimal in areas with high SSR's and maximal in areas with relatively lower SSR's, providing that the reservoir of nutrients below the pycnocline is ample. Shallow water on Georges Bank would be an exception, since nutrients are low through the water column during summer (Draxler et al., 1985; O'Reilly et al., 1987; Walsh et al., 1987; Bisagni, 1992) and new nitrogen must come into the well-mixed region laterally across the mixing front at approximately 50–60 m isobath.

Fall Bloom

During late summer and early fall in stratified water, the shallow upper mixed layer begins to deepen due to seasonal decreases in solar radiation and seasonal increases in wind and convective mixing. The pycnocline begins to erode and the euphotic layer gains access to fresh supplies of nutrients previously trapped below. The ensuing increase in phytoplankton biomass is termed the "fall bloom."

Conditions leading to fall bloom are quite different from those leading to WS-bloom. The critical mixed depth model, described above, helps to understand these differences. During WS-bloom in deep water, the mixed layer is shoaling, incident radiation is seasonally increasing, and consequently the mean level of light available to phytoplankton in the mixed layer is increasing; during fall bloom the opposite trend occurs. Phytoplankton are exposed to decreasing mean light levels in the mixed layer with seasonal decreases in solar radiation compounded by the mixed layer becoming deeper as destratification proceeds. Thus, the extent of the fall bloom will depend upon the extent to which nutrient enhancement of growth is offset by decreases in light and by deepening of the mixed layer below the critical depth (Yentsch, 1981).

It is these basic differences outlined above which appear to explain why fall bloom is usually subordinate in magnitude to WS-bloom. This is the general case for the Middle Atlantic Bank, Georges Bank, and Wilkinson and Georges basins, where chlorophyll *a* is roughly one-half the WS-bloom values. Fall bloom in other subareas of the Gulf of Maine, such as the Scotian Shelf, Jordan Basin, and northern and western Gulf of Maine, may surpass WS-bloom. Because sampling during spring was not always adequate, this conclusion must be tentative. The significance of fall blooms in the Gulf of Maine is underscored by the observation that chlorophyll *a* near surface during October is greater in the western gulf than in any other area of the shelf except the southern nearshore Middle Atlantic Bight (cf. Figs. 23, 24, and 25).

Unlike the WS-bloom where chlorophyll *a* becomes elevated throughout most of the water column, biomass increases during fall bloom are largely restricted to the upper ~20–30 m of the column. Fall bloom is thus identified as a disappearance of bell-shaped vertical biomass profiles characteristically seen during the stratified season (Figs. 23–25). Moreover, because surface chlorophyll *a* is low in stratified water prior to the bloom, the relative biomass increase near surface during the fall bloom is generally greater than during the WS-bloom. Conversely, prior to WS-bloom, biomass near bottom is generally quite low, but during and following the WS-bloom peak, phytoplankton biomass reaches annual maxima in the lower portion of the water column.

The emergence of fall bloom is temporally associated with decreases in the stability$_{40}$ below 1 sigma-*t* (Fig. 27). In the Gulf of Maine, fall bloom appears in September in weakly stratified eastern subareas which destratify early (Jordan Basin, Georges Basin, Scotian Shelf). Later, during October, it appears in the relatively more stratified western portion (Wilkinson Basin, western Gulf of Maine; see Fig. 27 and Mountain and Manning, 1994). In the northern Gulf of Maine subarea, near surface biomass increases during September but does not peak until October. In the Middle Atlantic Bight, the fall bloom occurs during October, and perhaps begins during September in the central nearshore, as indicated by the disappearance of the summer bell-shaped profile and the noisy composite profile for September (Fig. 23).

The fall bloom is not strongly dominated by netplankton as is the WS-bloom, and there are differences among areas in the mean size composition of fall blooms. In the Middle Atlantic Bight and Georges Bank, and the northern Gulf of Maine and Jordan Basin, netplankton and nanoplankton are approximately equal; throughout the rest of the gulf and the northern and southern slope areas, nanoplankton tend to dominate fall bloom.

Moderate increases in biomass are evident in September (Fig. 24) in tidally-mixed unstratified areas of Georges Bank, where stability$_{40}$ is usually less than 1 sigma-*t* unit throughout summer (Fig. 27). If these pulses signify fall bloom and are responses to nutrient enrichment, then the critical mixed depth-stratification model does not directly apply. Nutrients in the well-mixed water are uniformly low during summer but abundant below seasonal pycnoclines in the surrounding water (Draxler et al., 1985; O'Reilly et al., 1987). The new nutrients presumed needed for these biomass

increases might be derived by advection and subsequent tidal mixing of nutrient-enriched surface water from surrounding water undergoing destratification. Alternatively, the additional nutrients, if required, could potentially be supplied from enhanced nutrient recycling which would be expected to peak during September when temperature of the well-mixed water (Bisagni and Sano, 1993) reaches its annual peak. Other hypotheses meriting examination concern whether the sharp drop in zooplankton biomass (Sherman et al., 1987) and abundance of herbivorous copepods (Davis, 1987; Meise and O'Reilly, 1996) represent a relaxation in grazing pressure during fall and early winter. We also note that the photosynthetic efficiency of phytoplankton is highest not during summer solstice, when photosynthetically active radiation is highest, but during fall (O'Reilly et al., 1987). This may be due to the species composition or to environmental factors.

Summary

The broad scale features in the horizontal, vertical, and seasonal distribution of chlorophyll *a* on the northeast U.S. continental shelf are described based on 57,088 measurements made during 78 oceanographic surveys from 1977 through 1988. The $mean_g$ for all observations is 0.84 μg/l. The distribution of chlorophyll *a*, considered here as an index of autotrophic phytoplankton biomass, is strongly influenced by physical factors. Bathymetry, vertical mixing by strong tidal currents, and seasonal and regional differences in the intensity and duration of vertical stratification appear to explain a large fraction of the variability in chlorophyll *a*. Vertical density stratification ranges widely; areas of the Middle Atlantic Bight are among the most stratified in the world and the shallow water on Georges Bank (where vigorous tidal mixing occurs) is essentially vertically homogeneous year-round. The wide range in measured chlorophyll *a* (<0.01–57.8 μg l^{-1}) reflects wide seasonal and regional variations in hydrographic conditions throughout this ecosystem.

Highest mean Chl_w is usually observed in nearshore areas adjacent to the mouths of the Hudson-Raritan, Delaware, and Chesapeake estuaries, over the shallow water on Georges Bank, and in a small area along the southeast edge of Nantucket Shoals. Occasionally, high Chl_w concentrations are found in Middle Atlantic Bight coastal waters not in close proximity to estuaries, and may reflect upwelling episodes. Lowest Chl_w (<0.125 μg l^{-1}) is usually restricted to the most seaward stations sampled along the shelf-break and the central deep waters in the Gulf of Maine. When relatively high Chl_w occurs in the Gulf of Maine, it is in the nearshore western portion, between Penobscot and Casco bays.

The annual cycle of phytoplankton biomass follows the paradigm for temperate continental shelf ecosystems. There is at least a twofold seasonal variation in all areas. The highest phytoplankton concentrations (m^3) and highest integrated standing stocks (m^2) occur during the WS-bloom; the lowest occur during summer, when vertical density stratification is maximal. In most regions, a secondary phytoplankton biomass pulse is evident during convective destratification in fall, usually in October.

The timing, duration, and intensity of WS-bloom vary by region. In the Middle Atlantic Bight the WS-bloom progresses from nearshore to the slope, occurring during January–March in the nearshore and midshelf regions, and March in outer shelf and adjacent southern slope water. On Georges Bank, WS-bloom peaks during March, except in the Great South Channel along the southern flank and in the northern slope waters, where the peak is reached during April. Winter-spring bloom appears during February–March in the nearshore western gulf and during April throughout the gulf's deeper waters. Greatest concentrations of biomass near surface appear in the Wilkinson Basin during April.

In shallow nearshore Middle Atlantic Bight, fall bloom appears during September–October. In the midshelf and outer shelf regions and along the Middle Atlantic Bight shelf-break, fall bloom occurs one month later in October and follows the expected delay in destratification of deeper water. In the shallow water on Georges Bank, chlorophyll *a* increases above the summer minimum during September, but continues through November. In the deeper water, fall bloom appears during October, followed by decreases in Chl_w during November and December. Fall bloom in some areas of the Gulf of Maine approaches the magnitude of the WS-bloom, but Georges Bank and Middle Atlantic Bight fall blooms are clearly subordinate to WS-blooms.

Generally, mean Chl_w decreases from nearshore to the shelf-break. These cross-shelf gradients are usually present in the Middle Atlantic Bight. On Georges Bank, an annular pattern is usually evident, where Chl_w decreases from shallow to deep water surrounding the shoals. In the Gulf of Maine, Chl_w is not well correlated with water column depth and bathymetric gradients are much weaker than those for the Middle Atlantic Bight and Georges Bank, where there is a regular seasonal progression. Cross-shelf gradients are steeper during the unstratified season than during the stratified season. They are most pronounced during January–February when the WS-bloom appears in the nearshore Middle Atlantic Bight and in the shallow water on Georges Bank, and least pronounced during April when the WS-bloom appears in deeper water.

Measurements of chlorophyll in two size-fractions of the phytoplankton, netplankton (>20 μm) and nano-

plankton (<20 μm), reveal that the smaller nanoplankton are responsible for most of the phytoplankton biomass on the northeast U.S. shelf. Considering all samples, the median size composition is 70% nanoplankton, 30% netplankton. Strong dominance (>90%) by nanoplankton was common while strong dominance by netplankton was rare. Most of the annual phytoplankton primary production on the shelf is also by the nanoplankton (O'Reilly et al., 1987).

There are distinct patterns in seasonal, regional, and vertical variation in size composition, which presumably reflect variations in the species-composition of the phytoplankton. Cross-shelf gradients in phytoplankton size composition are frequently observed in contour maps of individual surveys and in the two-month composite contours. Netplankton dominate nearshore areas of the Middle Atlantic Bight and shallow water on Georges Bank, where chlorophyll *a* is usually high; nanoplankton (<20 μm) dominate deeper water at the shelf-break and deep water in the Gulf of Maine, where Chl_w is usually low. As a general rule, the percent of phytoplankton in the netplankton size-fraction increases with increasing depth below surface and decreases proceeding offshore.

Size-fractionated measurements of chlorophyll into netplankton (>20 μm) and nanoplankton (<20 μm) also provide a useful rough index of major changes in the phytoplankton composition that occur during spring and fall blooms and between stratified and unstratified conditions. Overall, netplankton dominate standing stocks during the WS-bloom, whereas the fall bloom is strongly dominated by nanoplankton offshore and weakly dominated by nanoplankton nearshore. Our findings support the emerging ecological paradigm (Malone et al., 1983b) that netplankton (presumably large diatoms or chain and colonial small diatoms) prevail during the unstratified period when turbulence, vertical mixing, and nutrients are high and photosynthetically active radiation (PAR) in the upper mixed layer is variable; and that smaller nanoplankton and motile species prevail during density stratification, when turbulence is low and average PAR is high in the upper mixed layer.

Composite vertical profiles of mean chlorophyll *a* concentration in 11 layers of the water column constructed for 26 subareas provide additional insight on regional and seasonal differences in the vertical distribution of chlorophyll *a* and percent netplankton. Four basic profile shapes are evident: uniform, declining, bell, and inverted.

Vertically uniform chlorophyll *a* profiles are most obvious from November through February, the period of minimal density stratification, and year-round in the tidally well-mixed shallow water on Georges Bank. Declining vertical profiles occur during the winter-spring and fall blooms, when highest biomass is in the upper 20–30 m of the column. Inverted profiles occur relatively infrequently. They are most obvious following the WS-bloom, when elevated concentrations of chlorophyll *a* appear near the bottom of the water column in the midshelf region of the Middle Atlantic Bight, but not on Georges Bank and in the Gulf of Maine. The inverted profiles indicate that the near-term fate of the WS-bloom in some areas of the shelf is sedimentation and accumulation near bottom. Thus there are significant differences among regions with respect to the fate of the WS-bloom and the extent of its potential availability to benthic animals. The intense and prolonged WS-bloom throughout the water column in midshelf and outer shelf MAB is followed by a major diatom sinking event, as indicated by increases in chlorophyll *a* from surface to bottom and by disproportionally more netplankton at the bottom of the water column than near surface.

Bell-shaped profiles characterize periods of vertical density stratification. Chlorophyll *a* is relatively low near surface, progressively increases to the subsurface chlorophyll maximum layer (generally in the pycnocline 20–35 m below surface), and then progressively decreases over the remaining deeper portion of the profile. Subsurface chlorophyll *a* maxima are ubiquitous during summer in stratified water. Chlorophyll *a* in the subsurface maximum layer is generally 2–8 times the concentration in the overlying and underlying water and approaches 50–75% of the levels observed in surface water during WS-bloom. This concentration of phytoplankton biomass in and just below the seasonal pycnocline makes this layer a highly localized and potentially important source of organic carbon for herbivorous copepods.

The SSR during summer parallels the shelfwide pattern for stability, indexed as the difference in density (sigma-*t*) between 40 m and surface. The weakest stability and lowest SSR's are found in shallow tidally-mixed water on Georges Bank; the greatest stability and highest SSR's (8–12:1) are along the mid and outer MAB shelf, over the winter residual water known as the "cold pool." On Georges Bank, the distribution of SSR and the $stability_{40}$ are roughly congruent with the pattern for maximum surface tidal current velocity, with values above 50 cms^{-1} defining SSR's less than 2:1 and the well-mixed area.

A strong seasonality is evident in the magnitude of chlorophyll, the size composition of the phytoplankton chlorophyll, and in the shape of the vertical profile of chlorophyll. In areas that stratify during summer, chlorophyll *a* concentrations at depths between 20–35 m below surface are less variable over an annual cycle than those in surface and bottom waters. Surface water exhibits the most pronounced seasonal change. Chlorophyll concentrations are generally lowest during the period of vertical density stratification and highest dur-

ing the WS-bloom. Chlorophyll concentrations 20–35 m below surface are less variable over the annual cycle as a consequence of the establishment of a seasonal thermocline. At this depth there is approximately a 2:1 range in chlorophyll concentration over the annual cycle, whereas in surface, the range is 8:1.

The composite profiles of chlorophyll *a* also reveal large vertical gradients in the size composition of phytoplankton during the stratified season. Usually, percent netplankton increases with increasing depth below surface. In some areas, such as the midshelf and outer shelf Middle Atlantic Bight, percent netplankton increases from ~10–20% near surface to 40–70% 50 m below surface, suggesting large differences in phytoplankton species composition. Similar but less sharp gradients are observed in the deeper stratified water on Georges Bank and in the Gulf of Maine.

Although size composition of the phytoplankton varies throughout the annual cycle and throughout the water column in regular patterns in many shelf areas, there remains much uncertainty about the precise species composition of the phytoplankton, particularly during the stratified period when largest vertical gradients in size composition are observed. This is a neglected area and warrants further field studies.

These characterizations of the seasonal and regional differences in the magnitude of Chl_w, annual cycles, and the shape of the mean chlorophyll *a* profile should prove useful in understanding regional differences in fisheries productivity. They will also help increase the precision of ecosystem-wide estimates of euphotic standing stocks and primary productivity, when combined with synoptic satellite measurements of the surficial layer of the ocean.

Acknowledgments

In any extensive endeavor spanning a decade, a number of individuals are responsible. We would like to acknowledge J. Pearce, K. Sherman, and R. Murchelano for providing sustained support and guidance, and W. Smith for his efficient coordination of MARMAP field surveys. We thank J. Sibunka, F. Steimle, P. Berrien, and D. Mountain for serving as Chief Scientist during many of the field surveys. Their wise decisions at sea led to the most comprehensive sampling possible.

We are fortunate to have worked with many highly competent technicians involved in data collection and analysis: J. Anderson, S. Barker, R. Bruno, J. Cain, J. Duggan, T. Finneran, A. Fischer, P. Forunier, S. Fromm, S. Fromm, B. Hogelin, C. Ingham, B. Lamp, C. Muchant Cain, J. Nickels, A. Pratt, J. Prezioso, S. Ward, and K. Workman.

We thank J. Thomas for his assistance with the initial sampling design and methods; P. Fournier, S. Fromm, and R. Pikanowski for their assistance in developing computer routines and database management; D. Mountain, J. Manning, and T. Holzworth for providing hydrographic data; E. Escowitz for providing bathymetric data; R. Armstrong, J. Bisagni, and J. Landry for their suggestions on data analyses; and S. Arenas for many helpful editorial suggestions.

Literature Cited

Anderson, G. C.
1964. The seasonal geographic distribution of primary productivity off the Washington and Oregon coasts. Limnol. Oceanogr. 9:284–302.

Antoine, D., J.-M. André, and A. Morel.
1996. Oceanic Primary Production 2. Estimation at global scale from satellite (CZCS) chlorophyll. Glob. Biochem. Cycles 10(1):57–69.

Balch, W., R. Evans, J. Brown, G. Feldman, C. McClain, and W. Esaias.
1992. The remote sensing of primary productivity. Use of a new data compilation to test satellite algorithms. J. Geophys. Res. 97(C2):2279–2293.

Banse, K.
1977. Determining the carbon-to-chlorophyll ratio of natural phytoplankton. Mar. Biol. 41:199–212.

Benway, R. L., J. W. Jossi, K. P. Thomas, and J. R. Goulet.
1993. Variability of temperature and salinity in the Middle Atlantic Bight and Gulf of Maine. U.S. Dep. Commer., NOAA Tech. Rep. NMFS 112, 108 p.

Bigelow, H.
1926. Plankton of the offshore waters of the Gulf of Maine. U.S. Bur. Fish. 40(2), 509 p.

Bigelow, H., and M. Sears.
1935. Studies of the waters of the continental shelf, Cape Cod to Chesapeake Bay II: Salinity. Pop. Phys. Oceanogr. Meteorol. 4(1):1–94.

Bigelow, H., L. Lillick, and M. Sears.
1940. Phytoplankton and planktonic protozoa of the offshore waters of the Gulf of Maine. Part I. Numerical distribution. Transact. Am. Philos. Soc. 31(3):149–191.

Bisagni, J. J.
1983. Lagrangian current measurements within the eastern margin of a warm-core Gulf Stream ring. J. Phys. Oceanogr. 13:709–715.
1992. Differences in annual stratification cycle over short spatial scales on southern Georges Bank. Cont. Shelf Res. 12:415–435.

Bisagni, J. J., and M. Sano.
1993. Satellite observations of short time scale sea surface temperature variability on southern Georges Bank. Cont. Shelf Res. 13:1045–1064.

Bisagni, J. J., R. C. Beardsley, C. J. Ruhsam, J. P. Manning, and W. C. Williams.
1996a. Historical and recent evidence concerning the presence of Scotian Shelf water on southern Georges Bank. Deep-Sea Res. II, 43(7–8):1439–1471.

Bisagni, J. J., D. J. Gifford, and C. M. Ruhsam.
1996b. The spatial and temporal distribution of the Maine coastal current during 1992. Cont. Shelf Res. 16:1–24.

Bishop, S. S., J. A. Yoder, and G. A. Paffenhofer.
1980. Phytoplankton and nutrient variability along a cross-shelf transect off Savannah, Georgia, U.S.A. Estuar. Coast. Mar. Sci. 11:359–368.

Bowman, M. J., and L. D. Wunderlich.
1977. Hydrographic properties. MESA New York Bight atlas monograph 1. N.Y. Sea Grant Inst., Albany, 78 p.

Broeker, W. S., T. Takahashi, H. J. Simpson, and T.-H. Peng.
1979. Fate of fossil fuel carbon dioxide and the global carbon budget. Science 206:409–418.

Brown, W. S., and J. D. Irish.
1993. The annual variation of water mass structure in the Gulf of Maine: 1986–1987. J. Mar. Res. 51:53–107.

Bumpus, D. F.
1976. Review of the physical oceanography of Georges Bank. Int. Comm. NW Atl. Fish. Res. Bull. 12:119–134.

Butman, B.
1987. Physical processes causing surficial sediment movement. *In* R. H. Backus and D. W. Bourne (eds.), Georges Bank, p. 147–162. MIT Press, Cambridge, Mass.

Butman, B., and R. Beardsley.
1987. Physical oceanography. *In* R. H. Backus and D. W. Bourne (eds.), Georges Bank, p. 88–98. MIT Press, Cambridge, Mass.

Campbell, J. W., and W. E. Esais.
1985. Spatial patterns in temperature and chlorophyll on Nantucket Shoals from airborne remote sensing data, May 7–9, 1981. J. Mar. Res. 43:139–161.

Campbell, J. W., and J. E. O'Reilly.
1988. Role of satellites in estimating primary productivity on the northwest Atlantic continental shelf. Cont. Shelf Res. 8(2):179–204.

Churchill, J. H., and P. C. Cornillon.
1991. Gulf Stream water on the shelf and upper slope north of Cape Hatteras. Cont. Shelf Res. 11(5):409–431.

Cohen, E.
1976. An overview of the plankton communities of the Gulf of Maine. Int. Comm. NW Atl. Fish. Sel. Papers 1, p. 89–105.

Cohen, E., and M. Grosslein.
1987. Production on Georges Bank compared with other shelf ecosystems. *In* R. H. Backus and D. W. Bourne (eds.), Georges Bank, p. 383–391. MIT Press, Cambridge, Mass.

Collins, D. J.
1989. The remote sensing of oceanic primary productivity - A review. Proc. SPIE 1129:92–106.

Colton, J. B.
1972. Short-term variation in estimates of chlorophyll abundance. Int. Comm. NW Atl. Fish., Res. Bull. 9:81–84.

Colton, J. B., and J. L. Anderson.
1983. Residual drift and residence time of Georges Bank surface waters with reference to the distribution, transport, and survival of larval fishes. U.S. Dep. Commer., NOAA Tech. Memo. NMFS-F/NEC–24, 44 p.

Colton, J. B., J. L. Anderson, J. E. O'Reilly, C. A. Evans-Zetlin, and H. G. Marshall.
1985. The shelf/slope front south of Nantucket Shoals and Georges Bank as delineated by satellite infrared imagery and shipboard hydrographic and plankton observatons. U.S. Dep. Commer., NOAA Tech. Memo. NMFS-F/NEC-38, 22 p.

Colton, J .B., R. R. Marak, S. Nickerson, and R. R. Stoddard.
1968. Physical, chemical, and biological observations on the continental shelf, Nova Scotia to Long Island, 1964–1966. U.S. Fish Wildl. Serv. Data Rep. 23. 189 p.

Cosper, Elizabeth M., and J. C. Stephien.
1984. Phytoplankton-zooplankton coupling in the outer continental shelf and slope waters of the Mid-Atlantic Bight, June 1979. Estuar. Coast. Shelf Sci. (18):145–155.

Cox, J. L., P. H. Wiebe, P. Ortner, and S. Boyd.
1981. Seasonal development of subsurface chlorophyll maxima in slope water and northern Sargasso Sea of the Northwestern Atlantic Ocean. Biol. Oceanogr. 1(3):271–285.

Cullen, J. J.
1982. The deep chlorophyll maximum: comparing vertical profiles of chlorophyll *a*. Can. J. Fish. Aquat. Sci. 39:791–803.

Cullen, J. J., and R. W. Eppley.
1981. Chlorophyll maximum layers of the Southern California Bight and possible mechanisms of their formation and maintenance. Oceanol. Acta 4:23–32.

Cullen, J. J., F. M. H. Reid, and E. Stewart.
1982. Phytoplankton in the surface and chlorophyll maximum off southern California in August, 1978. J. Plankton Res. 4(3):665–694.

Curra, J. J.
1987. Phytoplankton. *In* R. H. Backus and D. W. Bourne (eds.), Georges Bank, p. 213–218. MIT Press, Cambridge, Mass.

Dagg, M. J., and J. T. Turner.
1982. The impact of copepod grazing on phytoplankton of Georges Bank and the New York Bight. Can. J. Fish. Aquat. Sci. 39:979–990.

Davis, C.
1987. Zooplankton life cycles. *In* R. H. Backus and D. W. Bourne (eds.), Georges Bank, p. 256–267. MIT Press, Cambridge, Mass.

Downs, J. N., and C. J. Lorenzen.
1985. Carbon:phaeopigment ratios of zooplankton fecal pellets as an index of herbivorous feeding. Limnol. Oceanogr. 30(5):1024–1036.

Draxler, A. F. J., A. Matte, R. Waldhauer, and J. E. O'Reilly.
1985. Nutrient distributions for Georges Bank and adjacent waters in 1979. U.S. Dep. Commer., NOAA Tech. Rep. NMFS 32, 34 p.

Eppley, R. W., C. Sapienza, and E. H. Renger.
1978. Gradients in phytoplankton stocks and nutrients off Southern California in 1974–76. Estuar. Coast. Mar. Sci. 7:291–301.

Eppley, R. W., P. Koeller, and G. T. Wallace.
1987. Stirring influences the phytoplankton species composition within enclosed columns of coastal sea water. J. Exp. Mar. Biol. Ecol. 32:219–239.

Esaias, W. E., G. C. Feldman, C. R. McClain, and J. A. Elrod.
1986. Monthly satellite-derived phytoplankton pigment distribution for the north Atlantic Ocean basin. EOS 67:835–837.

Eslinger, D. L., and R. L. Iverson.
1986. Wind effects on coastal zone color scanner chlorophyll patterns in the U.S. Mid-Atlantic Bight during spring 1979. J. Geophys. Res. 91(C11):12985–12992.

Evans, C. A., J. E. O'Reilly, and J. P. Thomas.
1987. A handbook for the measurement of chlorophyll *a* and primary production. Volume 8. Biological Investigations of Marine Antarctic Systems and Stocks (BIOMASS). Texas A&M Univ., College Station, 114 p.

Evans, R. H., K. S. Baker, O. B. Brown, and R. C. Smith.
1985. Chronology of warm-core ring 82B. J. Geophys. Res. 90(C5):8803–8811.

Falkowski, P. G.
1991. A carbon budget for the northeast continental shelf ecosystem: Results of the shelf edge exchange process studies. *In* K. Sherman, L. M. Alexander, and B. D. Gold (eds.), Food chains, yields, models, and management of large marine ecosystems, p. 35–48. Westview Press, Boulder, Colo.

Falkowski, P. G., J. Vidal, T. S. Hopkins, G. T. Rowe, T. E. Whitledge, and W. G. Harrison.
1983. Summer nutrient dynamics in the Middle Atlantic Bight:

primary production and the utilization of phytoplankton carbon. J. Plankton Res. 5:515–537.

Falkowski, P., C. Flagg, G. Rowe, S. Smith, T. Whitledge, and C. Wirick.
1988. The fate of a spring phytoplankton bloom: export or oxidation? Cont. Shelf Res. 8(5–7):457–484.

Fedosh, M. S., and J. C. Munday.
1982. Satellite analysis of estuarine plume behavior. OCEANS '82 IEEE: 464–469.

Feldman, G., N. Kuring, C. Ng, W. Esaias, C. McClain, J. Elrod, N. Maynard, D. Endres, R. Evans, J. Brown, S. Walsh, M. Carle, and G. Podesta.
1989. Ocean Color: Availability of the global data set. Eos 70:634–641.

Flagg, C.
1987. Hydrographic structure and variability. *In* R. H. Backus and D. W. Bourne, (eds.), Georges Bank, p. 109–124. MIT Press, Cambridge, Mass.

Franks, P. J. S., and D. M. Anderson.
1992a. Alongshore transport of a toxic phytoplankton bloom in a buoyancy current: *Alexandrium tamarense* in the Gulf of Maine. Mar. Biol. 112:153–164.
1992b. Toxic phytoplankton blooms in the southwestern Gulf of Maine: testing hypotheses of physical control using historical data. Mar. Biol. 112:165–174.

Garrett, C. J. R., and R. H. Loucks.
1976. Upwelling along the Yarmouth shore of Nova Scotia. J. Fish. Res. Bd. Can. 33:116–117.

Gordon, H. R.
1987. Calibration requirements and methodology for remote sensors viewing the ocean in the visible. Remote Sens. Environ. 22:103–126.

Gordon, H. R., D. K. Clark, J. L. Mueller, and W. A. Hovis.
1980. Phytoplankton pigments from the Nimbus–7 Coastal Zone Color Scanner: comparisons with surface measurements. Science 210:63–66.

Green, P. J., and R. Sibson.
1978. Computing Dirichlet tessellations in the plane. Computer J. 21:168–173.

Haines, E. B., and W. M. Dunstan.
1975. The distribution and relation of particulate organic material and primary productivity in the Georgia Bight, 1973–1974. Estuar. Coast. Mar. Sci. 3:431–441.

Herbland, A., and B. Voituriez.
1979. Hydrological structure analysis for estimating the primary production in the tropical Atlantic Ocean. J. Mar. Res. 37:87–101.

Hinga, K. R., A. A. Keller, and C. A. Oviatt.
1991. Atmospheric deposition and nitrogen inputs to coastal waters. Royal Swed. Acad. Sci., Ambio 20(6):256–260.

Hitchcock, G., and T. J. Smayda.
1977. The importance of light in the initiation of the 1972–1973 winter-spring diatom bloom in Narragansett Bay. Limnol. Oceanogr. 22:126–131.

Hjort, J.
1941. Fluctuations in the great fisheries of northern Europe viewed in the light of biological research. Rapp. P.-v. Reun. Cons. Perm. Int. Explor. Mer 20:1–223.

Holligan, P. M.
1978. Patchiness in subsurface phytoplankton populations on the northwest European continental shelf. *In* J. H. Steele (ed.), Spatial patterns in plankton communities, p. 221–238. Plenum Press, N.Y.

Holligan, P. M., W. M. Balch, and C. M. Yentsch.
1984. The significance of subsurface chlorophyll, nitrite and ammonium maxima in relation to nitrogen for phytoplankton growth in stratified waters of the Gulf of Maine. J. Mar. Res. 42:1051–1073.

Holm-Hansen, O., and B. Riemann.
1978. Chlorophyll *a* determination: Improvements in methodology. Oikos 30:438–447.

Holm-Hansen, O., C. J. Lorenzen, R. W. Holmes, and J. D. H. Strickland.
1965. Fluorometric determination of chlorophyll. J. Cons. Perm. Int. Explor. Mer. 30(1):3–15.

Hooker, S. B., and W. E. Esaias.
1993. An overview of the SeaWiFS project. Am. Geophys. Union 74(21):245–246.

Hooker, S. B., C. R. McClain, and A. Holmes.
1993. Ocean color imaging: CZCS to SeaWiFS. Mar. Technol. Soc. 27(1):3–15.

Hopkins, T., and N. Garfield.
1979. Gulf of Maine intermediate water. J. Mar. Res. 37:103–139.

Horne, E. P. W., J. W. Loder, W. G. Harrison, R. Mohn, M. R. Lewis, B. Irwin, and T. Platt.
1988. Nitrate supply and demand at the Georges Bank tidal front. Scient. Mar. 53(2–3):145–158.

Houghton, R. W., R. Schlitz, R. C. Beardsley, B. Butman, and J. L. Chamberlin.
1982. The Middle Atlantic Bight cold pool: evolution of the temperature structure during summer 1979. J. Physical Oceanogr. 12:1019–1029.

Hunter, J. R.
1981. Feeding ecology and predation of marine fish larvae. *In* R. Lasker (ed.), Marine fish larvae morphology, ecology, and relation to fisheries, p. 33–77. Univ. Wash. Press, Seattle.

Ingham, M. C., and J. Eberwine.
1984. Evidence of nearshore summer upwelling off Atlantic City, New Jersey. U.S. Dep. Commer., NOAA Tech. Memo. NMFS-F/NEC-31, 10 p.

Ingham, M. C., R. S. Armstrong, J. L. Chamberlin, S. K. Cook, D. G. Mountain, R. J. Schlitz, J. P. Thomas, J. J. Bisagni, J. F. Paul, and C. E. Warsh.
1982. Summary of the physical oceanographic processes and features pertinent to pollution distribution in the coastal and offshore waters of the northeastern United States, Virginia to Maine. U.S. Dep. Commer., NOAA Tech. Memo. NMFS-F/NEC–17, 166 p.

Iverson, R. L.
1990. Control of marine fish production. Limnol. Oceanogr. 35(7):1593–1604.

Keeling, C. D., J. A. Adams, C. A. Ekdahl, and P. R. Guenther.
1976. Atmospheric CO_2 variations at Mauna Loa Observatory, Hawaii. Tellus 28:538–551.

Ketchum, B., and N. Corwin.
1964. The persistance of "winter" water on the continental shelf south of Long Island, New York. Limnol. Oceanogr. 9:467–475.

Kiefer, D., and J. Kremer.
1981. Origins of vertical patterns of phytoplankton and nutrients in the temperate, open ocean: a stratigraphic hypothesis. Deep-Sea Res. 28A(10):1087–1105.

Kuring, N., M. R. Lewis, T. Platt, and J. E. O'Reilly.
1990. Satellite-derived estimates of primary production on the northwest Atlantic continental shelf. Cont. Shelf Res. 10(5):461–484.

Larsson, U., R. Elmgren, and F. Wulff.
1985. Eutrophication and the Baltic Sea: Causes and consequences. Ambio 14(1):9–15.

Lasker, R.
1975. Field criteria for survival of anchovy larvae: The rela-

tion between inshore chlorophyll maximum layers and successful first feeding. Fish. Bull. 73:453–462.

1978. The relationship between oceanographic conditions and larval anchovy food in the California current: Identification of factors contributing to recruitment failure. Rapp. P.-v. Reun. Cons. Int. Explor. Mer. 173:212–230.

1981. Factors contributing to variable recruitment of the northern anchovy (*Engraulis mordax*) in the California current: Contrasting years 1975 through 1978. Rapp. P.-v. Reun. Cons. Int. Explor. Mer. 178:375–388.

Lignell, R., A.-S. Heiskanen, H. Kuosa, K. Gundersen, P. Kuuppo-Leinikki, R. Pajuniemi, and A. Uitto.
1993. Fate of a phytoplankton spring bloom: sedimentation and carbon flow in the planktonic food web in the northern Baltic. Mar. Ecol. Progr. Ser. 94(3):239–252.

Lillick, L. C.
1937. Seasonal studies of the phytoplankton off Woods Hole, Massachusetts. Biol. Bull. 73:488–503.

Limeburner, R., and R. C. Beardsley.
1996. Near-surface recirculation over Georges Bank. Deep-Sea Res. II, 43(7–8):1547–1574.

Loder, J. W., and D. A. Greenberg.
1986. Predicted positions of tidal fronts in the Gulf of Maine region. Cont. Shelf Res. 6:397–414.

Mahoney, J. B., P. Olsen, and M. Cohn.
1990. Blooms of a dinoflagellate *Gyrodinium cf. aureolum* in New Jersey coastal waters and their occurrence and effects worldwide. J. Coast. Res. 6(1):121–135.

Malone, T. C.
1976. Phytoplankton productivity in the apex of the New York Bight: environmental regulation of productivity/chlorophyll *a*. *In* M. G. Gross (ed.), Middle Atlantic continental shelf and the New York Bight, special symposia, vol. 2, p. 260–272. Allen Press, Lawrence, Kansas.

Malone, T. C., P. J. Neale, and D. Boardman.
1979. Influences of estuarine circulation on the distribution and biomass of phytoplankton size fractions. *In* V. S. Kennedy (ed.), Estuarine perspectives, p. 249–262. Acad. Press, New York.

Malone, T. C.
1984. Anthropogenic nitrogen loading and assimilation capacity of the Hudson river estuarine system, USA. *In* V. S. Kennedy (ed.), The estuary as a filter, p. 291–311. Acad. Press, New York.

Malone, T. C., P. G. Falkowski, T. S. Hopkins, G. T. Rowe, and T. E. Whitledge.
1983a. Mesoscale response of diatom populations to a wind event in the plume of the Hudson River. Deep-Sea Res. 30(2A):149–170.

Malone, T. C., T. S. Hopkins, P. G. Falkowski, and T. E. Whitledge.
1983b. Production and transport of phytoplankton biomass over the continental shelf of the New York Bight. Cont. Shelf Res. 1:305–337.

Mandelli, E. F., P. R. Burkholder, T. E. Doheny, and R. Brody.
1970. Studies of primary productivity in coastal waters of southern Long Island, New York. Mar. Biol. 7:153–160.

Mann, K. H.
1993. Physical oceanography, food chains, and fish stocks: a review. ICES J. Mar. Sci. 50:105–119.

Manning, J.
1991. Middle Atlantic Bight salinity: interannual variability. Cont. Shelf Res. 11(2):123–137.

Marra, J., R. W. Houghton, D. C. Boardman, and P. J. Neale.
1982. Variability in surface chlorophyll *a* at a shelf-break front. J. Mar. Res. 40:575–591.

Marra, J., R. W. Houghton, and C. Garside.
1990. Phytoplankton growth at the shelf-break front in the Middle Atlantic Bight. J. Mar. Res. 49:851–868.

Marshall, H. G.
1976. Phytoplankton distribution along the eastern coast of the U.S.A. I. Phytoplankton composition. Mar. Biol. 38: 81–89.

1984. Phytoplankton of the northeastern continental shelf of the United States in relation to abundance, composition, cell volume, seasonal and regional assemblages. Rapp. P.-v. Reun. Cons. Int. Explor. Mer 183:41–50.

May, R. C.
1974. Larval mortality in marine fishes and the critical period concept. *In* J. H. S. Blaxter (ed.), The early life history of fish, p. 3–19. Springer-Verlag, Berlin.

Meise, C. J., and J. E. O'Reilly.
1996. Spatial and seasonal patterns in abundance and age-composition of *Calanus finmarchicus* in the Gulf of Maine and on Georges Bank: 1977–1987. Physical-biological interactions on Georges Bank and its environs. Deep Sea Res. 43(7–8):1473–1501.

Moody, J. A., B. Butman, R. C. Beardsley, W. S. Brown, P. Daifuku, J. D. Irish, D. A. Mayer, H. O. Mofjeld, B. Petrie, S. Ramp, P. Smith, and W. R. Wright.
1984. Atlas of tidal elevation and current observations on the northeast American continental shelf and slope. U.S. Geol. Surv. Bull. 1611, 122 p.

Mooers, C. N. K., R. W. Garvine, and W. W. Martin.
1979. Summertime synoptic varibility of the middle Atlantic shelf water/slope water front. J. Geophys. Res. 84:4837–4854.

Morse, W. W., M. P. Fahay, and W. G. Smith.
1987. MARMAP surveys of the continental shelf from Cape Hatteras, North Carolina, to Cape Sable, Nova Scotia (1977–1984). Atlas No. 2. Annual distribution patterns of fish larvae. NOAA Tech. Memo. NMFS-F/NEC-47, 215 p.

Mountain, D., and P. Jessen.
1987. Bottom waters of the Gulf of Maine, 1978–1983. J. Mar. Res. 45:319–345.

Mountain, D. G., and T. J. Holzwarth.
1989. Surface and bottom temperature distribution for the northeast continental shelf. NOAA Tech. Memo. NMFS-F/NEC-73, 39 p.

Mountain, D. G., and J. P. Manning.
1994. Seasonal and interannual variability in the properties of the surface waters of the Gulf of Maine. Cont. Shelf Res. 14(13/14):1555–1581.

Nielsen, T. G., B. Lokkegaard, K. Richardson, F. B. Pedersen, and L. Hansen.
1993. Structure of plankton communities in the Dogger Bank area (North Sea) during a stratified season. Mar. Ecol. Prog. Ser. 95:115–131.

Nixon, S. W.
1988. Physical energy inputs and the comparative ecology of lake and marine ecosystems. Limnol. Oceanogr. 33(4, part 2):1005–1025.

1992. Quantifying the relationship between nitrogen input and the productivity of marine ecosystems. Proc. Adv. Mar. Tech. Conf. 5, p. 57–83.

O'Reilly, J. E., and J. P. Thomas.
1983. A manual for measurement of total primary production using ^{14}C-simulated *in situ* sunlight inclubation. Biomass Handbook No.10, SCAR/SCOR/IABO/ACMRR, 70 p.

O'Reilly, J. E., C. Evans-Zetlin, and D. A. Busch.
1987. Primary production. *In* R. H. Backus and D. W. Bourne (eds.), Georges Bank, p. 220–233. MIT Press, Cambridge, Mass.

Parsons, T. R., Y. Maita, and C. M. Lalli.
1985. A manual of chemical and biological methods for seawater analysis. Pergamon Press, Oxford, U.K., 187 p.

Pearce, J. B.
1981. Monitoring the health of the northeast continental shelf. OCEANS '81 IEEE:744-751.

Perry R. I., G. C. Harding, J. W. Loder, M. J. Tremblay, M. M. Sinclair, and K. F. Drinkwater.
1993. Zooplankton distributions at the Georges Bank frontal system: retention or dispersion? Cont. Shelf Res. 13:357–383.

Pingree, R. D.
1978. Mixing and stabilization of phytoplankton distributions on the northwest European continental shelf. *In* J. H. Steele (ed.), Spatial patterns in plankton communities, p. 181–220. Plenum Press, New York.

Pingree, R. D., P. M. Holligan, G. T. Mardell, and R. N. Head.
1976. The influence of physical stability on spring, summer and autumn phytoplankton blooms in the Celtic Sea. J. Mar. Biol. Assoc. U.K. 56:845–873.

Platt, T., C. Caverhill, and S. Sathyendranath.
1991. Basin-scale estimates of oceanic primary production by remote sensing: the North Atlantic. J. Geophys. Res. 96(C8):15147–15159.

Radach, G., J. Berg, and E. Hagmeier.
1990. Long-term changes of the annual cycles of meteorological, hydrographic, nutrient and phytoplankton time series at Helgoland and at LV ELBE 1 in the German Bight. Cont. Shelf Res. 10(4):305–328.

Ramp, S., R. Schlitz, and W. R. Wright.
1985. The deep flow through Northeast Channel, Gulf of Maine. J. Phys. Oceanogr. 15:1790–1808.

Raymont, J. E. C.
1949. Further observations on changes in the bottom fauna of a fertilized sea-loch. J. Mar. Biol. Assoc. U.K. 28:9–19.

Richardson, K., and A. Christoffersen.
1991. Seasonal distribution and production of phytoplankton in the southern Kattegat. Mar. Ecol. Prog. Ser. 78:217–227.

Riley, G.
1941. Plankton studies. IV. Georges Bank. Bingham Oceanogr. Collect. 7(art. 4):1–73.
1952. Phytoplankton of Block Island Sound, 1949. Bull. Bingham Oceanogr. Collect. 13:40–64.

Riley, G. A.
1956. Review of the oceanography of the Long Island Sound. Deep-Sea Res. 3:224–238.
1957. Phytoplankton of the north central Sargasso Sea, 1950–52. Limnol. Oceanogr. 2:252–270.

Ripley, B. D.
1980. Spatial statistics. John Wiley & Sons, New York, 252 p.

Rosenberg, R.
1985. Eutrophication — The future marine coastal nuisance? Mar. Poll. Bull. 16(6):227–231.

Rowe, G. T., S. Smith, P. Falkowski, T. Whitledge, R. Theroux, W. Phoel, and H. Ducklow.
1986. Do continental shelves export organic matter? Nature 324:559–561.

Ryther, J. H., and C. S. Yentsch.
1958. Primary production of continental shelf waters off New York. Limnol. Oceanogr. 3:327–335.

Sampson, R. J.
1988. SURFACE III users manual. Kansas Geological Survey. Interactive Concepts Inc., Lawrence, Kans., 277 p.

SAS Institute Inc.
1990. SAS/STAT User's Guide, Version 6, Fourth Edition, Volume 1, Cary NC: SAS Inst. Inc., 943 p.

Sathyendranath, S., and T. Platt.
1981. Remote sensing of ocean chlorophyll: consequence of nonuniform pigment profile. Appl. Optics 28(3):490–495.

Sathyendranath, S., T. Platt, E. P. W. Horne, W. G. Harrison, O. Ulloa, R. Outerbridge, and N. Hoepffner.
1991. Estimation of new production in the ocean by compound remote sensing. Nature 253:129–133.

Sherman, K.
1980. MARMAP, a fisheries ecosystem study in the NW Atlantic: fluctuations in ichthyoplankton-zooplankton components and their potential for impact on the system. *In* F. P. Diemer, F. J. Vernbert, and D. Z. Merkes (eds.), Advanced concepts in ocean measurement for marine biology, p. 9–37. Univ. S.C. Press, Columbia.

Sherman, K., W. Smith, W. Morse, M. Berman, J. Green, and L. Ejsymont.
1984. Spawning strategies of fishes in relation to circulation, phytoplankton production, and pulses in zooplankton off the northeastern United States. Mar. Ecol. Prog. Ser. 18: 1–19.

Sherman, K., W. G. Smith, J. R. Green, E. B. Cohen, M. S. Berman, K. A. Marti, and J. R. Goulet.
1987. Zooplankton production and the fisheries of the northeastern shelf. *In* R. H. Backus and D. W. Bourne (eds.), Georges Bank, p. 269–282. MIT Press, Cambridge, Mass.

Sherman, K., M. Grosslein, D. Mountain, D. Busch, J. O'Reilly, and R. Theroux.
1988. The continental shelf ecosystem off the northeast coast of the United States. *In* H. Postma and J. J. Zijlstra (eds.), Ecosystems of the world, vol. 27, p. 279–337. Elsevier Press, The Netherlands.

Sibunka, J., and M. Silverman.
1989. MARMAP surveys of the continental shelf from Cape Hatteras, North Carolina, to Cape Sable, Nova Scotia (1984–87). Atlas no. 3. Summary of operations. NOAA Tech. Memo. NMFS-F/NEC–68, 197 p.

Smayda, T.
1990. Novel and nuisance phytoplankton blooms in the sea: evidence for a global epidemic. *In* E. Graneli, B. Sundstrom, L. Edler, and D. M. Anderson (eds.), Toxic marine phytoplankton, p 29–40. Elsevier Sci. Publ. Co., Amsterdam.
1990. Global epidemic of noxious phytoplankton blooms and food chain consequences in large ecosystems. *In* K.Sherman, L. M. Alexander, and B. D. Gold (eds.), Food chains, yields, models, and management of large marine ecosystems, p. 275–307. Westview Press, Boulder, Colo.

Smith, P. E., and R. W. Eppley.
1982. Primary production and the anchovy population in the Southern California Bight: Comparison of time series. Limnol. Oceanogr. 27:1–17.

Smith, R. A., R. B. Alexander, and M. G. Wolman.
1987. Water-quality trends in the nation's rivers. Science 235:1607–1615.

Smith, R. C.
1981. Remote sensing and depth distribution of ocean chlorophyll. Mar. Ecol. Progr. Ser. 5:359–361.

Smith, R. C., and K. S. Baker.
1982. Oceanic chlorophyll concentrations as determined by satellite (Nimbus-7 Coastal Zone Color Scanner). Mar. Biol. 66:269–279.

Snyder J. P.
1987. Map projections-a working manual. U.S. Geol. Surv. Prof. Pap. 1395, 383 p.

Steven, D. M.
1975. Biological production in the Gulf of Saint Lawrence. *In* T. W. M. Cameron and L. W. Billingsley (eds.), Energy

flow—its abiological dimensions, a summary of the IBP in Canada 1964–1975, p. 229–248. R. Soc. Can., Ottawa.

Stoddard, A., J. E. O'Reilly, T. E. Whitledge, T. C. Malone, and J. F. Herbard.
1986. The application and development of a compatible historical data base for the analysis of water quality management issues in the New York Bight. IEEE Oceans '86 Conference Proc., Wash. D.C., p. 1030–1035.

Sverdrup, H.
1955. The place of physical oceanography in oceanographic research. J. Mar. Res. 14(4):287–294.

Townsend, D., and L. M. Cammen.
1988. Potential importance of the timing of spring plankton blooms to benthic-pelagic coupling and recruitment of juvenile demersal fishes. Biol. Oceanogr. 5:215–229.

Townsend, D., and R. Spinrad.
1986. Early spring phytoplankton blooms in the Gulf of Maine. Cont. Shelf Res. 6(4):515–529.

Townsend, D., J. Christensen, D. Stevenson, J. Graham, and S. Chenoweth.
1987. The importance of a plume of tidally-mixed water to the biological oceanography of the Gulf of Maine. J. Mar. Res. 45:699–728.

Townsend, D., T. Cucci, and T. Berman.
1984. Subsurface chlorophyll maxima and vertical distribution of zooplankton in the Gulf of Maine. J. Plankton Res. 6(5):793–802.

Trees, C. C., M. C. Kennicutt, and J. M. Brooks.
1985. Errors associated with the standard fluorimetric determination of chlorophylls and phaeopigments. Mar. Chem. 17:1–12.

TRIGOM.
1974. A socio-economic and environmental inventory of the North Atlantic region. The Research Institute of the Gulf of Maine, South Portland, Maine, Book III, Vol. I.

Twichell, D., B. Butman, and R. Lewis.
1987. Shallow structure, surficial geology, and the processes currently shaping the Bank. *In* R. H. Backus and D. W. Bourne (eds.), Georges Bank, p. 31–37. MIT Press, Cambridge, Mass.

Uchupi, E.
1965. Map showing relation of land and submarine topography, Nova Scotia to Florida. U.S.G.S. Misc. Geol. Invest. Map I–451.

Uchupi, E., and J. A. Austin.
1987. Morphology. *In* R. H. Backus and D. W. Bourne (eds.), Georges Bank, p. 25–30. MIT Press, Cambridge, Mass.

UNESCO.
1966. Determination of photosynthetic pigments in seawater. Monogr. Oceanogr. Methodol. 1, 69 p.

Venrick, E. L.
1978. Systematic sampling in a planktonic ecosystem. Fish. Bull. 76(3):617:627.

Venrick, E. L., J. A. McGowan, D. R. Cayan, and T. L. Hayward.
1987. Climate and chlorophyll *a*: long-term trends in the central North Pacific Ocean. Science 238:70–72.

Walsh, J.
1981. Shelf-sea ecosystem. *In* A. R. Longhurst (ed.), Analysis of marine ecosystems. p. 159–196. Acad. Press, New York.

Walsh, J., T. Whitledge, F. Barvenik, C. Wirick, O. Howe, W. Esaias, and J. Scott.
1978. Wind events and food chain dynamics within the New York Bight Limnol. Oceanogr. 23:659–683.

Walsh, J., G. T. Rowe, R. L. Iverson, and C. P. McRoy.
1981. Biological export of shelf carbon is a sink of the global CO_2 cycle. Nature 291:196–201.

Walsh, J. J., T. E. Whitledge, J. E. O'Reilly, W. C. Phoel, and A. F. Draxler.
1987. Nitrogen cycling on Georges Bank and the New York shelf: A comparison between well-mixed and seasonally stratified waters. *In* R. H. Backus (ed.), Georges Bank, p. 234–246. MIT Press, Cambridge, Mass.

Welschmeyer, N. A.
1994. Fluorometric analysis of chlorophyll *a* in the presence of chlorophyll *b* and phaeopigments. Limnol. Oceanogr. 39(8):1985–1992.

Wright, W. R.
1976. The limits of shelf water south of Cape Cod, 1941–1972. J. Mar. Res. 34(1):1–14.

Yentsch, C. S.
1977. Plankton production. MESA New York Bight atlas monograph 12. N.Y. Sea Grant Inst., Albany, 25 p.
1981. Vertical mixing, a constraint to primary production: an extension of the concept of an optimal mixing zone. *In* J. C. J. Nihoul (ed.), Ecohydrodynamics, p. 67–78. Elsevier, Amst.

Yentsch, C. S., and N. Garfield.
1981. Principal areas of vertical mixing in the waters of the Gulf of Maine, with reference to the total productivity of the area. *In* J. F. R. Gower (ed.), Oceanography and space, p. 303–322. Plenum, N.Y.

Yentsch, C. S., and D. W. Menzel.
1963. A method for the determination of phytoplankton chlorophyll and phaeophytin by fluorescence. Deep-Sea Res. 10:221–231.

Yentsch, C. S., D. A. Phinney, and J. W. Campbell.
1994. Color banding on Georges Bank as viewed by coastal zone color scanner. J.Geophys. Res. 99:7401–7410.

Yoder, J. A., L. P. Atkinson, S. S. Bishop, E E. Hofmann, and T. N. Lee.
1983. Effect of upwelling on phytoplankton productivity on the outer southeastern United States continental shelf. Cont. Shelf Res. 1(4):385–404.

Yoder, J. A., L. P. Atkinson, S. S. Bishop, J. O. Blanton, T. N. Lee, and L. J. Pietrafesa.
1985. Phytoplankton dynamics within Gulf Stream intrusions on the southeastern United States continental shelf during summer 1981. Cont. Shelf Res. 4(6):611–635.

Yoder, J. A., W. E. Esaias, G. C. Feldman, and C. R. McClain.
1988. Satellite ocean color-status report. Oceanogr. Mag. 1:18–20,35.

APPENDIX A

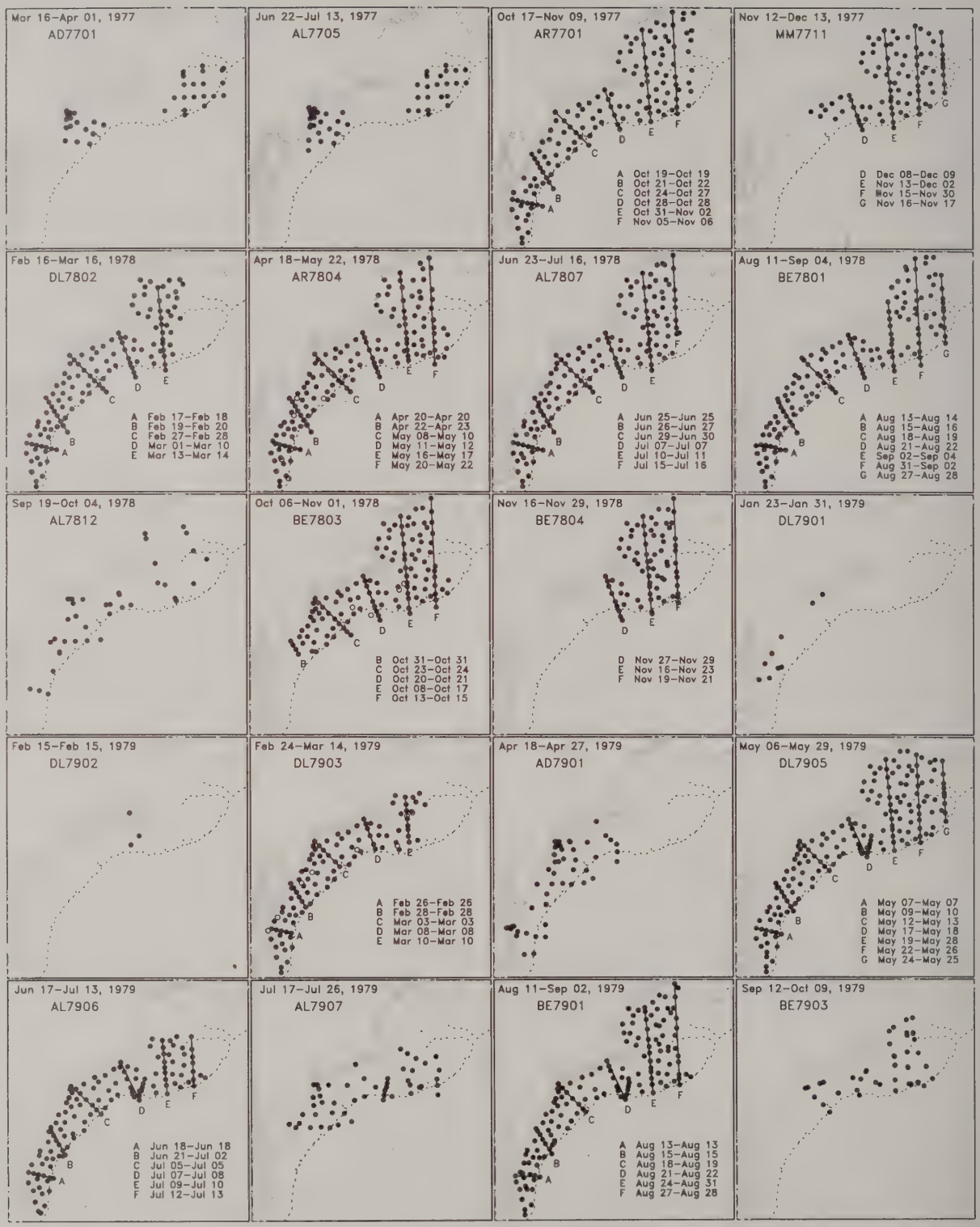

Appendix Figure A1

Locations of stations sampled during the 78 surveys considered in this report. Surveys are presented in chronological order. The survey period and the survey name are shown in the upper left area of each panel. The dates of occupations of standard transects (A, B, C, D, E, F, G) are shown in the lower right area for MARMAP surveys. Stations east of the map area are not shown for survey AL 8011.

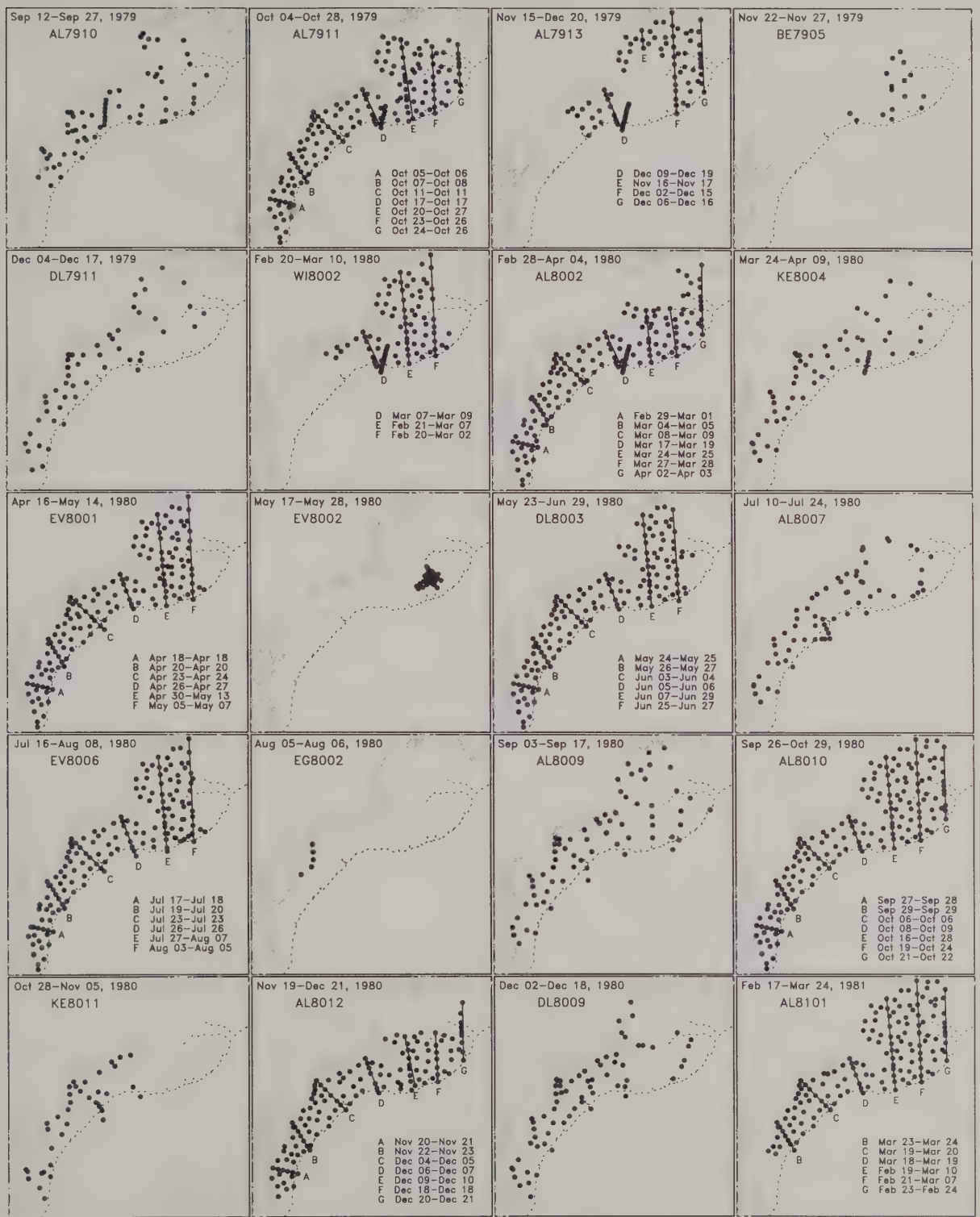

Appendix Figure A1 (continued)

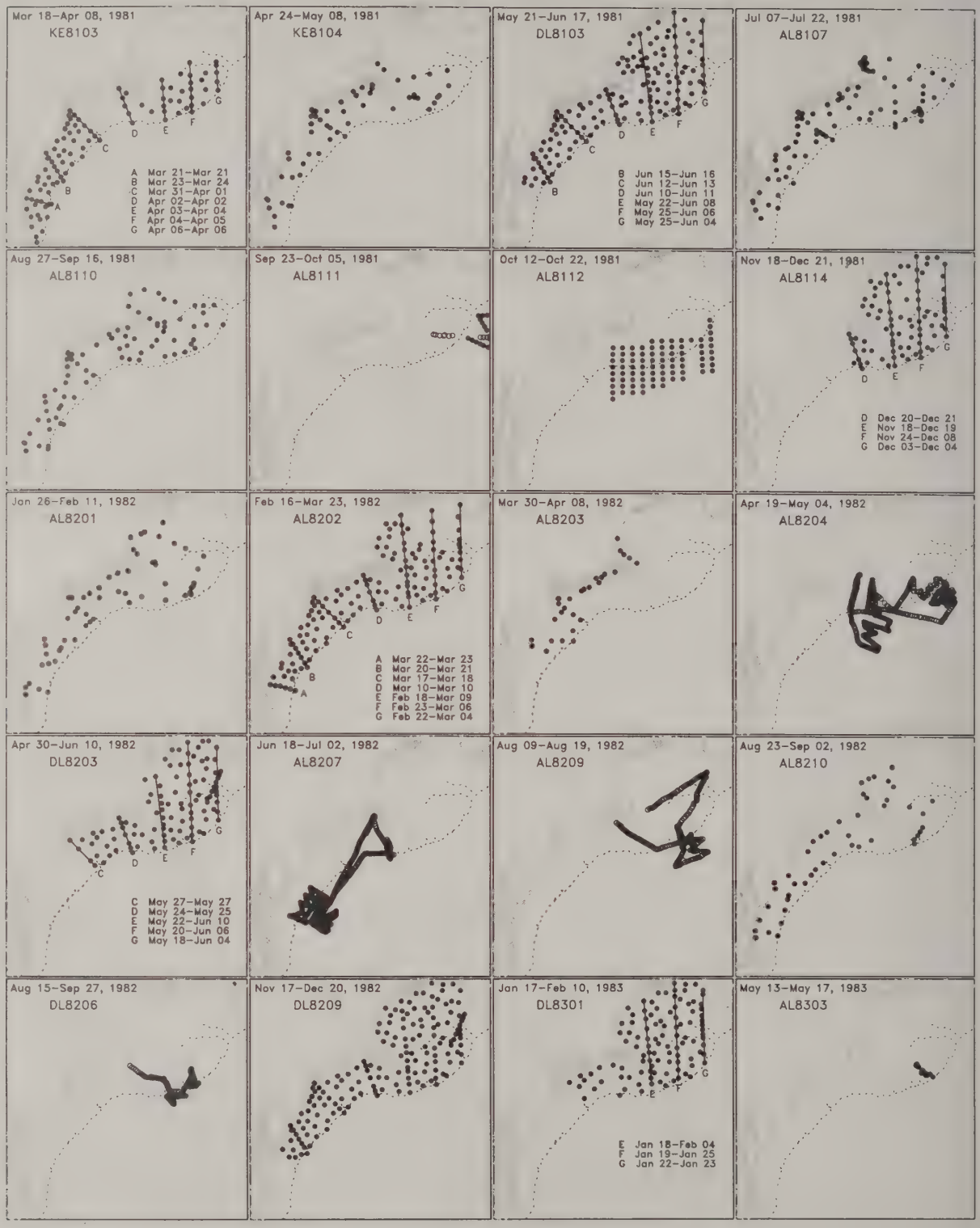

Appendix Figure A1 (continued)

Appendix Figure A1 (continued)

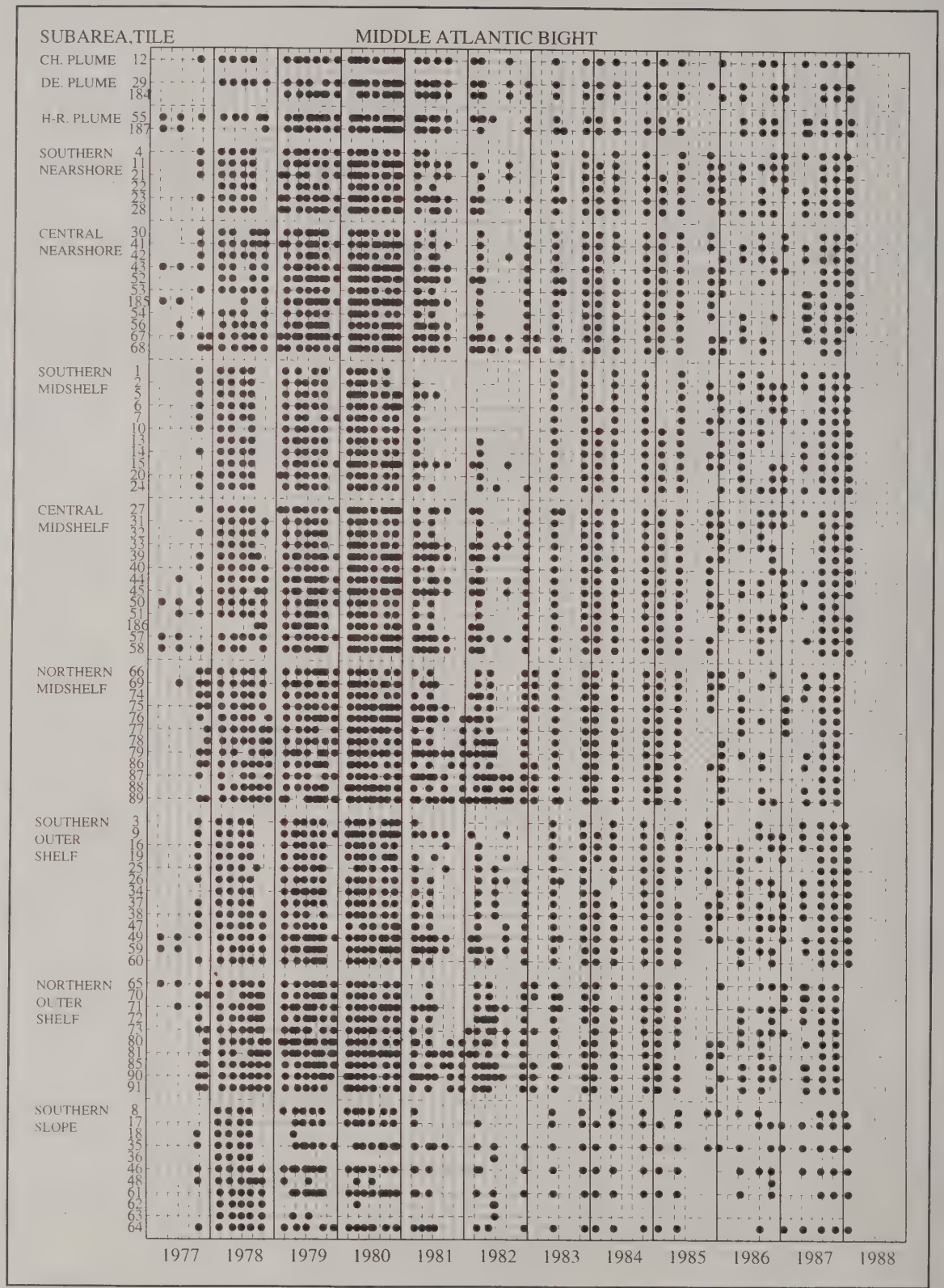
SUBAREA,TILE
MIDDLE ATLANTIC BIGHT
CH. PLUME 12
DE. PLUME 29 184
H-R. PLUME 55 187
SOUTHERN NEARSHORE 4 11 21 22 23 25 28
CENTRAL NEARSHORE 30 41 42 43 52 53 185 54 56 67 68
SOUTHERN MIDSHELF 1 2 5 6 7 10 13 14 15 20 24
CENTRAL MIDSHELF 27 31 32 33 39 40 44 45 50 51 186 57 58
NORTHERN MIDSHELF 66 69 74 75 76 77 78 79 86 87 88 89
SOUTHERN OUTER SHELF 3 9 16 19 25 26 34 37 38 47 49 59 60
NORTHERN OUTER SHELF 65 70 71 72 73 80 81 85 90 91
SOUTHERN SLOPE 8 17 18 35 36 46 48 61 62 63 64
1977 1978 1979 1980 1981 1982 1983 1984 1985 1986 1987 1988

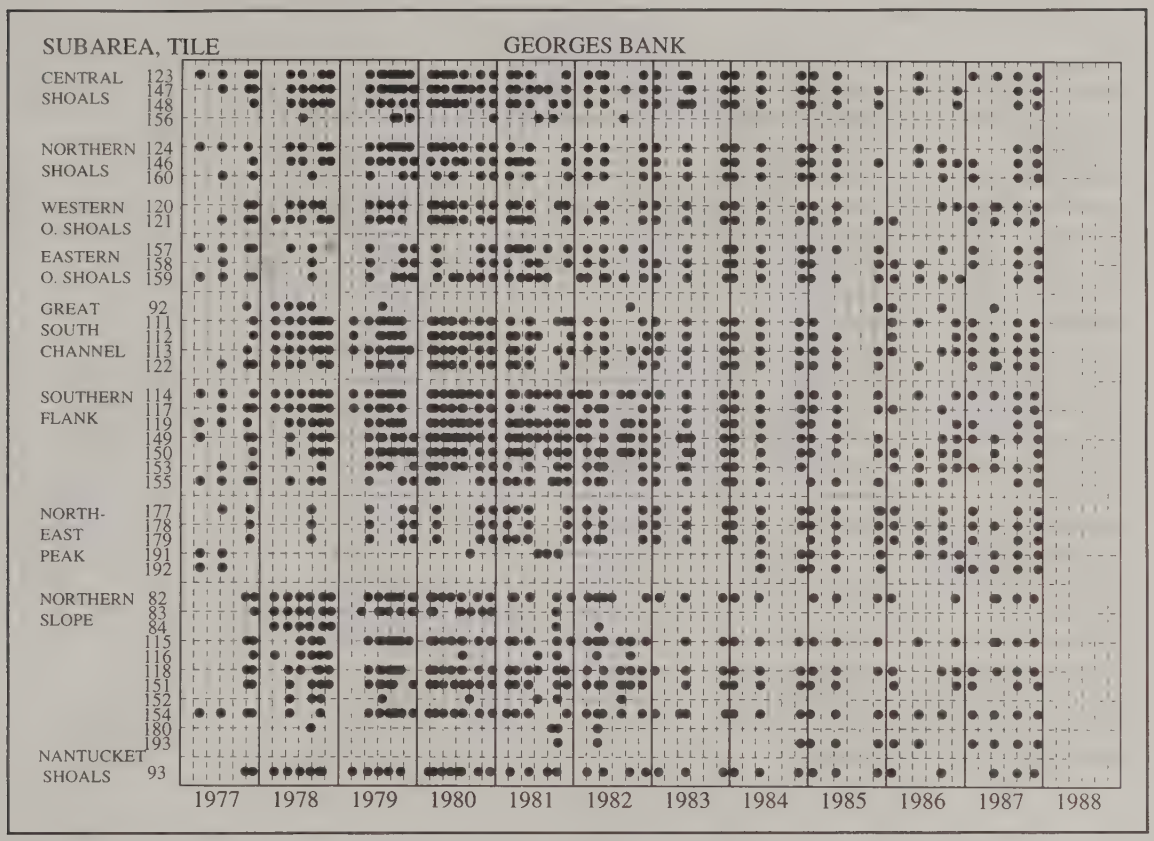

Appendix Figure A2 (facing page and above)

Temporal distribution of chlorophyll sampling in subareas of the Middle Atlantic Bight, Georges Bank, and Gulf of Maine, 1977–88. Values in the left column are standard tile numbers (see Figs. 5, 8).

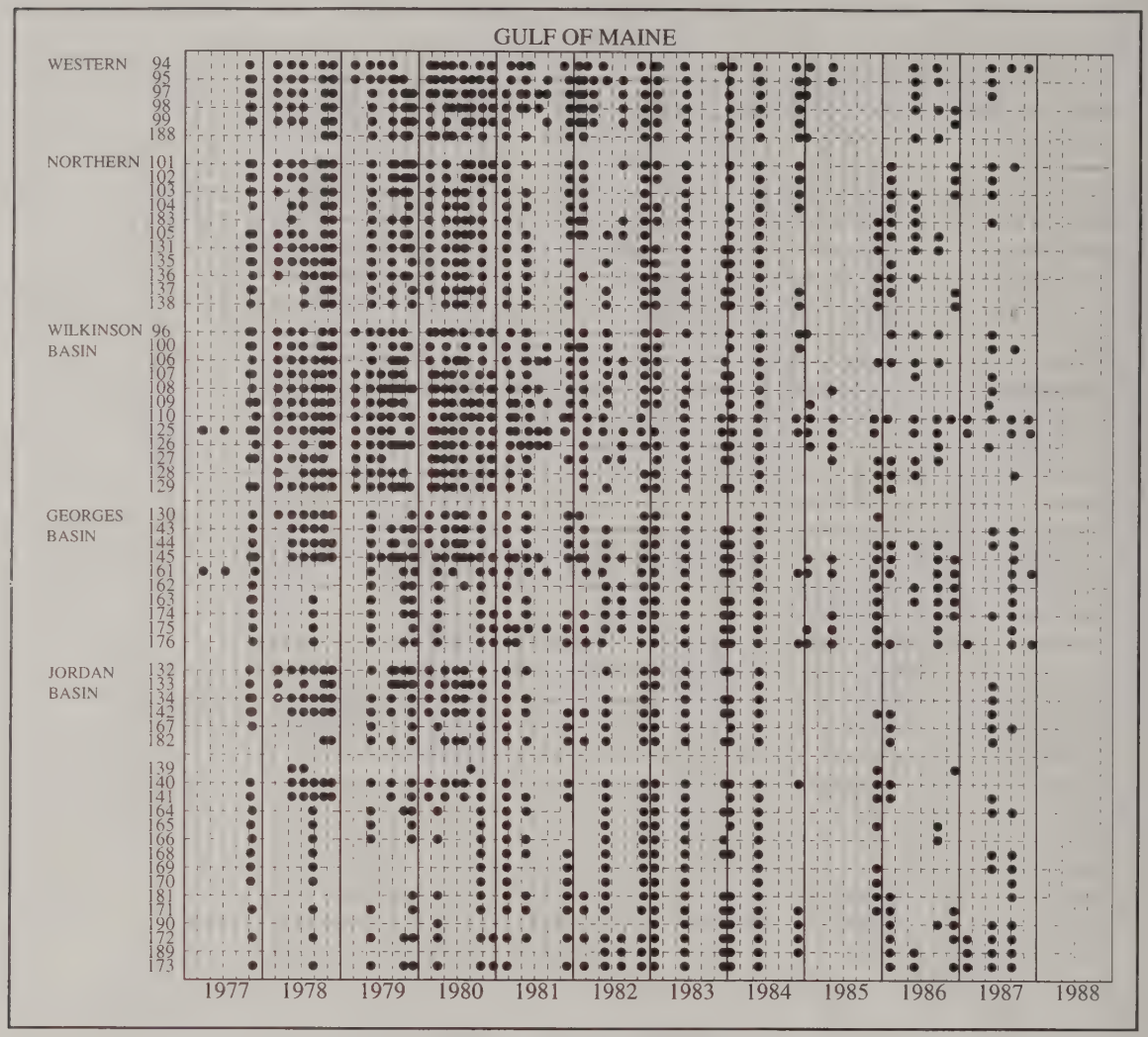

Appendix Figure A2 (continued)

APPENDIX B

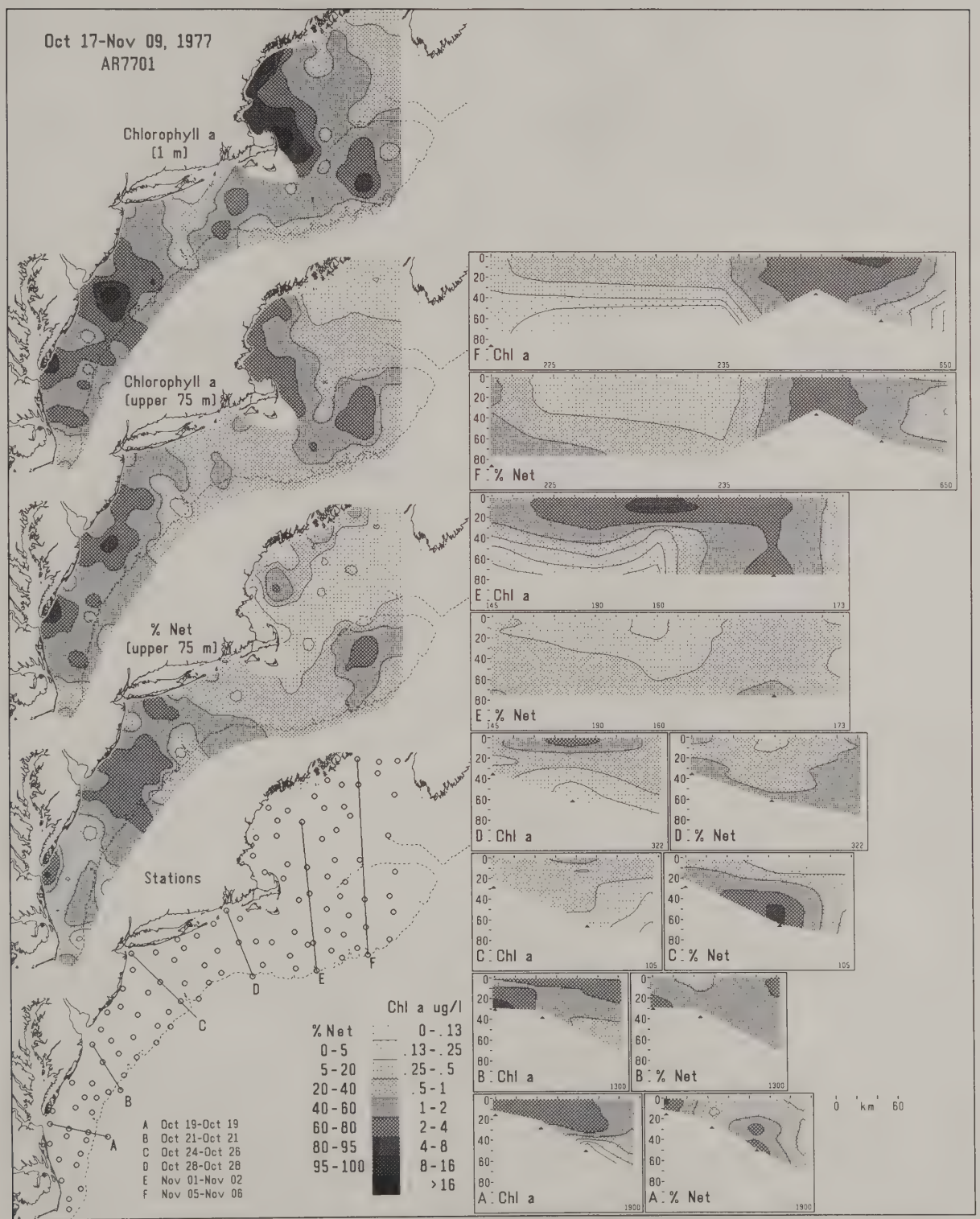

Appendix Figure B1

The distribution of chlorophyll *a* (Chl *a*) and percent netplankton (% Net) during survey AR7701.

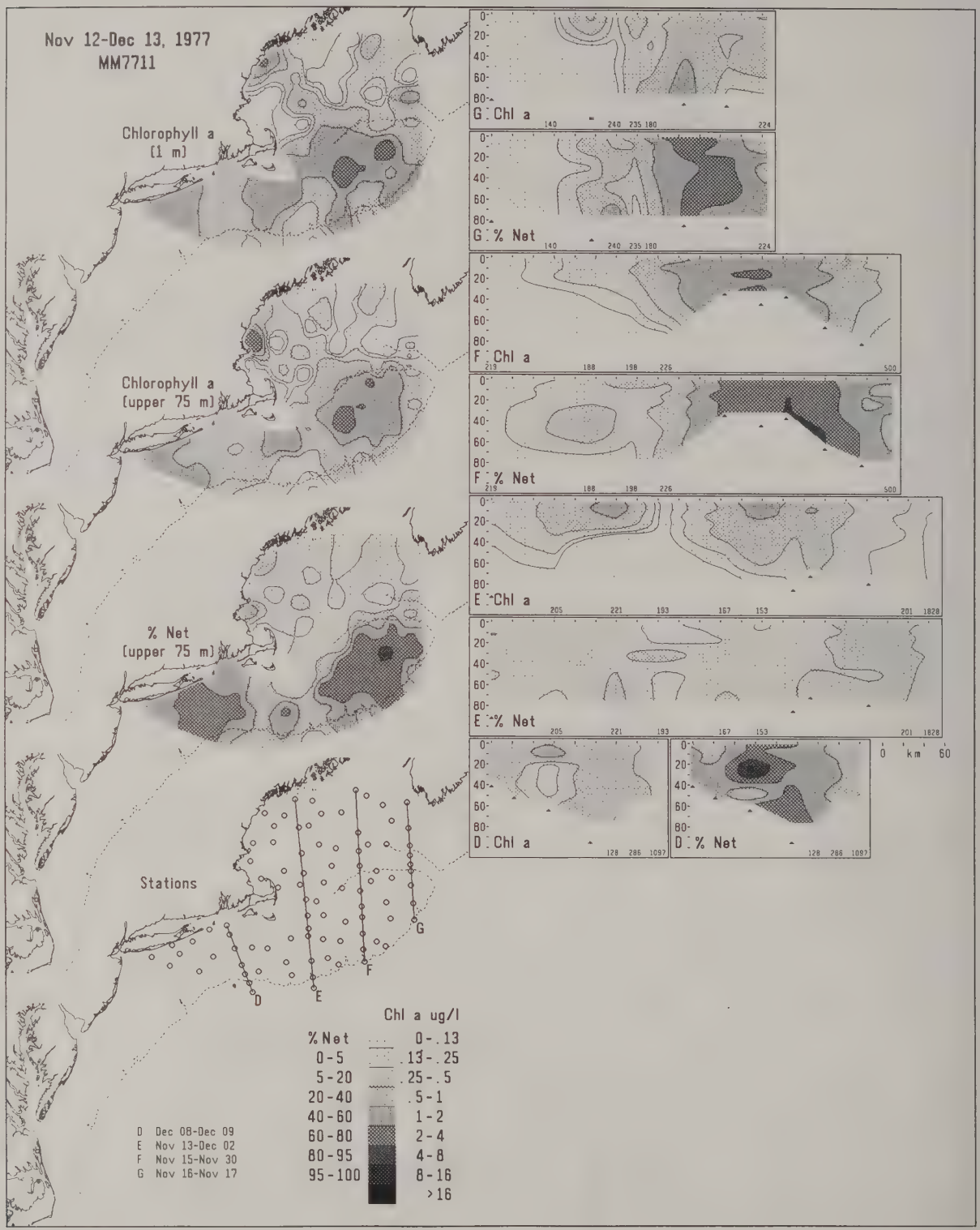

Appendix Figure B2
The distribution of chlorophyll *a* and percent netplankton during survey MM7711.

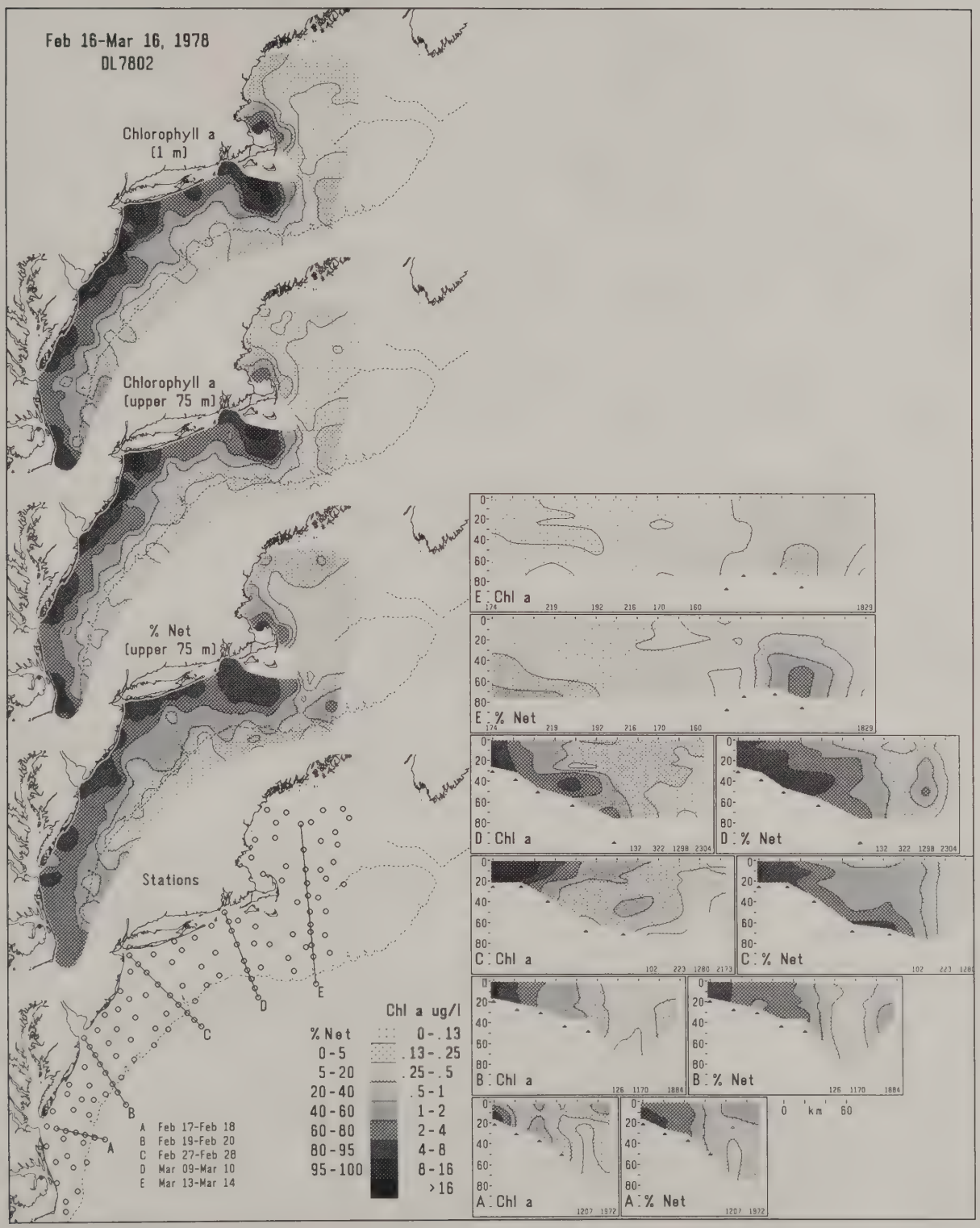

Appendix Figure B3
The distribution of chlorophyll *a* and percent netplankton during survey DL7802.

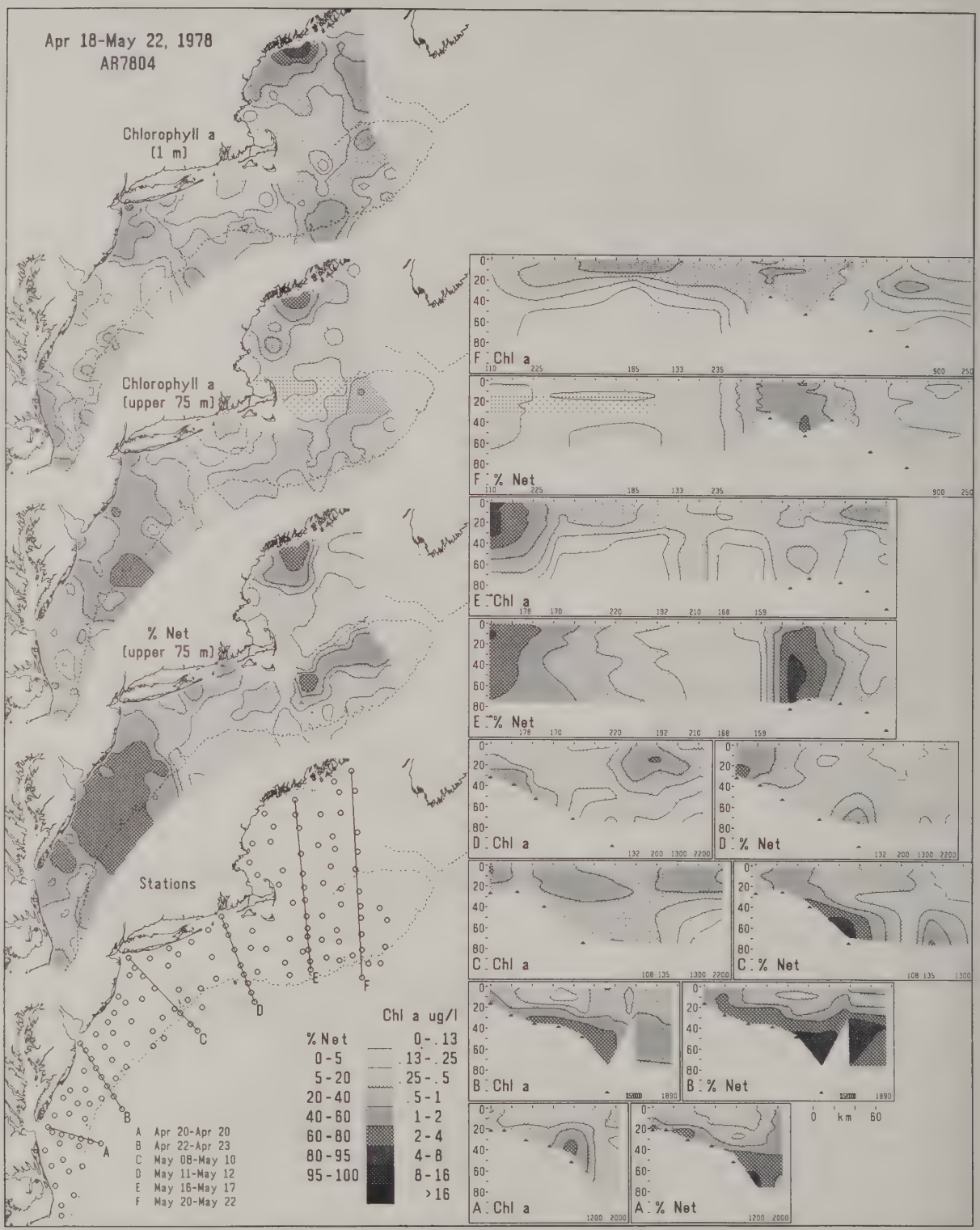

Appendix Figure B4
The distribution of chlorophyll *a* and percent netplankton during survey AR7804.

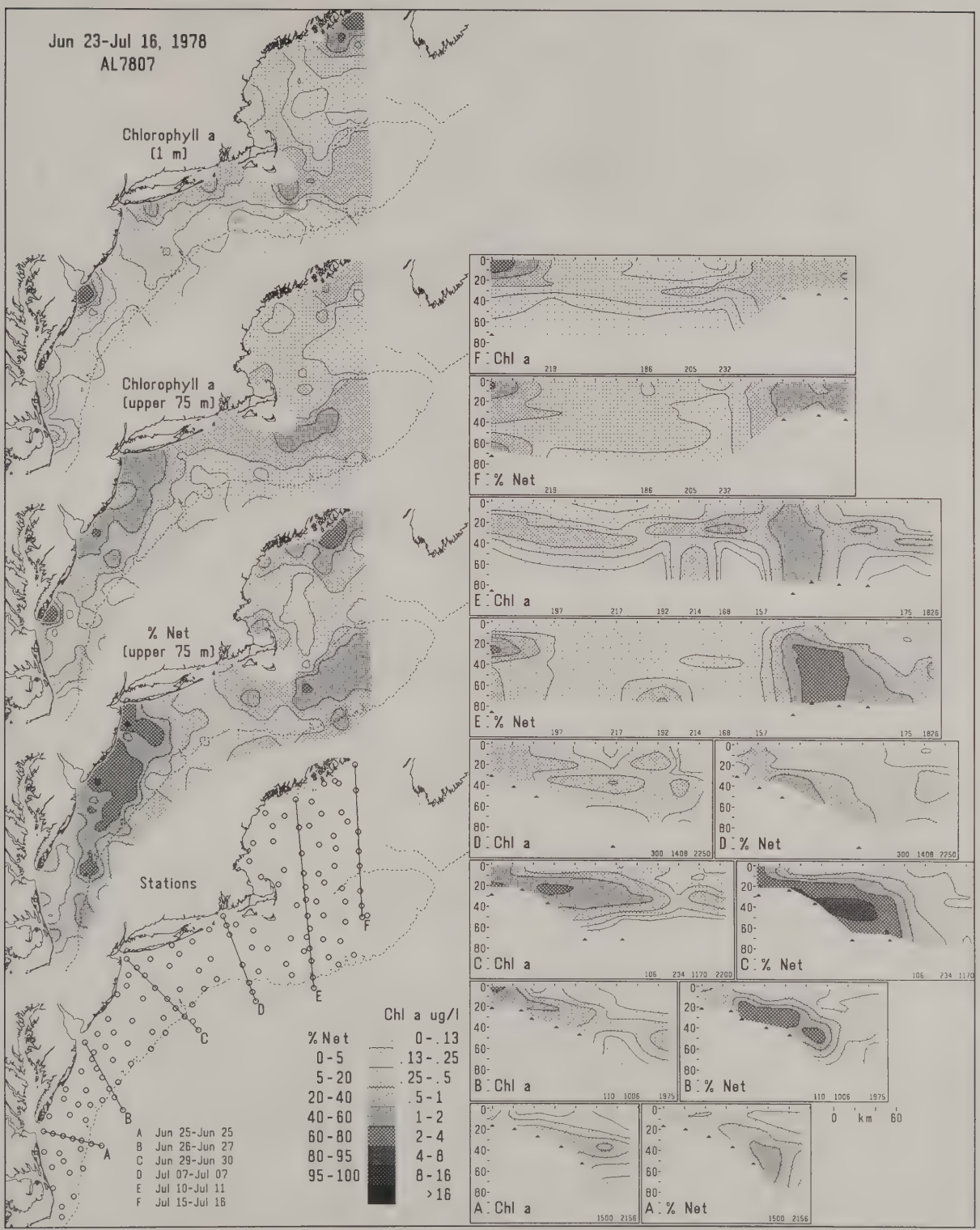

Appendix Figure B5
The distribution of chlorophyll *a* and percent netplankton during survey AL7807.

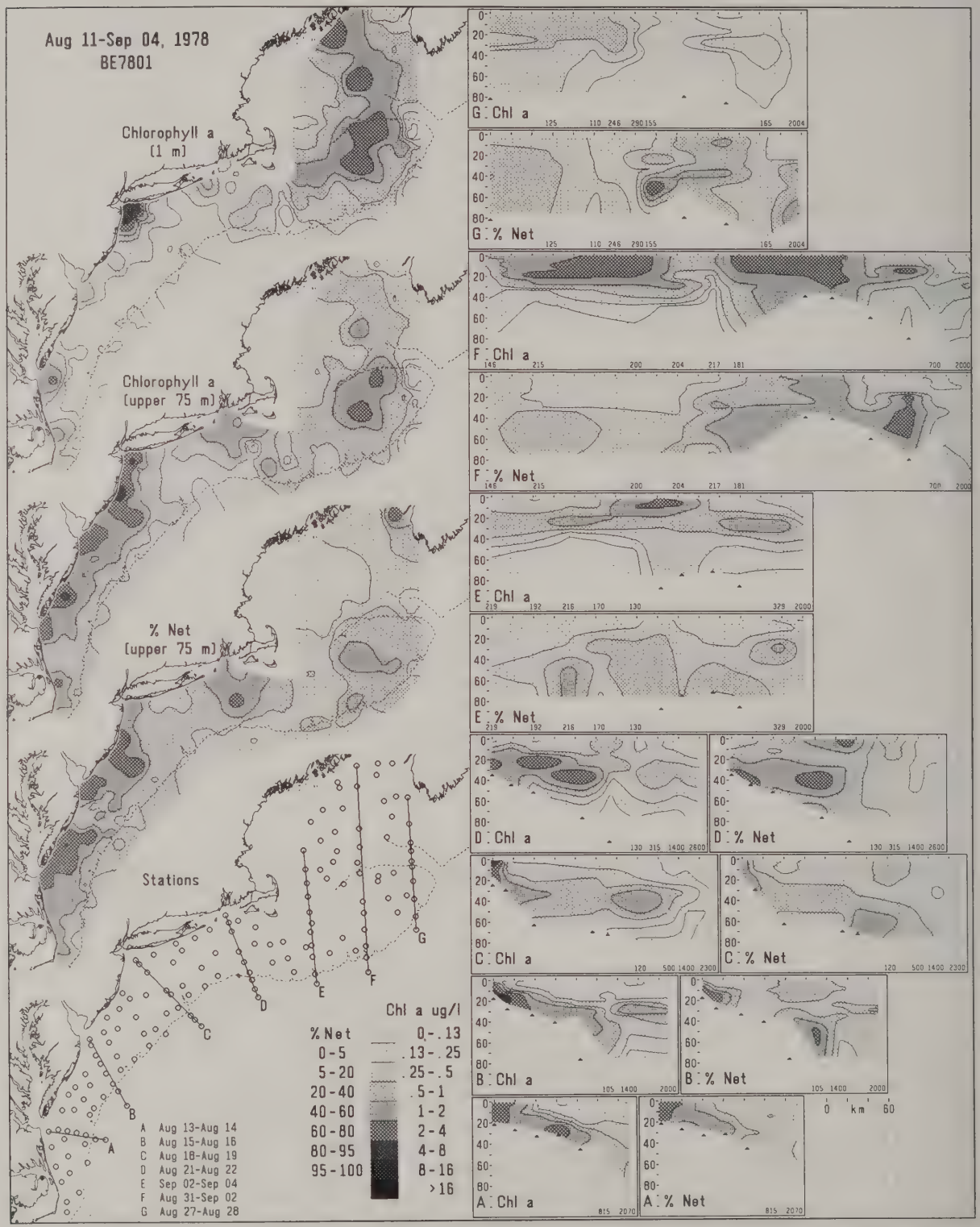

Appendix Figure B6
The distribution of chlorophyll *a* and percent netplankton during survey BE7801.

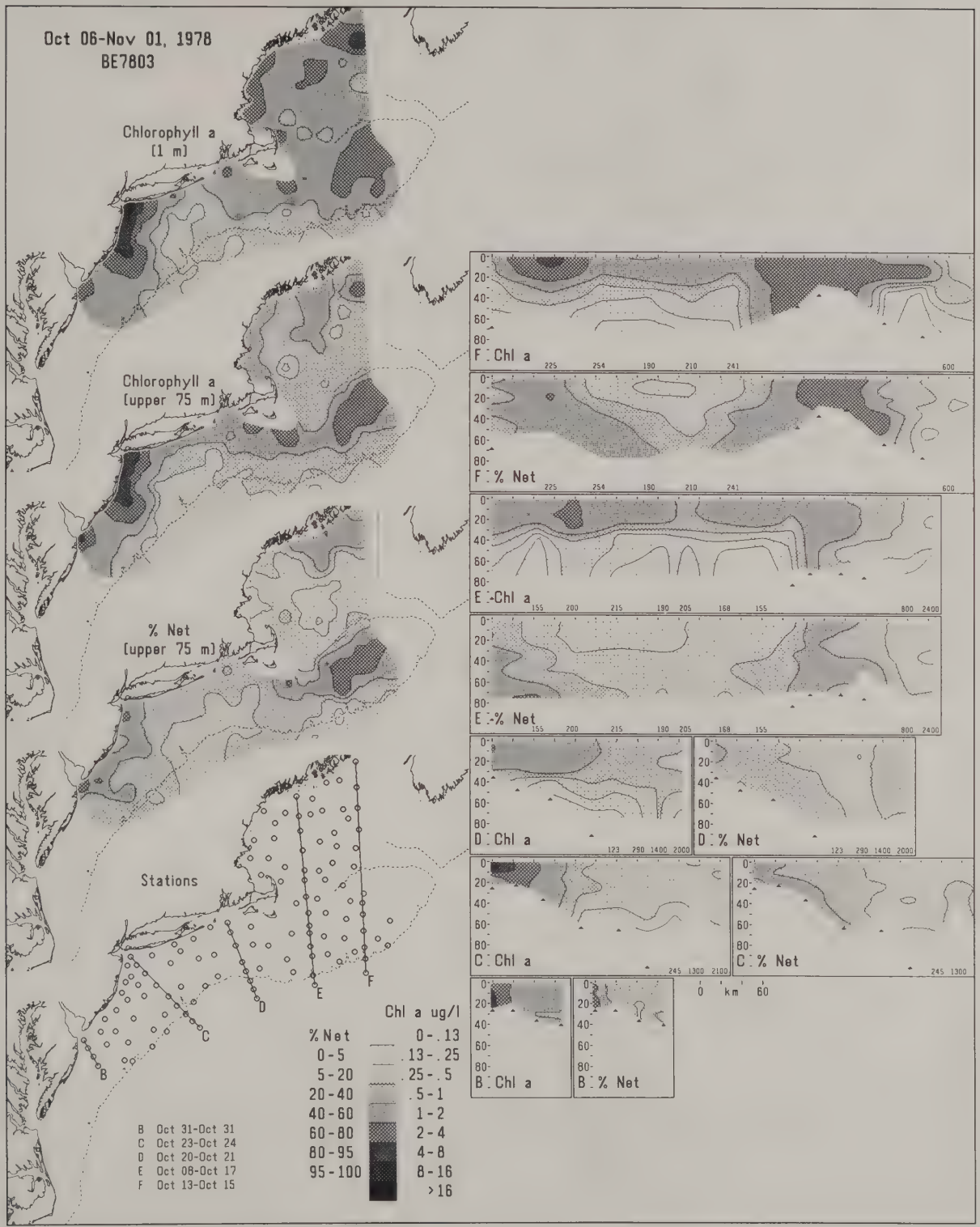

Appendix Figure B7
The distribution of chlorophyll *a* and percent netplankton during survey BE7803.

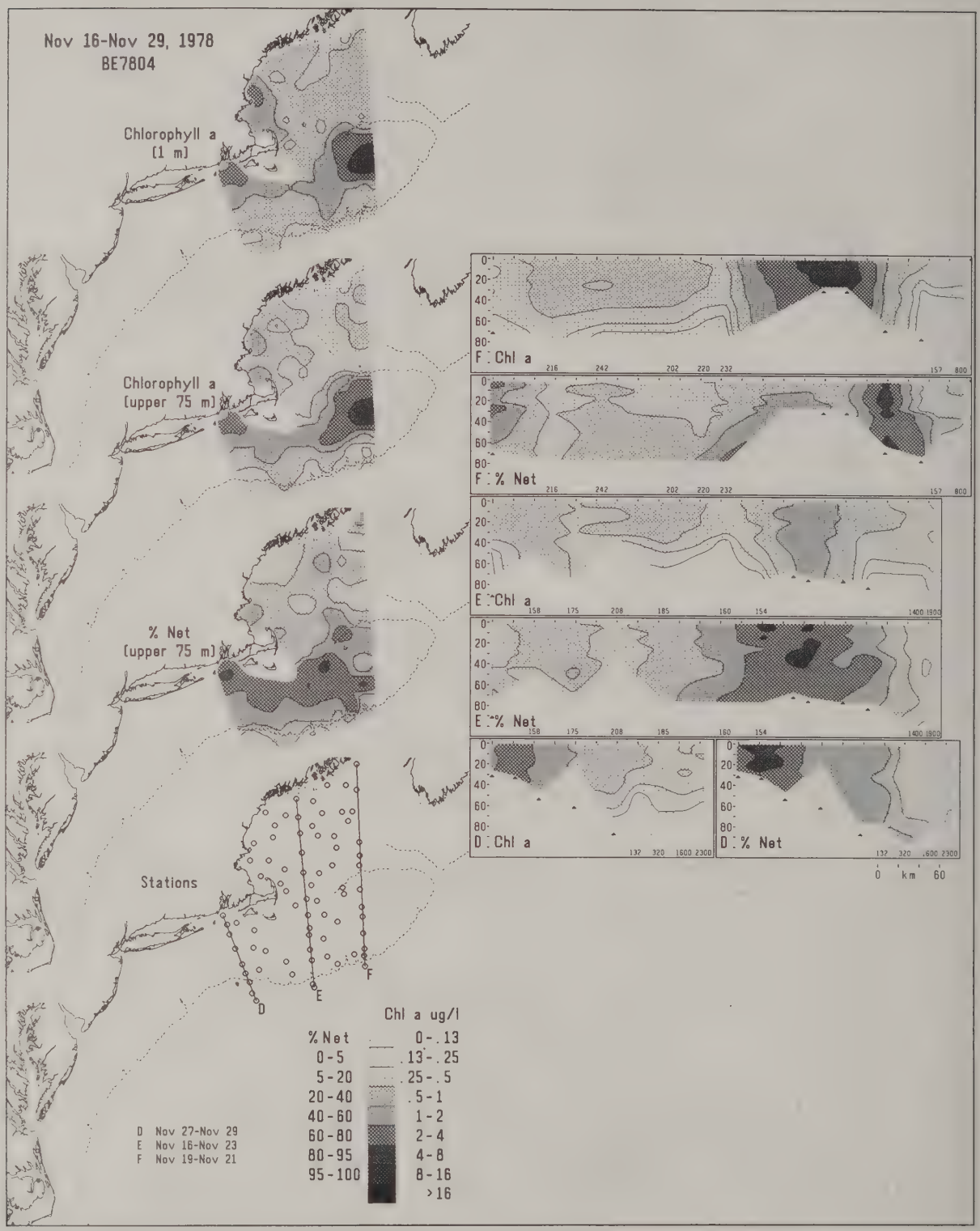

Appendix Figure B8
The distribution of chlorophyll *a* and percent netplankton during survey BE7804.

Appendix Figure B9
The distribution of chlorophyll *a* and percent netplankton during survey DL7903.

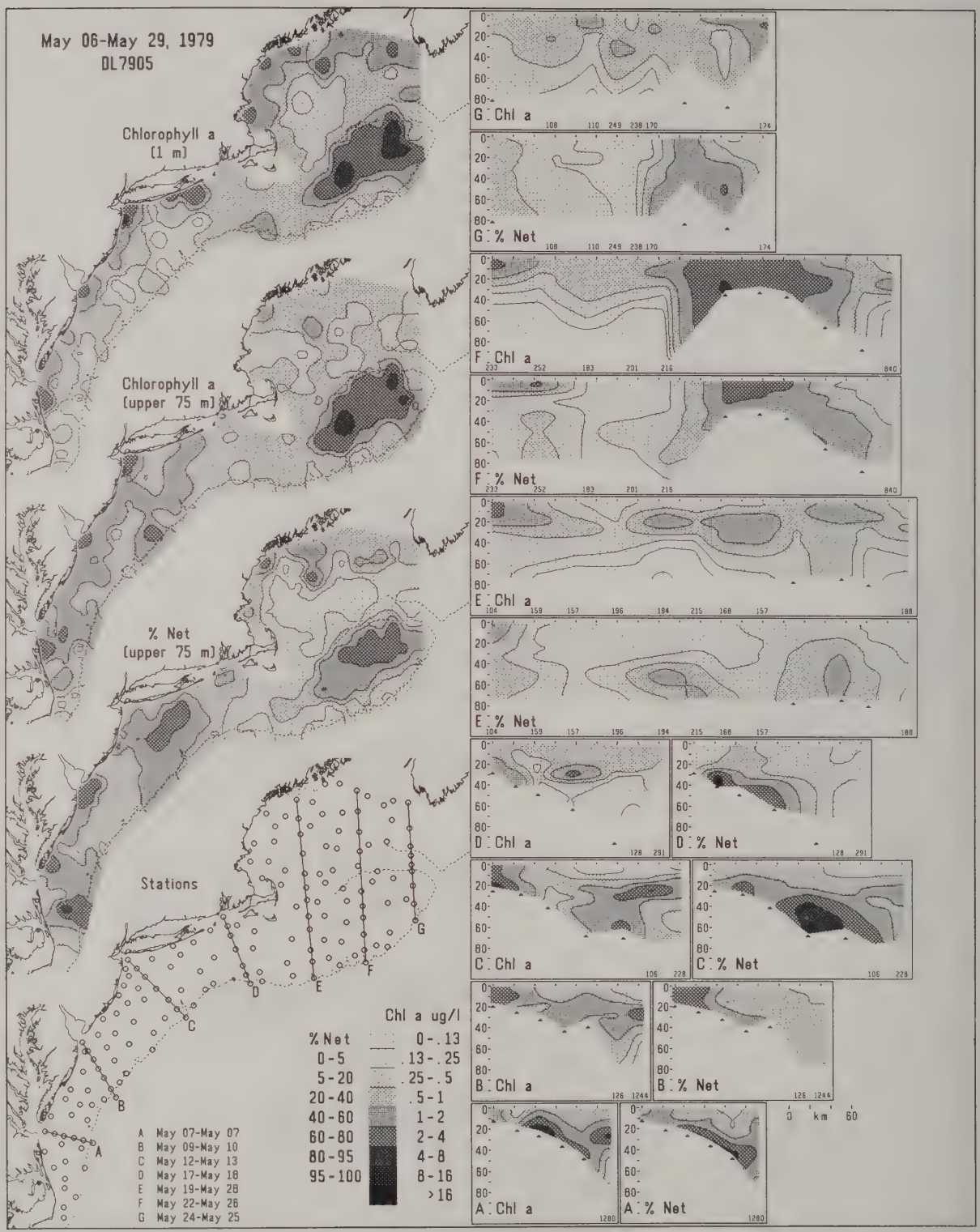

Appendix Figure B10
The distribution of chlorophyll *a* and percent netplankton during survey DL7905.

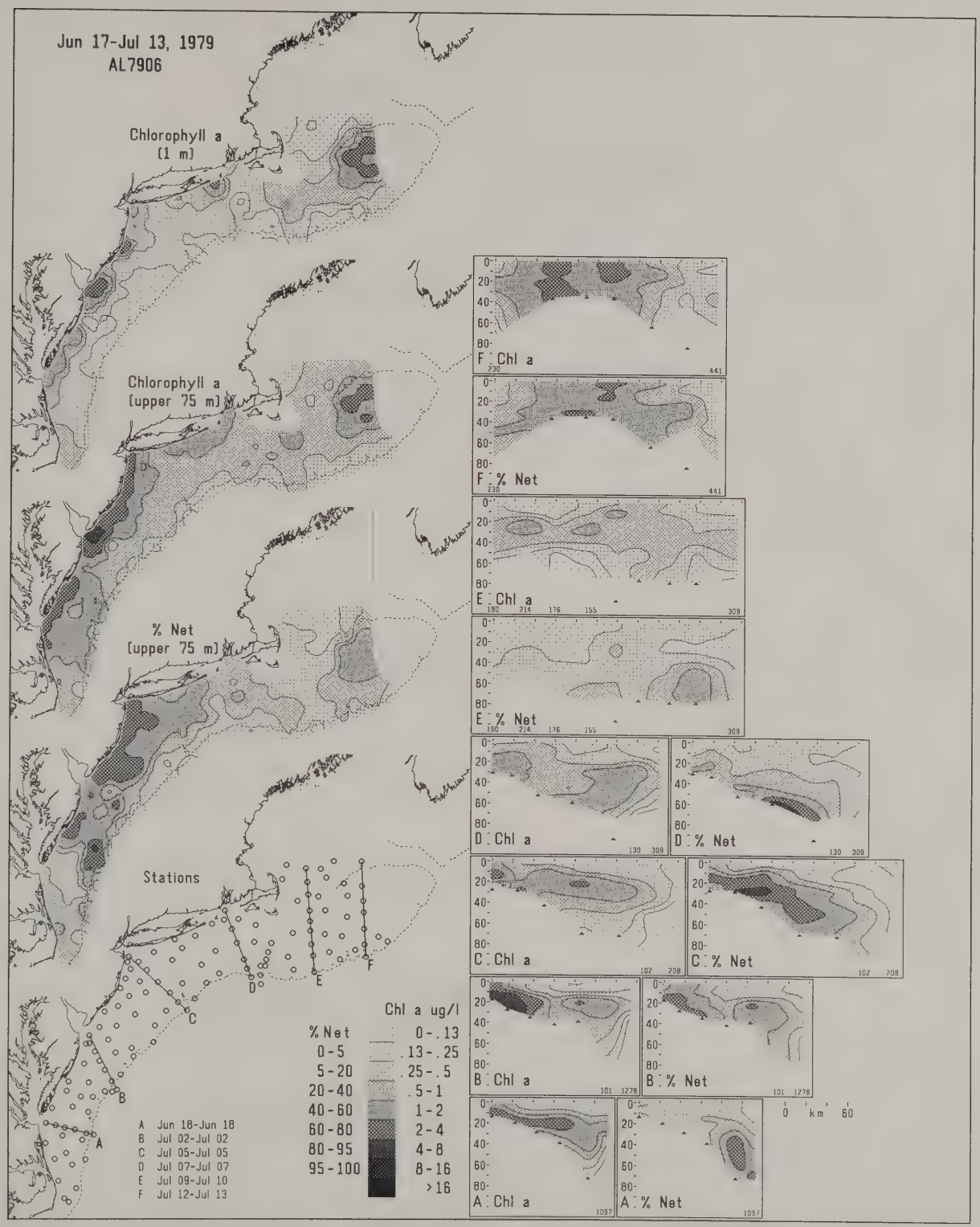

Appendix Figure B11
The distribution of chlorophyll *a* and percent netplankton during survey AL7906.

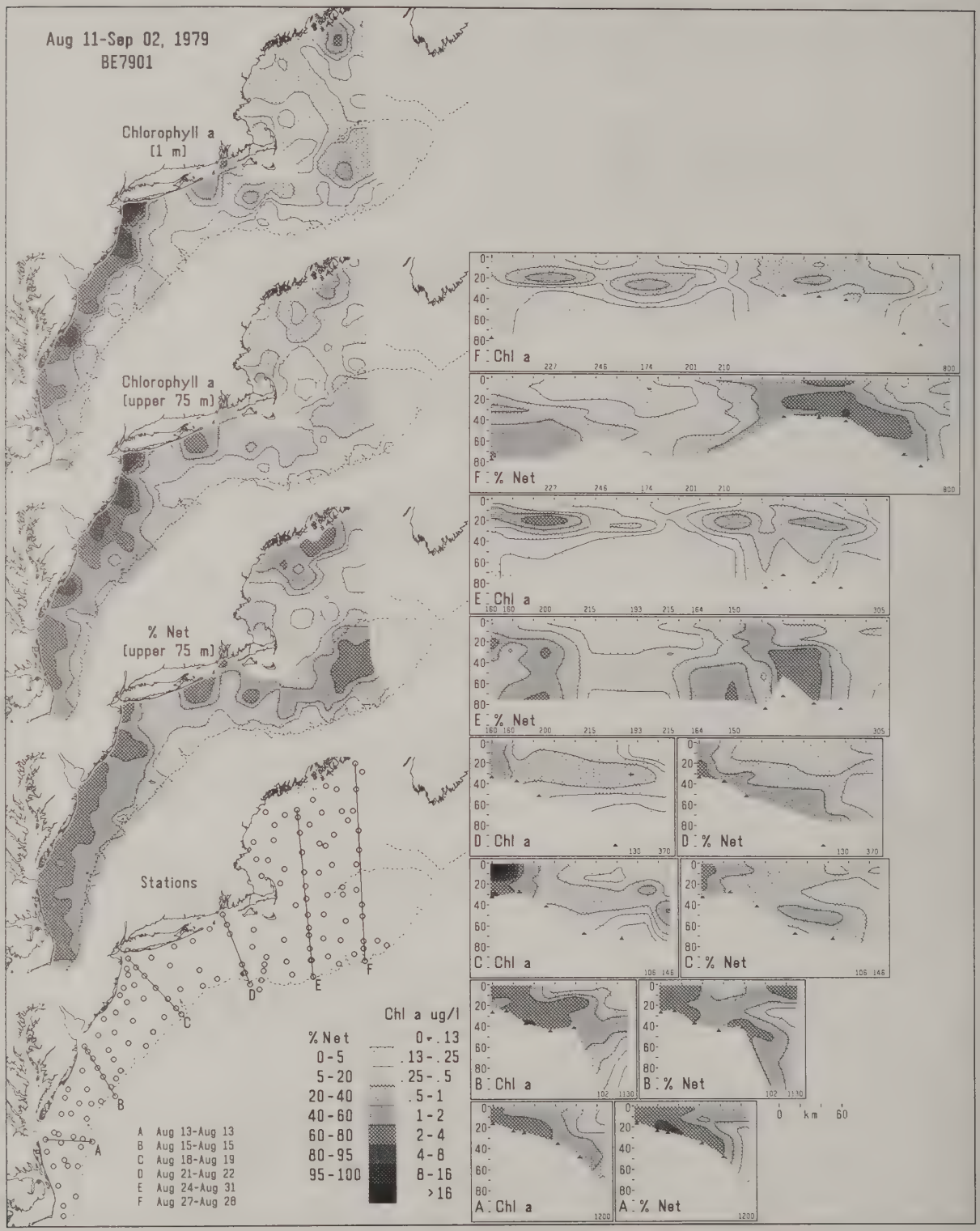

Appendix Figure B12
The distribution of chlorophyll *a* and percent netplankton during survey BE7901.

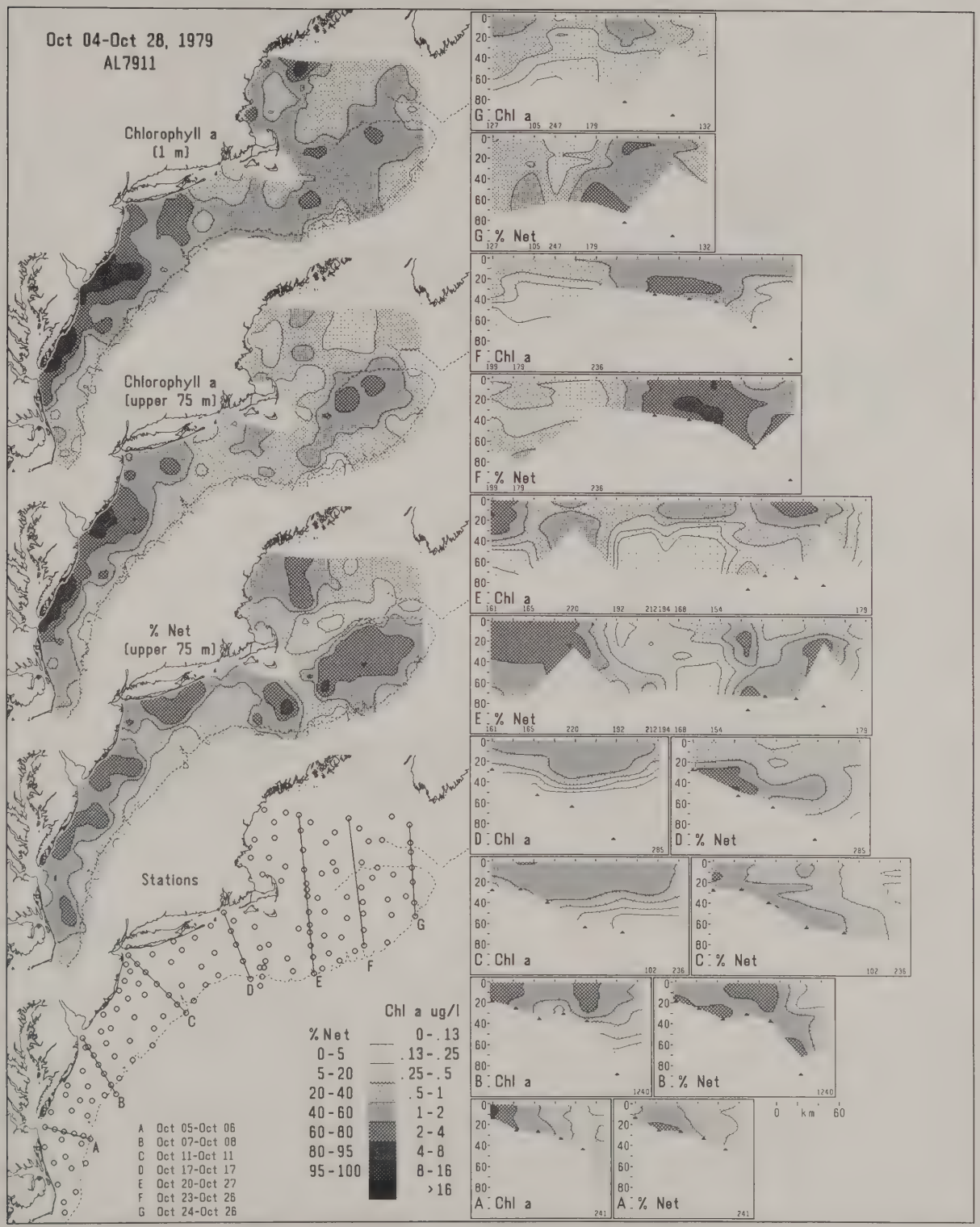

Appendix Figure B13
The distribution of chlorophyll *a* and percent netplankton during survey AL7911.

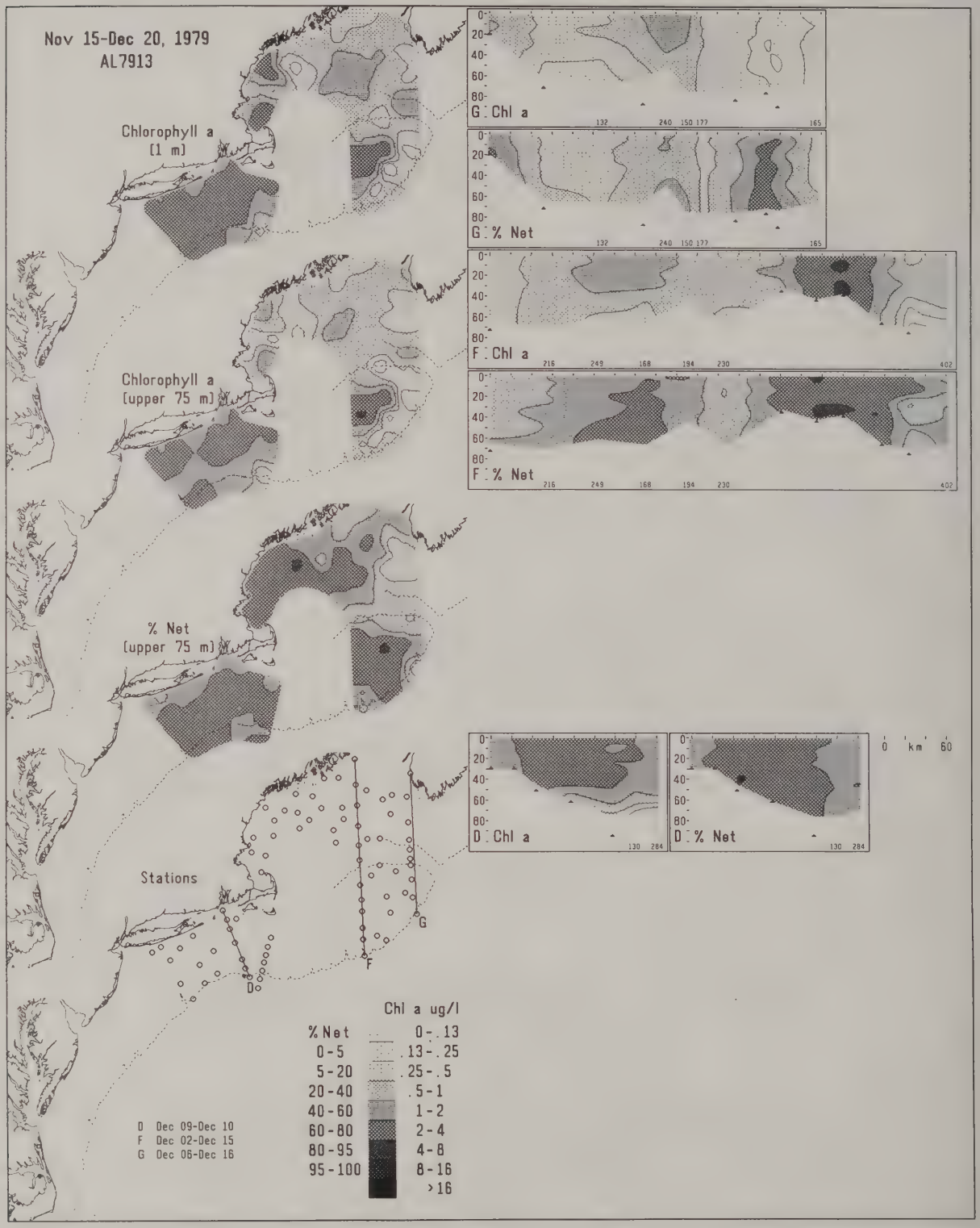

Appendix Figure B14
The distribution of chlorophyll *a* and percent netplankton during survey AL7913.

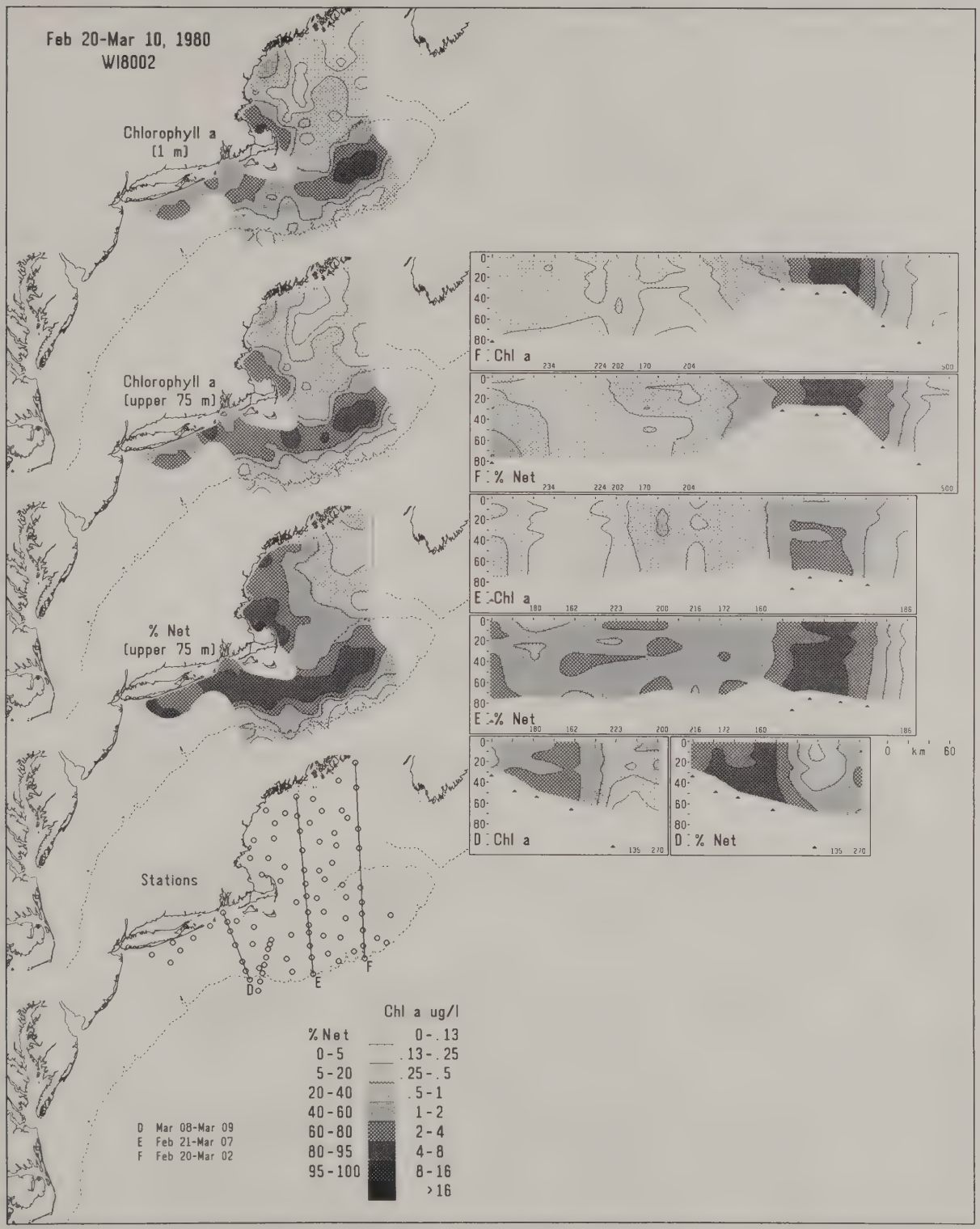

Appendix Figure B15
The distribution of chlorophyll *a* and percent netplankton during survey WI8002.

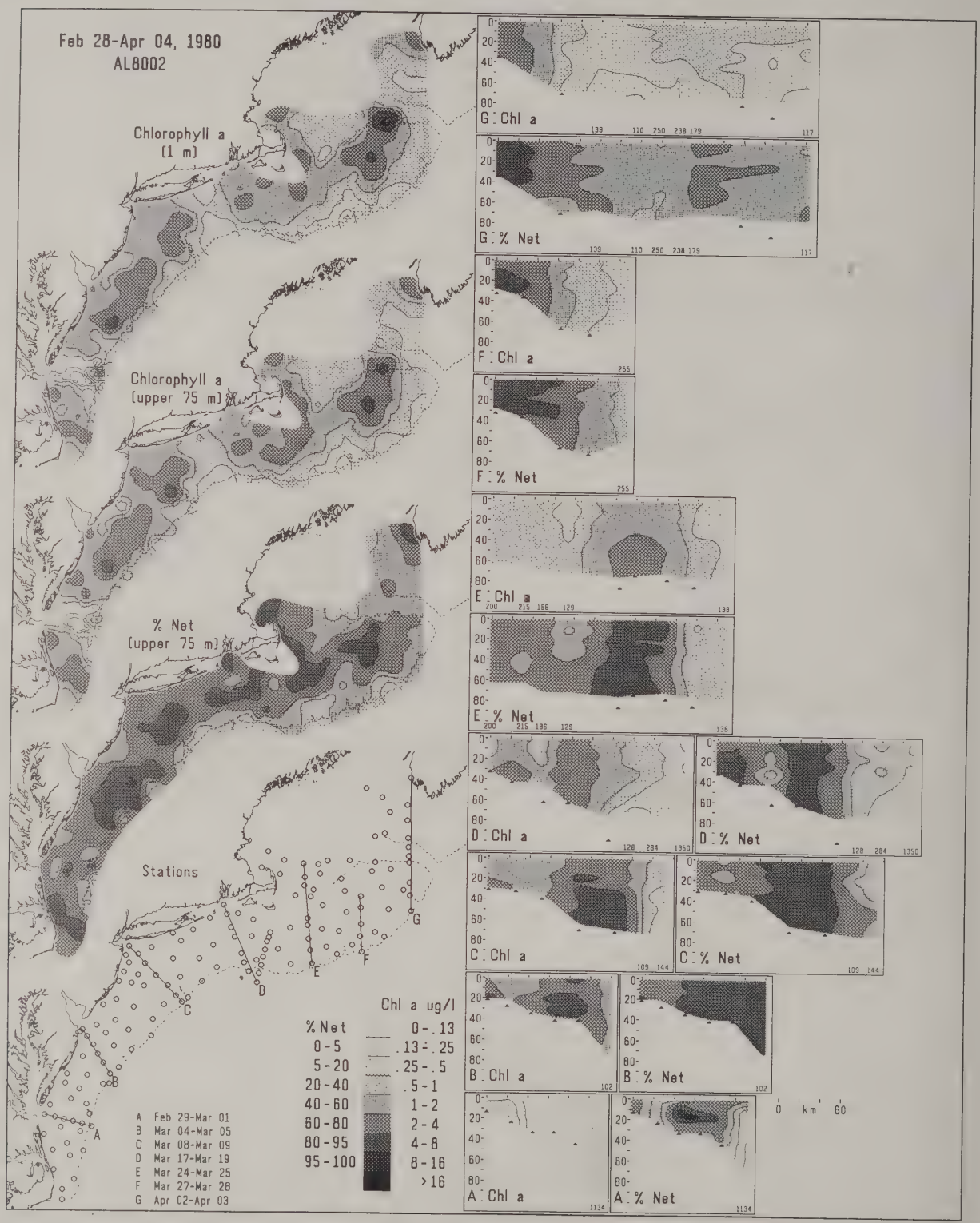

Appendix Figure B16
The distribution of chlorophyll *a* and percent netplankton during survey AL8002.

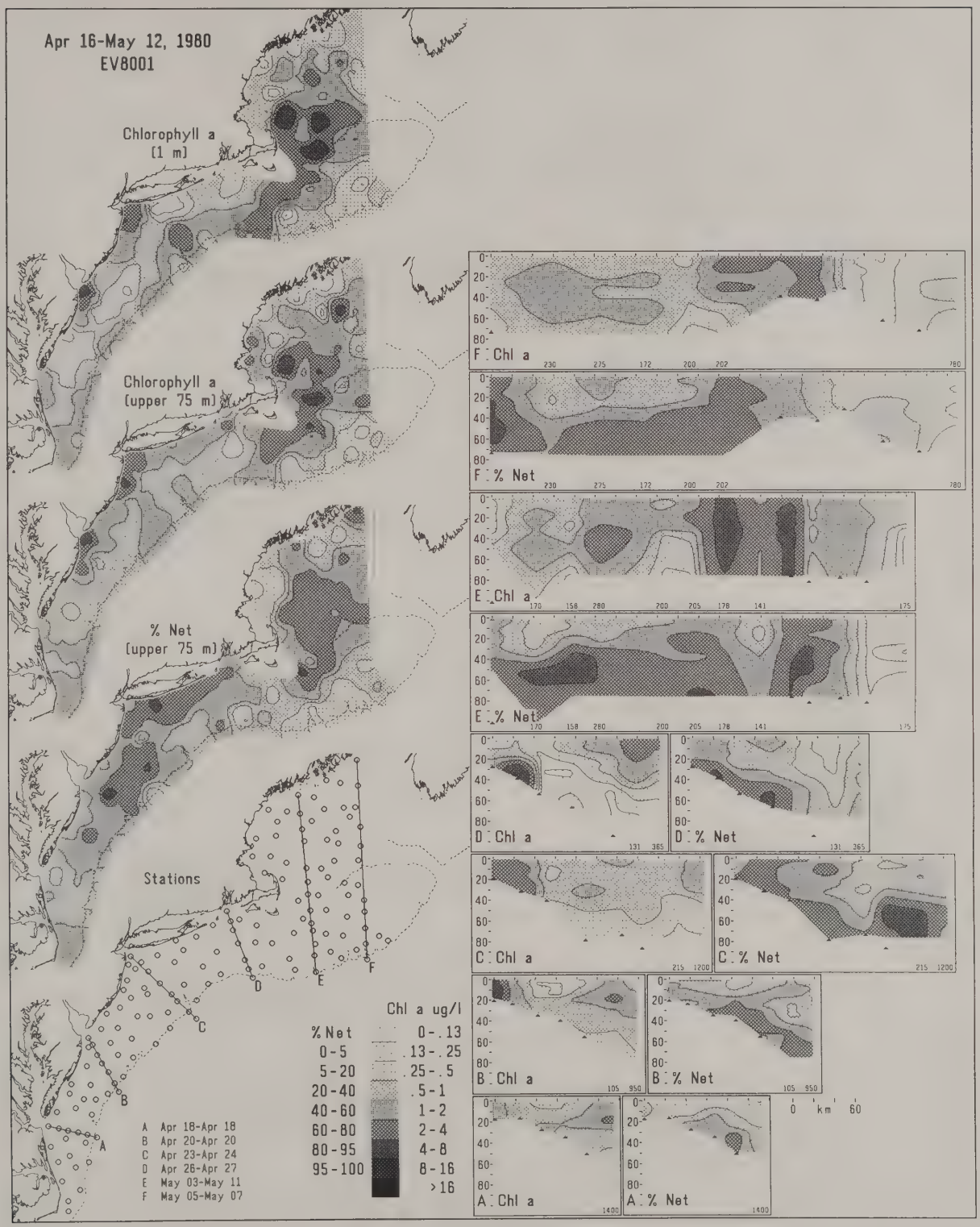

Appendix Figure B17
The distribution of chlorophyll *a* and percent netplankton during survey EV8001.

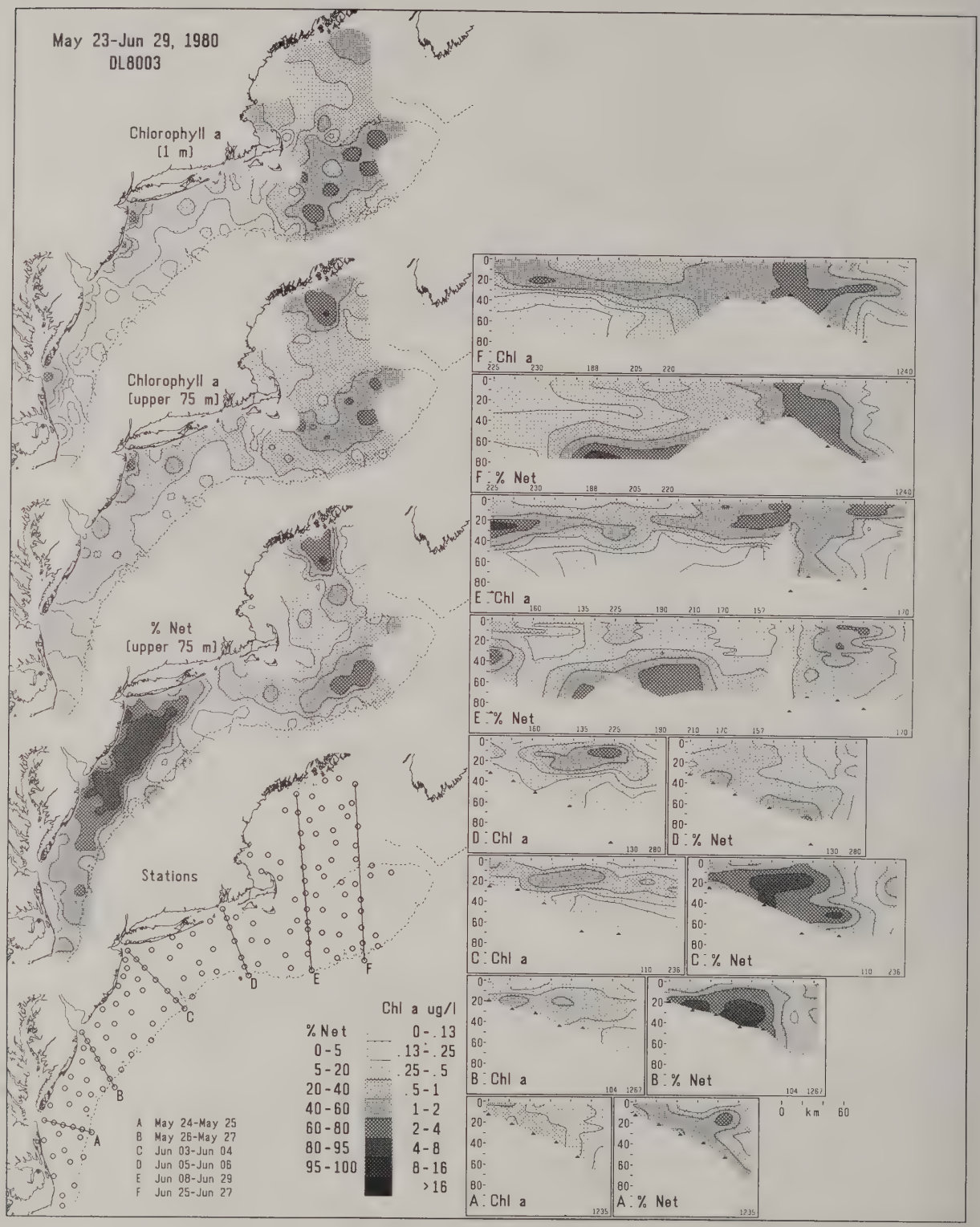

Appendix Figure B18
The distribution of chlorophyll *a* and percent netplankton during survey DL8003.

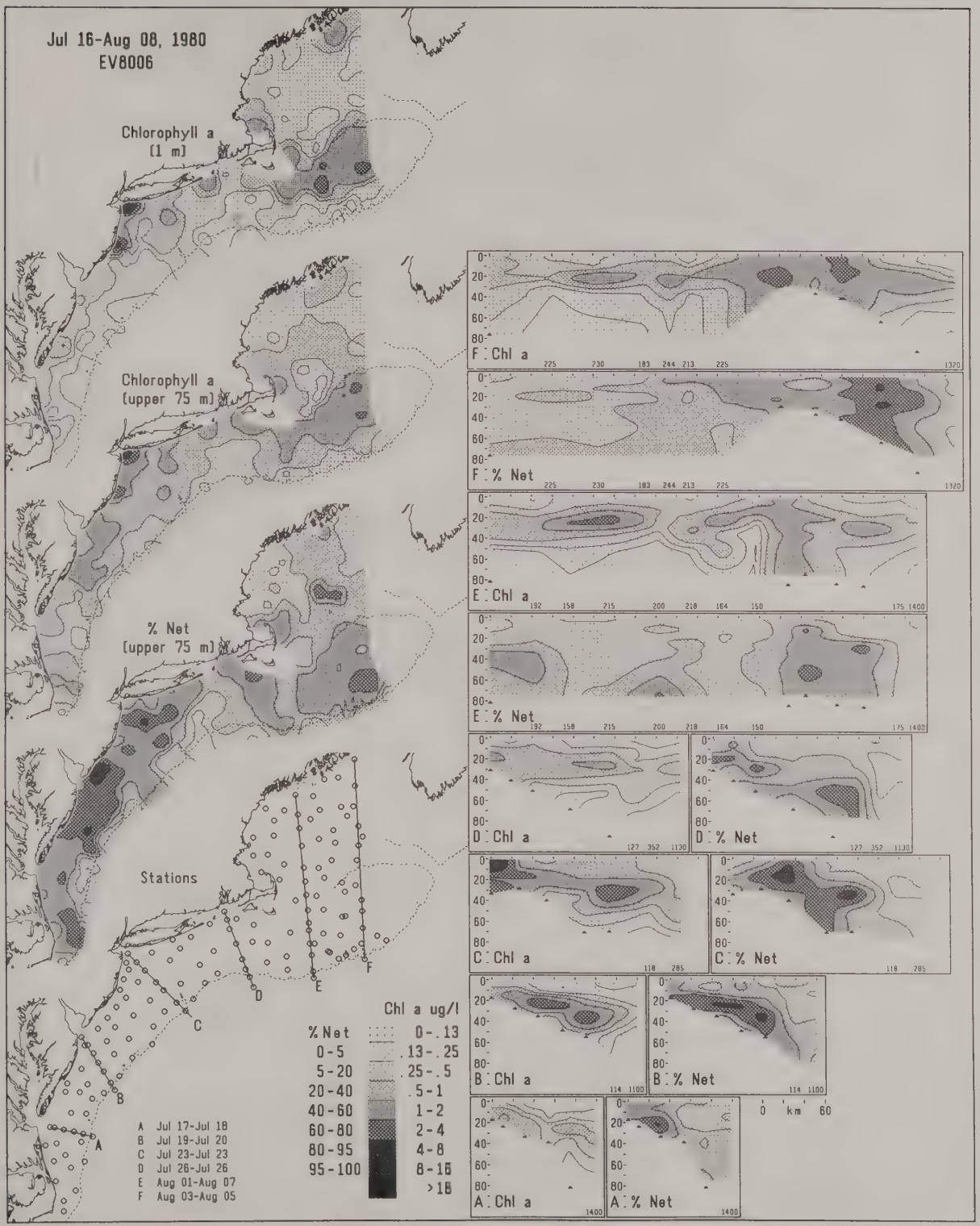

Appendix Figure B19
The distribution of chlorophyll *a* and percent netplankton during survey EV8006.

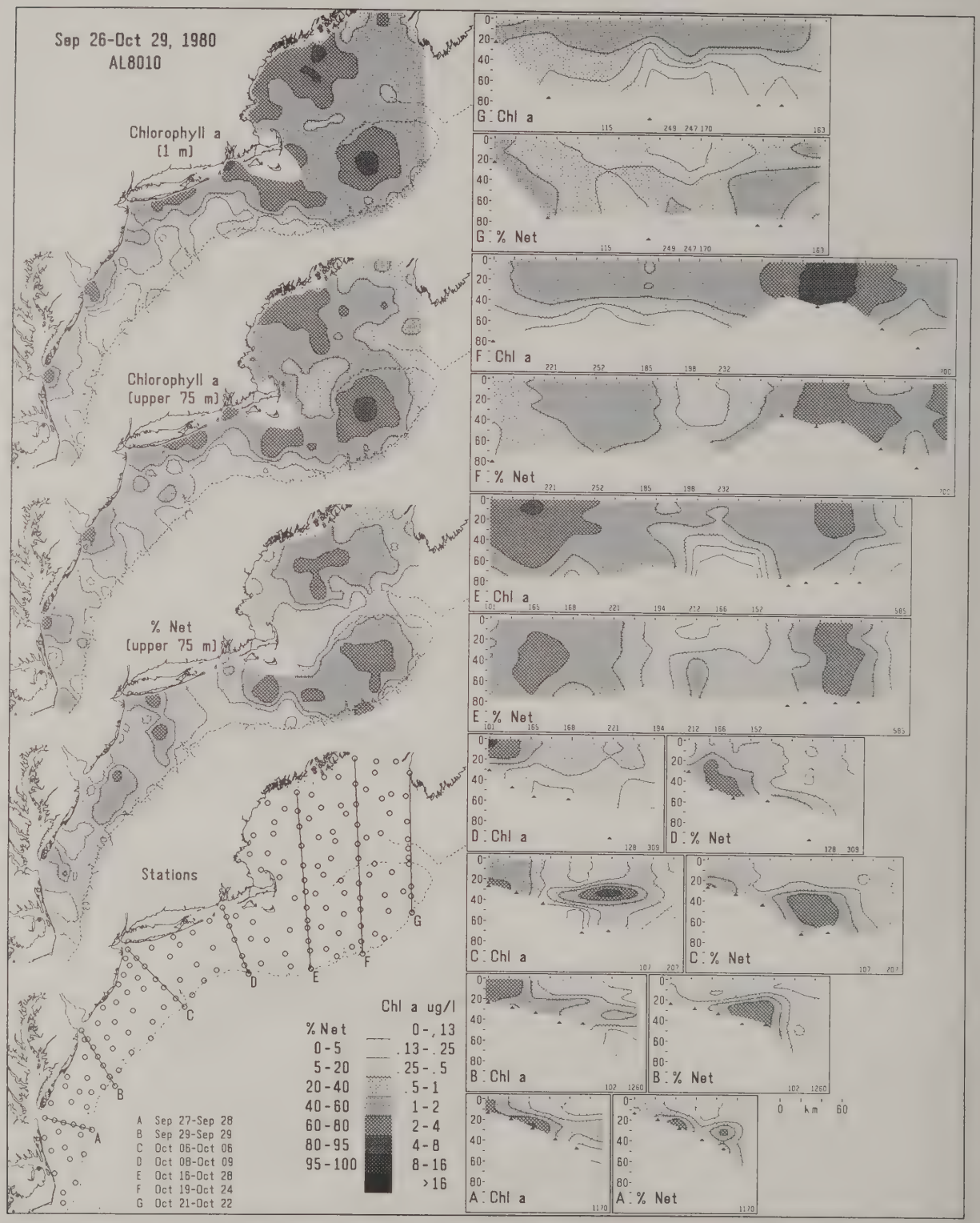

Appendix Figure B20
The distribution of chlorophyll *a* and percent netplankton during survey AL8010.

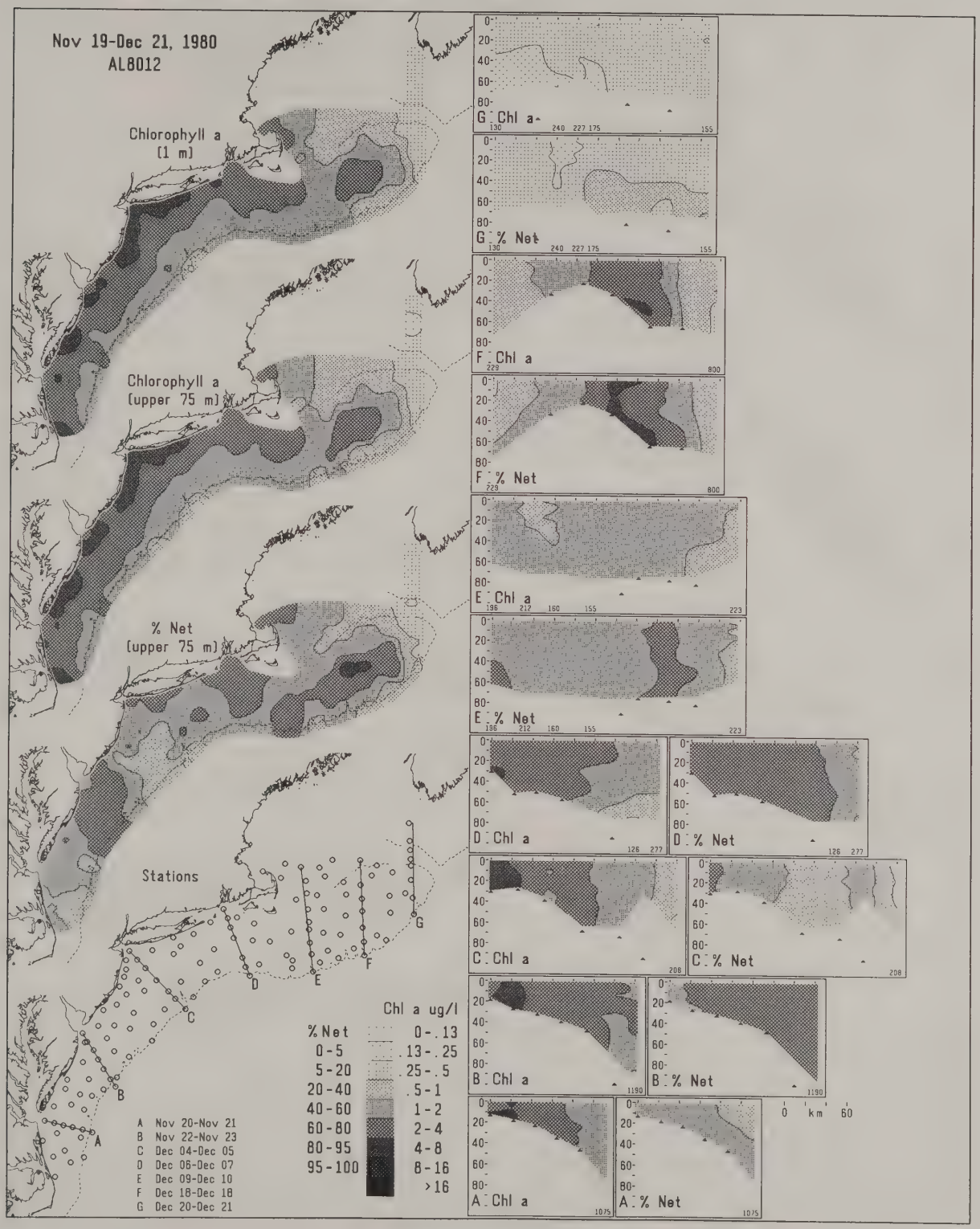

Appendix Figure B21
The distribution of chlorophyll *a* and percent netplankton during survey AL8012.

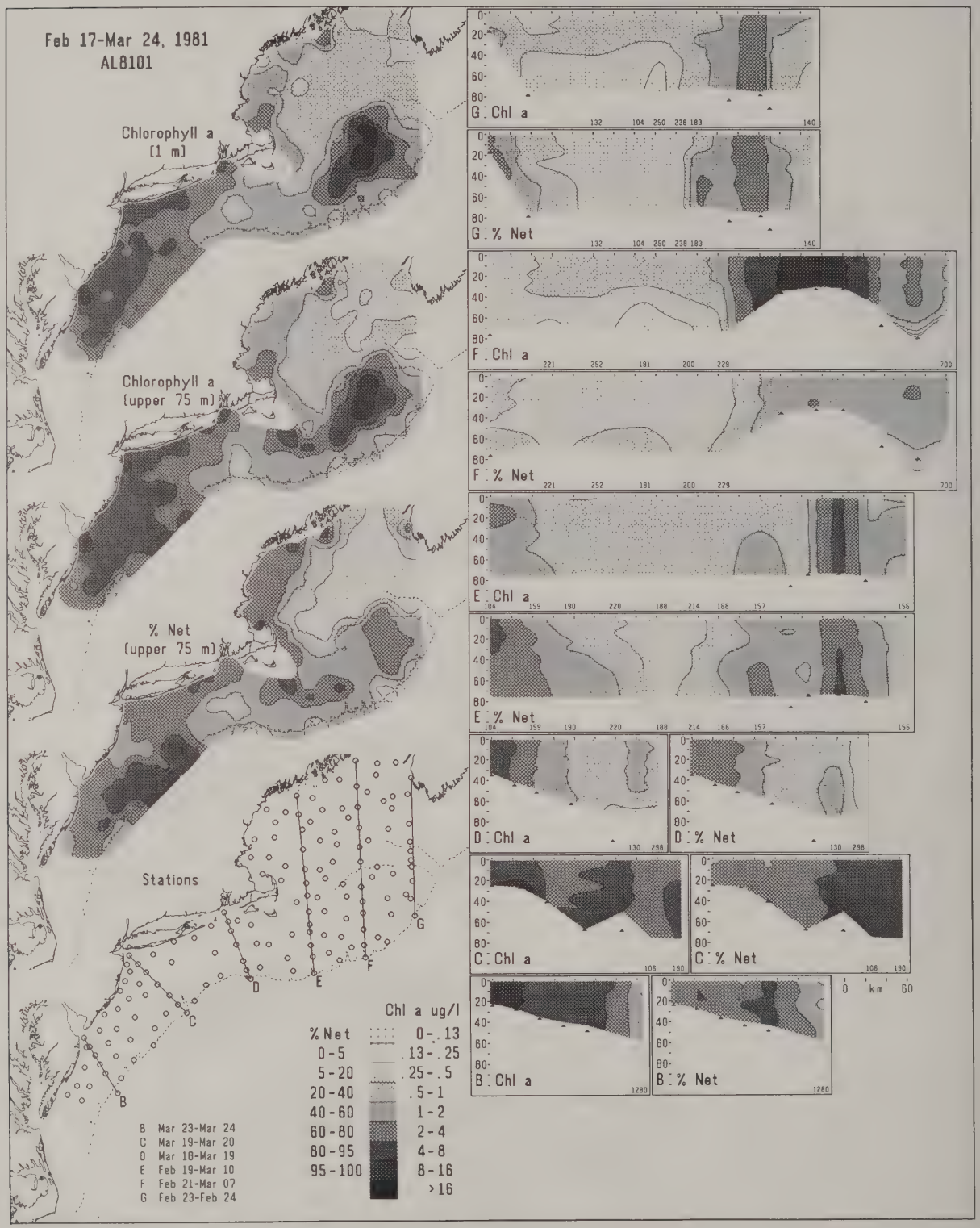

Appendix Figure B22
The distribution of chlorophyll *a* and percent netplankton during survey AL8101.

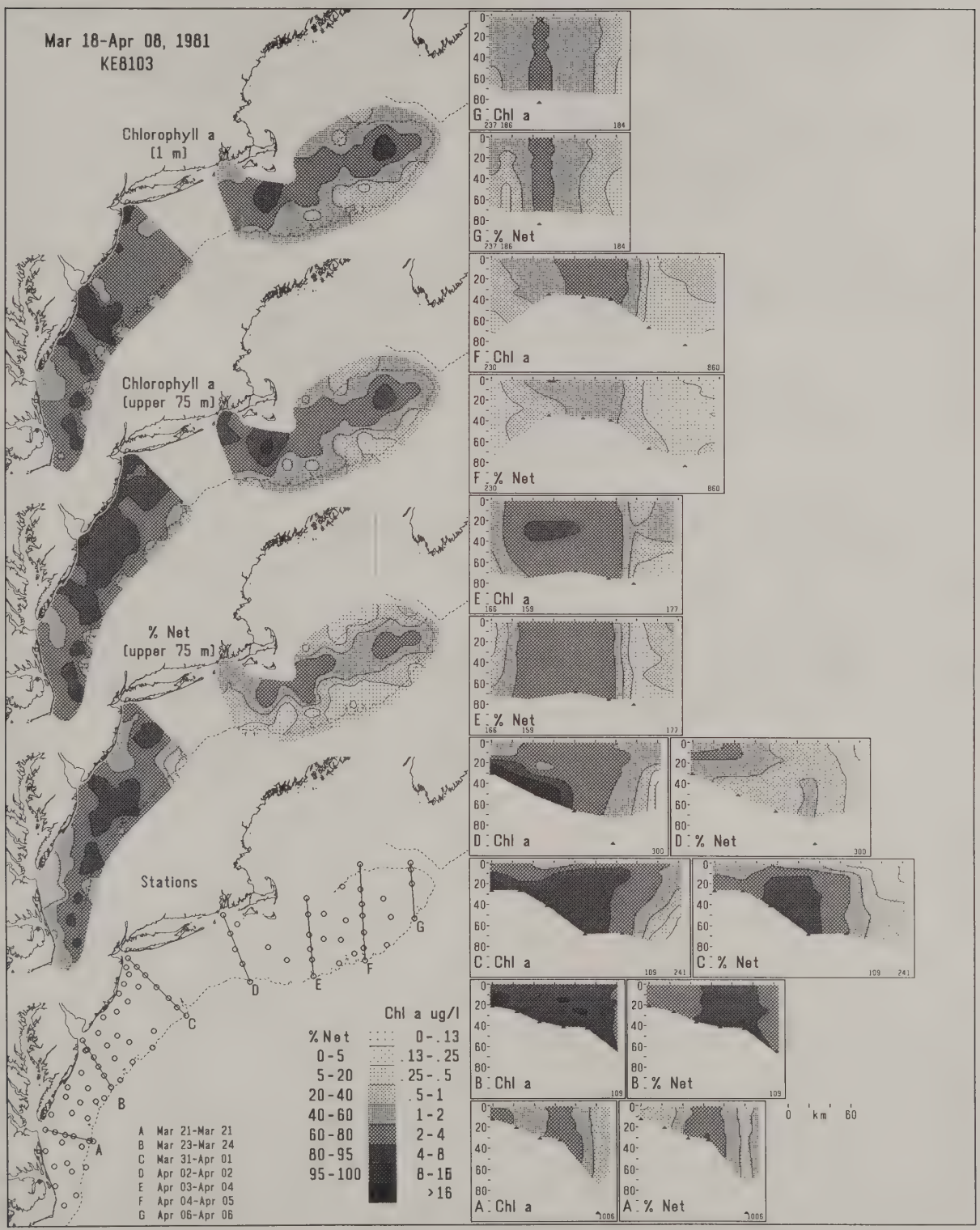

Appendix Figure B23
The distribution of chlorophyll *a* and percent netplankton during survey KE8103.

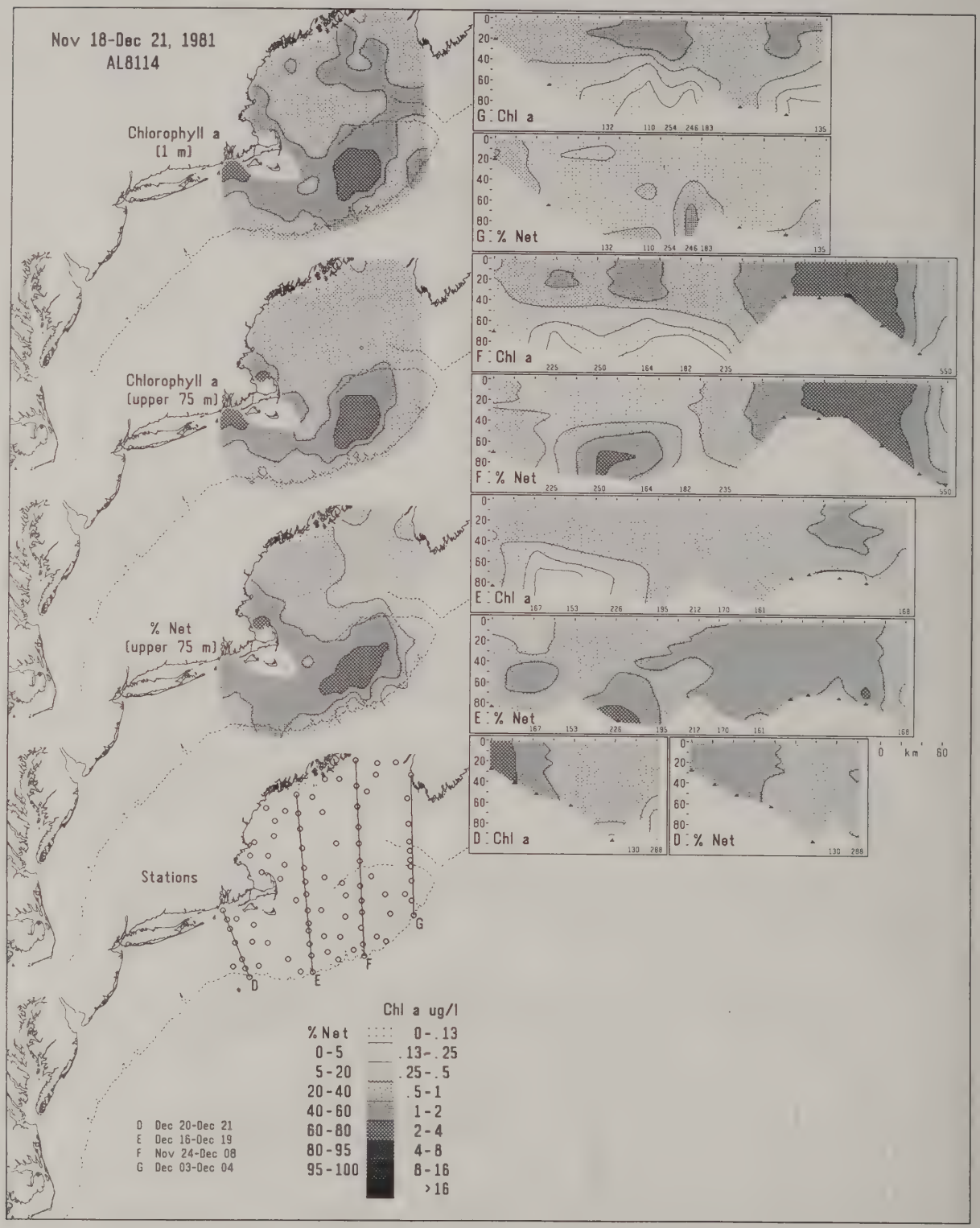

Appendix Figure B24
The distribution of chlorophyll *a* and percent netplankton during survey DL8103.

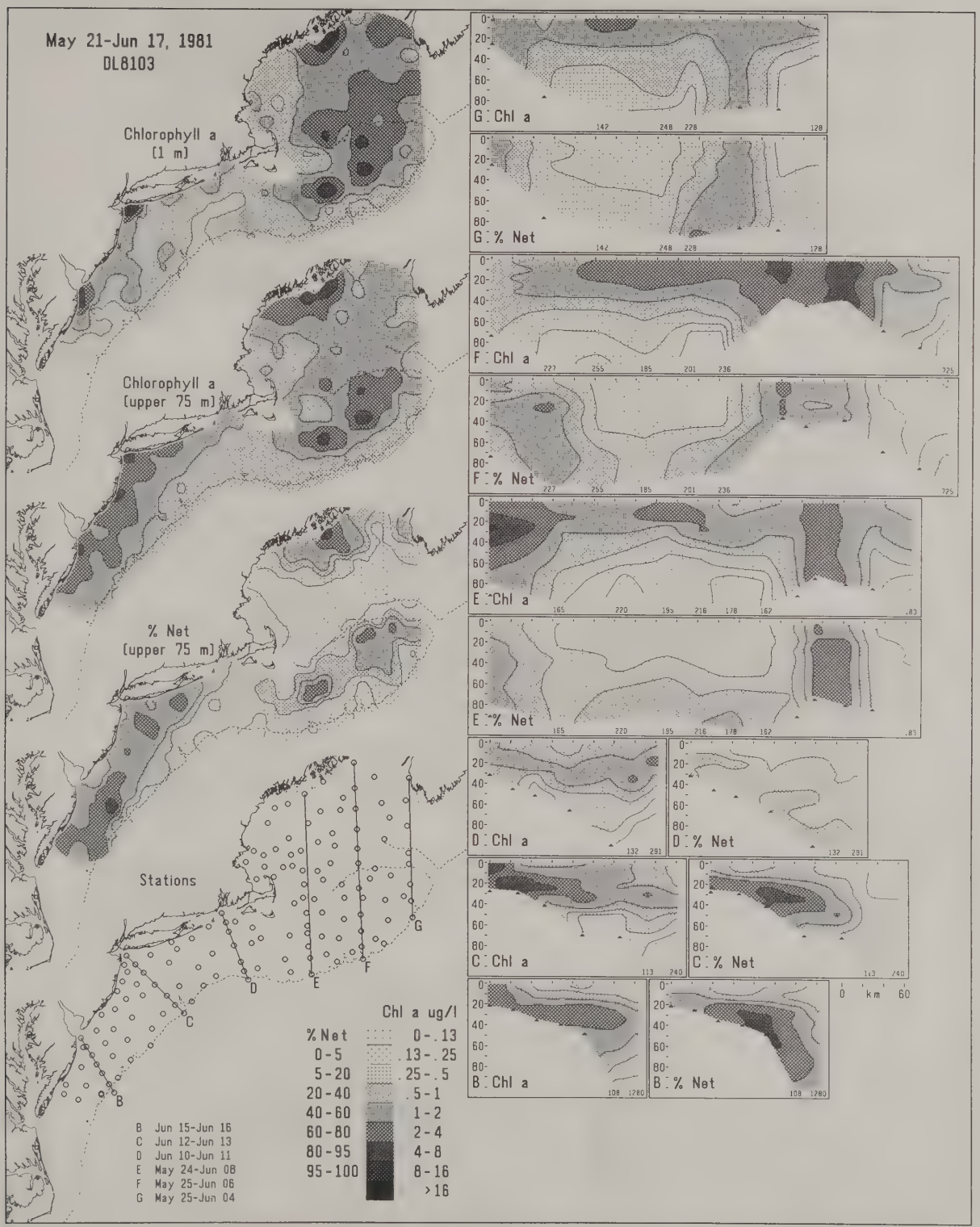

Appendix Figure B25
The distribution of chlorophyll *a* and percent netplankton during survey AL8114.

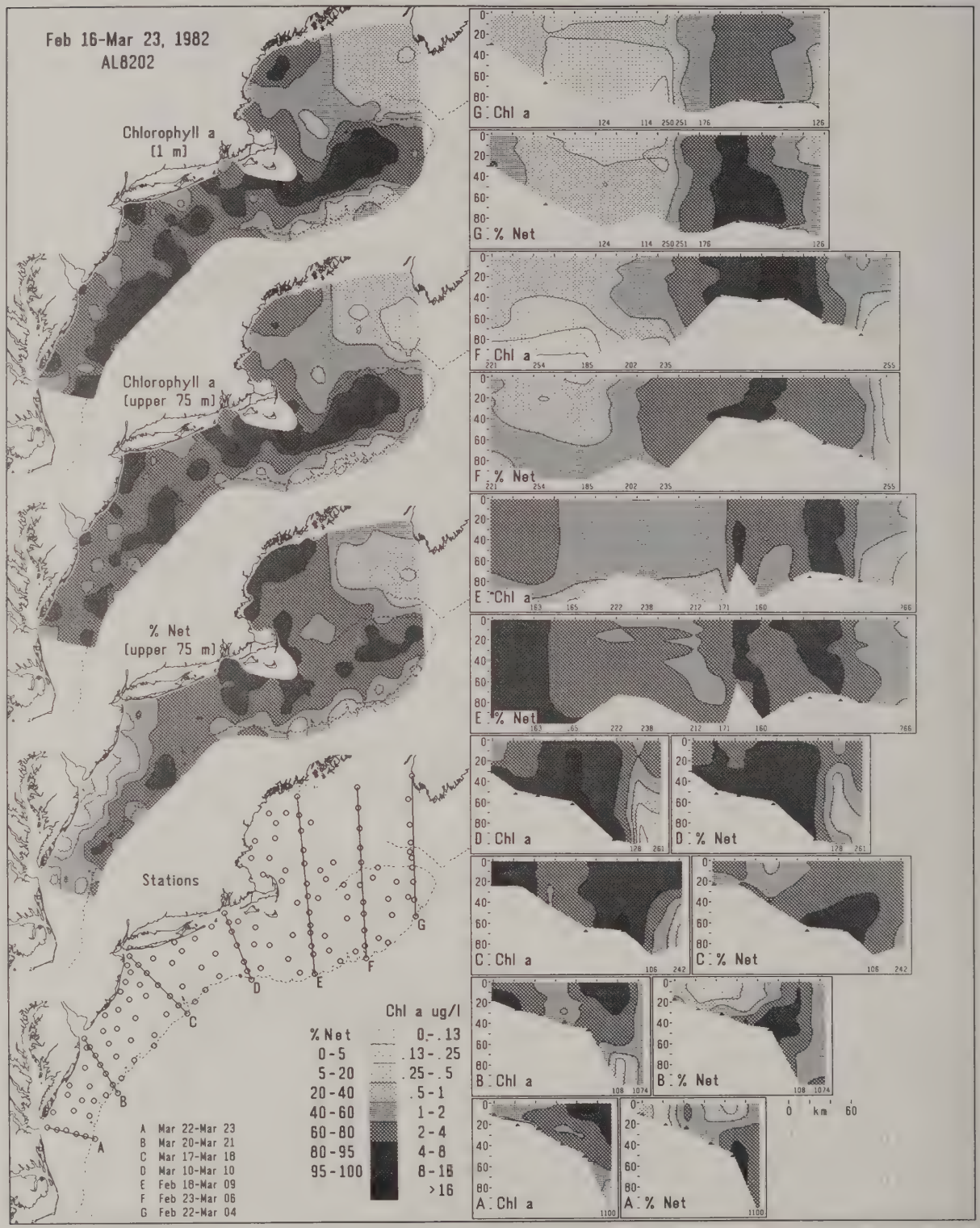

Appendix Figure B26
The distribution of chlorophyll *a* and percent netplankton during survey AL8202.

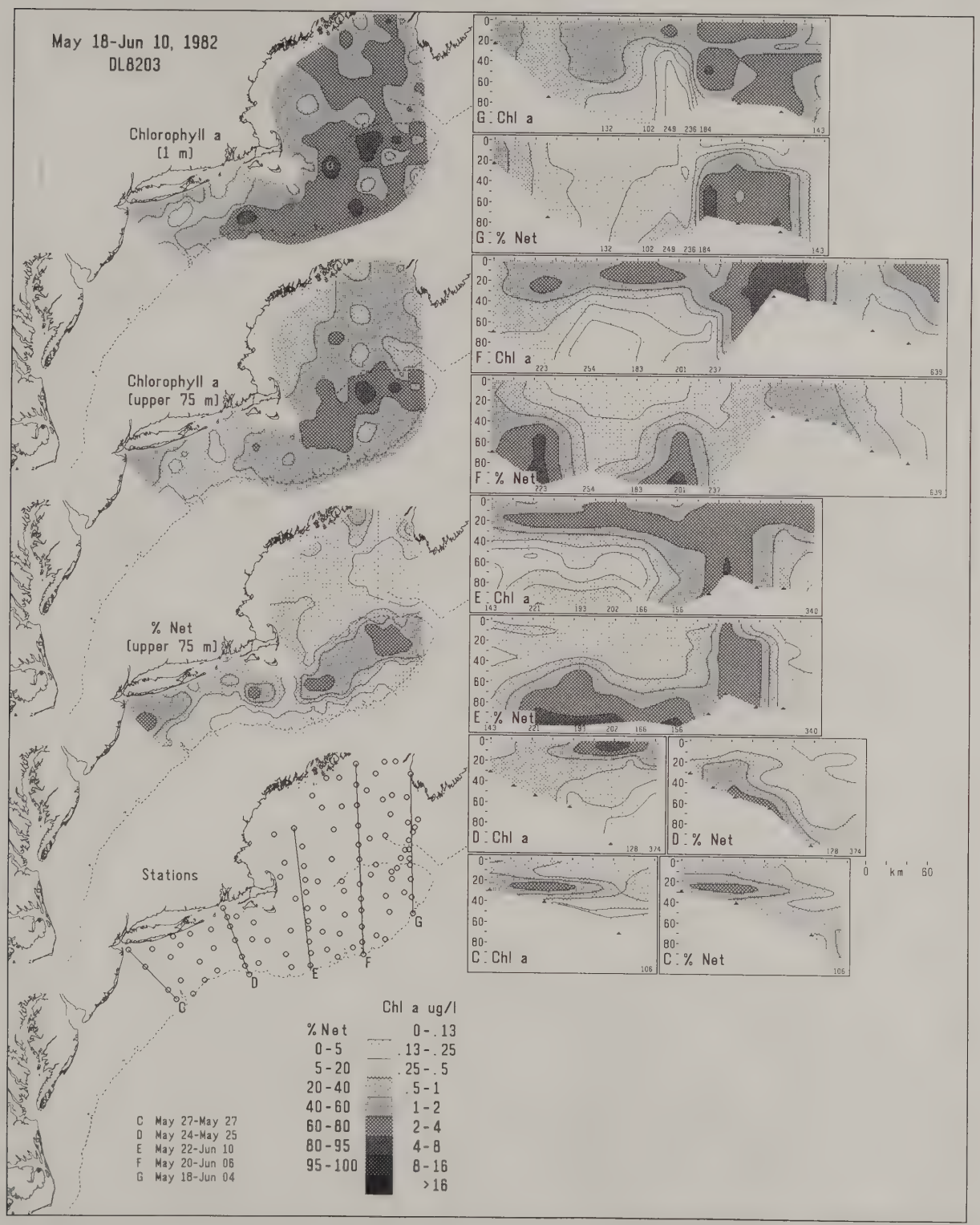

Appendix Figure B27
The distribution of chlorophyll *a* and percent netplankton during survey DL8203.

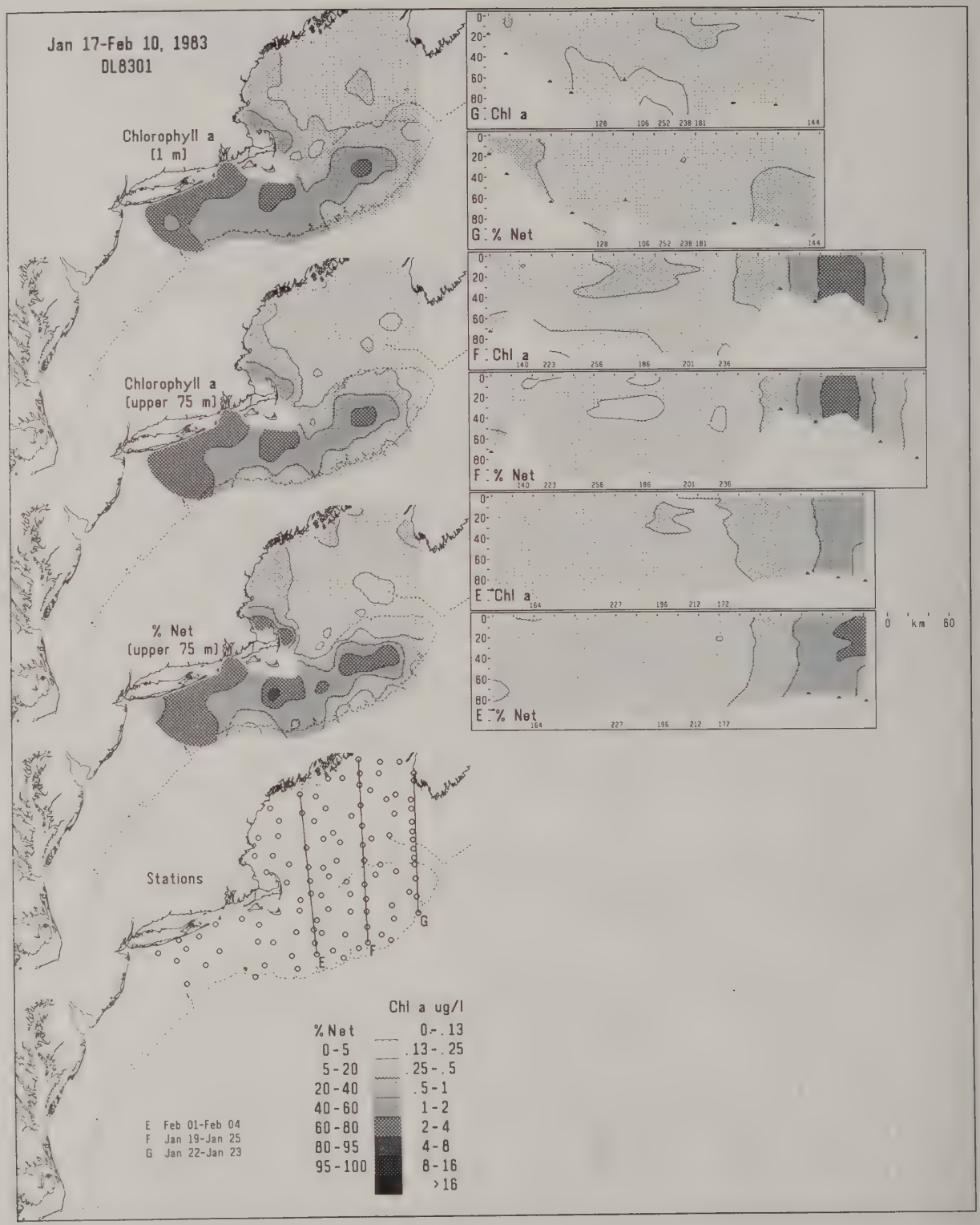

Appendix Figure B28
The distribution of chlorophyll *a* and percent netplankton during survey DL8301.

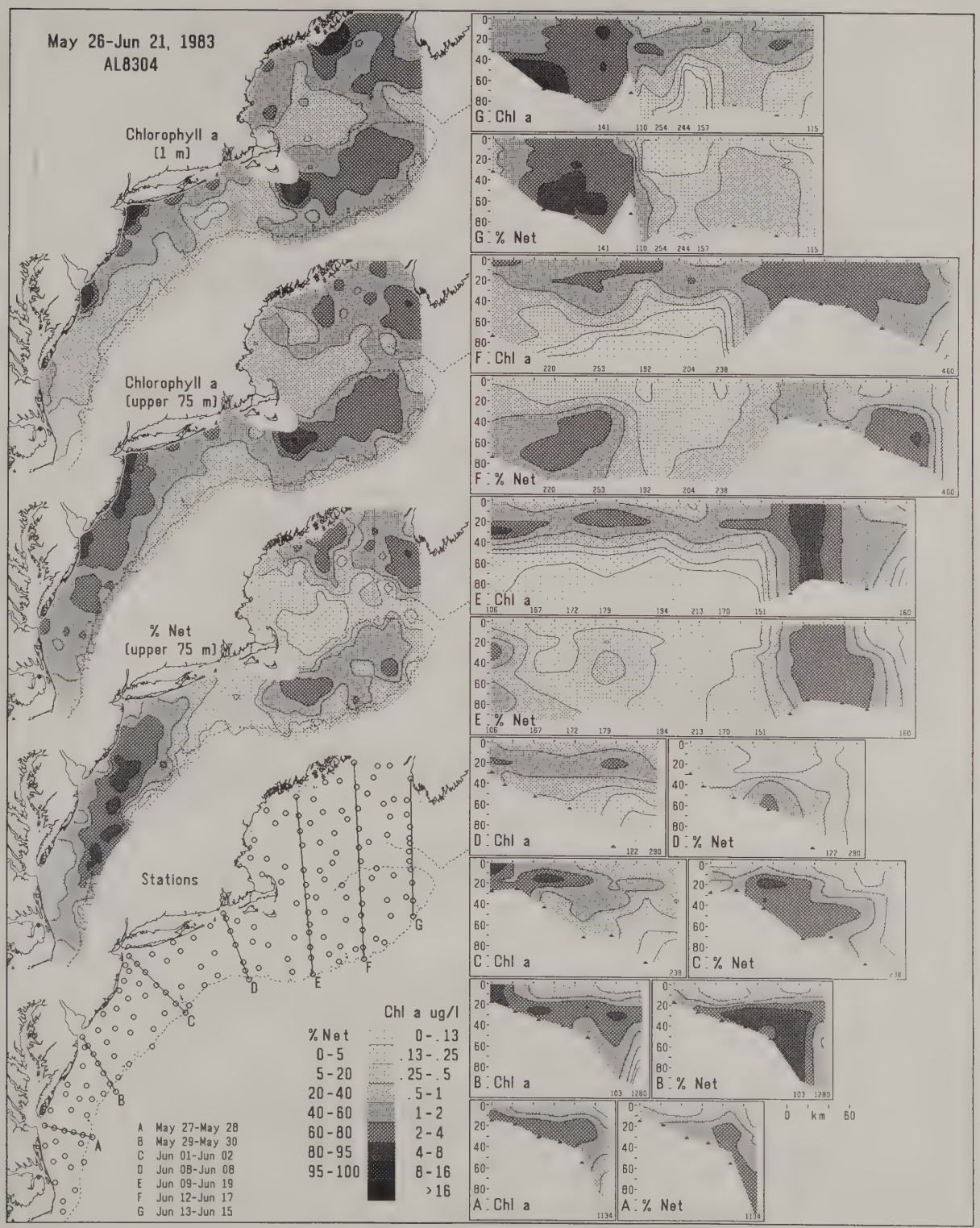

Appendix Figure B29
The distribution of chlorophyll *a* and percent netplankton during survey AL8304.

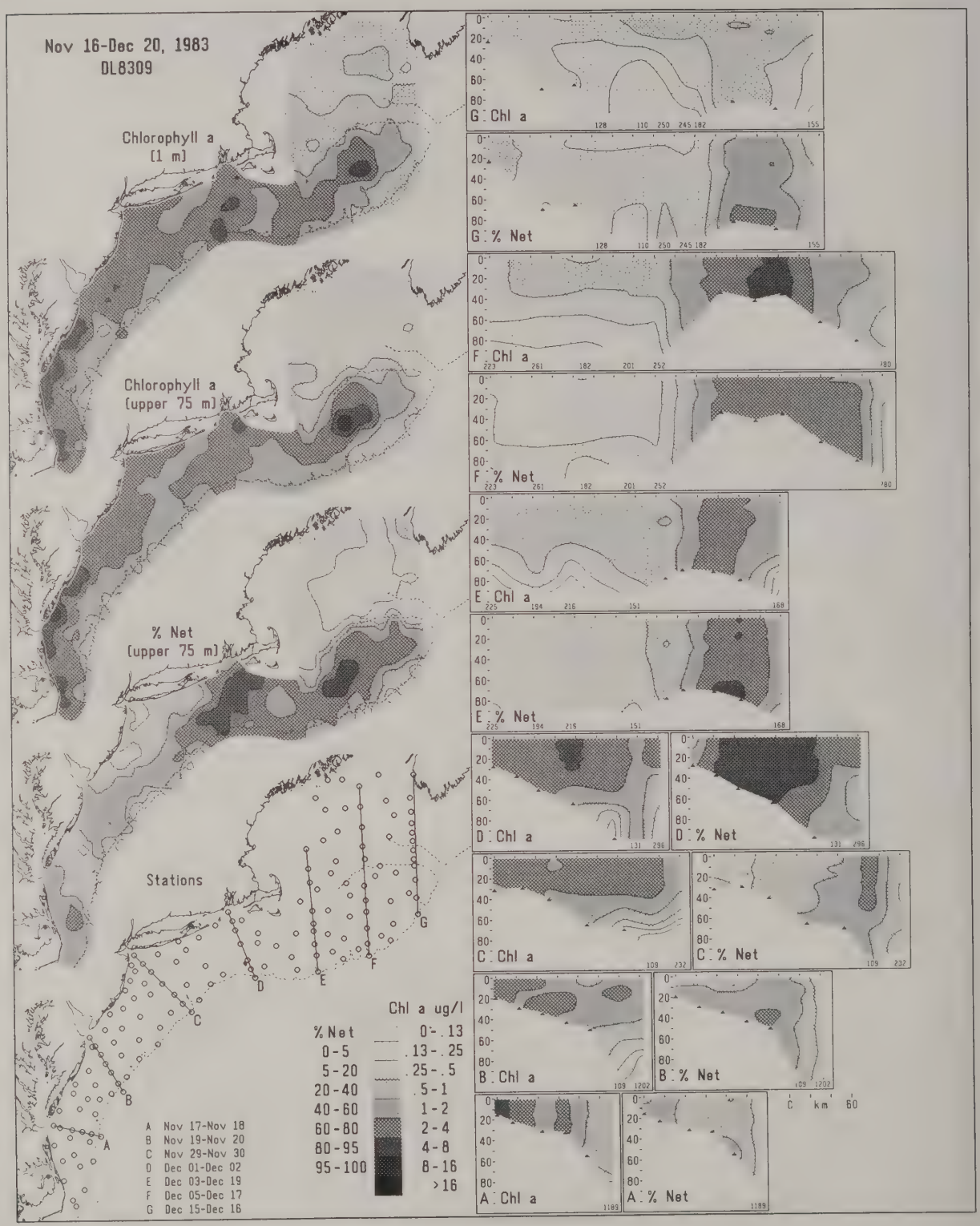

Appendix Figure B30
The distribution of chlorophyll *a* and percent netplankton during survey DL8309.

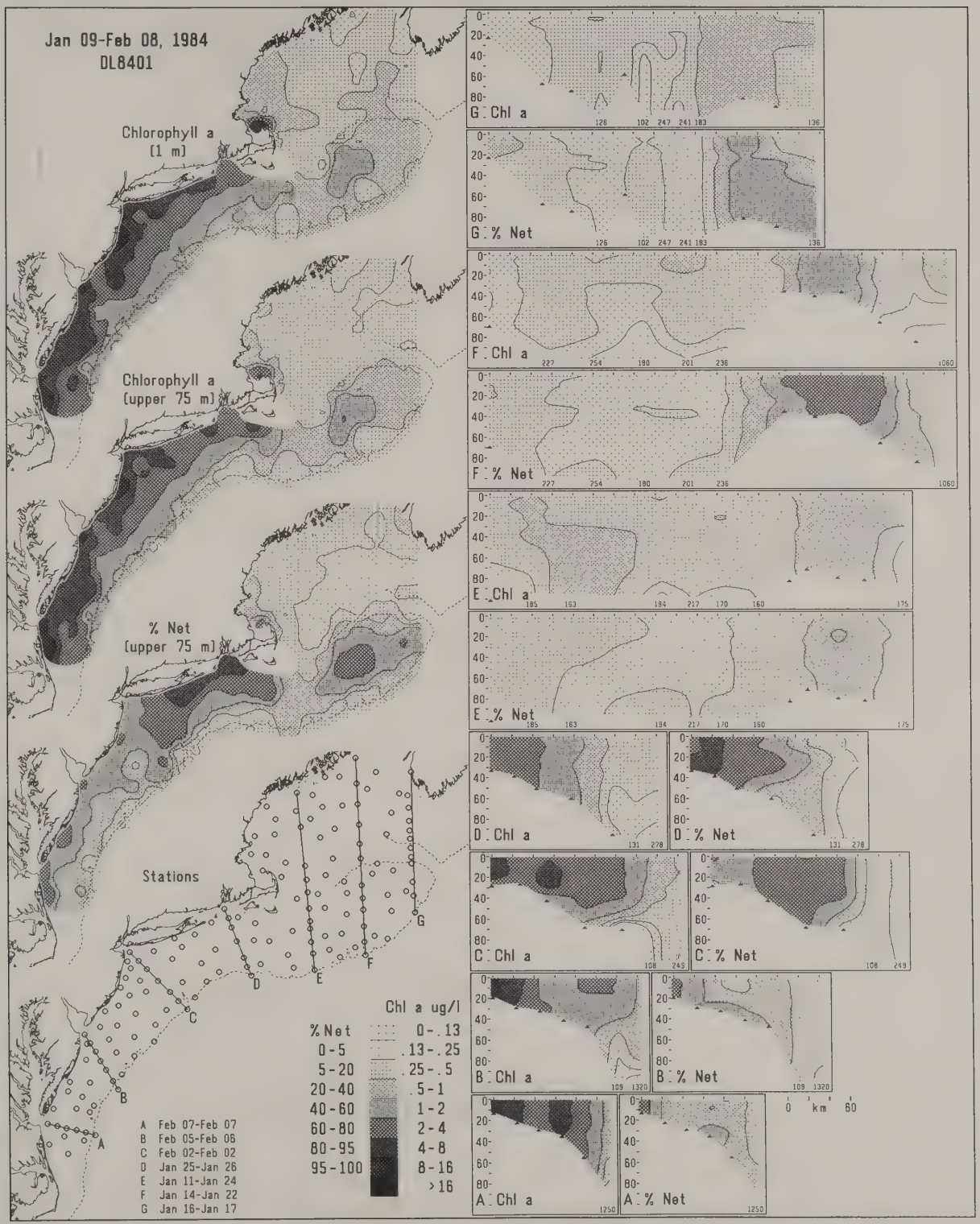

Appendix Figure B31
The distribution of chlorophyll *a* and percent netplankton during survey DL8401.

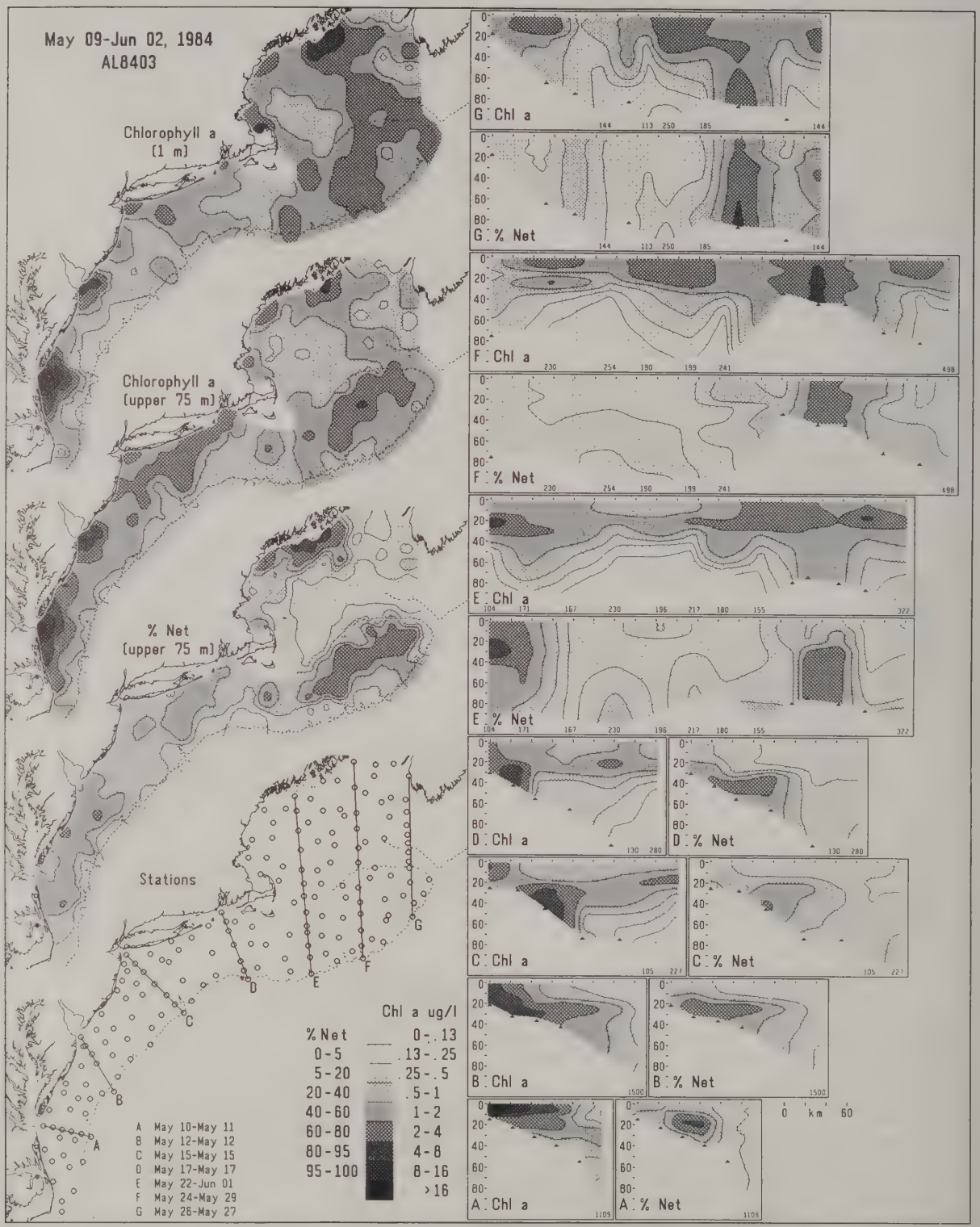

Appendix Figure B32
The distribution of chlorophyll *a* and percent netplankton during survey AL8403.

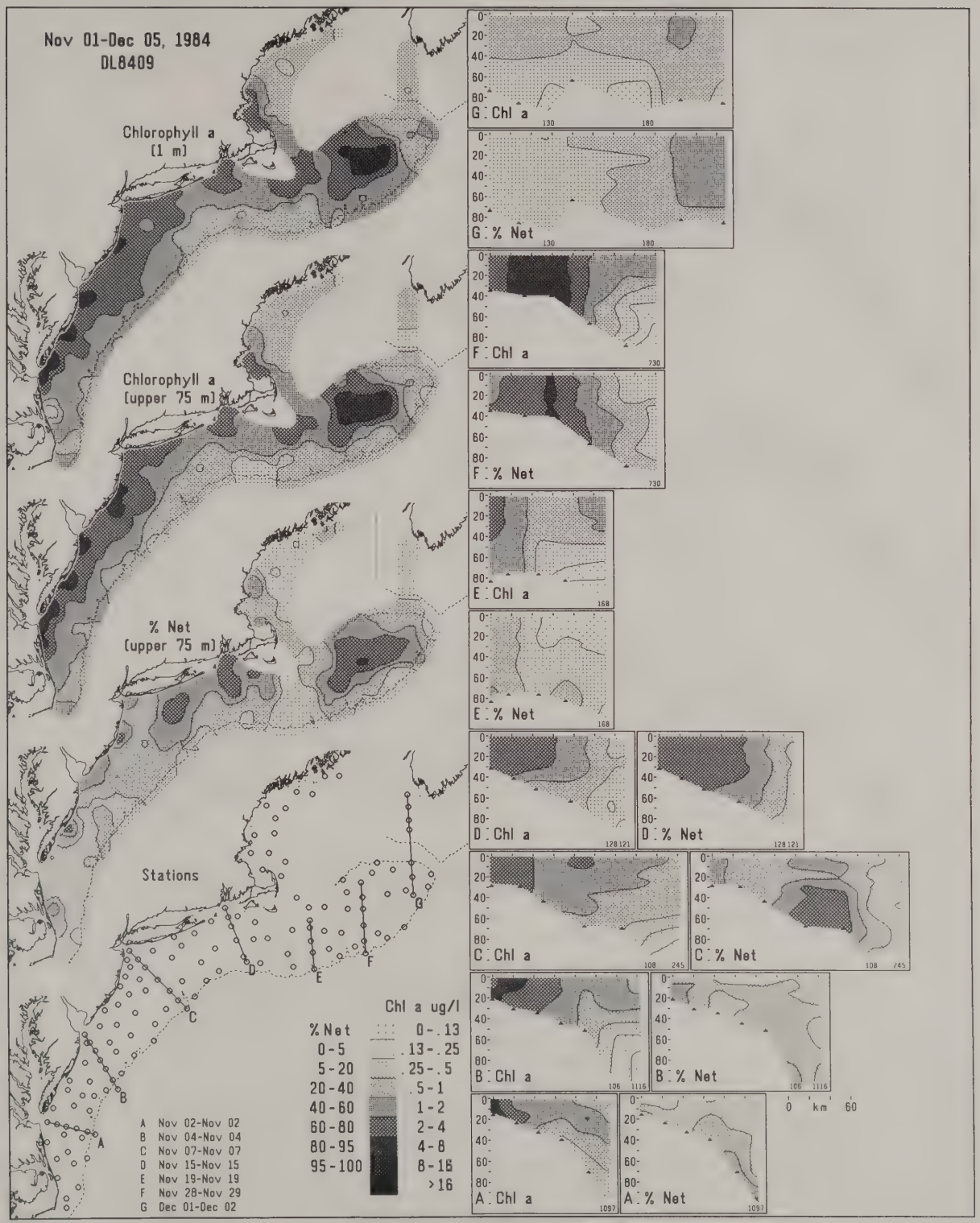

Appendix Figure B33
The distribution of chlorophyll *a* and percent netplankton during survey DL8409.

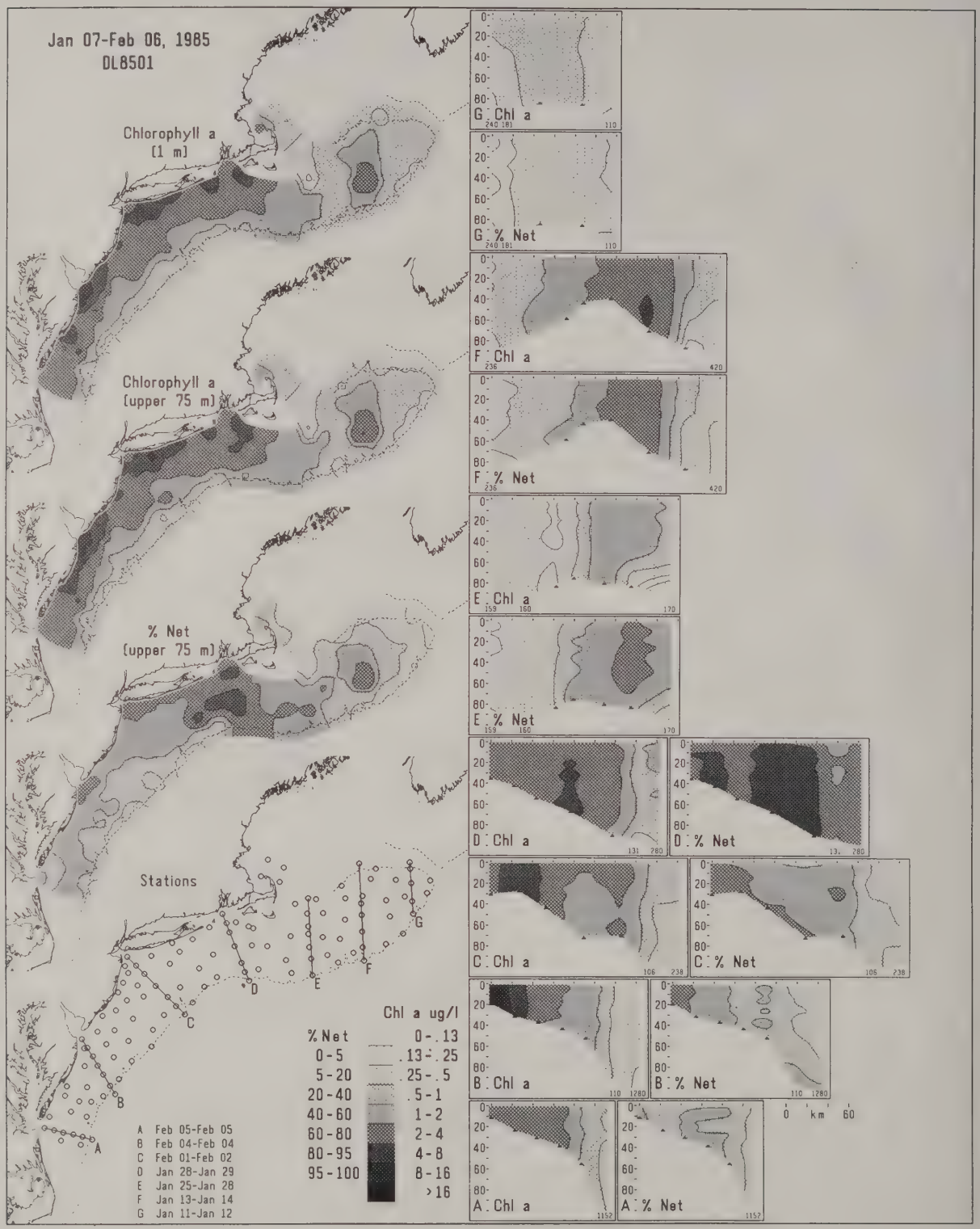

Appendix Figure B34
The distribution of chlorophyll *a* and percent netplankton during survey DL8501.

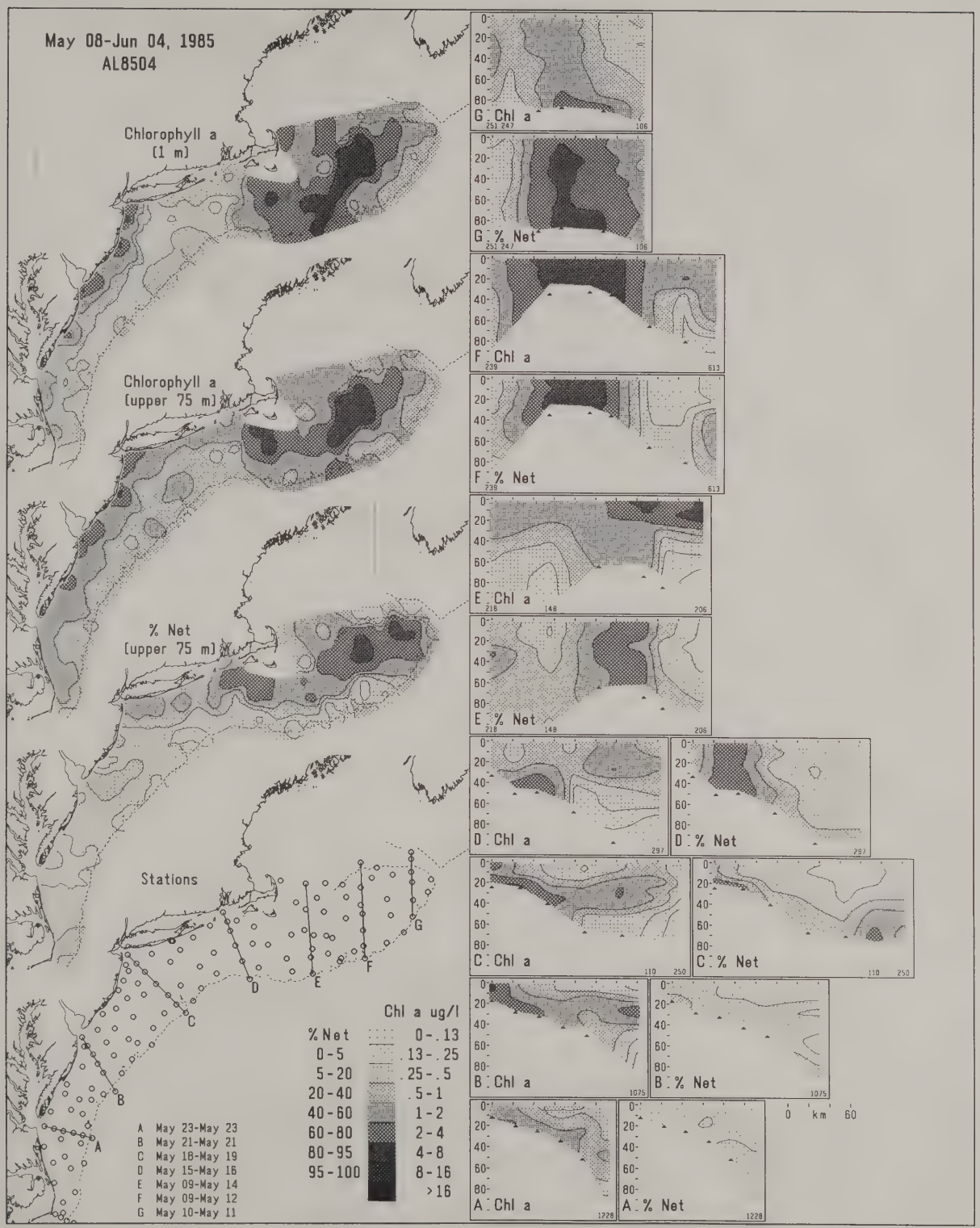

Appendix Figure B35
The distribution of chlorophyll *a* and percent netplankton during survey AL8504.

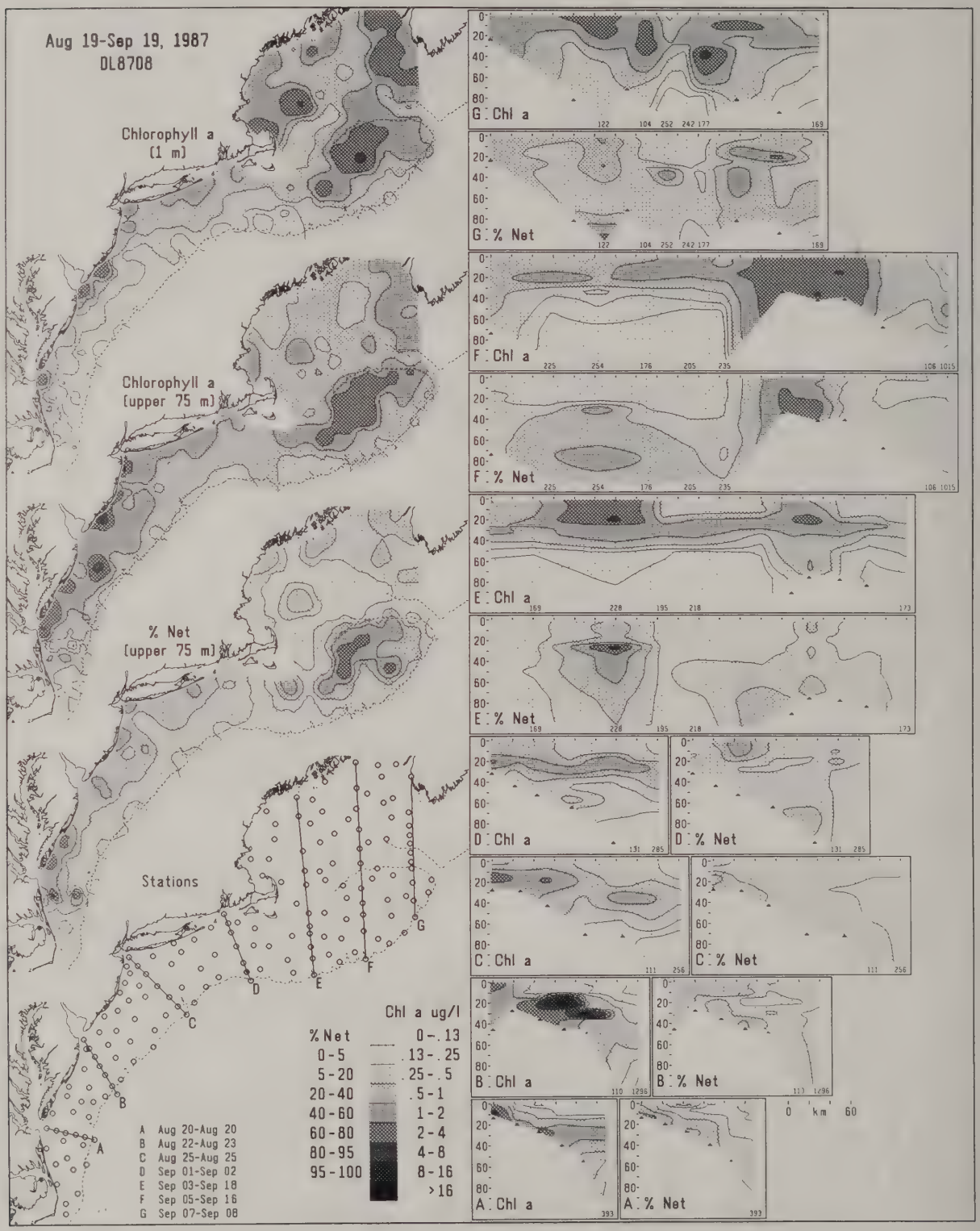

Appendix Figure B36
The distribution of chlorophyll *a* and percent netplankton during survey DL8708.

Appendix Figure B37
The distribution of chlorophyll *a* and percent netplankton during survey DL8710.

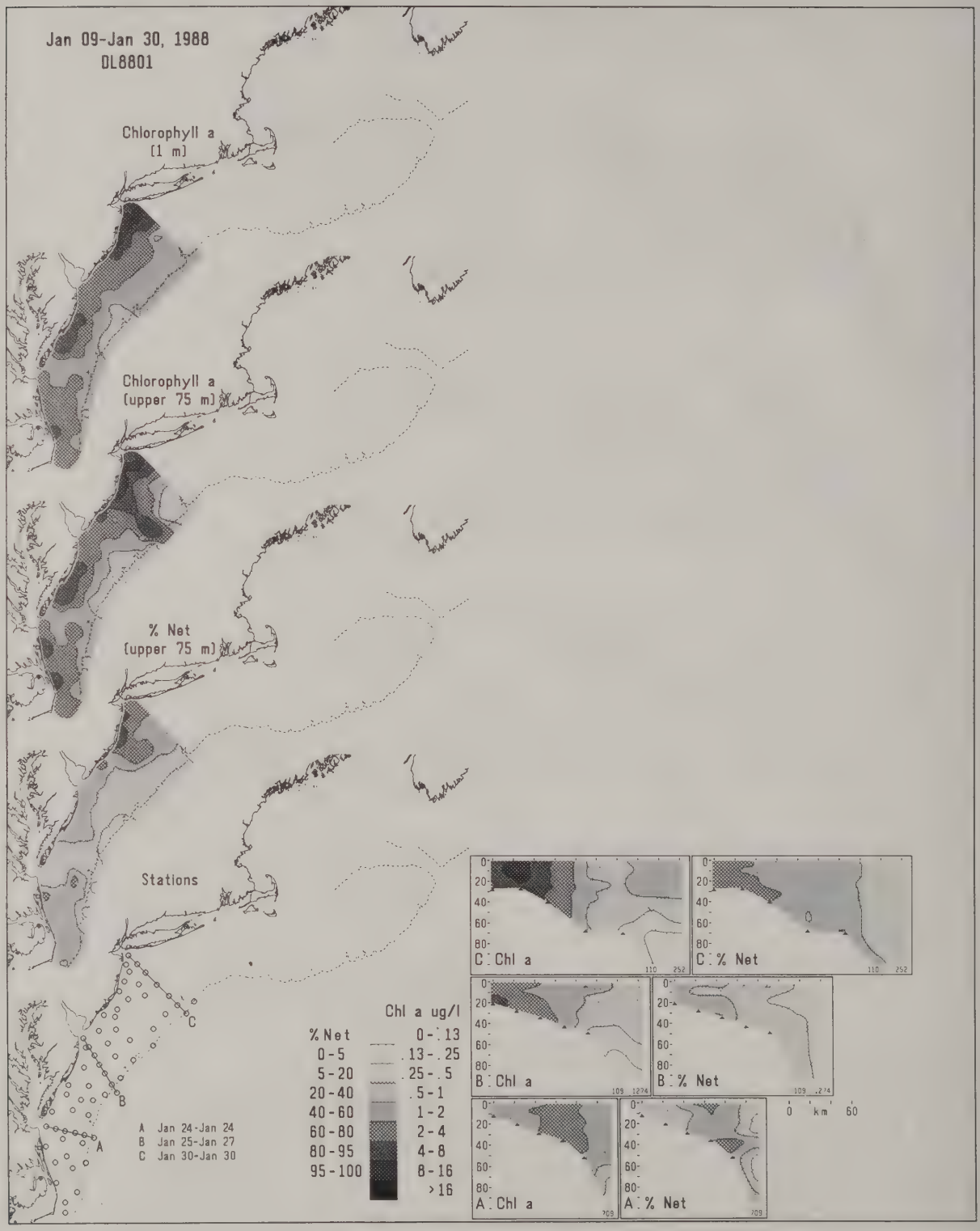

Appendix Figure B38
The distribution of chlorophyll *a* and percent netplankton during survey DL8801.

APPENDIX C

Table C1

Chronological listing of surveys, dates of sampling, number of vertical profiles, number of samples, number of samples taken 3 m below surface while underway, and summary by field program.

Cruise[1]	Program	Start	Finish	Profiles	Samples	Underway
AD7701	Other	Mar 16,77	Apr 01,77	29	179	
AL7705	Other	Jun 22,77	Jul 13,77	45	304	
AR7701	MARMAP[2]	Oct 17,77	Nov 09,77	116	807	
MM7711	MARMAP	Nov 12,77	Dec 13,77	90	677	
DL7802	MARMAP	Feb 16,78	Mar 16,78	131	1,073	
AR7804	MARMAP	Apr 18,78	May 22,78	156	1,322	
AL7807	MARMAP	Jun 23,78	Jul 16,78	146	1,230	
BE7801	MARMAP	Aug 11,78	Sep 04,78	154	1,358	
AL7812	NEMP[3]	Sep 20,78	Oct 04,78	23	210	
BE7803	MARMAP	Oct 06,78	Nov 01,78	129	1,169	
BE7804	MARMAP	Nov 16,78	Nov 29,78	77	720	
DL7901	NEMP	Jan 23,79	Jan 31,79	10	73	
DL7902	NEMP	Feb 15,79	Feb 15,79	2	19	
DL7903	MARMAP	Feb 24,79	Mar 14,79	111	849	
AD7901	Other	Apr 18,79	Apr 26,79	48	347	
DL7905	MARMAP	May 06,79	May 29,79	168	1,390	
AL7906	MARMAP	Jun 17,79	Jul 13,79	131	1,140	
AL7907	NEMP	Jul 17,79	Jul 26,79	50	449	
BE7901	MARMAP	Aug 11,79	Sep 02,79	149	1,351	
BE7903	Other	Sep 12,79	Oct 09,79	54	498	
AL7910	NEMP	Sep 12,79	Sep 27,79	55	486	
AL7911	MARMAP	Oct 04,79	Oct 28,79	155	1,342	
AL7913	MARMAP	Nov 15,79	Dec 20,79	82	785	
BE7905	Other	Nov 22,79	Nov 27,79	16	151	
DL7911	NEMP	Dec 04,79	Dec 17,79	50	375	
WI8002	MARMAP	Feb 20,80	Mar 10,80	87	806	
AL8002	MARMAP	Feb 28,80	Apr 04,80	154	1,361	
KE8004	NEMP	Mar 24,80	Mar 30,80	29	198	
EV8001	MARMAP	Apr 16,80	May 12,80	153	1,413	
EV8002	Other	May 18,80	May 28,80	48	453	
DL8003	MARMAP	May 23,80	Jun 29,80	149	1,332	
AL8007	NEMP	Jul 10,80	Jul 23,80	56	475	
EV8006	MARMAP	Jul 16,80	Aug 08,80	159	1,445	
EG8002	Other	Aug 05,80	Aug 06,80	5	20	
AL8009	NEMP	Sep 03,80	Sep 17,80	69	557	
AL8010	MARMAP	Sep 26,80	Oct 29,80	175	1,601	
KE8011	NEMP	Oct 28,80	Nov 05,80	34	260	
AL8012	MARMAP	Nov 19,80	Dec 21,80	137	1,211	
DL8009	NEMP	Dec 02,80	Dec 18,80	66	516	
AL8101	MARMAP	Feb 17,81	Mar 24,81	150	1,374	
KE8103	MARMAP	Mar 18,81	Apr 08,81	93	773	
KE8104	NEMP	Apr 24,81	May 08,81	54	431	
DL8103	MARMAP	May 21,81	Jun 17,81	148	1,428	
AL8107	NEMP	Jul 07,81	Jul 21,81	65	542	
AL8110	NEMP	Aug 27,81	Sep 16,81	67	583	
AL8111	WCR[4]	Sep 23,81	Oct 05,81	62	552	25
AL8112	WCR	Oct 12,81	Oct 22,81	73	530	
AL8114	MARMAP	Nov 18,81	Dec 21,81	88	917	
AL8201	NEMP	Jan 26,82	Feb 10,82	49	421	
AL8202	MARMAP	Feb 16,82	Mar 23,82	145	1,356	
AL8203	NEMP	Mar 30,82	Apr 06,82	23	178	
AL8204	WCR	Apr 19,82	May 03,82	64	792	8
DL8203	MARMAP	May 18,82	Jun 10,82	110	1,104	

continued on next page

Table C1 (continued)

Cruise[1]	Program	Start	Finish	Profiles	Samples	Underway
AL8207	WCR	Jun 18,82	Jul 01,82	88	874	82
AL8209	WCR	Aug 09,82	Aug 19,82	53	420	54
AL8210	NEMP	Aug 23,82	Sep 02,82	44	397	
DL8206	WCR	Sep 22,82	Sep 27,82	33	284	12
DL8209	WCR	Nov 17,82	Dec 20,82	161	1,559	
DL8301	MARMAP	Jan 17,83	Feb 10,83	103	1,039	
AL8303	Other	May 13,83	May 17,83	30	199	
AL8304	MARMAP	May 26,83	Jun 21,83	176	1,640	
AL8305	NEMP	Jul 04,83	Jul 13,83	24	254	
DL8309	MARMAP	Nov 16,83	Dec 20,83	152	1,387	
DL8401	MARMAP	Jan 09,84	Feb 08,84	160	1,491	
AL8403	MARMAP	May 09,84	Jun 02,84	177	1,655	
DL8409	MARMAP	Nov 01,84	Dec 05,84	141	1,273	
DL8501	MARMAP	Jan 07,85	Feb 06,85	130	1,187	
AL8504	MARMAP	May 08,85	Jun 04,85	167	1,403	
DL8510	MARMAP	Nov 07,85	Dec 10,85	0	338	338
DL8601	MARMAP	Jan 10,86	Feb 11,86	0	297	297
DL8603	MARMAP	May 08,86	Jun 05,86	0	277	277
DL8607	MARMAP	Aug 27,86	Sep 22,86	0	283	283
DL8610	MARMAP	Nov 05,86	Dec 10,86	0	256	256
DL8701	MARMAP	Jan 07,87	Feb 08,87	0	188	188
DL8704	MARMAP	May 07,87	Jun 06,87	0	415	415
DL8708	MARMAP	Aug 19,87	Sep 19,87	170	1,738	1
DL8710	MARMAP	Nov 04,87	Dec 10,87	125	1,212	67
DL8801	MARMAP	Jan 09,88	Jan 30,88	63	534	27

Program	Profiles	Samples	Underway
MARMAP	5,107	47,947	2,149
NEMP	770	6,424	0
WCR	534	5,011	181
Other	275	2,151	0
Grand total	6,686	61,533	2,330

[1] Vessel Codes: AD=Advance IV, AL=Albatross IV, AR=Argus, BE=Belogorsk, DL=Delaware, EG=Evergreen, EV=Evrika, KE=Kelez, MM=Mount Mitchel, WI=Wieczno.
[2] MARMAP=Marine Resource Monitoring and Prediction.
[3] NEMP=Northeast Monitoring Program.
[4] WCR=Warm Core Ring Studies.

Table C2
Coordinates of standard MARMAP stations used in the Dirichlet tesselation to define tiles.

Region/Subarea	Tile	Lat. N	Long. W	Depth (m)	Area (km^2)
MAB[1] Chesapeake plume	12	36°57'	75°48'	13.7	966
MAB Delaware plume	29	38°45'	74°57'	19.8	649
	184	38°34'	74°53'	19.3	544
MAB Hudson-Raritan plume	55	40°26'	73°50'	23.7	718
	187	40°15'	73°54'	22.8	342
MAB southern nearshore	4	35°51'	75°29'	21.1	1,197
	11	36°33'	75°47'	17.1	1,055
	21	37°15'	75°40'	13.5	1,163
	22	37°37'	75°19'	20.3	1,195
	23	37°48'	75°17'	17.5	1,041
	28	38°10'	74°54'	20.4	1,522
MAB central nearshore	30	38°35'	74°48'	24.7	562
	41	38°55'	74°33'	20.9	1,282
	42	39°14'	74°26'	17.7	934
	43	39°21'	74°06'	25.8	1,307
	52	39°34'	73°49'	24.0	1,176
	53	39°43'	74°03'	15.3	565
	185	39°55'	73°56'	21.6	684
	54	40°07'	73°48'	29.3	620
	56	40°16'	73°36'	27.2	829
	67	40°28'	73°13'	31.4	1,681
	68	40°44'	72°40'	26.4	836
MAB southern midshelf	1	35°16'	75°14'	31.0	1152
	2	35°28'	75°15'	27.5	1,193
	5	36°15'	75°32'	24.9	1,348
	6	36°23'	75°15'	33.7	1,224
	7	36°09'	75°06'	35.7	1,499
	10	36°43'	75°22'	20.2	1,020
	13	36°55'	75°33'	20.0	853
	14	36°53'	75°19'	27.7	729
	15	36°51'	75°04'	33.8	899
	20	37°18'	75°09'	26.9	1,454
	24	37°31'	74°57'	30.9	969
MAB central midshelf	27	37°48'	74°46'	38.8	1,465
	31	38°25'	74°39'	32.6	868
	32	38°14'	74°31'	40.5	874
	33	38°04'	74°22'	48.7	1,107
	39	38°25'	74°07'	53.9	1,535
	40	38°40'	74°19'	42.6	1,260
	44	38°57'	74°07'	41.8	1,460
	45	38°45'	73°45'	55.3	1,991
	50	39°12'	73°39'	42.7	2,143
	51	39°39'	73°23'	34.2	1,667
	186	39°52'	73°33'	34.1	971
	57	40°06'	73°23'	46.6	1,188
	58	39°52'	73°05'	68.4	1,618
MAB northern midshelf	66	40°19'	72°43'	50.0	2,225
	69	40°34'	72°28'	44.6	1,476
	74	40°49'	72°08'	37.9	1,696
	75	41°04'	71°42'	43.1	1,179
	76	41°20'	71°21'	30.0	765
	77	41°09'	71°15'	40.2	653
	78	40°58'	71°10'	50.6	1,252
	79	40°41'	71°02'	62.3	1,651
	86	40°42'	70°35'	57.5	1,521
	87	41°10'	71°00'	33.8	966
	88	41°03'	70°33'	44.4	1,400

continued on next page

Table C2 (continued)

Region/Subarea	Tile	Lat. N	Long. W	Depth (m)	Area (km^2)
MAB northern midshelf (continued)	89	40°41'	70°11'	49.6	2,348
MAB southern outer shelf	3	35°41'	74°58'	50.8	1,570
	9	36°39'	74°52'	56.9	1,120
	16	36°49'	74°50'	53.9	711
	19	37°13'	74°45'	65.0	1,773
	25	37°31'	74°39'	62.2	1,087
	26	37°38'	74°21'	145.5	1,279
	34	37°51'	74°11'	105.8	714
	37	37°59'	73°58'	215.2	1,428
	38	38°21'	73°39'	186.5	1,894
	47	38°59'	73°08'	78.7	1,676
	49	39°17'	72°51'	77.6	1,721
	59	39°39'	72°46'	70.2	1,310
	60	39°28'	72°33'	106.0	982
MAB norhern outer shelf	65	39°51'	72°27'	72.8	2,119
	70	40°14'	71°57'	66.1	2,265
	71	39°52'	71°49'	145.5	2,209
	72	40°04'	71°30'	137.3	2,633
	73	40°31'	71°36'	70.1	2,503
	80	40°21'	70°51'	96.9	1,595
	81	40°10'	70°46'	133.4	1,061
	85	40°13'	70°25'	114.9	2,204
	90	40°24'	69°42'	70.1	2,095
	91	40°08'	69°34'	91.7	1,735
Southern slope	8	36°16'	74°46'	318.0	1,380
	17	36°46'	74°35'	1059.0	1,082
	18	36°44'	74°20'	2055.0	1,314
	35	37°41'	74°03'	1217.7	1,036
	36	37°26'	73°50'	2044.9	1,675
	46	38°39'	73°09'	198.5	1,773
	48	38°58'	72°48'	735.1	1,535
	61	39°18'	72°19'	239.3	1,071
	62	39°10'	72°07'	1275.0	1,149
	63	39°02'	71°57'	2250.0	1,174
	64	39°33'	72°07'	307.0	1,785
GB[2] central shoals	123	41°11'	68°08'	37.5	1,933
	147	41°30'	67°41'	38.1	1,211
	148	41°16'	67°41'	37.2	822
	156	41°18'	67°33'	54.7	1,196
GB northern shoals	124	41°37'	68°06'	37.1	1,633
	146	41°48'	67°42'	35.4	1,479
	160	41°59'	67°24'	35.7	1,450
GB western outer shoals	120	40°48'	68°17'	54.1	1,786
	121	40°51'	68°44'	61.9	1,519
GB eastern outer shoals	157	41°33'	67°01'	60.8	2,084
	158	41°36'	66°31'	78.8	1,263
	159	42°02'	66°50'	69.8	2,119
GB Great South Channel	92	40°37'	69°14'	62.0	996
	111	41°04'	69°06'	79.9	1,093
	112	40°55'	69°06'	73.1	793
	113	40°39'	69°05'	72.6	710
	122	41°20'	68°42'	86.9	1,857
GB southern flank	114	40°25'	69°03'	80.5	1,275
	117	40°29'	68°37'	82.2	1,419
	119	40°31'	67°56'	126.7	1,240
	149	40°56'	67°41'	60.5	1,559
	150	40°37'	67°41'	84.9	1,022
	153	40°46'	67°19'	91.2	1,399

continued on next page

Table C2 (continued)

Region/Subarea	Tile	Lat. N	Long. W	Depth (m)	Area (km^2)
GB southern flank (continued)	155	41°13'	66°56'	69.3	2,161
GB northeast peak	177	41°52'	66°20'	81.7	1,331
	178	41°30'	66°20'	88.0	1,213
	179	41°10'	66°19'	152.5	1,759
	191	41°39'	65°55'	123.5	1,472
	192	41°54'	65°49'	130.8	1,570
GB northern slope	82	39°59'	70°40'	311.5	1,237
	83	39°48'	70°35'	1,224.3	1,361
	84	39°37'	70°30'	2,261.7	1,334
	115	40°05'	69°01'	275.1	1,585
	116	39°52'	69°00'	1,812.9	1,666
	118	40°20'	68°21'	162.3	1,643
	151	40°22'	67°40'	820.0	1,415
	152	40°04'	67°41'	2,116.8	1,799
	154	40°40'	67°05'	267.0	1,974
	180	40°53'	66°19'	1,932.8	1,069
	193	40°52'	66°37'	542.3	1,619
GB Nantucket shoals	93	40°53'	69°34'	37.2	1,967
GOM[3] western	94	41°32'	69°26'	68.4	1,392
	95	41°58'	69°50'	98.0	1,588
	97	42°06'	70°20'	59.7	1,103
	98	42°26'	70°38'	71.1	1,267
	99	42°48'	70°32'	88.5	1,848
	188	42°26'	70°09'	78.0	1,752
GOM northern	101	43°08'	69°58'	145.0	1,554
	102	43°24'	70°12'	91.9	1,616
	103	43°20'	69°41'	177.8	1,533
	104	43°40'	69°22'	96.5	1,426
	183	43°17'	69°20'	165.3	1,240
	105	42°58'	69°17'	163.3	1,717
	131	42°45'	68°46'	183.7	1,791
	135	43°22'	68°41'	135.2	1,841
	136	43°08'	69°01'	161.8	1,344
	137	43°37'	68°56'	116.5	1,661
	138	43°58'	68°35'	81.5	951
GOM Wilkinson Basin	96	42°15'	69°43'	228.8	1,846
	100	42°50'	70°00'	184.0	2,119
	106	42°35'	69°14'	217.6	2,231
	107	42°11'	69°12'	195.3	1,463
	108	41°54'	69°10'	207.0	1,400
	109	41°39'	69°09'	168.5	792
	110	41°20'	69°07'	151.4	1,190
	125	41°52'	68°11'	161.2	1,789
	126	41°37'	68°53'	127.3	1,352
	127	41°59'	68°39'	165.5	1,398
	128	42°10'	68°48'	187.1	1,231
	129	42°19'	68°27'	197.5	1,982
GOM Georges Basin	130	42°40'	68°19'	202.9	1,612
	143	42°59'	67°42'	182.8	1,989
	144	42°36'	67°42'	198.4	1,434
	145	42°18'	67°42'	228.5	2,014
	161	42°11'	67°15'	188.3	1,803
	162	42°43'	67°28'	210.7	1,519
	163	42°46'	66°58'	180.0	2,658
	174	42°28'	66°20'	250.7	1,217
	175	42°17'	66°20'	243.5	1,046
	176	42°09'	66°20'	173.9	1,122
GOM Jordan Basin	132	42°55'	68°22'	163.6	1,700

continued on next page

Table C2 (continued)

Region/Subarea	Tile	Lat. N	Long. W	Depth (m)	Area (km^2)
GOM Jordan Basin (continued)	133	43°12'	67°59'	200.6	1,113
	134	43°23'	68°08'	206.3	1,790
	142	43°49'	67°43'	220.6	1,751
	167	43°42'	67°26'	208.8	1,415
	182	43°24'	67°43'	251.0	1,779
GOM Scotian Shelf	139	44°01'	68°17'	88.3	646
	140	43°58'	68°11'	135.8	1,452
	141	44°20'	67°43'	83.4	1,804
	164	43°12'	66°48'	142.3	2,027
	165	43°35'	66°44'	118.0	1,673
	166	43°30'	67°00'	204.1	1,612
	168	44°02'	67°10'	139.9	1,957
	169	44°16'	67°07'	140.8	1,449
	170	44°16'	66°36'	197.1	1,570
	181	44°00'	66°12'	23.0	1,093
	171	43°32'	66°20'	71.4	1,490
	190	43°17'	66°20'	74.6	1,241
	172	43°01'	66°20'	127.6	1,210
	189	42°49'	66°20'	61.5	1,020
	173	42°39'	66°20'	105.2	1,006
				Total Area = 272,807 km^2	

[1] MAB=Middle Atlantic Bight.
[2] GB=Georges Bank.
[3] GOM=Gulf of Maine.

Table C3

Mean water column concentration of chlorophyll *a* and associated statistics by tile and by two-month periods.

	January–February								March–April								May–June							
Tile	Y[1] #	P[2] #	Min. Chl *a* µg l^{-1}	Max. Chl *a* µg l^{-1}	Mean Chl *a* µg l^{-1}	C.V.[3] Chl *a* %	Net.[4] %	Pha.[5] %	Y #	P #	Min. Chl *a* µg l^{-1}	Max. Chl *a* µg l^{-1}	Mean Chl *a* µg l^{-1}	C.V. Chl *a* %	Net. %	Pha. %	Y #	P #	Min. Chl *a* µg l^{-1}	Max. Chl *a* µg l^{-1}	Mean Chl *a* µg l^{-1}	C.V. Chl *a* %	Net. %	Pha. %
MAB Chesapeake Plume 14 m																								
12	6	7	1.53	9.37	3.75	64.7	62.4	22.3	5	10	0.28	22.60	5.85	109.4	58.5	21.8	7	9	0.64	19.16	3.55	156.2	34.1	22.3
MAB Delaware Plume 20 m																								
29	6	6	3.92	18.55	10.74	43.8	70.4	19.6	4	9	0.76	9.70	5.54	57.8	58.4	20.4	7	8	0.46	6.32	3.72	49.1	43.1	26.6
184	5	5	4.05	12.03	8.97	31.0	66.7	19.1	3	5	2.36	7.97	5.16	42.6	50.8	15.5	6	7	1.25	6.52	3.65	51.1	49.0	23.8
MAB Hudson-Raritan Plume 23 m																								
55	5	6	2.72	13.90	8.03	46.6	82.1	15.4	5	17	0.13	15.37	5.79	71.7	64.1	17.5	9	12	0.77	6.87	3.44	54.7	28.6	24.7
187	3	3	5.94	9.78	8.01	19.8	68.1	15.9	5	10	1.05	12.30	5.75	67.7	55.5	19.2	7	8	1.35	10.63	4.20	65.4	37.0	25.1
MAB Southern Nearshore 15–20 m																								
4	4	4	2.29	5.75	4.04	32.6	64.3	24.0	4	4	1.02	2.13	1.58	26.8	34.1	31.0	7	8	0.37	3.88	1.31	77.3	28.9	29.9
11	6	6	2.38	15.01	5.71	74.9	68.6	20.6	4	5	0.90	3.42	1.92	48.2	43.4	22.3	7	8	0.65	6.00	2.27	70.9	29.3	22.3
21	5	6	1.61	8.71	4.93	46.3	50.3	30.7	4	6	0.36	7.16	1.93	122.9	42.0	28.2	6	7	0.48	7.58	2.54	86.9	28.6	19.4
22	5	5	1.99	9.59	5.29	48.2	53.4	20.2	4	6	0.67	3.52	1.90	58.1	38.8	29.6	7	8	0.37	2.85	1.55	52.4	42.9	24.8
23	6	7	2.58	10.67	6.88	33.5	56.5	21.1	4	7	0.39	5.20	2.31	67.5	47.8	29.1	7	9	0.63	4.12	2.04	51.2	55.0	27.6
28	6	8	3.63	9.51	6.49	33.8	60.7	16.3	4	7	1.29	3.38	2.20	37.6	46.3	25.4	7	7	0.67	3.53	1.61	53.5	38.5	26.4
MAB Central Nearshore 15–30 m																								
30	5	5	2.72	8.92	5.40	38.9	64.9	19.2	5	7	0.70	9.52	3.85	79.1	61.9	23.1	6	6	0.90	4.55	2.16	53.8	52.6	23.9
41	5	5	3.20	5.88	4.25	25.3	59.8	22.0	5	7	0.65	7.37	3.40	76.8	71.6	22.7	7	7	1.45	5.02	2.53	45.3	55.7	22.9
42	4	4	4.32	7.27	5.21	23.0	65.6	28.6	5	7	0.61	10.21	3.95	87.8	68.6	26.1	7	7	0.30	2.43	1.46	46.1	19.4	30.2
43	4	5	1.61	6.00	3.90	39.8	61.0	28.4	6	11	0.33	6.06	2.84	65.4	53.2	24.4	6	6	0.78	4.50	2.05	57.2	52.0	22.9
52	5	5	1.14	4.79	3.28	40.7	60.5	19.4	5	11	0.24	7.24	2.41	88.2	59.0	20.8	6	7	0.92	3.66	1.74	53.8	50.3	24.0
53	4	4	4.94	15.29	10.36	35.5	81.7	18.3	5	7	1.26	9.72	4.18	63.4	56.0	24.0	7	7	0.96	5.79	3.27	56.7	49.7	28.3
185	3	3	3.01	11.10	7.80	44.4	66.5	13.7	5	10	1.30	9.30	4.92	54.5	58.7	20.0	8	11	0.62	4.60	1.75	60.9	38.5	31.3
54	4	4	2.28	7.29	4.19	44.7	64.4	18.5	5	8	1.27	5.48	3.08	50.1	57.4	20.4	7	7	0.75	3.56	1.76	52.5	55.1	25.7
56	4	4	2.30	11.67	7.63	46.0	71.5	16.3	4	8	0.57	7.44	3.37	69.8	64.7	16.0	8	9	0.58	3.64	1.51	57.6	45.5	27.4
67	6	6	2.74	8.19	4.82	35.6	67.8	20.3	4	11	0.83	4.53	1.77	53.6	68.0	19.1	9	9	0.41	1.97	1.27	48.9	36.0	27.4
68	6	6	1.84	7.21	3.80	44.8	73.4	22.0	4	10	0.96	6.41	2.37	79.6	72.2	17.4	8	9	0.29	3.03	1.34	60.4	30.2	30.2
MAB Southern Midshelf 20–40 m																								
1	4	4	0.71	3.85	2.46	46.2	67.0	25.9	2	2	1.08	1.24	1.16	6.9	52.2	36.3	6	9	0.20	1.60	0.60	68.2	18.1	33.5
2	4	4	0.59	5.70	2.66	70.3	60.7	24.6	3	3	0.54	2.39	1.47	51.4	51.0	44.3	6	8	0.15	1.11	0.60	49.5	30.3	34.1
5	4	4	0.97	3.13	2.36	36.1	68.8	21.6	3	4	0.66	3.40	1.73	65.3	43.9	24.8	7	8	0.27	1.43	0.83	50.0	24.5	33.6
6	5	5	1.51	3.86	2.46	33.0	54.4	21.9	3	3	0.32	3.61	1.74	79.3	64.2	20.9	6	8	0.30	1.84	0.94	53.5	43.7	26.5
7	4	4	1.87	2.83	2.36	17.0	65.7	23.4	3	3	0.43	5.66	2.30	103.5	74.4	14.8	6	7	0.30	1.58	0.93	40.7	32.1	31.1
10	6	6	1.17	4.57	2.83	44.9	54.1	21.8	3	3	0.72	1.78	1.17	38.2	30.5	26.9	5	6	0.61	2.65	1.26	60.7	32.5	20.3
13	5	5	1.73	5.00	3.59	31.8	50.1	23.6	5	6	0.33	1.94	1.14	60.5	27.6	30.1	6	7	0.19	8.06	1.89	135.9	31.9	20.6
14	5	5	0.54	3.26	2.30	43.0	45.9	25.8	4	5	0.02	2.45	1.04	80.3	58.1	18.1	6	7	0.28	3.85	1.67	73.1	41.9	25.4
15	6	6	1.14	5.04	3.22	42.4	56.2	19.1	5	8	0.03	4.10	2.12	69.0	69.2	20.6	7	8	0.33	2.54	1.24	55.6	40.1	27.0
20	5	6	1.74	5.13	2.77	40.9	51.8	26.5	4	5	0.26	2.42	1.16	74.9	54.0	21.1	6	7	0.21	1.74	1.03	50.0	31.1	30.0
24	5	5	1.68	7.66	4.36	50.0	58.2	20.1	4	6	0.67	5.28	2.38	64.5	68.5	18.2	8	9	0.51	2.43	1.25	49.1	40.9	23.8
MAB Central Midshelf 30–60 m																								
27	6	8	1.65	6.78	3.62	47.7	55.0	18.3	5	8	0.96	5.00	2.11	67.9	71.6	19.8	7	8	0.71	3.06	1.27	58.1	53.3	22.6
31	5	5	1.80	6.55	2.93	62.2	58.1	20.6	4	6	0.44	5.10	2.47	67.4	69.1	19.3	7	8	0.39	2.36	1.27	49.0	51.0	25.7
32	5	5	1.40	7.35	2.78	82.8	62.0	23.2	4	6	0.43	7.30	3.18	79.9	78.4	13.8	7	7	0.65	1.98	1.29	36.6	57.7	25.9
33	6	6	0.78	3.94	2.03	55.1	62.7	22.5	4	7	0.67	7.37	3.47	70.6	82.1	13.0	7	8	0.45	1.80	1.21	41.0	60.6	23.4
39	5	6	0.77	2.86	1.63	48.8	47.4	24.9	5	10	0.68	7.54	3.19	74.6	78.0	16.9	8	10	0.47	2.73	1.36	56.5	65.8	23.6
40	4	4	1.52	2.47	1.95	17.5	45.8	29.1	5	8	0.80	6.16	3.09	58.7	79.5	19.3	7	7	0.60	2.27	1.40	46.1	58.0	25.2
44	5	5	1.65	4.48	2.72	36.9	49.5	24.2	5	9	0.62	7.63	2.77	80.3	75.9	17.1	8	8	0.33	3.18	1.24	70.1	61.7	25.8
45	5	5	0.51	2.59	1.46	48.8	49.4	25.2	5	10	0.85	6.49	3.28	58.3	75.1	15.2	7	10	0.44	2.00	1.18	49.0	54.3	23.4
50	3	3	2.13	2.97	2.54	13.5	24.8	26.4	6	8	0.85	6.94	2.55	73.4	74.2	15.0	8	8	0.48	2.10	1.23	52.1	54.5	25.5
51	4	4	1.26	3.01	2.21	28.3	52.6	23.0	5	6	1.14	5.13	2.77	52.8	60.8	16.3	8	8	0.67	2.43	1.39	43.1	49.6	24.8
186	4	4	2.14	3.73	3.10	20.8	56.6	23.8	4	8	0.98	6.12	2.89	57.6	70.9	17.9	6	6	0.54	2.26	1.45	43.5	55.6	22.8
57	5	5	2.19	4.17	3.32	22.5	63.2	18.4	5	8	0.52	4.51	2.15	67.6	71.7	17.3	9	11	0.46	2.96	1.34	57.9	60.1	23.5
58	5	5	0.83	2.21	1.52	36.7	56.2	24.4	5	10	0.72	6.22	2.89	57.3	76.7	15.5	8	11	0.62	1.32	0.96	21.2	51.7	28.9
MAB Northern Midshelf 30–60 m																								
66	4	4	0.82	4.13	2.35	50.5	62.9	23.7	4	6	0.77	3.71	2.52	35.3	77.7	15.4	8	9	0.44	2.33	1.32	47.0	50.4	19.5
69	4	4	2.25	3.37	2.96	15.2	71.7	18.4	3	7	0.56	2.99	1.53	50.2	73.8	21.2	9	10	0.45	2.68	1.05	64.9	51.9	26.6
74	5	5	2.12	4.58	3.35	23.4	70.9	20.4	4	7	0.48	3.89	1.89	52.7	73.7	22.2	8	8	0.18	2.94	1.18	64.4	37.9	30.6
75	3	3	3.99	4.89	4.40	8.5	75.2	25.8	5	8	1.22	5.57	3.13	51.6	78.6	21.2	8	8	0.43	3.12	1.42	64.0	36.8	30.0
76	3	3	1.25	2.72	2.15	29.9	73.8	18.6	5	11	0.67	8.04	3.60	69.0	70.2	20.3	8	8	0.44	2.58	1.09	61.6	25.6	29.7
77	2	2	3.24	3.65	3.44	6.0	85.9	14.2	5	8	1.49	3.99	2.95	28.0	82.2	21.6	8	8	0.27	3.54	1.17	79.7	42.3	29.5
78	2	2	2.12	3.21	2.67	20.5	71.7	23.1	5	8	0.20	5.43	2.27	67.5	63.4	22.3	8	8	0.31	1.64	0.79	49.8	38.2	35.7
79	3	3	0.85	4.12	2.03	73.2	74.0	23.1	5	9	0.33	8.88	2.45	100.7	77.0	19.7	8	9	0.24	0.87	0.62	32.1	19.3	38.1
86	3	4	0.67	4.45	2.40	62.4	73.8	23.3	5	7	0.82	5.22	2.84	55.3	81.5	18.6	8	8	0.19	3.37	1.19	83.3	46.7	30.4
87	3	4	2.86	5.55	4.19	29.8	79.6	21.8	5	9	0.42	4.58	2.38	61.5	75.8	23.5	7	7	0.55	1.92	1.03	44.6	23.6	29.5
88	4	5	1.74	5.47	3.60	36.7	69.3	26.4	5	6	0.99	12.04	5.09	75.4	85.6	18.2	8	8	0.20	4.53	1.10	120.7	42.8	27.7
89	5	6	0.83	3.72	1.76	53.9	63.1	26.9	5	14	1.21	8.41	3.40	62.5	72.4	24.8	7	7	0.44	4.48	1.73	71.1	53.2	27.0
MAB Southern Outer Shelf 60–200 m																								
3	4	5	1.00	2.52	1.74	27.7	71.0	24.3	3	3	0.47	4.51	2.02	87.8	73.0	22.6	6	7	0.21	0.98	0.48	59.3	33.8	41.4
9	7	7	0.55	4.72	1.87	71.8	55.0	23.7	4	5	0.52	5.83	2.15	90.4	72.3	19.8	7	9	0.11	2.22	1.17	52.8	35.6	26.9
16	5	5	0.51	4.22	2.00	65.0	59.0	24.0	3	4	0.08	4.62	1.75	98.7	31.5	16.3	6	8	0.30	2.22	0.86	68.1	45.2	28.8
19	5	6	0.47	2.13	1.07	48.7	41.4	31.4	4	6	0.21	4.57	1.82	84.3	69.7	17.2	6	7	0.41	1.85	0.98	44.5	50.4	28.9
25	4	4	0.71	1.74	1.04	40.1	46.0	32.4	4	4	0.62	6.77	3.57	70.4	80.0	16.0	7	10	0.35	2.42	1.01	68.2	58.0	25.8
26	4	4	0.49	1.30	0.73	45.8	34.7	36.0	4	6	0.63	4.55	1.62	84.9	75.8	19.8	8	12	0.31	1.82	0.86	56.1	44.4	25.2
34	5	5	0.27	1.40	0.73	63.0	29.4	32.9	5	6	0.81	4.27	2.17	60.4	73.1	22.5	6	9	0.14	2.24	0.86	68.6	46.4	25.3
37	5	5	0.36	0.94	0.58	34.2	14.1	39.5	4	6	0.81	3.45	1.80	57.1	66.3	21.4	8	10	0.15	1.59	0.70	55.1	32.1	29.3
38	4	4	0.29	0.86	0.54	38.0	12.4	39.2	5	8	0.79	2.88	1.90	34.8	74.2	20.8	8	14	0.25	0.90	0.50	41.7	14.5	34.9
47	4	4	0.39	5.98	2.12	106.7	28.2	41.9	5	6	0.28	5.03	2.59	69.2	83.2	17.8	7	7	0.33	2.54	0.95	73.4	33.2	31.6
49	5	5	0.47	2.81	1.31	66.2	55.3	23.8	6	9	0.61	5.22	2.17	77.1	71.1	15.6	8	9	0.24	1.24	0.78	38.9	38.0	33.4
59	5	6	0.84	2.39	1.52	38.0	56.0	25.1	5	9	0.69	6.70	2.82	71.1	71.6	14.3	9	10	0.23	1.53	0.85	45.9	41.1	30.8
60	4	4	0.58	0.83	0.71	13.6	28.3	34.1	4	6	0.59	3.76	1.89	58.6	69.4	17.1	8	9	0.36	1.15	0.68	36.8	16.6	32.0

continued on next page

Table C3 (continued)

	July–August								September–October								November–December							
Tile	Y[1] #	P[2] #	Min. Chl *a* µg l^{-1}	Max. Chl *a* µg l^{-1}	Mean Chl *a* µg l^{-1}	C.V.[3] Chl *a* %	Net.[4] %	Pha.[5] %	Y #	P #	Min. Chl *a* µg l^{-1}	Max. Chl *a* µg l^{-1}	Mean Chl *a* µg l^{-1}	C.V. Chl *a* %	Net. %	Pha. %	Y #	P #	Min. Chl *a* µg l^{-1}	Max. Chl *a* µg l^{-1}	Mean Chl *a* µg l^{-1}	C.V. Chl *a* %	Net. %	Pha. %
MAB Chesapeake Plume 14 m																								
12	6	8	1.38	6.99	3.42	49.2	46.0	23.6	4	8	1.33	12.40	4.74	84.3	21.5	32.4	5	7	1.91	8.37	4.78	40.8	44.7	27.3
MAB Delaware Plume 20 m																								
29	5	6	0.52	4.94	2.93	50.7	40.4	29.2	5	6	2.83	8.89	5.36	46.2	45.4	35.3	6	8	0.93	6.29	3.52	46.4	58.2	33.2
184	4	6	0.83	6.69	2.42	81.2	32.6	27.3	4	6	0.49	6.81	3.97	55.7	26.9	29.7	6	8	1.90	7.12	4.84	29.8	49.6	23.2
MAB Hudson-Raritan Plume 23 m																								
55	4	8	1.20	16.12	5.39	87.1	42.5	25.7	5	14	0.55	18.61	5.36	102.9	47.6	22.3	6	12	2.00	5.13	3.57	32.7	50.6	23.9
187	5	10	1.35	5.43	3.13	42.5	47.8	27.4	4	5	0.98	12.33	5.24	83.3	49.1	22.1	6	8	2.69	6.32	4.38	28.1	42.8	21.8
MAB Southern Nearshore 15–20 m																								
4	4	4	1.10	2.21	1.64	32.7	47.9	24.1	3	3	0.64	1.57	1.03	38.5	39.3	39.1	5	5	0.80	7.81	3.82	67.1	60.0	22.2
11	6	7	0.40	4.08	2.02	66.8	41.8	30.4	4	6	0.55	6.92	2.16	100.2	22.8	35.2	5	6	1.36	7.26	4.61	39.5	53.1	25.8
21	5	5	1.03	3.53	2.38	40.5	42.3	29.2	4	5	0.28	6.30	3.36	76.6	51.8	26.3	5	6	2.29	9.37	4.87	49.1	40.4	24.5
22	4	4	0.74	4.61	2.54	58.3	75.6	18.6	2	2	0.80	4.92	2.86	72.0	64.0	30.2	4	4	0.13	4.88	2.57	65.1	41.3	34.4
23	7	8	0.93	6.69	2.61	67.9	51.9	24.1	4	6	0.68	6.30	2.46	84.3	41.8	35.4	6	7	1.26	7.40	4.12	60.5	50.8	26.7
28	5	7	0.53	3.29	1.40	59.6	45.9	21.8	3	5	0.37	5.12	2.33	69.5	35.4	27.4	6	7	1.84	4.61	3.22	30.3	39.4	30.9
MAB Central Nearshore 15–30 m																								
30	4	6	0.77	3.78	1.79	59.0	59.4	21.5	4	6	1.75	4.88	2.88	33.0	42.4	25.8	5	5	2.25	5.22	3.93	24.8	51.4	23.4
41	4	8	0.40	4.71	2.26	62.8	64.5	20.7	5	7	1.04	8.64	2.96	88.4	47.4	26.7	6	8	1.86	6.81	3.63	39.9	58.8	23.4
42	5	7	0.97	5.23	2.67	61.2	49.0	21.9	5	5	1.26	10.74	3.52	103.0	49.7	28.6	5	5	2.46	3.62	3.07	13.7	37.9	31.3
43	5	8	0.41	2.72	1.61	52.8	50.4	24.5	5	6	0.17	3.95	2.09	61.6	60.4	27.9	6	8	2.13	5.15	3.62	28.7	33.9	24.8
52	6	10	0.44	4.59	1.64	73.3	48.5	28.1	4	7	0.60	4.40	2.11	73.1	50.5	24.6	6	7	2.64	4.46	3.39	18.7	13.9	26.6
53	5	6	2.73	5.53	3.95	26.5	59.8	23.6	4	4	0.89	5.05	2.70	55.4	38.2	35.7	4	4	2.23	5.92	4.77	31.0	49.6	28.5
185	4	8	0.72	9.99	2.52	114.6	63.0	20.8	4	6	0.61	5.97	2.49	86.0	47.8	25.5	6	8	2.12	6.55	4.28	36.1	38.0	22.7
54	3	4	0.67	2.00	1.33	37.8	52.5	23.6	4	4	0.81	3.34	1.87	54.6	50.7	31.2	5	5	2.25	4.84	3.73	25.6	22.4	22.9
56	5	8	0.65	4.81	2.07	66.9	50.7	28.6	4	9	0.31	3.25	1.34	63.6	40.2	34.7	5	5	2.13	3.98	2.99	20.2	23.6	27.4
67	5	10	0.54	2.42	1.35	43.5	36.6	25.9	6	8	0.37	2.00	1.44	39.9	52.1	32.6	7	11	1.27	5.23	2.98	43.3	45.5	29.5
68	6	10	0.48	2.82	1.62	49.1	28.6	29.2	6	7	0.58	2.92	2.01	39.8	36.8	31.4	7	10	1.26	10.93	4.45	73.0	54.0	30.3
MAB Southern Midshelf 20–40 m																								
1	4	4	0.20	1.17	0.66	57.0	33.3	34.7	3	3	0.70	1.17	0.98	20.6	29.4	47.4	3	3	0.68	2.96	1.70	55.5	35.4	35.1
2	4	4	0.58	1.25	0.91	35.4	47.8	30.1	3	3	0.83	1.43	1.18	21.6	22.3	43.0	3	3	0.82	4.57	2.10	82.9	42.2	25.0
5	5	6	0.27	2.38	1.10	62.4	52.7	27.1	3	4	0.17	1.54	0.70	81.0	27.9	37.5	4	5	0.92	2.92	2.18	33.6	39.7	32.5
6	4	5	0.51	1.19	0.91	29.8	54.1	26.7	3	3	0.60	2.27	1.35	51.3	44.4	35.1	4	6	1.26	3.12	2.16	35.5	34.6	26.8
7	3	3	0.35	0.87	0.69	34.9	45.4	26.6	3	3	0.62	1.99	1.41	41.1	55.9	34.2	5	5	0.97	3.63	1.96	46.2	52.4	28.5
10	4	4	0.30	2.67	1.06	89.5	46.3	24.3	3	3	0.99	2.12	1.45	33.4	43.9	32.2	4	4	1.03	2.65	1.84	35.0	38.7	28.2
13	4	5	0.51	2.53	1.20	61.1	61.5	24.5	2	2	1.14	1.83	1.49	23.2	51.5	33.9	4	4	1.50	4.29	2.75	40.9	40.7	23.4
14	4	4	0.51	2.48	1.17	67.3	67.2	32.1	3	3	1.13	2.13	1.59	25.8	41.0	34.3	4	4	1.35	2.14	1.60	19.8	26.9	27.3
15	6	7	0.22	1.42	0.88	47.5	38.8	28.5	3	5	0.46	2.92	1.15	79.1	46.9	30.3	5	7	0.92	2.97	1.92	34.0	34.9	27.0
20	4	5	0.30	1.71	0.95	48.9	53.9	24.5	3	3	0.74	2.31	1.59	40.8	33.6	35.1	4	4	1.36	2.72	1.96	28.9	32.3	28.5
24	4	4	0.39	1.38	1.03	36.8	42.3	26.5	3	3	0.53	1.75	1.25	41.7	25.5	43.6	5	5	1.17	3.17	1.92	37.9	26.0	29.1
MAB Central Midshelf 30–60 m																								
27	6	7	0.81	3.95	1.66	60.2	55.3	23.2	4	6	0.23	1.29	0.78	50.9	27.0	36.6	6	7	0.58	2.84	1.67	48.7	38.1	28.0
31	4	5	0.87	2.59	1.75	35.4	48.0	21.1	3	3	0.96	1.10	1.01	6.1	38.8	36.8	5	5	1.93	2.69	2.35	11.9	41.5	25.9
32	5	6	0.63	5.54	1.86	91.9	25.2	23.5	4	5	0.47	1.82	1.03	44.5	46.2	32.6	5	5	1.16	2.61	1.84	26.1	43.6	29.5
33	6	8	0.61	1.94	1.21	36.9	43.1	24.9	3	4	0.63	2.35	1.32	50.5	57.2	21.4	5	5	0.78	2.56	1.29	50.1	47.9	29.4
39	5	7	0.75	1.53	1.02	28.9	55.7	24.9	5	9	0.44	2.93	1.06	66.6	57.0	28.8	6	7	0.36	2.81	1.49	52.2	42.8	28.7
40	4	5	0.28	1.66	1.09	41.8	46.3	26.8	4	4	1.05	5.37	2.40	72.0	64.6	23.3	5	5	1.40	3.38	2.33	35.0	47.9	25.4
44	6	9	0.57	1.99	1.29	32.8	52.8	24.1	3	6	0.42	2.98	1.42	73.1	62.9	21.5	7	8	0.85	3.59	2.16	42.9	43.0	26.8
45	5	7	0.34	2.33	1.03	63.2	39.5	25.3	5	8	0.27	2.29	0.94	67.3	49.4	29.3	6	7	0.78	2.78	1.68	41.2	39.0	27.9
50	4	6	0.65	2.48	1.41	40.9	56.2	27.3	4	4	0.75	4.03	2.14	55.6	56.3	28.2	6	6	1.18	2.37	1.79	25.1	30.3	30.1
51	4	6	0.51	1.71	1.04	41.2	49.0	28.8	4	4	0.75	2.50	1.60	42.9	50.7	29.8	5	5	1.66	3.28	2.43	26.9	18.9	29.2
186	3	5	0.75	1.95	1.25	34.5	47.9	26.0	3	5	1.00	1.42	1.14	13.2	49.7	30.0	5	6	1.88	3.86	2.76	31.2	41.5	25.0
57	5	7	0.64	1.27	0.98	25.8	49.6	27.4	5	7	0.32	1.61	1.08	45.6	41.6	35.4	6	7	0.75	2.06	1.53	30.5	31.5	27.8
58	4	6	0.45	1.71	0.93	50.7	58.0	23.1	5	10	0.30	0.96	0.54	34.6	39.8	39.3	5	5	0.64	2.38	1.44	46.9	33.8	28.0
MAB Northern Midshelf 30–60 m																								
66	4	6	0.41	1.12	0.78	28.7	45.4	37.0	4	6	0.33	2.31	0.94	71.8	57.9	30.5	7	7	0.60	2.49	1.76	37.5	50.2	24.8
69	5	7	0.45	0.96	0.73	23.2	29.9	31.9	4	6	0.16	3.10	1.27	72.7	58.8	33.8	7	11	0.54	2.95	1.73	44.7	46.4	29.7
74	4	6	0.53	2.87	1.32	62.7	54.5	28.2	4	4	0.48	2.61	1.16	74.9	24.4	50.3	7	7	1.00	3.09	1.65	37.5	46.7	30.3
75	5	9	0.62	3.15	1.70	43.0	39.2	29.5	5	6	0.42	3.15	1.50	61.0	45.2	31.7	7	8	0.73	3.96	1.73	58.9	60.0	34.2
76	4	7	0.76	4.19	1.85	62.7	25.2	31.0	5	7	0.62	2.86	1.41	56.3	21.4	34.4	8	11	1.00	4.10	2.54	40.9	59.4	23.3
77	3	5	0.49	1.19	0.85	33.3	36.2	33.7	3	4	0.67	1.80	1.15	42.3	39.4	35.8	9	9	0.92	3.45	2.41	37.3	68.9	21.8
78	3	5	0.55	1.30	0.75	38.2	33.9	33.0	4	4	0.53	0.90	0.72	18.6	30.5	36.7	9	9	0.65	3.80	2.24	49.7	66.8	23.0
79	4	4	0.41	1.23	0.84	43.7	40.6	28.9	6	12	0.49	3.48	1.02	77.3	38.7	31.9	9	9	0.45	3.24	1.59	56.1	65.1	25.4
86	3	5	0.09	1.06	0.57	60.4	54.4	31.2	6	8	0.72	1.12	0.96	14.2	28.6	33.4	8	8	0.51	1.92	1.27	32.6	53.9	26.6
87	5	6	0.64	1.90	1.11	39.4	27.0	31.5	4	4	0.46	1.84	1.10	44.5	29.5	39.2	8	9	1.29	6.42	3.25	46.6	67.4	21.9
88	4	7	0.52	1.59	0.95	40.0	39.3	29.1	4	8	0.39	2.24	1.23	44.7	32.0	30.8	7	8	1.29	2.88	2.05	29.9	64.2	22.0
89	6	14	0.37	3.74	1.10	77.4	20.1	33.3	6	11	0.50	3.53	1.38	61.5	43.4	31.0	9	13	0.74	2.72	1.59	30.9	56.0	29.6
MAB Southern Outer Shelf 60–200 m																								
3	4	5	0.31	1.09	0.61	44.4	40.0	37.1	3	3	0.26	0.63	0.51	34.4	21.7	48.6	4	5	0.33	1.46	0.85	45.2	28.4	35.2
9	6	7	0.20	1.18	0.71	45.5	34.3	33.1	4	6	0.52	1.17	0.84	27.0	36.7	32.7	5	6	0.35	1.86	1.06	45.2	24.1	31.6
16	4	4	0.22	0.87	0.58	40.9	28.8	32.4	4	4	0.30	1.98	0.84	81.0	37.5	35.9	4	4	0.88	1.79	1.19	29.8	31.7	31.6
19	6	7	0.51	1.01	0.76	25.9	34.1	31.4	3	4	0.46	0.78	0.59	23.3	43.9	37.1	4	4	0.90	1.63	1.15	24.8	24.8	33.6
25	3	3	0.72	1.32	0.93	30.0	48.9	25.1	5	6	0.50	2.67	0.97	78.8	31.9	29.7	5	5	0.70	2.90	1.47	53.5	42.9	30.0
26	6	7	0.34	1.06	0.65	41.0	20.2	31.5	3	3	0.14	1.43	0.77	68.5	43.7	36.4	5	5	0.34	1.81	0.92	56.4	40.2	30.9
34	4	5	0.29	0.78	0.53	33.9	35.9	32.9	2	3	0.42	0.66	0.50	22.0	23.8	34.1	5	5	0.47	1.91	1.08	48.0	42.4	29.9
37	4	6	0.17	1.10	0.59	62.7	23.2	31.4	3	3	0.46	1.60	0.90	55.6	38.2	25.0	5	5	0.26	1.61	0.82	57.9	41.9	31.8
38	4	5	0.27	0.64	0.42	35.6	13.5	33.5	4	5	0.31	1.11	0.64	46.8	45.5	35.9	5	5	0.22	1.24	0.72	48.2	23.6	31.4
47	5	8	0.27	0.86	0.57	31.5	26.5	35.9	4	4	0.59	1.38	0.87	35.3	39.2	36.1	5	6	0.51	1.34	0.90	39.2	33.2	32.4
49	7	11	0.37	1.09	0.64	27.9	16.4	35.4	5	8	0.25	0.83	0.48	36.3	31.2	36.9	6	7	0.42	1.70	1.13	44.5	44.8	30.7
59	6	11	0.35	1.26	0.74	34.9	39.6	30.3	4	8	0.29	1.52	0.76	56.4	29.4	33.3	5	6	0.52	1.86	1.18	43.3	42.8	25.8
60	4	5	0.33	0.75	0.54	25.6	10.7	34.1	4	5	0.30	0.84	0.47	44.2	13.1	41.9	5	5	0.65	1.86	1.05	44.1	42.8	26.5

continued on next page

Table C3 (continued)

	January–February								March–April								May–June							
Tile	Y[1] #	P[2] #	Min. Chl *a* µg l^{-1}	Max. Chl *a* µg l^{-1}	Mean Chl *a* µg l^{-1}	C.V.[3] Chl *a* %	Net.[4] %	Pha.[5] %	Y #	P #	Min. Chl *a* µg l^{-1}	Max. Chl *a* µg l^{-1}	Mean Chl *a* µg l^{-1}	C.V. Chl *a* %	Net. %	Pha. %	Y #	P #	Min. Chl *a* µg l^{-1}	Max. Chl *a* µg l^{-1}	Mean Chl *a* µg l^{-1}	C.V. Chl *a* %	Net. %	Pha. %
MAB Northern Outer Shelf 60–200 m																								
65	4	4	0.51	2.20	1.41	42.9	61.6	22.1	4	5	0.72	2.34	1.43	38.4	52.3	19.6	9	9	0.37	2.55	1.04	67.1	30.3	32.4
70	3	3	1.68	2.28	2.03	12.6	68.9	21.3	4	5	0.53	5.13	1.57	113.6	71.2	18.7	6	6	0.25	1.07	0.74	35.2	18.9	33.9
71	3	3	0.35	0.70	0.57	27.4	17.0	38.7	4	6	0.29	2.87	1.17	82.2	62.2	21.5	9	11	0.27	0.94	0.65	29.6	13.1	35.0
72	3	3	0.40	0.80	0.56	30.9	32.7	29.1	4	5	0.30	2.17	1.23	55.7	63.5	21.7	8	12	0.19	1.41	0.69	54.5	8.6	35.9
73	4	4	0.81	3.70	1.81	62.0	63.8	23.9	5	7	0.43	3.38	1.30	82.1	59.3	18.3	8	8	0.17	0.94	0.53	45.2	22.0	43.1
80	3	3	0.28	2.74	1.33	78.2	75.6	20.4	5	10	0.49	4.82	1.99	75.5	65.1	16.7	8	8	0.37	1.28	0.80	36.2	6.9	37.1
81	3	3	0.31	0.84	0.61	36.4	44.6	27.3	5	8	0.47	1.44	0.92	33.2	34.1	30.4	7	7	0.40	1.04	0.71	30.4	5.5	38.4
85	3	4	0.58	2.79	1.30	66.6	61.3	27.3	5	11	0.39	2.00	1.05	49.6	59.3	29.5	8	9	0.34	1.38	0.76	45.0	4.7	36.7
90	4	4	0.33	1.33	0.84	45.0	55.8	23.0	5	8	0.28	2.91	1.41	59.5	64.1	28.8	8	8	0.60	1.70	0.96	35.4	26.2	34.7
91	4	5	0.29	1.76	0.85	58.3	49.8	29.8	5	6	0.38	1.30	0.69	46.1	44.3	33.8	8	8	0.32	1.85	0.86	54.8	6.8	32.8
Southern Slope 200–2,000 m																								
8	4	4	0.31	1.04	0.66	44.8	30.0	32.0	3	3	0.79	1.24	0.96	21.1	43.9	31.0	6	7	0.34	1.37	0.66	48.5	39.5	31.9
17	5	5	0.02	1.19	0.49	79.3	18.5	34.9	4	5	0.39	3.97	1.43	91.4	51.3	25.1	6	7	0.14	1.23	0.59	54.2	28.4	32.0
18	1	1	0.52	0.52	0.52		46.2	41.6	2	2	0.35	0.89	0.62	43.5	26.6	36.7	1	1	0.21	0.21	0.21		14.3	51.2
35	4	4	0.29	0.77	0.53	41.7	10.9	39.8	4	4	0.89	1.29	1.07	14.3	52.2	26.7	8	11	0.16	1.06	0.60	41.0	23.6	29.6
36	1	1	0.59	0.59	0.59		44.1	46.8	1	1	1.08	1.08	1.08		66.7	23.9	2	6	0.33	0.66	0.50	20.1	5.6	38.1
46	4	4	0.21	0.71	0.47	38.8	20.4	42.2	5	9	0.22	4.05	1.69	67.2	56.4	23.5	7	7	0.25	1.40	0.67	51.8	22.6	28.7
48	1	1	0.25	0.25	0.25		8.0	52.8	3	3	0.51	2.20	1.25	56.2	62.8	21.8	1	1	0.34	0.34	0.34		8.8	44.3
61	4	4	0.44	0.89	0.57	31.8	14.8	39.2	4	7	0.46	4.59	1.62	85.4	57.1	23.2	7	8	0.18	0.72	0.49	42.3	17.3	34.5
62	1	1	0.39	0.39	0.39		10.3	50.6	1	1	1.00	1.00	1.00		35.0	32.9	1	2	0.24	0.63	0.44	44.8	4.6	46.6
63	1	1	0.32	0.32	0.32		12.5	52.2	1	1	1.06	1.06	1.06		45.3	29.8	1	2	0.30	0.47	0.39	22.1	3.9	43.8
64	4	4	0.25	0.93	0.55	45.3	8.7	37.0	4	5	0.46	3.41	2.18	50.7	68.1	20.1	8	11	0.16	1.00	0.49	44.9	17.6	37.4
GB Central Shoals 35–55 m																								
123	3	3	0.74	2.03	1.53	37.0	67.6	32.6	4	6	0.94	11.91	6.41	60.9	71.6	21.5	8	13	0.58	6.41	2.46	71.8	54.6	27.9
147	3	3	1.55	1.81	1.72	6.9	54.0	35.1	3	5	2.87	11.54	6.27	49.3	72.0	17.6	8	9	0.73	4.86	2.88	44.3	60.2	25.2
148	3	3	1.59	3.23	2.44	27.5	73.6	38.5	3	5	3.27	11.00	6.62	43.8	68.5	21.4	8	20	0.34	5.68	2.33	69.6	54.8	27.2
156																								
GB Northern Shoals 30–40 m																								
124	3	3	1.24	1.37	1.30	4.2	55.8	36.9	4	5	3.11	6.95	4.06	36.0	71.5	24.2	8	9	0.45	7.23	2.70	67.0	59.6	27.1
146	3	3	0.48	1.35	0.85	43.2	39.2	38.8	3	5	1.24	8.29	3.35	82.2	59.2	20.4	8	9	1.01	5.90	3.15	50.8	54.9	21.2
160	3	3	0.64	1.03	0.81	19.9	28.7	38.1	3	3	2.57	10.82	6.62	50.9	79.4	14.6	7	7	1.98	3.87	3.06	23.9	63.8	18.4
GB Western Outer Shoals 50–60 m																								
120	3	3	0.53	1.33	1.03	34.5	49.7	36.1	2	4	0.49	5.20	2.09	90.3	75.7	30.1	8	9	0.33	4.90	2.40	60.9	52.0	26.4
121	3	3	0.90	1.70	1.27	26.1	62.9	33.2	4	8	0.79	6.43	3.16	57.3	59.8	22.0	8	10	0.37	4.81	2.48	52.0	58.7	26.6
GB Eastern Outer Shoals 60–80 m																								
157	2	2	0.69	0.74	0.71	3.5	36.4	50.2	4	6	2.07	9.14	5.63	44.2	78.2	20.7	7	7	0.68	2.98	1.99	39.7	63.9	29.4
158	4	4	0.57	3.62	1.45	87.3	67.9	23.7	2	2	0.68	3.09	1.89	63.9	83.0	16.4	5	5	0.67	4.95	2.41	58.4	60.2	21.8
159	4	4	0.51	0.95	0.67	25.4	28.7	36.8	4	5	1.04	7.03	2.94	75.1	65.0	14.3	7	9	0.79	5.18	2.91	44.6	64.7	19.6
GB Great South Channel 60–100 m																								
92	1	1	0.33	0.33	0.33	15.2	47.6	1	1	0.82	0.82	0.82	42.7	34.4										
111	3	3	0.23	0.46	0.37	27.3	25.0	38.1	5	7	0.23	2.66	1.65	46.9	77.9	24.3	7	9	0.50	4.87	1.96	68.2	44.6	24.6
112	3	3	0.37	0.82	0.60	30.8	36.9	42.4	5	7	0.26	4.40	2.27	61.2	78.2	20.9	7	9	0.52	5.69	2.52	63.5	62.2	21.5
113	3	3	0.63	1.52	1.19	33.5	53.6	32.3	5	7	0.40	4.91	2.67	57.3	79.9	22.0	8	9	0.41	2.52	1.50	39.5	58.0	28.2
122	3	3	0.24	0.77	0.53	41.3	28.8	34.4	3	5	0.39	3.92	1.58	80.2	64.5	22.2	8	9	0.23	2.74	1.20	61.4	50.9	26.4
GB Southern Flank 60–200 m																								
114	4	4	0.63	1.21	0.98	22.3	56.0	28.5	6	8	0.48	8.74	2.02	128.6	55.1	24.6	8	10	0.47	1.50	0.96	42.9	18.4	37.3
117	3	3	0.57	0.91	0.68	23.5	30.7	35.7	5	6	0.44	1.75	0.97	49.5	54.9	33.0	8	9	0.35	1.44	0.88	37.1	10.4	35.8
119	4	4	0.59	1.02	0.75	21.6	32.7	31.2	4	8	0.40	1.36	0.67	43.2	27.8	32.9	8	9	0.16	1.78	0.71	64.1	19.4	33.6
149	4	5	0.35	4.10	1.64	78.0	68.1	26.7	4	8	0.35	3.06	1.57	55.0	60.7	30.0	8	59	0.15	16.60	1.54	144.7	30.3	32.1
150	3	3	0.24	0.85	0.59	43.6	19.2	34.4	3	6	0.37	1.93	0.83	62.7	45.4	29.6	8	10	0.43	1.81	0.80	50.5	20.7	32.7
153	4	4	0.27	0.94	0.58	43.4	25.3	27.4	2	3	0.34	1.09	0.69	44.7	43.0	26.6	6	17	0.53	1.81	1.12	37.4	7.7	33.3
155	5	6	0.45	1.88	1.01	55.0	59.6	28.9	4	6	0.96	3.49	1.98	43.1	71.7	28.0	7	8	0.20	3.11	1.29	63.9	43.4	31.7
GB Northeast Peak 80–200 m																								
177	4	4	0.44	1.17	0.71	38.3	38.8	34.1	3	3	0.51	3.50	2.07	59.1	79.1	17.2	6	6	0.68	2.08	1.40	38.0	64.6	30.0
178	4	4	0.42	0.99	0.60	37.5	35.3	33.2	2	2	0.36	2.11	1.24	70.9	59.5	17.9	6	6	0.52	2.38	0.97	66.1	40.0	32.1
179	4	4	0.37	0.63	0.48	19.8	19.4	36.1	3	4	0.42	1.48	0.84	50.1	40.3	23.7	6	6	0.38	1.81	0.97	52.9	21.5	30.6
191	1	1	0.44	0.44	0.44		4.6	35.3	1	1	1.15	1.15	1.15		66.1	24.3	2	2	0.55	1.34	0.94	41.8	20.6	36.8
192	1	1	0.66	0.66	0.66		3.0	35.3	1	1	3.70	3.70	3.70		84.9	8.6	2	2	0.91	1.23	1.07	15.0	17.3	35.2
Northern Slope 200–2,000 m																								
82	3	3	0.28	1.01	0.68	44.5	41.9	25.4	4	10	0.24	1.82	0.74	58.6	35.2	28.2	8	8	0.15	0.86	0.60	35.8	5.6	40.0
83									3	4	0.16	1.18	0.51	78.8	14.7	39.3	1	1	0.55	0.55	0.55		7.3	45.5
84									1	1	0.36	0.36	0.36		11.1	46.3	2	3	0.38	1.98	1.31	51.8	12.9	29.9
115	2	2	0.38	0.72	0.55	30.9	37.3	28.6	3	6	0.41	1.33	0.83	39.6	23.8	30.2	7	8	0.34	1.70	0.91	56.4	3.2	33.2
116									1	1	0.24	0.24	0.24		8.3	52.0								
118	3	3	0.28	0.47	0.40	21.0	19.3	31.2	3	6	0.15	1.19	0.54	58.6	25.8	35.6	8	10	0.25	4.13	1.08	99.9	5.4	29.9
151	2	2	0.52	0.53	0.53	1.0	6.7	36.4	3	7	0.34	1.03	0.74	38.6	20.9	30.3	8	9	0.35	1.75	0.77	60.0	10.8	35.2
152																	1	1	0.40	0.40	0.40		2.5	49.4
154	5	5	0.32	0.78	0.50	31.6	12.9	34.4	4	7	0.31	1.05	0.58	40.4	30.9	32.6	8	10	0.26	1.64	0.76	54.9	9.7	33.9
180									1	2	0.62	0.74	0.68	8.8	10.3	33.3								
193	1	1	0.42	0.42	0.42		7.1	40.8	1	1	0.76	0.76	0.76		6.6	39.7	1	1	1.13	1.13	1.13		34.5	36.5
GB Nantucket Shoals 37 m																								
93	4	4	0.96	6.32	2.90	70.9	78.3	20.8	5	6	1.22	15.13	5.67	82.6	80.6	17.6	8	8	0.49	8.17	2.05	119.0	50.3	26.7
GOM Western 60–100 m																								
94	5	6	0.29	0.92	0.55	37.7	38.6	29.4	5	7	0.23	5.43	2.58	65.5	65.2	22.7	8	8	0.18	1.22	0.83	42.5	16.1	34.7
95	5	6	0.45	3.26	1.58	71.8	75.7	17.3	5	6	0.81	2.08	1.22	37.0	68.1	25.2	8	8	0.39	1.48	0.70	45.8	21.5	43.4
97	6	7	0.85	4.23	2.69	44.4	76.9	19.7	4	4	1.08	2.79	1.63	41.4	65.1	23.1	6	7	0.25	1.94	0.90	61.0	22.6	36.2
98	5	6	0.50	4.03	1.90	74.5	67.7	15.2	3	3	0.70	4.67	2.09	87.6	24.9	22.9	6	8	0.18	2.18	1.02	67.0	14.8	37.4
99	5	6	0.51	1.42	0.86	35.1	57.6	24.5	2	2	0.48	0.67	0.57	16.5	36.5	32.7	5	5	0.34	2.11	0.83	79.8	9.0	39.5
188	6	6	0.38	2.86	1.27	66.3	68.4	20.1	1	1	2.39	2.39	2.39		83.7	22.1	5	7	0.20	1.15	0.53	52.5	7.6	38.6

continued on next page

Table C3 (continued)

Tile	July–August Y[1] #	P[2] #	Min. Chl *a* µg l^{-1}	Max. Chl *a* µg l^{-1}	Mean Chl *a* µg l^{-1}	C.V.[3] Chl *a* %	Net.[4] %	Pha.[5] %	September–October Y #	P #	Min. Chl *a* µg l^{-1}	Max. Chl *a* µg l^{-1}	Mean Chl *a* µg l^{-1}	C.V. Chl *a* %	Net. %	Pha. %	November–December Y #	P #	Min. Chl *a* µg l^{-1}	Max. Chl *a* µg l^{-1}	Mean Chl *a* µg l^{-1}	C.V. Chl *a* %	Net. %	Pha. %
MAB Northern Outer Shelf 60–200 m																								
65	4	6	0.29	0.71	0.51	31.8	24.2	37.0	4	5	0.28	1.04	0.62	49.0	21.8	35.9	6	7	0.60	2.31	1.38	39.6	54.7	23.8
70	5	7	0.21	0.92	0.60	45.2	19.0	33.3	4	7	0.33	0.89	0.49	37.3	25.3	37.1	7	8	0.49	2.90	1.32	50.2	67.1	22.9
71	7	9	0.17	0.79	0.41	41.9	8.3	35.8	4	7	0.19	1.02	0.56	49.0	35.4	33.5	6	8	0.34	2.23	1.07	52.0	53.8	27.6
72	4	7	0.28	0.56	0.42	20.2	11.9	36.4	4	5	0.32	1.12	0.57	50.9	28.0	39.9	6	6	0.34	3.54	1.38	77.1	64.4	22.4
73	4	8	0.41	1.22	0.69	38.7	19.8	32.9	5	7	0.28	1.14	0.63	51.1	18.0	39.5	6	8	0.56	2.95	1.31	51.4	56.2	25.6
80	4	7	0.36	1.04	0.53	45.5	22.3	36.8	5	5	0.41	2.75	1.00	88.1	32.6	31.5	9	11	0.38	2.45	1.06	58.1	56.8	26.4
81	5	7	0.29	0.80	0.51	40.3	11.5	33.7	5	9	0.25	1.01	0.49	42.4	14.3	33.8	9	13	0.30	1.42	0.84	38.7	41.9	28.2
85	4	14	0.20	1.26	0.45	65.2	19.6	34.8	6	12	0.24	1.36	0.79	41.9	36.4	30.7	9	12	0.22	1.51	0.69	57.8	47.8	28.9
90	4	6	0.20	1.92	0.82	67.1	31.7	31.5	6	8	0.33	2.93	1.02	82.4	47.7	31.5	9	10	0.35	2.00	1.16	50.4	54.5	25.7
91	3	5	0.22	0.61	0.38	46.7	20.4	34.4	6	7	0.31	3.44	1.01	100.8	41.4	29.4	8	8	0.27	1.94	0.75	71.4	48.8	31.1
Southern Slope 200–2,000 m																								
8	4	4	0.32	0.72	0.59	27.0	22.3	35.0	2	2	0.34	0.94	0.64	46.9	36.7	33.3	4	4	0.82	1.02	0.90	8.2	24.9	33.7
17	4	4	0.28	0.56	0.42	28.0	12.5	37.3	2	2	0.35	0.39	0.37	5.4	9.5	43.1	4	4	0.75	1.29	0.93	23.1	23.5	32.2
18	1	1	0.34	0.34	0.34		5.9	59.5	1	1	0.75	0.75	0.75		16.0	49.3								
35	5	7	0.14	0.87	0.46	52.9	10.3	35.2	4	5	0.22	1.40	0.62	65.7	31.9	31.9	6	8	0.21	1.96	0.86	54.5	30.6	31.7
36	1	1	0.38	0.38	0.38		21.1	41.5																
46	4	6	0.23	1.13	0.54	53.2	25.9	32.7	4	5	0.32	0.80	0.51	35.4	21.6	39.3	5	5	0.31	0.77	0.54	33.6	17.7	34.8
48	3	3	0.34	0.44	0.40	10.8	15.0	42.9	2	3	0.28	0.56	0.45	27.1	14.1	36.6								
61	4	7	0.12	0.86	0.40	60.0	7.5	37.4	3	7	0.17	0.59	0.35	47.6	11.8	37.4	5	6	0.38	0.88	0.60	25.9	17.9	32.7
62	1	1	0.19	0.19	0.19		5.3	53.7	1	1	0.42	0.42	0.42		19.1	40.8								
63	2	2	0.12	0.34	0.23	47.8	4.4	43.9	1	1	0.42	0.42	0.42		14.3	41.7								
64	5	6	0.25	0.54	0.41	28.2	5.3	38.8	4	4	0.42	0.57	0.47	12.7	10.6	45.3	6	6	0.31	2.16	0.99	61.2	37.8	24.5
GB Central Shoals 35–55 m																								
123	4	7	0.91	1.73	1.39	22.2	45.2	29.4	4	6	1.71	3.40	2.61	26.9	65.6	24.1	9	10	1.20	9.88	3.46	68.0	77.0	21.7
147	7	11	0.74	3.08	1.84	48.8	36.6	28.1	4	9	1.05	5.54	3.04	42.6	61.5	24.5	9	11	0.78	5.27	3.00	44.5	64.7	27.3
148	4	5	0.63	2.82	1.74	47.1	51.2	26.6	4	5	1.81	4.54	3.16	31.3	55.6	25.0	9	9	1.53	5.88	3.88	35.9	70.1	24.2
156	2	2	0.77	2.11	1.44	46.5	30.9	37.9	1	2	0.83	1.31	1.07	22.4	50.5	31.8	2	2	1.00	2.01	1.50	33.6	70.8	25.3
GB Northern Shoals 30–40 m																								
124	4	5	0.82	2.49	1.44	48.2	48.1	29.8	4	6	1.53	3.85	2.84	31.2	62.6	22.0	9	9	0.59	5.26	2.18	61.5	58.6	24.6
146	3	4	0.78	2.26	1.55	44.6	49.4	30.2	4	4	1.94	3.33	2.71	21.4	59.4	23.9	9	9	0.99	3.39	1.83	42.7	57.7	29.0
160	2	3	1.77	2.42	2.05	13.2	39.3	28.5	3	3	2.40	3.85	2.95	21.8	64.9	20.1	8	8	0.53	2.20	1.34	47.6	50.2	27.2
GB Western Outer Shoals 50–60 m																								
120	3	4	0.49	1.22	0.92	29.0	49.3	34.3	5	6	0.60	2.19	1.51	41.9	52.3	28.1	7	8	0.75	3.34	1.98	42.0	65.8	29.8
121	4	5	0.23	2.57	1.21	65.6	47.1	25.3	4	4	1.25	2.75	1.80	31.5	61.5	23.7	8	9	0.50	3.72	1.70	51.2	66.2	27.7
GB Eastern Outer Shoals 60–80 m																								
157	3	3	0.85	2.56	1.43	55.9	53.2	27.4	3	3	0.65	2.08	1.41	41.6	60.3	23.0	8	10	0.69	4.78	1.70	66.5	72.9	28.3
158	3	3	1.08	1.50	1.25	14.4	42.1	30.2	3	3	1.24	1.33	1.29	2.9	54.0	27.9	7	7	0.17	1.80	0.77	63.3	54.9	32.5
159	5	8	1.07	2.73	1.80	33.2	38.6	26.0	3	5	1.19	2.15	1.73	18.1	50.3	26.4	7	12	0.39	1.60	0.82	46.8	45.9	29.8
GB Great South Channel 60–100 m																								
92	2	3	0.48	0.94	0.77	26.6	30.4	28.8	1	1	1.06	1.06	1.06	20.8	44.2									
111	3	5	0.49	2.35	1.27	53.5	30.0	29.9	5	9	0.54	1.55	0.93	37.6	29.1	32.2	8	9	0.46	2.46	1.03	53.8	40.4	30.3
112	4	6	0.55	1.73	1.08	42.1	49.5	27.1	4	8	0.53	1.85	1.09	38.9	37.1	31.9	8	8	0.47	1.69	1.01	39.6	45.1	31.8
113	3	5	0.47	0.73	0.60	13.9	44.2	32.7	6	9	0.41	2.16	1.09	54.9	42.7	30.1	9	9	0.51	2.87	1.27	60.4	52.8	27.9
122	4	6	0.24	1.58	0.92	49.6	38.3	33.3	4	4	0.50	2.05	1.11	51.4	58.4	27.9	8	9	0.24	1.34	0.88	37.4	45.2	31.8
GB Southern Flank 60–200 m																								
114	5	11	0.31	1.69	0.70	59.9	33.1	30.5	6	12	0.25	2.87	1.00	81.2	37.9	28.1	8	8	0.29	2.01	0.80	65.0	51.8	29.2
117	4	7	0.27	0.63	0.42	29.0	29.7	36.2	5	7	0.27	1.20	0.66	52.9	30.7	34.8	8	9	0.52	2.27	1.10	54.8	52.9	31.3
119	6	11	0.25	1.21	0.58	49.2	24.6	33.1	6	13	0.22	1.60	0.64	51.0	28.1	32.8	8	9	0.45	0.77	0.62	18.3	39.1	32.6
149	5	10	0.55	2.56	1.29	41.0	43.4	25.8	6	10	0.37	2.13	0.95	49.8	34.7	30.6	9	11	0.78	3.27	1.77	50.1	69.3	28.1
150	5	10	0.14	1.28	0.58	57.1	35.2	30.1	5	13	0.33	1.96	0.86	43.7	21.4	31.8	9	10	0.17	0.92	0.61	33.3	42.9	34.4
153	3	4	0.34	1.15	0.61	51.5	44.5	31.4	4	4	0.42	1.62	0.85	56.2	47.8	32.1	8	8	0.25	1.14	0.60	39.9	39.8	32.5
155	2	2	0.72	0.90	0.81	11.1	27.8	33.6	5	5	0.40	2.27	1.06	60.3	57.3	29.8	7	8	0.22	1.36	0.76	44.5	56.1	35.0
GB Northeast Peak 80–200 m																								
177	2	2	0.08	0.75	0.41	80.7	36.1	38.5	3	3	0.72	1.10	0.88	18.5	43.0	38.1	8	8	0.36	1.05	0.66	38.1	38.6	34.0
178	1	1	0.16	0.16	0.16		31.3	50.0	3	3	0.57	0.87	0.77	18.4	35.5	37.9	8	8	0.13	0.86	0.49	41.3	34.7	32.7
179	1	1	0.30	0.30	0.30		6.7	46.4	3	3	0.36	0.58	0.47	19.0	27.5	36.3	7	7	0.30	0.69	0.44	29.8	17.1	38.7
191	2	3	0.40	0.78	0.55	29.6	10.2	34.4	3	4	0.25	0.73	0.51	35.8	25.0	31.1	2	2	0.30	0.69	0.50	39.4	13.1	31.7
192	1	1	0.57	0.57	0.57		3.5	44.7	1	1	0.72	0.72	0.72		1.4	32.7	2	2	0.54	0.66	0.60	10.0	5.8	38.8
Northern Slope 200–2,000 m																								
82	3	5	0.18	0.49	0.32	38.2	8.1	39.6	6	7	0.28	0.61	0.46	27.4	14.9	40.3	8	9	0.27	1.47	0.75	54.4	41.1	28.5
83	3	7	0.17	0.39	0.28	23.3	9.6	41.4	4	5	0.29	0.68	0.46	28.7	13.8	36.8	4	6	0.33	0.62	0.46	25.0	36.6	35.5
84	1	2	0.19	0.38	0.28	33.3	17.5	47.7	2	2	0.36	0.43	0.40	8.9	20.3	43.2	1	1	0.29	0.29	0.29		10.3	42.0
115	3	6	0.11	0.45	0.36	32.8	7.9	40.2	6	12	0.13	0.69	0.41	42.4	9.4	38.0	8	10	0.19	1.12	0.68	43.2	26.4	32.0
116	3	3	0.28	0.43	0.36	17.2	17.8	40.2	3	7	0.22	0.56	0.39	27.6	4.8	42.8	2	3	0.10	0.31	0.22	40.1	6.0	46.0
118	4	8	0.16	0.53	0.38	30.0	27.6	33.6	6	10	0.06	0.66	0.35	52.9	12.8	38.4	8	9	0.38	1.17	0.68	36.3	40.7	32.7
151	3	15	0.10	1.01	0.42	54.3	6.0	31.1	6	10	0.16	1.47	0.52	65.7	25.6	35.8	9	11	0.22	0.69	0.48	34.9	19.3	35.9
152	3	7	0.14	0.82	0.35	59.4	3.7	30.2	3	4	0.21	0.75	0.41	49.7	19.9	36.6								
154	4	25	0.09	0.70	0.45	33.0	3.1	32.8	4	6	0.25	0.62	0.48	25.5	18.2	35.3	8	9	0.32	0.74	0.56	20.7	30.4	34.8
180	1	1	0.04	0.04	0.04		25.0	55.6	1	2	0.28	0.40	0.34	17.6	5.9	42.4								
193									2	3	0.42	0.52	0.46	9.4	8.7	37.0	2	2	0.49	1.08	0.79	37.6	7.6	34.9
GB Nantucket Shoals 37 m																								
93	3	6	0.35	1.90	1.19	45.2	35.1	29.6	6	8	0.75	3.49	2.06	48.0	35.5	30.7	6	6	0.51	3.79	2.22	49.8	37.4	27.7
GOM Western 60–100 m																								
94	3	3	0.36	0.86	0.63	32.8	11.2	35.8	5	5	0.14	2.59	1.09	74.6	9.7	33.9	7	8	0.49	1.80	1.03	44.7	27.3	31.3
95	4	4	0.29	1.21	0.72	52.5	33.3	37.4	5	8	0.29	2.60	1.29	58.7	17.2	26.3	6	8	0.02	1.65	0.89	54.7	45.3	25.9
97	4	5	0.64	1.47	0.87	35.6	23.4	39.1	4	6	1.04	2.70	1.50	38.4	19.6	21.9	7	9	0.01	3.46	2.03	51.2	60.3	21.3
98	4	6	0.29	2.17	0.98	59.5	10.8	39.8	4	6	0.33	3.88	1.48	80.6	15.1	24.9	7	8	0.02	2.21	1.10	61.1	50.2	25.7
99	4	5	0.32	3.46	1.24	94.3	20.8	35.1	4	6	0.29	3.26	1.24	84.3	10.8	28.3	7	8	0.31	3.45	1.42	65.8	39.2	24.8
188	1	1	0.65	0.65	0.65		3.1	35.0	3	4	0.29	1.85	0.94	60.3	19.4	29.8	5	5	0.62	1.47	0.86	36.8	49.8	26.0

continued on next page

Table C3 (continued)

	January–February							March–April							May–June						
Tile	Y[1] #	P[2] #	Min. Chl *a* µg l^{-1}	Max. Chl *a* µg l^{-1}	Mean Chl *a* µg l^{-1}	C.V.[3] Chl *a* %	Net.[4] %	Pha.[5] %	Y #	P #	Min. Chl *a* µg l^{-1}	Max. Chl *a* µg l^{-1}	Mean Chl *a* µg l^{-1}	C.V. Chl *a* %	Net. %	Pha. %	Y #	P #	Min. Chl *a* µg l^{-1}	Max. Chl *a* µg l^{-1}	Mean Chl *a* µg l^{-1}	C.V. Chl *a* %	Net. %	Pha. %
GOM Northern 80–200 m																								
101	5	5	0.40	4.19	1.47	97.1	75.0	13.6	1	1	0.23	0.23	0.23		17.4	53.1	6	6	0.40	1.43	0.79	46.2	10.8	34.8
102	5	5	0.51	3.25	1.30	79.7	75.9	17.2	1	1	0.54	0.54	0.54		42.6	36.5	5	5	0.26	4.05	1.45	92.1	66.3	35.2
103	3	3	0.53	3.62	1.84	71.1	85.5	13.2	1	1	0.24	0.24	0.24		33.3	38.5	5	6	0.52	3.87	1.39	82.5	25.0	26.8
104	5	5	0.37	2.47	1.12	76.4	72.6	18.3									6	7	0.21	2.95	1.65	51.6	64.3	34.2
183	5	6	0.21	3.14	0.93	109.2	66.8	18.4									5	6	0.58	1.53	1.01	34.5	42.2	33.9
105	4	5	0.16	1.30	0.57	71.6	46.5	23.0	1	1	0.28	0.28	0.28		21.4	49.1	7	8	0.29	0.98	0.63	38.1	15.0	32.9
131	4	4	0.40	0.68	0.55	23.3	18.6	31.1	1	1	0.18	0.18	0.18		16.7	51.4	6	7	0.30	1.25	0.74	43.7	18.8	30.2
135	4	4	0.21	0.57	0.41	31.5	16.5	30.5	1	1	0.34	0.34	0.34		41.2	41.4	7	8	0.18	4.14	1.60	85.2	57.7	28.3
136	5	5	0.20	1.14	0.54	61.6	41.6	24.0	1	1	0.24	0.24	0.24		33.3	45.5	5	6	0.48	2.02	1.24	43.3	46.8	30.8
137	4	4	0.34	0.53	0.41	17.9	26.1	30.4									6	7	0.50	4.45	1.91	68.7	58.6	28.0
138	3	3	0.41	4.16	1.69	103.0	81.1	15.5									6	7	0.12	5.88	2.26	95.0	75.7	23.6
GOM Wilkinson Basin 100–250 m																								
96	5	5	0.40	2.85	0.94	101.7	60.4	21.7	4	5	0.28	6.16	1.83	119.1	71.8	20.7	7	8	0.26	0.92	0.65	34.1	5.6	33.7
100	5	6	0.42	1.15	0.70	45.5	51.9	24.0	1	1	0.26	0.26	0.26		15.4	49.0	6	6	0.24	1.23	0.66	56.3	10.1	33.9
106	4	4	0.29	1.17	0.66	51.1	45.4	25.1	1	1	0.22	0.22	0.22		9.1	51.1	7	9	0.23	2.28	0.87	66.4	26.6	30.4
107	3	3	0.46	1.26	0.74	50.3	40.7	24.6	4	5	0.23	1.01	0.74	39.8	47.8	28.8	7	8	0.19	1.12	0.66	44.3	18.8	30.6
108	3	3	0.45	1.17	0.70	47.5	35.2	27.1	4	5	0.19	1.28	0.70	52.8	38.3	29.3	8	9	0.34	1.12	0.76	38.4	21.2	31.4
109	4	4	0.33	1.17	0.61	54.2	32.9	33.0	4	6	0.21	1.36	0.79	42.4	49.7	28.1	7	8	0.14	5.00	1.45	96.2	29.6	24.1
110	2	2	0.30	0.39	0.34	13.0	10.1	36.7	5	6	0.18	3.55	1.46	74.6	66.3	21.5	8	9	0.18	2.14	1.07	52.0	12.2	31.9
125	3	3	0.21	0.48	0.38	32.0	11.3	38.5	6	9	0.25	2.22	1.04	63.7	48.1	25.7	8	9	0.15	1.79	0.84	59.1	17.8	31.8
126	4	4	0.46	1.15	0.66	43.4	35.4	29.9	4	7	0.16	1.22	0.67	52.0	33.1	28.6	6	7	0.38	5.01	1.37	111.5	48.9	26.0
127	3	3	0.46	1.00	0.65	38.7	23.7	27.9	4	5	0.18	1.15	0.65	48.1	39.1	30.9	8	9	0.23	2.49	1.21	63.6	22.1	26.7
128	2	2	0.51	0.85	0.68	25.0	39.0	26.9	4	5	0.13	0.88	0.62	45.8	37.9	29.6	5	6	0.58	4.34	1.65	86.5	36.4	25.4
129	3	3	0.36	1.64	0.81	73.1	52.9	23.7	4	5	0.22	0.84	0.58	35.9	31.9	31.9	7	8	0.22	2.06	0.90	59.6	23.5	30.8
GOM Georges Basin 150–250 m																								
130	4	4	0.45	0.62	0.52	12.4	28.2	29.6	1	1	0.26	0.26	0.26		19.2	50.0	6	7	0.17	2.09	0.84	66.6	32.5	28.8
143	5	5	0.19	0.49	0.35	33.4	14.4	36.5									7	8	0.37	1.41	0.85	41.2	10.2	33.1
144	5	5	0.24	1.10	0.55	52.9	26.6	31.3									7	8	0.36	1.78	0.82	54.8	10.5	31.1
145	4	5	0.30	1.43	0.64	63.7	45.0	25.7	2	3	0.50	0.87	0.67	22.8	19.4	29.5	8	9	0.36	1.42	0.78	41.5	22.6	31.5
161	3	3	0.40	0.49	0.46	8.8	5.8	35.4	4	4	1.06	4.69	2.86	47.5	54.4	18.8	7	7	0.70	2.24	1.07	49.2	11.2	26.1
162	2	2	0.53	0.53	0.53	0.0	5.7	32.9	1	1	0.45	0.45	0.45		57.8	32.8	4	4	0.85	1.43	1.07	22.0	15.4	28.1
163	3	3	0.32	0.62	0.42	32.9	5.5	34.2	1	1	0.66	0.66	0.66		63.6	27.5	5	5	0.47	1.49	1.00	39.7	2.4	30.1
174	4	4	0.27	0.41	0.35	14.8	12.1	35.0	1	1	0.43	0.43	0.43		44.2	34.8	6	7	0.69	2.03	1.09	38.8	5.1	28.7
175	5	5	0.24	1.02	0.51	52.2	26.1	32.7	2	2	0.44	1.11	0.78	43.2	45.8	29.2	6	7	0.50	0.86	0.64	18.6	6.5	32.0
176	4	4	0.48	0.88	0.60	26.8	22.4	32.5	3	3	0.57	1.50	1.07	35.8	54.5	20.7	5	5	0.52	2.95	1.29	69.0	44.2	20.9
GOM Jordan Basin 150–250 m																								
132	4	4	0.39	0.58	0.50	15.2	16.7	33.6	1	1	0.17	0.17	0.17		11.8	57.5	7	8	0.21	2.09	0.95	61.3	22.0	32.6
133	3	3	0.45	0.57	0.49	11.0	13.5	32.7	1	1	0.19	0.19	0.19		15.8	48.6	3	4	0.45	1.23	0.83	43.1	25.2	38.0
134	3	3	0.20	0.47	0.36	32.3	9.2	33.1	1	1	0.27	0.27	0.27		22.2	40.0	7	9	0.31	5.04	1.37	100.5	47.5	29.3
142	5	6	0.37	0.64	0.45	20.2	17.0	30.7									7	8	0.32	1.36	0.86	42.7	26.0	35.4
167	3	3	0.19	0.51	0.38	36.1	11.4	33.3	1	1	0.63	0.63	0.63		36.5	30.0	4	4	0.65	2.26	1.31	45.3	35.6	28.4
182	4	4	0.24	0.50	0.41	24.9	15.2	33.7									6	7	0.26	1.43	0.80	49.2	25.7	29.3
GOM Scotian Shelf 60–200 m																								
139																	1	1	0.50	0.50	0.50		8.0	39.8
140	4	4	0.14	0.43	0.26	46.8	25.7	34.7									6	7	0.30	2.06	1.21	52.1	38.1	26.7
141	4	4	0.13	0.40	0.30	34.2	25.2	46.6									6	6	0.22	0.97	0.60	38.0	39.7	34.8
164	3	3	0.18	0.47	0.36	35.6	6.5	40.0	1	1	0.45	0.45	0.45		44.4	31.8	5	5	0.38	2.55	1.26	60.2	28.3	25.9
165	3	3	0.16	0.48	0.34	39.3	8.8	39.3									4	4	0.50	3.11	1.35	77.1	44.7	25.4
166	2	2	0.39	0.47	0.43	9.3	12.8	34.8	1	1	0.49	0.49	0.49		49.0	35.5	5	5	0.47	1.98	1.17	44.7	15.3	25.1
168	3	3	0.33	0.45	0.41	13.8	9.8	37.9									4	4	1.35	1.73	1.55	8.8	19.4	26.2
169	2	2	0.32	0.41	0.36	12.3	13.7	37.6									3	3	0.44	2.49	1.52	55.3	27.9	24.8
170	2	2	0.28	0.38	0.33	15.2	19.7	38.9									3	3	0.35	1.70	1.00	55.2	32.0	31.5
181	4	5	0.18	0.85	0.52	49.9	49.4	48.4	1	1	3.16	3.16	3.16		93.4	19.0	4	4	1.18	1.97	1.41	23.0	40.7	30.5
171	4	4	0.20	0.49	0.36	29.6	22.9	40.0									5	5	0.43	4.19	1.56	88.8	47.0	32.2
190	2	2	0.26	0.44	0.35	25.7	8.6	43.5	1	1	0.55	0.55	0.55		63.6	32.9	2	2	0.34	2.41	1.38	75.3	73.8	27.8
172	4	4	0.28	0.52	0.38	24.8	11.1	37.5	1	1	0.29	0.29	0.29		55.2	34.1	5	7	0.39	3.76	1.36	78.6	32.1	23.2
189	2	2	0.28	0.39	0.34	16.4	6.0	40.7									3	3	1.04	1.67	1.38	18.8	26.1	23.8
173	4	4	0.19	0.47	0.35	32.1	15.7	36.4	1	1	0.32	0.32	0.32		46.9	37.3	4	5	0.42	1.05	0.71	36.1	7.6	32.3

continued on next page

Table C3 (continued)

Tile	July–August Y[1] #	P[2] #	Min. Chl *a* µg l^{-1}	Max. Chl *a* µg l^{-1}	Mean Chl *a* µg l^{-1}	C.V.[3] Chl *a* %	Net.[4] %	Pha.[5] %	September–October Y #	P #	Min. Chl *a* µg l^{-1}	Max. Chl *a* µg l^{-1}	Mean Chl *a* µg l^{-1}	C.V. Chl *a* %	Net. %	Pha. %	November–December Y #	P #	Min. Chl *a* µg l^{-1}	Max. Chl *a* µg l^{-1}	Mean Chl *a* µg l^{-1}	C.V. Chl *a* %	Net. %	Pha. %
GOM Northern 80–200 m																								
101	4	4	0.20	0.62	0.35	46.6	10.1	43.7	4	7	0.38	1.83	0.83	58.6	39.5	29.6	7	8	0.21	1.14	0.58	55.1	38.6	30.0
102	3	3	0.21	0.36	0.28	22.0	31.0	54.1	4	7	0.37	2.77	1.40	62.7	20.9	26.3	7	8	0.39	1.30	0.80	36.0	47.1	28.6
103	3	3	0.21	0.69	0.46	42.5	36.0	44.4	4	5	0.74	2.36	1.42	51.2	28.8	26.1	6	6	0.29	0.82	0.52	33.5	19.9	35.0
104	2	2	0.28	0.35	0.32	11.1	34.9	50.4	2	2	1.00	2.27	1.64	38.8	41.3	26.8	6	6	0.16	0.67	0.47	37.2	21.8	38.7
183	3	4	0.34	0.59	0.45	20.7	28.9	39.2	3	4	0.57	3.46	1.66	69.8	60.1	23.9	4	4	0.27	0.62	0.48	27.1	28.4	33.1
105	4	4	0.34	0.97	0.65	34.6	16.2	34.3	3	4	0.47	1.55	0.93	49.7	38.3	28.0	5	6	0.21	0.70	0.46	32.8	25.5	38.5
131	3	5	0.19	0.91	0.42	61.4	32.7	33.2	3	3	0.49	2.78	1.47	65.3	50.5	23.8	5	6	0.32	0.86	0.47	38.6	18.7	39.6
135	3	4	0.31	0.55	0.44	19.4	27.1	42.7	2	2	1.19	1.29	1.24	4.0	55.2	23.0	6	7	0.25	0.73	0.44	34.1	23.6	35.2
136	3	4	0.34	0.70	0.51	32.5	24.0	38.6	3	3	0.50	3.13	1.82	59.0	51.5	18.4	4	4	0.00	0.55	0.34	60.0	31.9	31.7
137	3	3	0.31	0.62	0.51	28.0	44.2	52.6	2	3	0.39	2.92	1.46	73.2	52.7	23.6	7	9	0.21	0.77	0.45	39.6	28.3	34.9
138	3	3	0.91	1.73	1.25	27.9	68.8	29.8	2	2	1.16	1.97	1.56	25.9	56.6	22.3	7	7	0.34	0.68	0.50	26.0	37.4	35.2
GOM Wilkinson Basin 100–250 m																								
96	3	3	0.30	0.60	0.40	34.5	23.1	37.3	4	6	0.18	2.21	0.76	91.8	16.2	33.3	6	6	0.29	1.54	0.72	56.7	34.8	32.1
100	3	3	0.23	1.14	0.59	67.0	27.1	37.2	4	6	0.34	1.19	0.80	39.7	30.8	31.1	6	6	0.00	0.91	0.51	65.0	22.8	34.0
106	5	7	0.18	0.97	0.63	44.4	5.9	41.1	3	6	0.23	1.67	0.80	63.6	37.7	27.4	5	5	0.38	0.63	0.51	18.2	18.8	36.3
107	4	5	0.16	1.02	0.43	75.0	4.7	34.8	3	5	0.26	1.03	0.53	51.6	4.5	36.8	6	7	0.03	1.74	0.75	69.2	26.6	31.3
108	4	7	0.06	0.77	0.51	43.4	5.6	34.6	3	9	0.24	0.86	0.53	32.2	18.1	31.9	7	9	0.37	1.16	0.65	43.3	44.9	30.2
109	3	4	0.12	0.64	0.35	53.2	4.2	38.3	4	7	0.35	0.83	0.52	28.5	14.4	39.0	5	8	0.23	1.51	0.68	58.7	28.8	34.6
110	3	4	0.33	0.50	0.44	15.3	14.7	36.1	4	6	0.40	0.89	0.64	28.4	19.4	33.5	9	10	0.42	1.90	0.88	48.7	28.2	29.0
125	6	9	0.65	2.99	1.21	57.1	38.3	27.5	4	4	0.83	1.55	1.16	22.2	26.3	29.7	9	10	0.57	1.53	0.96	30.6	39.9	28.8
126	4	5	0.15	0.86	0.48	65.8	8.8	37.0	4	6	0.13	0.85	0.57	41.4	11.4	36.0	6	6	0.48	1.34	0.84	35.5	33.5	28.3
127	3	4	0.20	0.47	0.34	30.8	7.3	43.0	2	2	0.46	0.68	0.57	19.3	9.7	40.0	4	5	0.45	0.79	0.60	21.5	23.0	33.3
128	3	5	0.14	0.72	0.35	56.9	6.8	39.4	3	3	0.43	0.78	0.61	23.5	8.2	39.6	3	3	0.36	0.91	0.62	36.7	30.8	28.0
129	3	6	0.18	1.24	0.61	52.6	5.2	34.2	3	6	0.53	1.12	0.78	27.7	10.9	29.6	6	7	0.40	0.86	0.64	24.7	24.8	30.4
GOM Georges Basin 150–250 m																								
130	2	3	0.19	0.68	0.43	47.0	39.8	38.7	2	2	0.76	1.46	1.11	31.5	31.1	27.9	5	5	0.01	0.86	0.45	63.9	30.4	34.9
143	3	3	0.22	0.45	0.35	27.6	10.4	38.4	3	4	0.27	1.18	0.76	42.9	17.6	30.4	5	5	0.18	0.84	0.50	57.0	28.8	35.1
144	3	4	0.18	0.78	0.39	61.7	19.4	36.2	3	4	0.44	1.21	0.82	33.8	6.4	33.8	6	7	0.27	0.88	0.47	42.2	22.6	37.1
145	4	6	0.08	1.02	0.56	62.9	18.3	33.2	3	12	0.24	1.26	0.66	52.2	14.3	32.0	7	10	0.24	0.68	0.55	23.4	20.0	35.5
161	2	3	0.83	1.30	1.01	20.3	3.3	35.6	3	3	0.73	1.48	1.14	27.2	18.7	29.6	7	7	0.16	0.69	0.44	41.5	25.6	32.5
162	1	1	0.62	0.62	0.62		29.0	31.9	2	2	0.28	0.91	0.59	52.9	39.5	31.2	3	3	0.00	0.92	0.42	90.4	45.2	23.6
163	1	1	0.73	0.73	0.73		12.3	38.1	2	2	0.79	1.00	0.90	11.7	15.1	32.5	4	5	0.00	0.67	0.39	62.3	13.9	37.2
174	2	2	0.44	0.62	0.53	17.0	1.9	36.9	3	3	0.32	0.61	0.47	25.4	12.1	33.0	6	7	0.08	1.41	0.58	71.4	17.9	30.0
175	3	3	0.13	0.80	0.52	54.7	2.6	38.1	2	2	0.65	0.78	0.71	9.1	4.2	29.6	6	7	0.38	0.88	0.51	32.8	15.6	34.5
176	1	1	0.04	0.04	0.04		25.0	50.0	3	3	0.35	2.28	1.09	78.4	6.1	36.3	8	8	0.29	0.66	0.44	25.9	15.2	40.8
GOM Jordan Basin 150–250 m																								
132	3	4	0.20	0.65	0.40	42.5	16.4	45.3	3	4	0.43	0.89	0.59	30.8	22.6	34.5	5	6	0.35	1.19	0.61	54.0	35.6	32.1
133	3	3	0.22	0.47	0.31	36.6	17.2	43.6	3	6	0.44	1.86	0.86	56.8	28.0	31.7	4	5	0.28	1.16	0.58	52.4	43.5	31.8
134	3	4	0.19	0.34	0.28	20.2	13.2	46.7	2	2	0.45	2.10	1.27	64.7	55.3	24.8	5	6	0.00	0.99	0.46	65.8	32.4	32.4
142	3	4	0.19	0.75	0.38	59.6	8.7	40.9	2	2	1.31	2.37	1.84	28.8	52.5	22.4	6	7	0.00	0.70	0.42	53.5	19.9	35.2
167	2	2	0.45	1.52	0.98	54.3	41.6	27.8									4	4	0.30	0.89	0.57	37.6	32.2	36.7
182	2	2	0.18	0.43	0.30	41.0	13.1	33.0	2	2	0.50	1.03	0.77	34.6	41.8	34.3	5	5	0.34	1.00	0.58	39.8	28.2	31.7
GOM Scotian Shelf 60–200 m																								
139	1	1	0.78	0.78	0.78		70.5	44.7	1	1	1.37	1.37	1.37		74.5	22.2								
140	3	5	0.50	0.99	0.76	24.2	36.4	39.1	2	2	0.60	0.83	0.71	16.1	39.2	35.3	7	7	0.16	0.90	0.43	49.3	19.1	32.6
141	3	5	0.21	0.89	0.47	47.9	31.8	38.1	2	2	0.50	0.53	0.52	2.9	30.1	33.5	5	5	0.23	0.44	0.30	24.9	36.9	40.2
164	1	1	0.57	0.57	0.57		12.3	36.7	2	2	0.55	0.79	0.67	17.9	39.6	30.9	4	4	0.14	0.40	0.33	33.3	8.4	40.1
165	1	1	0.21	0.21	0.21		23.8	48.8	1	1	0.88	0.88	0.88		15.9	31.8	3	3	0.36	0.41	0.39	5.5	9.4	44.3
166	1	1	0.77	0.77	0.77		6.5	44.2	1	1	2.13	2.13	2.13		59.2	23.4	4	4	0.23	0.95	0.46	61.9	28.7	33.2
168	1	1	0.62	0.62	0.62		4.8	39.8	2	2	0.75	0.77	0.76	1.3	30.9	28.3	4	4	0.24	0.71	0.39	49.5	9.7	39.4
169	1	1	0.09	0.09	0.09		11.1	43.8	2	2	1.09	1.17	1.13	3.5	25.2	28.5	3	3	0.23	0.70	0.44	43.8	15.0	39.6
170	1	1	0.16	0.16	0.16		68.8	27.3	2	2	0.95	1.28	1.12	14.8	18.4	31.0	3	3	0.25	0.54	0.35	37.4	15.1	46.8
181									2	2	1.03	1.31	1.17	12.0	35.9	35.0	4	4	0.37	1.05	0.66	37.9	47.0	63.5
171	1	1	0.50	0.50	0.50		22.0	46.2	1	1	0.65	0.65	0.65		33.9	37.5	6	6	0.00	0.55	0.34	53.7	13.3	39.4
190									1	2	0.66	1.19	0.93	28.6	12.4	38.9	2	2	0.26	0.55	0.41	35.8	8.6	43.4
172	2	3	0.50	1.93	1.14	52.0	10.5	26.0	3	3	0.82	1.37	1.11	20.3	27.4	27.5	7	9	0.00	0.60	0.33	52.9	10.1	41.0
189	1	1	1.44	1.44	1.44		10.4	22.6	1	1	0.93	0.93	0.93		11.8	32.1	3	3	0.40	0.47	0.42	7.8	7.9	37.1
173	2	2	0.35	1.89	1.12	68.8	6.7	26.8	3	3	0.58	1.81	0.99	58.6	13.5	29.8	6	6	0.21	0.73	0.39	53.9	18.2	38.9

[1] Y: Number of years with observations.

[2] P: Number of stations per two-month period.

[3] C.V.: Coefficient of variation.

[4] Net.: Netplankton.

[5] Pha.: Phaeopigment.

NOAA Technical Reports NMFS

Technical Reports of the *Fishery Bulletin*

Guide for Contributors

Preparation

Title page should include authors' full names and mailing addresses and the senior author's telephone and FAX number.

Abstract should not exceed one double-spaced typed page. It should state the main scope of the research but emphasize its conclusions and relevant findings. Because abstracts are circulated by abstracting agencies, it is important that they represent the research clearly and concisely.

Text must be typed double-spaced throughout. A brief introduction should portray the broad significance of the paper; the remainder of the paper should be divided into the following sections: **Materials and methods, Results, Discussion** (or **Conclusions**), and **Acknowledgments**. Headings within each section must be short, reflect a logical sequence, and follow the rules of multiple subdivision (i.e. there can be no subdivision without at least two items). The entire text should be intelligible to interdisciplinary readers; therefore, all acronyms, abbreviations, and technical terms should be spelled out the first time they are mentioned. The scientific names of species must be written out the first time they are mentioned; subsequent mention of scientific names may be abbreviated. Follow the *U.S. Government Printing Office Style Manual* (1984 ed.) and the *CBE Style Manual* (5th ed.) for editorial style, and the most current issue of the *American Fisheries Society's Common and Scientific Names of Fishes from the United States and Canada* for fish nomenclature. Dates should be written as follows: 11 November 1991. Measurements should be expressed in metric units, e.g., metric tons as (t); if other units of measurement are used, please make this fact explicit to the reader. The numeral one (1) should be typed as a one, not as a lower-case el (l).

Text footnotes should be numbered with Arabic numerals and typed on a separate sheet of paper. Footnote all personal communications, unpublished data, and unpublished manuscripts with full address of the communicator or author, or, as in the case of unpublished data, where the data are on file. Authors are advised to avoid references to nonstandard (gray) literature, such as internal, project, processed, or administrative reports, wherever possible. Where these references are used, please include whether they are available from NTIS (National Technical Information Service) or from some other public depository.

Literature cited comprises published works and those accepted for publication in peer-reviewed literature (in press). Follow the name and year system for citation format. In the text, cite Smith and Jones (1977) or (Smith and Jones, 1977). If there is a sequence of citations, list chronologically: Smith, 1932; Green, 1947; Smith and Jones, 1985. Abbreviations of serials should conform to abbreviations given in *Serial Sources for the BIOSIS Previews Database.* Authors are responsible for the accuracy and completeness of all citations.

Tables should not be excessive in size and must be cited in numerical order in the text. Headings should be short but ample enough to allow the table to be intelligible on its own. All unusual symbols must be explained in the table heading. Other incidental comments may be footnoted with italic numerals. Use asterisks for probability in statistical data. Because tables are typeset, they need only be submitted typed and formatted, with double-spaced legends. Zeros should precede all decimal points for values less than one.

Figures include line illustrations and photographs (or slides) and must be cited in numerical order in the text. Unless photographs are submitted on glossy paper with good contrast, we cannot guarantee a good final printed copy. Figures are to be labeled with author's name and number of figure. Use Times Roman font (upper and lowercase letters) to label within figures. Avoid vertical lettering except for y-axis labels. Zeros should precede all decimal points for values less than one. Figures may be submitted as computer software files (along with laser-printed copies), as photomechanical transfers (PMTs), or as high quality photographic prints. Send only xerox copies of figures to the Scientific Editor; original figures will be requested later when the manuscript has been accepted for publication. Figure legends should explain all symbols and abbreviations and should be double-spaced on a separate page at the end of the manuscript.

Copyright law does not cover government publications; they fall within the public domain. If an author reproduces any part of a government publication in his work, reference to source is considered correct form.

Submission

Send printed copies (original and two copies) to the Scientific Editor:

Dr. John B. Pearce, Scientific Editor
Northeast Fisheries Science Center
National Marine Fisheries Service, NOAA
166 Water Street
Woods Hole, MA 02543-1097

Once the manuscript has been accepted for publication, you will be asked to submit a software copy of your manuscript to the Managing Editor. The software copy should be submitted in *WordPerfect* text format (or in standard ASCII text format if *WordPerfect* is unavailable) and should be placed on a 5.25-inch or 3.5-inch disk that is double-sided, double or high density, and that is compatible with either DOS or Apple Macintosh systems.

Copies of published articles and notes are available free of charge to the senior author (50 copies) and to his or her laboratory (50 copies). Additional copies may be purchased in lots of 100 when the author receives page proofs.

UNITED STATES
DEPARTMENT OF COMMERCE
NATIONAL OCEANIC AND ATMOSPHERIC
ADMINISTRATION
NATIONAL MARINE FISHERIES SERVICE
SCIENTIFIC PUBLICATIONS OFFICE
BIN C15700
SEATTLE, WA 98115
OFFICIAL BUSINESS

Penalty for Private Use, $300

BULK RATE
POSTAGE & FEES PAID
U.S. Department of Commerce
Permit No. G-19

NOAA SCIENTIFIC AND TECHNICAL PUBLICATIONS

The National Oceanic and Atmospheric Administration was established as part of the Department of Commerce on October 13, 1970. The mission responsibilities of NOAA are to assess the socioeconomic impact of natural and technological changes in the environment and to monitor and predict the state of the solid Earth, the oceans and their living resources, the atmosphere, and the space environment of the Earth.

The major components of NOAA regularly produce various types of scientific and technical information in the following kinds of publications:

PROFESSIONAL PAPERS—Important definitive research results, major techniques, and special investigations.

CONTRACT AND GRANT REPORTS—Reports prepared by contractors or grantees under NOAA sponsorship.

ATLAS—Presentation of analyzed data generally in the form of maps showing distribution of rainfall, chemical and physical conditions of oceans and atmosphere, distribution of fishes and marine mammals, ionospheric conditions, etc.

TECHNICAL SERVICE PUBLICATIONS—Reports containing data, observations, instructions, etc. A partial listing includes data serials; predictions and outlook periodicals; technical manuals, training papers, planning reports, and information serials; and miscellaneous technical publications.

TECHNICAL REPORTS—Journal quality with extensive details, mathematical developments, or data listings.

TECHNICAL MEMORANDUMS—Reports of preliminary, partial, or negative research or technology results, interim instructions, and the like.

Information on availability of NOAA publications can be obtained from:

U.S. Department of Commerce
National Technical Information Service
5285 Port Royal Road
Springfield, VA 22161

☆ U. S. GOVERNMENT PRINTING OFFICE: 1998 PROG 2057-S/80001